

UNIVERSITY OF OSLO
Department of Physics

Viscous Universe Models

Master thesis

Nouraddin
Mostafapoor

May 31, 2010



Acknowledgements

I would like to express my deep-felt gratitude to my supervisor, Øyvind Grøn, for his valuable guidance, advice, encouragement and constant support. He has been an great inspiration for my work with this thesis, and his willingness to motivate me contributed tremendously to this work.

I am heartily thankful to my friends and fellow students at the department of physics and the department of mathematics, for their support and helpful advice and for many interesting discussions. In particular I want to mention Hans A. Winther, the numerous discussions I shared with him have helped clarifying many important issues, and he was so kind as to read through parts of this thesis.

Finally, an honorable mention goes to my family for their moral support.

This thesis is dedicated to my sister, Roja, and my brothers, Neco and Victor Vaco.

Oslo, May 2010
Nouraddin Mostafapoor

Abstract

This thesis begins with a brief introduction of Einstein's general theory of relativity, and the applications of this theory to modern cosmology. We will, in this application, go through some classical, spatially homogeneous and isotropic cosmological models of our Universe based on Friedmann-Robertson-Walker line element. Further, we introduce the statefinder formalism, and we apply this formalism to some classical and viscous fluid universe models. We rederive some well-known results, but, we also find new results for some of models. Following this introduction we investigate viscous fluid cosmological models of Bianchi Type-I with shear, bulk and nonlinear viscosity. Our primary goal is to analyze these viscous universe models by means of statefinder formalism.

Notation

We will in this thesis use the units where $\hbar \equiv c \equiv 1$.

The following acronyms will be used repeatedly throughout the text: GR = General Relativity, FRW = Friedmann-Robertson-Walker, FLRW = Friedmann-Lemaître-Robertson-Walker, BI = Bianchi type-I universe model, SF = Statefinder formalism, DE = Dark energy, DM = Dark matter, DP = Deceleration parameter.

We denote a general spacetime metric by $g_{\mu\nu}$. The metric signature that we use in this thesis is

$$\text{sign}(g_{\mu\nu}) = (-1, 1, 1, 1)$$

The Minkowski metric will be denoted by $\eta_{\mu\nu}$.

The following notation will be used for different derivatives

Total	derivatives:	$\frac{df}{dq}, \quad f' = \frac{df}{dq}, \quad \dot{f} = \frac{df}{dt}$
Partial	derivatives:	$\frac{\partial f}{\partial q} = \partial_q f = f_{,q}, \quad \nabla = \sum_{x_i=x,y,z} \frac{\partial}{\partial x_i} \vec{e}_{x_i}$
Covariant	derivatives:	$\nabla_\mu f = f_{;\mu}$

Einstein's summation convention will be used in Chapter 2. When an index appears twice in a single term, once in an upper and once in a lower position, it implies that we are summing over all of its possible values.

$$A^\mu B_\mu \equiv g_{\mu\nu} A^\mu B^\nu = \sum_{\mu,\nu=0} g_{\mu\nu} A^\mu B^\nu$$

Contents

	Page
Acknowledgements	ii
Abstract	iv
Notation	vi
Table of Contents	viii
List of Figures	xii
Chapter	
1 Introduction	1
1.1 Research Goals	2
1.2 Outline	2
2 General Relativity	4
2.1 Gravity and Space-Time	4
2.1.1 Newtonian Physics	4
2.1.2 Trajectory of Massive Body	5
2.1.3 Special Relativity	6
2.1.4 Trajectory of a Free Body	8
2.1.5 General Relativity and Curved Space-Time	8
2.2 Differential Geometry	10
2.2.1 Tensors	10
2.2.2 Geodesic Equations and Christoffel Symbols	12
2.2.3 Covariant Derivative and Parallel Transport	13
2.2.4 Curvature	15
2.3 Einstein's Equation	17
2.3.1 Conservation Equation	18
3 Cosmology	21
3.1 Cosmological and Copernican Principles	21
3.1.1 The Friedmann-Robertson-Walker Metric	21
3.1.2 The Cosmological Solution of Friedmann-Lemaître	22
3.1.3 Kinematic	22
3.1.4 Friedmann and Continuity Equations	24
3.2 Dynamics of Friedmann-Lemaître Space-Time	27
3.2.1 Solutions	27
3.2.2 Dynamical Evolution	28
3.2.3 Expansion and Contraction	29
3.3 Time and Distances	30
3.3.1 Age of the Universe	30
3.3.2 Proper Distance	31
3.3.3 Comoving Radial Distance	31
3.4 Horizons	31
3.4.1 Event Horizon	32
3.4.2 Particle Horizon	32
4 Statefinder Formalism	34
4.1 Earlier Applications of the Statefinder Formalism	35

4.1.1	The Friedmann Universe	35
4.1.2	The Flat Λ CDM Model	37
4.1.3	The Chaplygin Gas	37
4.1.4	Universe Models with a Scalar Field	41
4.1.5	Universe Models with Two Interacting Fluids	46
4.2	Statefinder Parameters for a New Coupled Quintessence Cosmological Model	48
5	Viscous Universe Models	56
5.1	Flat Friedmann-Robertson-Walker Universe Model with Viscous Dark Energy	56
5.2	Flat FRW Universe Models with Matter and Viscous Dark Energy	57
5.3	Bulk Viscous Dark Energy and the Λ CDM Model	58
5.4	Universe Models Dominated by a Viscous Cosmic Fluid	66
5.5	Quiescence Model with Constant Bulk Viscosity	69
5.6	Quiescence Model with Variable Bulk Viscosity	71
5.7	Models with variable bulk viscosity and equation of state	73
6	Bianchi Type-I Universe Models	83
6.1	Viscous Fluid Cosmology of Bianchi Type-I	83
6.1.1	Field equations and their solutions	85
6.1.2	Equations for determining τ , H and ρ	86
6.1.3	The Special Solutions with Constant Deceleration Parameter	87
6.1.4	Special Solutions in the Case with Variable Shear Viscosity and Constant Bulk Viscosity	96
6.2	Bianchi Type-I Universe Models with Nonlinear Viscosity	103
6.2.1	Energy-Momentum Tensor for a Fluid with Nonlinear Viscosity	103
6.2.2	Einstein's field equations	111
6.2.3	Energy Conservation Equation	113
6.2.4	Statefinder Formalism for Bianchi Type-I Universe Models with Nonlinear Viscous Fluid	113
6.2.5	Bianchi Type-I Universe Filled with Zel'dovich Fluid	114
7	Conclusion and Outlook	129
7.1	Results and Conclusions	129
7.2	General Overview and Outlook	131
Appendix		
A	Numerical values	132
A.1	Physical constants	132
A.2	Units	132
A.2.1	Natural units	132
A.2.2	Conversion factors	133
A.2.3	Cosmological quantities	133
B	Einstein's Field Equations	134
B.1	Einstein's Field Equations for Friedmann-Lemaître Metric	134
B.1.1	Christoffel symbols $\Gamma_{\mu\nu}^{\alpha}$	134
B.1.2	Riemann Tensor $R_{\mu\beta\nu}^{\alpha}$	135
B.1.3	Ricci Tensor $R_{\mu\nu}$ and Ricci Scalar R	136
B.1.4	Einstein Tensor $G_{\mu\nu}$	136
B.1.5	Energy-Momentum Tensor for a Perfect Fluid	137
B.1.6	Einstein's Field Equations	137
B.2	Einstein's Field Equations for Bianchi Type-I Metric	137
B.2.1	Energy-Momentum Tensor for a Viscous Fluid	138

B.2.2 Einstein Field Equations	138
References	140

List of Figures

2.1	The causal structure of Newtonian physics.	5
2.2	The causal structure of Minkowski space-time.	7
2.3	The tangent space of a two-dimensional sphere	10
2.4	The parallel transport of a vector along a closed curve.	14
2.5	The vector T^μ is parallel transported along the path P_1P_3 passing by either P_2 or P_4 to give, respectively, the vectors T_{123}^μ and T_{143}^μ	15
3.1	The curvature of space given by k	22
4.1	The s - r plane for the Chaplygin gas model	40
4.2	$r_0(q_0)$, $r_0(s_0)$ and $s_0(q_0)$ for a universe model with matter and quintessence with an exponential potential.	44
4.3	$r_0(q_0)$ and $r_0(s_0)$ for a universe model with matter and quintessence with a power-law potential.	45
4.4	The s_0 - r_0 plane for a universe model with with two interacting fluids	48
4.5	$q(z)$ for the coupled quintessence model.	51
4.6	$r(z)$ for the coupled quintessence model.	52
4.7	The q - r -plane for the coupled quintessence model.	53
4.8	The q - s -plane for the coupled quintessence model	54
4.9	The s - r -plane for the coupled quintessence model	55
5.1	The relation between density ρ and the scale factor a	59
5.2	The scale factor as a function of time for the Λ CDM model with and without viscosity	62
5.3	The energy density for the non-relativistic matter as a function of time for the Λ CDM model with and without viscosity	63
5.4	The deceleration parameter as a function of time for the Λ CDM model with and without viscosity	64
5.5	The q - r plane for the Λ CDM model with and without viscosity	65
5.6	The s - r plane for a model dominated by a viscous cosmic fluid	68
5.7	The relation between density ρ and the redshift z	70
5.8	The s - r -plane for the quiescence model	72
5.9	The Hubble parameter as a function of the redshift for the quiescence model	74
5.10	The total energy density as a function of the redshift for the quiescence model	75
5.11	The s - r -plane for the quiescence model	76
5.12	The scale factor $a(t)$ as a function of time	79
5.13	The s - r plane for a model with variable bulk viscosity and equation of state	81
5.14	The deceleration parameter $q(t)$, statefinder parameters $r(t)$ and $s(t)$	82
6.1	The s - r plane for a model with constant deceleration parameter.	88
6.2	The generalized Hubble parameter as a function of time for $0 < n \leq 1$	90
6.3	The anisotropy parameter as a function of time for $0 < n \leq 1$	90
6.4	The metric functions of cosmic time	91

6.5	Energy density, $\rho(t)$, as a function of time for different values of n	92
6.6	The ratio of energy density and expansion scalar	94
6.7	The scale factor as a function of time, $a(t)$, for the solution with $n = 0$	94
6.8	Anisotropy parameter as a function of cosmic time for $n = 0$	95
6.9	Shear scalar as a function of cosmic time for $n = 0$	95
6.10	Energy density as a function of cosmic time for $n = 0$	96
6.11	The volume expansion as a function of cosmic time	99
6.12	The volume expansion τ	100
6.13	The volume expansion as a function of cosmic time	101
6.14	The q - r -, q - s - and s - r -plane	102
6.15	The q - r -, q - s - and s - r -plane	104
6.16	The q - r -, q - s - and s - r -plane	105
6.17	The q - r -, q - s - and s - r -plane	106
6.18	The q - r -, q - s - and s - r -plane	107
6.19	The q - r -, q - s - and s - r -plane	108
6.20	The q - r - and q - s -plane	109
6.21	The s - r -plane	110
6.22	The Hubble parameter as a function of cosmic time, for the BI universe model with cosmological constant and Zel'dovich fluid	116
6.23	The volume expansion as a function of cosmic time, for the BI universe model with cosmological constant and Zel'dovich fluid	117
6.24	The energy density as a function of the redshift, for the BI universe model with cosmological constant and Zel'dovich fluid	118
6.25	The energy density as a function of the redshift, for the BI universe model with Zel'dovich fluid	119
6.26	The energy density as a function of the redshift, for the BI universe model with cosmological constant and Zel'dovich fluid	120
6.27	Statefinder parameter r as a function of time, for the BI universe model with cosmological constant and Zel'dovich fluid	123
6.28	Statefinder parameter s as a function of time, for the BI universe model with cosmological constant and Zel'dovich fluid	124
6.29	Deceleration parameter q as a function of time, for the BI universe model with cosmological constant and Zel'dovich fluid	125
6.30	The q - r plane for the BI universe model with cosmological constant and Zel'dovich fluid	126
6.31	The q - s plane for the BI universe model with cosmological constant and Zel'dovich fluid	127
6.32	The s - r plane for the BI universe model with cosmological constant and Zel'dovich fluid	128

Chapter 1

Introduction

A host of observations shows that our universe is currently undergoing an accelerating expansion. This has been confirmed by astronomical observations, such as observations of type Ia supernovae (SNIa) [19] [20], observations of large scale structure (LSS) [22] [23] and measurements of the cosmic microwave background (CMB) anisotropy [24] [25]. Physicists, today, have accepted the idea of dark energy: a fluid with negative pressure, to be responsible for this acceleration. There are many theoretical models of dark energy, but Einstein's cosmological constant Λ , is still the preferred model. The so-called Λ CDM model, which contains both a cosmological constant Λ and the cold dark matter (CDM), is the simplest cosmological model that provides an excellent explanation for the acceleration of the universe and the existing observational data.

But there are two problems that arise from the cosmological constant namely the "fine-tuning"- and the "cosmic coincidence"-problem. The "fine-tuning"-problem asks why the cosmological constant is around 120 orders of magnitude smaller than what one expects from quantum mechanics (vacuum energy) and the "cosmic coincidence"-problem asks why the energy densities of dark energy and matter happens to be of the same order today. All efforts that have been made by theorists to resolve the cosmological constant problem, so far, have been unsuccessful.

In order to solve these two problems, many dynamical dark energy models have been proposed, such as quintessence, K-essence, the Chaplygin gas, tachyon, braneworld models, phantom and quintom etc. ([52], [53], [55], [56], [54]) Many of them use a scalar field to play the role of dark energy and the negative pressure of these models is often produced by the slow-roll mechanism ([57]) in which the scalar-field is slowly rolling down a potential. This often leads to an equation of state which is no longer a constant, but evolves with time.

Also, interacting models, which suggest that there is an interaction between dark energy and dark matter, have been proposed to understand and resolve the coincidence problem ([46], [28]). The property of dark energy is strongly model dependent and there are many models that describe dark energy which is in agreement with current observations. But with so many models to choose from, how could we tell them apart? It's here the statefinder formalism comes into play as a diagnostic for distinguishing different dark energy models.

The Hubble parameter, $H = \dot{a}/a$, and the deceleration parameter, which is defined as

$$q = -\frac{\ddot{a}}{aH^2}, \quad (1.1)$$

where $a(t)$ is the scale factor of the Friedmann-Robertson-Walker (FRW) universe, are two geometric parameters that we use to characterize the expansion history of the universe. We know that if $\dot{a} > 0$, the universe is undergoing an expansion and if $\ddot{a} > 0$ the universe is experiencing an accelerated expansion. The cosmic acceleration indicates that q should be less than zero. However the deceleration parameter on its own does not characterize the current acceleration phase uniquely. The presence of a fairly large degeneracy in q is reflected in the fact that rival dark energy models can give rise to the same value of q_0 at the present time. Under

such circumstances, a robust diagnostic of dark energy, statefinder parameter pair $\{r(z), s(z)\}$, was introduced by Sahni et al. [11] and Alam et al. [17]. The statefinder probes the expansion dynamics of the universe through high derivatives of the scale factor \ddot{a} and $\ddot{\ddot{a}}$ and is a natural next step beyond the Hubble parameter H depending on \dot{a} and the deceleration parameter q depending on \ddot{a} . With the statefinder method one introduces parameters depending on higher-order derivatives of the scale factor and generalizing the deceleration parameter.

The statefinder diagnostic is a geometrical diagnostic, because it is constructed from the space-time metric directly, which is more universal than "physical" variables, which are model-dependent. Given some DE models we can plot the statefinder parameter diagram in order to see the difference between the cosmological behaviour of these models. Then, we can use the statefinder parameters for the spatially flat Λ CDM model, which as we will see in the next section, correspond to a fixed point $\{r, s\} = \{1, 0\}$ in these diagrams, as a reference. By comparing these dark energy models with the Λ CDM scenario we can find which model is a possible model of dark energy.

1.1 Research Goals

In this thesis we will explore and analyze different universe models by means of the statefinder parameter formalism. Our main goals are:

- Apply the statefinder formalism to a new coupled quintessence cosmological model, presented by J. F. Jesus, R. C. Santos, J. S. Alcaniz and J. A. S. Lima [48].
- Explore the Λ CDM model with viscosity, and then, apply the statefinder formalism to this model.
- Explore the quiescence model with variable bulk viscosity, and then, apply the statefinder formalism to this model.
- Explore the Bianchi type-I universe model with cosmological constant and variable shear viscosity and constant bulk viscosity, and then, apply the statefinder formalism to this model.
- Based on the work of Grøn [12], explore further the nonlinear viscous fluid Bianchi type-I universe model filled with Zel'dovich fluid and with the cosmological constant, and then, apply the statefinder formalism to this model.

We have managed to achieve these goals in this thesis. Most of the quantitative results we obtain for these models are new.

1.2 Outline

This thesis is divided into two main parts. Chapters 2 and 3 are background theory chapters introducing the Einstein's general theory of relativity and its application to cosmology. Chapters 4 through 6 are the main part of the work where we go through different universe models and do calculations. Chapter 7 concludes and summarizes the work, focusing on the future possibilities. There is also an appendix where we solve Einstein's field equations for two different metrics, namely, Friedmann-Robertson-Walker metric and Bianchi type-I metric.

Chapter 2 gives a very short introduction of the Einstein's general theory of relativity.

Chapter 3 reviews the application of the Einstein's general theory of relativity to cosmology. We will give an introduction to the cosmological solution and the dynamics of the Friedmann-Lemaître space-time.

Chapter 4 starts with an introduction of the statefinder formalism. Following this introduction, we will go through the earlier applications of this formalism to the following cosmological models

- The Friedmann universe
- The flat Λ CDM model
- Chaplygin gas models
- Universe models with a scalar field
- Universe models with two interacting components

At the end of this chapter we will apply the statefinder formalism to a new coupled quintessence cosmological model.

Chapter 5 gives an introduction to viscous universe models and the application of statefinder formalism to the following universe models

- The flat Friedmann-Robertson-Walker universe model with matter and viscous dark energy
- Universe models dominated by a viscous cosmic fluid
- Quiescence model with constant bulk viscosity
- Quiescence model with variable bulk viscosity
- Universe models with variable bulk viscosity and equation of state

We will also consider the Λ CDM model with bulk viscosity. We will do some calculations to find the scale factor, the Hubble parameter and the energy density for this model. Then, we will apply the statefinder formalism to this model.

Chapter 6 begins with an introduction to the Bianchi Type-I universe models. We will write down the Einstein's field equations and find their solutions for the Bianchi type-I model with a cosmological constant and linear viscosity. We will do some calculations for the case with constant bulk viscosity and variable shear viscosity. Then, we will apply the statefinder formalism to this model. We will also give the solutions when we assume that the deceleration parameter is a constant.

At the end of this chapter we will consider the Bianchi type-I universe models with a cosmological constant and with nonlinear viscosity. We will write down the Einstein's field equations and also find their solutions for this case. We will also consider Bianchi type-I universe model filled with Zel'dovich fluid and with the cosmological constant. We will also do calculations to find the Hubble parameter and the volume expansion in the case with constant bulk and shear viscosity, and we will give a numerical solution for the energy density. Then, we will apply the statefinder diagnostics to this model.

Finally, in chapter 7 we summarise our results. We will also briefly discuss the need for a detailed analysis of the Bianchi type-I universe model, for a better knowledge about the cosmic evolution, and, how measurements of the statefinder parameters to a good accuracy in the future, could help finding the 'best' model of dark energy.

Chapter 2

General Relativity

The material of this chapter is mainly based on [1], [2], [4], [5] and [6].

Since gravity is the only long-range force that cannot be screened, the properties of the Universe on large scales will be determined by this force. In this chapter we want to recall the basic hypotheses and formulas of general relativity that are necessary for the rest of this thesis. We start by recalling the evolution of the mathematical concept of space-time from Newtonian physics to general relativity in Section 2.1. In Section 2.2 we summarize the main mathematical tools used in general relativity. We derive Einstein equations that determine the dynamics of space-time and conservation equations that determine the evolution of matter in Section 2.3.

2.1 Gravity and Space-Time

2.1.1 Newtonian Physics

In Newtonian physics, space and time are ideal and absolute. The space is Euclidean in 3 dimensions. We can therefore endow it with an origin and with 3 arbitrary axes, thus determining an absolute frame of reference. Time is independent of the motion of any observer. If we consider two events P at time t_1 , and Q at time t_2 there are three possible outcomes: (1) if $t_2 > t_1$ Q belongs to the future of P , (2) if $t_2 < t_1$ Q belongs to the past of P and (3) if $t_2 = t_1$ Q and P are simultaneous. This causal structure of Newtonian space-time is represented in Fig. 2.1.

Since space is assumed Euclidean, we can use Pythagoras' theorem to calculate the distance between two neighboring points

$$d\ell^2 = (dx^1)^2 + (dx^2)^2 + (dx^3)^2, \quad (2.1)$$

in Cartesian coordinates. We can rewrite this distance in shorter form as

$$d\ell^2 = \sum_{i=1}^3 (dx^i)^2 = \sum_{ij} \delta_{ij} dx^i dx^j \equiv \delta_{ij} dx^i dx^j, \quad (2.2)$$

where δ_{ij} is the Kronecker symbol equal to 1 if $i = j$ and 0 otherwise, and the latin indices $i, j, \dots = 1 \dots 3$. This form introduces the Einstein summation convention according to which we implicitly assume a sum over all repeated indices. The trajectory of any body is therefore given in the parametric form by $x^i(t)$. The travel time from point A at t_A to point B at t_B is given by $t_A - t_B$ and is independent of the trajectory between A and B . We can also calculate the distance in other coordinates, for example spherical or cylindrical coordinates. If we have a system of coordinates (y^i) related to Cartesian coordinates (x^j) by a relationship of the form $x^j(y^i)$, the vector $d\mathbf{x}$ of coordinates dx^i in the Cartesian system has coordinates $dy^i = \frac{\partial y^i}{\partial x^j} dx^j$. Therefore, the distance between two neighboring points, in any coordinate system, is

$$d\ell^2 = g_{ij}(y^k) dy^i dy^j, \quad g_{ij}(y^k) = \frac{\partial x^m}{\partial y^i} \frac{\partial x^n}{\partial y^j} \delta_{mn}, \quad (2.3)$$

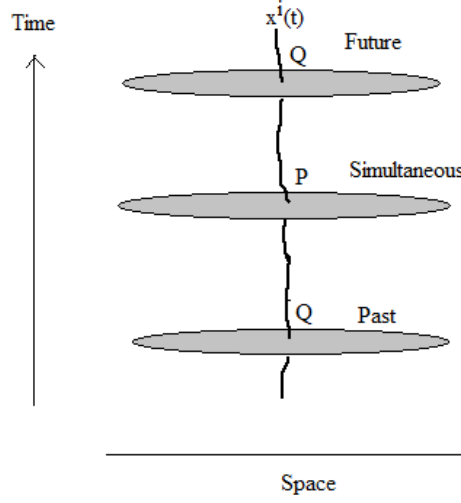


Figure 2.1: The causal structure of Newtonian physics.

where g_{ij} is the metric of space in the new coordinates. For example, spherical coordinates (r, θ, φ) are defined by

$$x = r \sin \theta \cos \varphi, \quad y = r \sin \theta \sin \varphi, \quad z = r \cos \theta. \quad (2.4)$$

By applying (2.3), we find that the non-zero components of the metric in spheric coordinates are

$$g_{rr} = 1, \quad g_{\theta\theta} = r^2, \quad g_{\varphi\varphi} = r^2 \sin^2 \theta. \quad (2.5)$$

The line-element (2.2) takes the form

$$ds^2 = dr^2 + r^2(d\theta^2 + \sin^2 \theta d\varphi^2). \quad (2.6)$$

2.1.2 Trajectory of Massive Body

The equation of motion of a body of mass m evolving in a gravitational potential ϕ can be obtained by determining the extremum of the Lagrangian constructed from the total energy of the particle

$$L = \frac{1}{2} m_I v^2 + m_G \phi = \frac{1}{2} m_I g_{ij}(x^k) \dot{x}^i \dot{x}^j + m_G \phi(x^k) \quad (2.7)$$

where we have considered that the *inertial mass*, m_I , and the *gravitational mass*, m_G , could a priori be different. The Euler-Lagrange equations

$$\frac{\partial L}{\partial x^i} - \frac{d}{dt} \left(\frac{\partial L}{\partial \dot{x}^i} \right) = 0, \quad (2.8)$$

are rewritten in any coordinate system as

$$\ddot{x}^i + \Gamma_{jk}^i \dot{x}^j \dot{x}^k = -\frac{m_G}{m_I} g^{ij} \partial_j \phi, \quad \Gamma_{jk}^i = \frac{1}{2} g^{ip} (\partial_j g_{kp} + \partial_k g_{jp} - \partial_p g_{jk}). \quad (2.9)$$

In Cartesian coordinates $g_{ij} = \delta_{ij}$ and $\Gamma_{jk}^i = 0$. We therefore recover the equation of motion in their classical form $\ddot{\mathbf{x}} = -\nabla\phi$, when $m_I = m_G$. Symbols Γ_{jk}^i represent the fictitious forces (centrifugal, Coriolis...) that have to be taken into account when the reference frame is not inertial.

We can see that (2.9) is independent of the mass of the body if $m_I = m_G$; all bodies fall identically, whatever their mass or chemical composition. This is what is called the *weak equivalence principle* or *universality of free fall*. Actually, in the Newtonian case, it is a priori possible to introduce two different masses and the equality between the gravitational mass and the inertial mass seems fortuitous. Using pendulums, Newton(1686) showed that

$$\frac{|m_G - m_I|}{m_G + m_I} < 10^{-3}. \quad (2.10)$$

The equality between the gravitational and the inertial mass was therefore only required up to one thousandth.

2.1.3 Special Relativity

The Maxwell laws of electromagnetism have the property of not being invariant under the Galilean transformations. The Galilean transformation between two inertial frames (reference frames that move with constant velocity relative to each other) with relative velocity v is then given by

$$x' = x - vt, \quad y' = y, \quad z' = z \quad (t' = t) \quad (2.11)$$

Maxwell deduced from his theory that light is an electromagnetic wave whose velocity of propagation, c , depends on permittivity and the permeability of the medium. Therefore, one had to introduce a special kind of medium in empty space which these waves could propagate, called the *aether*. The electromagnetic phenomena, in particular wave propagation, should then be physical phenomena taking place in this medium, much like the propagation of waves in water. The aether should fill the whole universe and there should be measurable corrections to Maxwell's equation in reference frames that moved relative to the aether. Michelson and Morley unsuccessfully tried to find such effects experimentally. In 1905 Albert Einstein offered a solution to the problem with aether that made the discussion about this medium completely irrelevant. He insisted on the fundamental character of Maxwell's equations and at the same time he upheld the idea of all inertial systems to be equivalent with respect to the fundamental laws of nature. His way of making this possible was to change the relations between coordinates and velocities as measured in different inertial frames. He introduced a new description of space and time by assuming the Lorentz transformations to give the correct transformations between inertial frames

$$x' = \gamma(x - vt), \quad y' = y, \quad z' = z, \quad t' = \gamma\left(t - \frac{v}{c^2}x\right) \quad (2.12)$$

where

$$\gamma = \frac{1}{\sqrt{1 - \frac{v^2}{c^2}}}. \quad (2.13)$$

The Lorentz transformations, which give the correct relativistic formula for the transition between the inertial frames S and S' is with v as the relative velocity of the two inertial frames. These transformations have the property of reducing to Galilean transformations when $v \ll c$ and keep the speed of light equal to c in all inertial reference frames. The expression for the

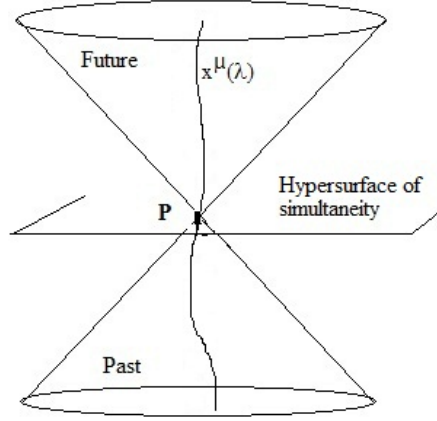


Figure 2.2: The causal structure of Minkowski space-time.

generalized distance between two points in space and time (often referred to as two events) is given by

$$ds^2 = -(dx^0)^2 + (dx^1)^2 + (dx^2)^2 + (dx^3)^2 \equiv \eta_{\mu\nu} dx^\mu dx^\nu, \quad (2.14)$$

with $x^0 \equiv ct$. The Greek indices vary between 0 and 3 and the Einstein summation convention is extended to these values. In this framework, space and time are united into a space-time, the *Minkowski space – time*. This space-time is absolute, just as in Newtonian framework. We note that contrary to the Euclidean metric, ds^2 can be negative or vanish for non-coincident events.

Depending on the relative position of the two space-time points the generalized invariant (2.14) it may be positive, zero or negative. If it is positive we refer to the separation of the two space-time points as being spacelike, if it is zero the separation is called lightlike and if it is negative the separation is timelike. The set of points such that $ds^2 = 0$ is known as the light cone and represents, for all points M in the space-time, the ensemble of points that can receive a light beam in M (future light cone) or received in M (past light cone). This light cone determines the causal structure of Minkowski space-time illustrated in Fig. 2.2. Indeed, since the velocity of all bodies is smaller than c , only pairs of points (M, P) such that $ds^2 < 0$, in other words such that M is at interior of the light cone in P , can be joined by trajectory emanating from P . The distance is then time-like and the proper time τ is generally introduced by relation

$$ds^2 = -c^2 d\tau^2. \quad (2.15)$$

If $ds^2 > 0$, the interval is said to be space-like and the points of the couple (M, P) cannot be joined by any physical trajectory.

The trajectory of any massive particles can be represented in the parametric form $x^\mu(\lambda)$, where λ is an arbitrary parameter. We can reparameterize this world-line as a function of the

proper time

$$\tau = \int \sqrt{-\eta_{\mu\nu} U^\mu U^\nu} d\lambda, \quad (2.16)$$

where $U^\mu = \frac{dx^\mu}{d\lambda}$ is the tangent vector to the worldline. In this new parameterization, the tangent vector is given by $u^\mu = \frac{dx^\mu}{d\tau}$ and it satisfies

$$u^\mu u_\mu = -c^2. \quad (2.17)$$

Let us consider an observer O' that moves with a velocity \mathbf{v} with respect to an inertial reference frame S , where an inertial observer O is located. As O is motionless, its trajectory is given by $x^i = \text{constant}$ and its proper time is $d\tau_O^2 = dt^2$. The moving observer O' has a trajectory such that $\frac{dx^i}{dt} = v^i$ with respect to the reference frame S . Its proper time is thus

$$d\tau_{O'}^2 = dt^2 - \delta_{ij} dx^i dx^j / c^2 = (1 - \frac{v^2}{c^2}) dt^2. \quad (2.18)$$

In conclusion, the proper times measured by two observers O and O' , obtained by eliminating the coordinate time, are related by

$$d\tau_{O'} = \frac{1}{\gamma} d\tau_O. \quad (2.19)$$

Thus, contrary to Newtonian case, the duration of the journey measured by O is not the same as that measured by O' , depending on their trajectory. If the clocks of O and O' have been initially synchronized, they will not be synchronous at another meeting point. This is what is called the phenomenon of *time dilation*.

Just as in Newtonian case, the metric (2.14) can be written in any coordinate system (y^μ) that is related to Minkowski coordinates (x^ν) by relation of the form $x^\nu(y^\mu)$. A vector dx^ν in Minkowski space has the coordinates $dy^\mu = \frac{\partial y^\mu}{\partial x^\nu} dx^\nu$. We thus deduce that the line-element (2.14) has the form

$$ds^2 = g_{\mu\nu}(y^\lambda) dy^\mu dy^\nu, \quad g_{\mu\nu}(y^\lambda) = \frac{\partial x^\alpha}{\partial y^\mu} \frac{\partial x^\beta}{\partial y^\nu} \eta_{\alpha\beta}. \quad (2.20)$$

2.1.4 Trajectory of a Free Body

In an analogous way to the Newtonian case, the trajectory of a massive free body can be obtained extremising the action

$$L = \frac{1}{2} g_{\mu\nu}(x^\lambda) \dot{x}^\mu \dot{x}^\nu \quad (2.21)$$

where a dot above a variable represents a derivative with respect to λ . Euler-Lagrange equations then take the form

$$\dot{u}^\mu + \Gamma_{\nu\lambda}^\mu u^\nu u^\lambda = 0, \quad \Gamma_{\nu\lambda}^\mu = \frac{1}{2} g^{\mu\sigma} (\partial_\nu g_{\lambda\sigma} + \partial_\lambda g_{\nu\sigma} - \partial_\sigma g_{\nu\lambda}), \quad (2.22)$$

where $u^\mu = \frac{dx^\mu}{d\lambda}$ and $\dot{u}^\mu = \frac{du^\mu}{d\lambda}$. In Minkowski coordinates, we find that an inertial observer must follow a trajectory of constant velocity

$$\dot{u}^\mu = 0 \Leftrightarrow u^\nu \partial_\nu u^\mu = 0. \quad (2.23)$$

2.1.5 General Relativity and Curved Space-Time

Special relativity reconciles the theory of electromagnetism and the principle of relativity at the price of replacing the Galilean principle of relativity by the principle of special relativity. However, another contradiction occurs. The theory of Newtonian gravity introduces instantaneous action at a distance, which is incompatible with the causal structure of special relativity. Einstein based his analysis on the fact that in Newtonian gravity all test objects fall in exactly the same way in an external gravitational field, whatever their mass or chemical composition. In Galilean and Newtonian physics, this *universality of free fall* comes from the equality between the inertial mass and the gravitational mass, *the equivalence principle*. Einstein's theory of general relativity is a theory of gravity. In this theory gravitation is a manifestation of the curvature of spacetime. The curvature is described by a tensor field $g_{\mu\nu}$, called the metric. Einstein built his theory mainly on two principles which we will briefly state below, see [7] for more details

- Principle of General Covariance

The principle of general covariance is a generalization of the principle of special covariance which is one of the fundamental building blocks of special relativity. While the special principle states that the laws of nature should be the same for all inertial observers, the general principle of covariance states that the laws of nature should be the same for all observers.

- Principle of Equivalence

The principle of equivalence states that there is no way to distinguish between the effects of uniform acceleration and a uniform gravitational field. Similarly there is no way to distinguish between a freely falling reference frame in a uniform gravitational field and an inertial frame in the absence of gravity. In other words freely falling reference frames are inertial and the presence of gravitational forces are due to deviations from inertial motion, just as inertial forces are due to acceleration.

The equivalence principle ensures that one can always find locally a reference frame in which the force of gravity is eliminated. This principle suggests that gravity is related to the geometry of spacetime itself. The principle of general covariance helps us to choose the appropriate mathematical objects to describe physical quantities, namely tensors.

Gravity as manifestation of geometry

Einstein's equivalence principle is at the heart of all metric theories of gravitation, which includes amongst other theory of general relativity. It is based on three conditions (see [6] for more details):

- *the weak equivalence principle* (or the universality of free fall) according to which the trajectory of a neutral test body is independent of its internal structure and its composition. This body must have a negligible binding gravitational energy and sufficiently small such that the inhomogeneities of the gravitational field can be ignored;
- *the local position invariance* according to which the result of all non-gravitational experiments is independent of the point in space-time where the experiment took place;

- *the local Lorentz invariance* according to which the results of all non-gravitational experiments are independent of the motion of the laboratory as long as it is free falling.

If the Einstein equivalence principle is valid then gravitation is the physical manifestation of curved space-time. Such a theory has the following three properties:

- the geometry of space-time is described by a metric,
- free bodies follow the geodesics of that geometry,
- in a local reference frame in free fall, the laws of physics take the same form as in spacial relativity.

2.2 Differential Geometry

From previous section we know that we can describe the motion of a free-falling body by a geodesic in four-dimensional curved space-time. Space-time is therefore described by a four-dimensional continuum so that one would need four values to locate each event, just as in special relativity.

2.2.1 Tensors

The notion of tensor is generalization of that of a vector, when one consider quantities that have multilinear dependencies under an infinitesimal transformation. General relativity is built upon a generalization of the special principle of relativity, naturally called the general principle of relativity, which states that the laws of nature should be the same in all reference frames. This means that the laws of nature should be formulated in a coordinate independent way and this is where tensors come in handy.

Given a vector space V_p , one can construct a dual space V_p^* composed of the linear maps from V_p to \mathbf{R} . This new vector space has a basis $\mathbf{y}^{\mu*}$ that can be defined by specifying their action on the elements of a basis \mathbf{y}_μ of V_p

$$\mathbf{y}^{\mu*}(\mathbf{y}_\nu) = \delta_\nu^\mu. \quad (2.24)$$

In particular, dx^ν represents the basis of V_p^* associated with the basis ∂_μ of V_p . dx^ν should therefore satisfy

$$dx^\nu(\partial_\mu) = \delta_\mu^\nu \quad (2.25)$$

and it associate any vector \mathbf{y} to its component y^ν defined by $dx^\nu(\mathbf{y}) = y^\nu$. In a coordinate transformation, dx^μ thus transforms as the components of a vector

$$dx^\mu \rightarrow dx'^\mu = \frac{\partial x'^\mu}{\partial x^\nu} dx^\nu. \quad (2.26)$$

A tensor T of rank (r, q) is a multilinear map from $(V_p)^r \times (V_p^*)^q$ to \mathbf{R} such that

$$T = T_{\nu_1 \dots \nu_q}^{\mu_1 \dots \mu_r} \partial_{\mu_1} \otimes \dots \otimes \partial_{\mu_r} \otimes dx^{\nu_1} \otimes \dots \otimes dx^{\nu_q}, \quad (2.27)$$

where \otimes is the tensor product. Such an object is said to be *r times contravariant and q times covariant*. In particular, a tensor of rank $(0, 0)$ is a scalar whose value is independent of the system of coordinates, tensor of $(1, 0)$ is a vector and a tensor of rank $(0, 1)$ is 1-form.

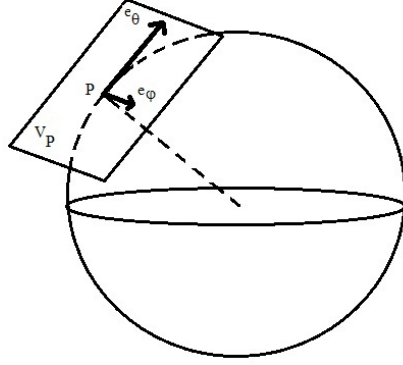


Figure 2.3: The tangent space of a two-dimensional sphere is a plane whose basis is given by $e_\theta = \partial_\theta$ and $e_\phi = \partial_\phi$.

Using the transformation laws for vectors and 1-forms, we can deduce that in a coordinate transformation, the components of a tensor transform as

$$T'^{\mu_1 \dots \mu_r}_{\nu_1 \dots \nu_q} = \frac{\partial x'^{\mu_1}}{\partial x^{\alpha_1}} \dots \frac{\partial x'^{\mu_p}}{\partial x^{\alpha_p}} \frac{\partial x^{\beta_1}}{\partial x'^{\nu_1}} \dots \frac{\partial x^{\beta_q}}{\partial x'^{\nu_q}} T^{\alpha_1 \dots \alpha_r}_{\beta_1 \dots \beta_q}. \quad (2.28)$$

A tangent space is associated to each point of the manifold. Tensors of the same nature defined at different points will therefore act different spaces. We now introduce the notion of a metric. Just as in Minkowski space-time in general coordinates, one has to use the metric to define the square of the distance between two neighboring points. The metric g should therefore be a symmetric and non-degenerate tensor of rank $(0, 2)$. The line-element between two events is then given by

$$ds^2 = g_{\mu\nu} dx^\mu dx^\nu, \quad (2.29)$$

where $g_{\mu\nu}$ is the metric tensor; it is symmetric and has hence 10 components. From the previous results, we can deduce that it transforms as

$$g'_{\mu\nu} = \frac{\partial x^\alpha}{\partial x'^\mu} \frac{\partial x^\beta}{\partial x'^\nu} g_{\alpha\beta}. \quad (2.30)$$

Tensors are thus a generalization of the notion of vector. Tensors of the same rank can be added

$$R^{\mu_1 \dots \mu_p}_{\nu_1 \dots \nu_q} = S^{\mu_1 \dots \mu_p}_{\nu_1 \dots \nu_q} + T^{\mu_1 \dots \mu_p}_{\nu_1 \dots \nu_q}, \quad (2.31)$$

and one can multiply tensors of different ranks to obtain a tensor of higher rank

$$R^{\mu_1 \dots \mu_r}_{\nu_1 \dots \nu_s} = S^{\mu_1 \dots \mu_p}_{\nu_1 \dots \nu_q} T^{\mu_{p+1} \dots \mu_r}_{\nu_{q+1} \dots \nu_s}. \quad (2.32)$$

The indices can be contracted to form a tensor whose rank is lowered by 2

$$R^{\mu_2 \dots \mu_p}_{\nu_2 \dots \nu_q} = S^{\mu_1 \mu_2 \dots \mu_p}_{\mu_1 \nu_2 \dots \nu_q} = S^{\mu_1 \mu_2 \dots \mu_p}_{\nu_1 \nu_2 \dots \nu_q} \delta_{\mu_1}^{\nu_1}. \quad (2.33)$$

This operation reduces to sum over the repeated index. This allows us to define a scalar by contracting all the indices. In particular, $T^\mu V_\mu = g_{\mu\nu} V^\mu T^\nu$ represents the scalar product of

two vectors. We conclude that $T_{\nu_1 \dots \nu_q}^{\mu_1 \dots \mu_p}$ is a tensor if and only if its contraction with any tensor of the form $R_{\mu_1 \dots \mu_p}^{\nu_1 \dots \nu_q}$ is an invariant. The metric can be used to raise or lower the indices

$$R^{\mu_1 \dots \mu_p \mu}_{\nu_2 \dots \nu_q} = R^{\mu_1 \dots \mu_p}_{\nu_1 \nu_2 \dots \nu_q} g^{\nu_1 \mu} \quad (2.34)$$

In particular, $T^\mu = g^{\mu\nu} T_\nu$. A tensor is symmetric if satisfies $T^{\mu\nu} = T^{\nu\mu}$ and is antisymmetric if $T^{\mu\nu} = -T^{\nu\mu}$. From any tensor, we can extract a symmetric and an antisymmetric tensor by

$$T_{(\mu\nu)} = \frac{1}{2} (T^{\mu\nu} + T^{\nu\mu}), \quad T_{[\mu\nu]} = \frac{1}{2} (T^{\mu\nu} - T^{\nu\mu}). \quad (2.35)$$

2.2.2 Geodesic Equations and Christoffel Symbols

Using the notion introduced in the previous section, we can go back to the trajectory of a free-falling body moving in a space-time with metric $g_{\mu\nu}$. Such a trajectory is a line of shortest length, such that its equation, $x^\mu(\lambda)$, can be obtained by maximizing the action

$$S = \int ds \quad (2.36)$$

However, as already mentioned in the Minkowski case, ds can be negative or null for some trajectories. It is therefore cleverer to maximize the action

$$S = \int L d\lambda, \quad L = g_{\mu\nu} \dot{x}^\mu \dot{x}^\nu, \quad (2.37)$$

with $\dot{x}^\mu = dx^\mu/d\lambda$. This is equivalent to maximizing $\int (ds^2/d\lambda^2) d\lambda$. We can show that extremizing these two actions comes to the same result if $ds \neq 0$, but using the second one allows us to get the correct result also for null geodesics ($ds = 0$). The Euler-Lagrange equations take the form

$$\frac{\delta L}{\delta x^\alpha} = \frac{d}{d\lambda} \left(\frac{\delta L}{\delta \dot{x}^\alpha} \right). \quad (2.38)$$

Since

$$\frac{\delta L}{\delta x^\alpha} = \partial_\alpha g_{\mu\nu} \dot{x}^\mu \dot{x}^\nu, \quad \frac{d}{d\lambda} \left(\frac{\delta L}{\delta \dot{x}^\alpha} \right) = \frac{d}{d\lambda} (2g_{\mu\alpha} \dot{x}^\mu) = 2g_{\mu\alpha} \ddot{x}^\mu + 2\partial_\beta g_{\mu\alpha} \dot{x}^\beta \dot{x}^\mu, \quad (2.39)$$

we have that

$$g_{\mu\alpha} \ddot{x}^\mu = \frac{1}{2} \left(\partial_\alpha g_{\mu\nu} \dot{x}^\mu \dot{x}^\nu - \partial_\beta g_{\mu\alpha} \dot{x}^\beta \dot{x}^\mu - \partial_\mu g_{\beta\alpha} \dot{x}^\beta \dot{x}^\mu \right) \quad (2.40)$$

where we have symmetrized the term $\partial_\beta g_{\mu\alpha} \dot{x}^\beta \dot{x}^\mu$. Introducing the Christoffel symbols

$$\Gamma_{\lambda\mu\nu} = \frac{1}{2} (\partial_\mu g_{\lambda\nu} + \partial_\nu g_{\mu\lambda} - \partial_\lambda g_{\mu\nu}), \quad (2.41)$$

and

$$\Gamma_{\mu\nu}^\alpha = g^{\lambda\alpha} \Gamma_{\lambda\mu\nu}, \quad (2.42)$$

and contracting our equation with $g^{\alpha\sigma}$, we get geodesic equation

$$\ddot{x}^\mu + \Gamma_{\nu\lambda}^\mu \dot{x}^\nu \dot{x}^\lambda = 0, \quad (2.43)$$

which is identical to (2.22) what we obtained in special relativity. As we have stressed, space-time curvature does not intervene in the equation of the trajectory of a single particle, but it

does in the deviation of close trajectory. From the definition of the Christoffel symbols (2.41), we have, since the metric is symmetric,

$$\Gamma_{\mu\nu}^{\alpha} = \Gamma_{\nu\mu}^{\alpha}, \quad (2.44)$$

as well as

$$\Gamma_{\alpha\mu\nu} = \Gamma_{\alpha\nu\mu}. \quad (2.45)$$

We note that in four dimensions there are $4 \times 10 = 40$ Christoffel symbols, which is precisely the number of partial derivatives of the metric $\partial_{\alpha}g_{\mu\nu}$. We can hence inverse the relation (2.41) to obtain, after some algebra

$$\partial_{\alpha}g_{\mu\nu} = g_{\lambda\mu}\Gamma_{\alpha\nu}^{\lambda} + g_{\lambda\nu}\Gamma_{\alpha\mu}^{\lambda}. \quad (2.46)$$

Using the geodesic equation, we can convince ourselves that the Christoffel symbols are not tensors since they transform as

$$\Gamma_{\mu\nu}^{\prime\alpha} = \frac{\partial x^{\prime\alpha}}{\partial x^{\beta}} \frac{\partial x^{\sigma}}{\partial x^{\prime\mu}} \frac{\partial x^{\rho}}{\partial x^{\prime\nu}} \Gamma_{\sigma\rho}^{\beta} - \frac{\partial^2 x^{\prime\alpha}}{\partial x^{\sigma} \partial x^{\rho}} \frac{\partial x^{\sigma}}{\partial x^{\prime\mu}} \frac{\partial x^{\rho}}{\partial x^{\prime\nu}} \quad (2.47)$$

under a coordinate transformation. The determinant of the metric is given by

$$g = \det g_{\mu\nu} = \pi_{0123}^{\alpha\beta\gamma\delta} g_{\alpha 0} g_{\beta 1} g_{\gamma 2} g_{\delta 3}, \quad (2.48)$$

where $\pi_{\mu\nu\rho\sigma}^{\alpha\beta\gamma\delta} = +1$ is an even permutation of $(\mu\nu\rho\sigma)$, -1 if it is an odd permutation and 0 otherwise. We thus obtain the derivative of the determinant

$$\partial_{\alpha}g = gg^{\mu\nu}\partial_{\alpha}g_{\mu\nu}. \quad (2.49)$$

2.2.3 Covariant Derivative and Parallel Transport

The laws of physics often take the form of partial differential equations. It is thus important to understand how a tensor field can be differentiated in way that preserves its tensor properties. The partial derivative of an arbitrary tensor field

$$\partial_{\alpha}T_{\nu_1 \dots \nu_q}^{\mu_1 \dots \mu_p}(x^{\beta}) = T_{\nu_1 \dots \nu_q, \alpha}^{\mu_1 \dots \mu_p} \quad (2.50)$$

is no longer a tensor, apart from the exceptional case of the derivative of a scalar that is a 1-form. To really understand this, let us consider the derivative of a vector T^{μ} and show how it transforms under a coordinate transformation

$$\frac{\partial T^{\mu}}{\partial x^{\prime\alpha}} = \frac{\partial}{\partial x^{\prime\alpha}} \left(\frac{\partial x^{\prime\mu}}{\partial x^{\nu}} T^{\nu} \right) = \frac{\partial x^{\prime\mu}}{\partial x^{\nu}} \frac{\partial x^{\sigma}}{\partial x^{\prime\alpha}} \frac{\partial T^{\nu}}{\partial x^{\sigma}} + \frac{\partial^2 x^{\prime\mu}}{\partial x^{\sigma} \partial x^{\nu}} \frac{\partial x^{\sigma}}{\partial x^{\prime\alpha}} T^{\nu}. \quad (2.51)$$

The reason for this is that this operation makes the difference between the value of the tensor at x^{α} and $x^{\alpha} + dx^{\alpha}$ and that at these points, the tensor has different transformation laws. Consider a constant vector of the Euclidean plane, with coordinates $T^x = 1, T^y = 0$. In polar coordinates, its coordinates depend on the position ($T^r = \sin\theta, T^{\theta} = \cos\theta$) simply because the direction of the coordinate lines change from one point to the other. It follows that $\partial_{\theta}T^r$ and $\partial_{\theta}T^{\theta}$ do not vanish even if T is a constant. What we should define is a derivative such that the components of a constant vector do no change when it is transported from x^{α} to $x^{\alpha} + dx^{\alpha}$. The covariant derivative is the differentiation operator that parallel transports the tensor from

x^α to $x^\alpha + dx^\alpha$ before subtracting its value at x^α . Since this operation is linear, one can always define such a covariant derivative by

$$\nabla_\mu T^\nu = \partial_\mu T^\nu + C_{\mu\alpha}^\nu T^\alpha, \quad \nabla_\mu T_\nu = \partial_\mu T_\nu - C_{\mu\nu}^\alpha T_\alpha, \quad (2.52)$$

where the quantities $C_{\mu\alpha}^\nu$ should be determined. For that, we notice that (2.51) implies that these quantities should transform as (2.47) during a change of coordinate. Working locally in Minkowski space and noting that then $\nabla_\alpha T^\mu = \partial_\alpha T^\mu$, we conclude that

$$C_{\mu\alpha}^\nu = \Gamma_{\mu\alpha}^\nu. \quad (2.53)$$

In the rest of this thesis, we will denote the covariant derivative either with the symbol ∇_μ or by $;\mu$ in subscript, with no distinction: $\nabla_\mu T^\nu = T^\nu_{;\mu}$. Similarly, we will use the notation $\partial_\mu T^\nu = T^\nu_{,\mu}$ for the ordinary partial derivative. The relation (2.52) can be generalized to an arbitrary tensor

$$\begin{aligned} \nabla_\alpha T^{\mu_1 \dots \mu_p}_{\nu_1 \dots \nu_q} &= \partial_\alpha T^{\mu_1 \dots \mu_p}_{\nu_1 \dots \nu_q} + \Gamma_{\alpha\lambda_1}^{\mu_1} T^{\lambda_1 \mu_2 \dots \mu_p}_{\nu_1 \dots \nu_q} + \dots + \Gamma_{\alpha\lambda_p}^{\mu_p} T^{\mu_1 \dots \mu_{p-1} \lambda_p}_{\nu_1 \dots \nu_q} \\ &\quad - \Gamma_{\alpha\nu_1}^{\lambda_1} T^{\mu_1 \dots \mu_p}_{\lambda_1 \nu_2 \dots \nu_q} - \dots - \Gamma_{\alpha\nu_q}^{\lambda_q} T^{\mu_1 \dots \mu_p}_{\nu_1 \dots \nu_{q-1} \lambda_q}. \end{aligned} \quad (2.54)$$

A consequence of this result is that $\nabla_\alpha g_{\mu\nu} = \partial_\alpha g_{\mu\nu} - \Gamma_{\alpha\mu}^\sigma g_{\sigma\nu} - \Gamma_{\alpha\nu}^\sigma g_{\sigma\mu}$. Using the expression (2.42) for the Christoffel symbols and (2.46) for the derivative of the metric, we get

$$\nabla_\alpha g_{\mu\nu} = 0. \quad (2.55)$$

To each metric, we can therefore associate a covariant derivative.

Parallel Transport

The covariant derivative allows us to define the notion of parallel transport. A vector is parallel transported if $DT^\mu \equiv dx^\nu \nabla_\nu T^\mu = 0$. We can use this condition to define the notion of parallel transport of a vector along a curve of equation $x^\mu(\tau)$ by $DT^\mu/D\tau = 0$, i.e. by

$$\frac{DT^\mu}{D\tau} = u^\nu \nabla_\nu T^\mu = \frac{dT^\mu}{d\tau} + \Gamma_{\nu\alpha}^\mu T^\alpha u^\nu = 0, \quad (2.56)$$

where $u^\mu = dx^\mu/d\tau$. The example of the sphere presented in Fig.2.4 shows that the result of this operation depends on which path is followed. A special case of transport along a curve is the auto-parallel transport, i.e. a curve such that the tangent vector is transported parallel to itself; it should therefore satisfy

$$\frac{Du^\mu}{D\tau} = u^\nu \nabla_\nu u^\mu = 0. \quad (2.57)$$

This is simply the equation of the geodesic(2.43) so that we conclude that the geodesics (curves of shortest path) are therefore auto-parallel.

Differential Operators

The covariant derivative allows us to define some mathematical operators such as the divergence and curl. Using (2.41), we get that

$$\nabla_\mu T^\mu = \partial_\mu T^\mu + \Gamma_{\mu\rho}^\mu T^\rho = \partial_\mu T^\mu + T^\rho \partial_\rho \ln \sqrt{-g}, \quad (2.58)$$

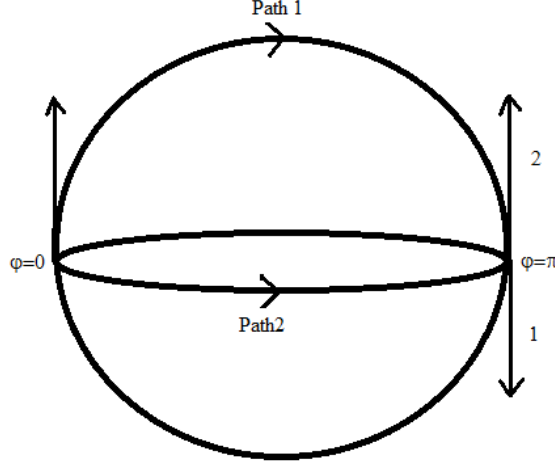


Figure 2.4: The parallel transport of a vector along a closed curve.

which can be used to express the divergence of any vector field by

$$\nabla_\mu T^\mu = \frac{1}{\sqrt{-g}} \partial_\mu (\sqrt{-g} T^\mu). \quad (2.59)$$

Similarly, we can check that divergence of any antisymmetric tensor is of the form

$$\nabla_\mu F^{\mu\nu} = \frac{1}{\sqrt{-g}} \partial_\mu (\sqrt{-g} F^{\mu\nu}), \quad (2.60)$$

where we used the fact that the contraction of a symmetric tensor with an antisymmetric one vanishes.

2.2.4 Curvature

As seen from Fig.2.4, the parallel transport of a vector along a closed curve does not bring the vector back to its initial state if the space is curved, contrary to what happens in a Euclidean space. Just like for the geodesic deflection, this characterizes the curvature space. Let us consider the parallel transport of a vector T^μ along the closed path shown in Fig.2.5. From P_1 to P_2 , the relation (2.56) implies that the variation of the vector T^μ is given by $\delta_{12} T^\mu = dx^\alpha \nabla_\alpha T^\mu = dT^\mu + \Gamma_{\alpha\sigma}^\mu T^\sigma dx^\alpha$. By iterating it, we get that the variation between P_1 and P_3 is given by $\delta_{123} T^\mu = dx^\alpha dx^\beta \nabla_\beta \nabla_\alpha T^\mu = d^2 T^\mu + 2\Gamma_{\alpha\nu}^\mu dx^\alpha dT^\nu + \left(\partial_\beta \Gamma_{\alpha\sigma}^\mu + \Gamma_{\beta\nu}^\mu \Gamma_{\alpha\sigma}^\nu \right) dx^\alpha dx^\beta T^\sigma$. The same variation passing through P_4 is given by $\delta_{143} T^\mu = dx^\alpha dx^\beta \nabla_\alpha \nabla_\beta T^\mu$. On comparing these two expressions, only the terms proportional to $dx^\alpha dx^\beta$ are different and we get that

$$(\nabla_\alpha \nabla_\beta - \nabla_\beta \nabla_\alpha) T^\mu = R_{\nu\alpha\beta}^\mu T^\nu, \quad (2.61)$$

where the Riemann tensor is given by

$$R_{\nu\alpha\beta}^\mu = \partial_\alpha \Gamma_{\nu\beta}^\mu - \partial_\beta \Gamma_{\nu\alpha}^\mu + \Gamma_{\sigma\alpha}^\mu \Gamma_{\nu\beta}^\sigma - \Gamma_{\sigma\beta}^\mu \Gamma_{\nu\alpha}^\sigma, \quad R_{\sigma\nu\alpha\beta} = g_{\sigma\mu} R_{\nu\alpha\beta}^\mu. \quad (2.62)$$

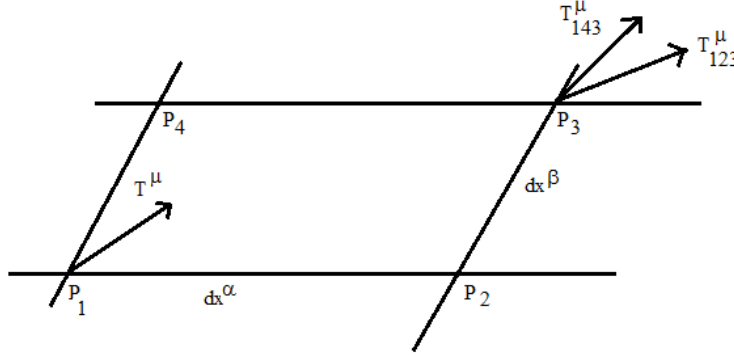


Figure 2.5: The vector T^μ is parallel transported along the path P_1P_3 passing by either P_2 or P_4 to give, respectively, the vectors T_{123}^μ and T_{143}^μ .

The definition (2.62) allows one to conclude that the Riemann tensor is antisymmetric in the permutation of the first or the second pair of indices

$$R_{\alpha\mu\nu\sigma} = -R_{\mu\alpha\nu\sigma} = -R_{\alpha\mu\sigma\nu}, \quad (2.63)$$

and that it is symmetric in the permutation of the two pairs

$$R_{\alpha\mu\nu\sigma} = R_{\nu\sigma\alpha\mu}. \quad (2.64)$$

We can also show that it satisfies the identity

$$3R_{\alpha[\mu\nu\sigma]} = R_{\alpha\mu\nu\sigma} + R_{\alpha\nu\sigma\mu} + R_{\alpha\sigma\mu\nu} = 0. \quad (2.65)$$

The two first symmetry properties imply that Riemann tensor has as many components as a 6×6 symmetric matrix, i.e. 21 components. The relation (2.65) independent of the first ones and thus adds one extra constraint to the number of components. The Riemann tensor therefore has 20 independent component. Finally, the derivative of the Riemann tensor enjoy a cyclic symmetry property that is

$$3R_{\alpha\mu[\nu\sigma;\beta]} = R_{\alpha\mu\nu\sigma;\beta} + R_{\alpha\mu\sigma\beta;\nu} + R_{\alpha\mu\beta\nu;\sigma} = 0, \quad (2.66)$$

called the Bianchi identity.

Ricci and Einstein Tensor

The symmetry properties of the Riemann tensor imply that we can construct only one tensor by contraction of two indices. This is the Ricci tensor, which is symmetric and defined by

$$R_{\mu\nu} = R_{\mu\alpha\nu}^{\alpha} = -R_{\mu\nu\alpha}^{\alpha}. \quad (2.67)$$

The Ricci tensor has 10 independent components. Its trace defines a scalar, the scalar curvature, also known as the Ricci scalar

$$R = R_{\mu\nu}g^{\mu\nu}. \quad (2.68)$$

Contracting the Bianchi identities (2.66), respectively, by $g^{\alpha\beta}$ and $g^{\alpha\beta}g^{\mu\sigma}$ implies that

$$R_{\mu\nu\sigma;\alpha} - R_{\mu\sigma;\nu} + R_{\mu\nu;\sigma} = 0, \quad R_{\nu;\alpha} - R_{;\nu} + R_{\nu;\alpha} = 0. \quad (2.69)$$

We can combine these two equations to construct a conserved tensor for the covariant derivative

$$G^{\mu\nu}_{;\nu} = 0, \quad G_{\mu\nu} = R_{\mu\nu} - \frac{1}{2}Rg_{\mu\nu}. \quad (2.70)$$

This tensor $G_{\mu\nu}$ is called the Einstein tensor.

2.3 Einstein's Equation

We will in this section derive Einstein's equation by treating $g_{\mu\nu}$ as a tensor field and then applying Hamilton's principle. For that, we need a Lagrangian density \mathcal{L} . Since curvature is related to the second derivative of the metric, the Lagrangian density must be dependent on the metric and its first derivatives only. Hilbert found that the Ricci scalar R is the simplest possible choice, and proposed that the Lagrangian density governing gravity is given by $\mathcal{L}_G = \kappa R$. Using this Lagrangian density we get the invariant Einstein-Hilbert action integral S by integrating over the invariant volume $dV = \sqrt{-g}d^4x$

$$S = \frac{1}{2\kappa} \int (R - 2\Lambda) \sqrt{-g}d^4x + \int \mathcal{L}_{mat}\sqrt{-g}d^4x, \quad (2.71)$$

where κ is coefficient to be determined by requiring that the theory reduces to Newtonian gravity in the weak-field limit; this is only free parameter of the theory. \mathcal{L}_{mat} is the Lagrangian of the matter field and Λ is a constant called the *cosmological constant*. We will now present the variation of these two terms. We start by varying the Einstein-Hilbert action

$$\delta \int R\sqrt{-g}d^4x = \int \delta (R_{\mu\nu}g^{\mu\nu}\sqrt{-g}) d^4x, \quad (2.72)$$

where we just used the definition of the scalar curvature. Expanding this expression, we get

$$\int \delta (R\sqrt{-g}) d^4x = \int R\delta\sqrt{-g}d^4x + \int g^{\mu\nu}\sqrt{-g}\delta R_{\mu\nu}d^4x + \int R_{\mu\nu}\sqrt{-g}\delta g^{\mu\nu}d^4x. \quad (2.73)$$

To evaluate the first term, we should vary the metric determinant. Using the result (2.49), we get

$$\delta g = g^{\mu\nu}g\delta g_{\mu\nu} = -g_{\mu\nu}g\delta g^{\mu\nu}, \quad (2.74)$$

which leads to the conclusion

$$\int \delta R\sqrt{-g}d^4x = -\frac{1}{2} \int R\sqrt{-g}g_{\mu\nu}g\delta g^{\mu\nu}d^4x. \quad (2.75)$$

The second term is more complicated to evaluate. For that, we work in locally inertial coordinate system, i.e. where $g_{\mu\nu} = \eta_{\mu\nu}$ and $\partial_\gamma g_{\mu\nu} = 0$ from which we deduce that $\Gamma^\alpha_{\mu\nu} = 0$ but the derivatives of Christoffel symbols do not vanish. We hence obtain

$$\delta R_{\mu\nu} = (\delta\Gamma^\sigma_{\mu\nu})_{;\sigma} - (\delta\Gamma^\sigma_{\sigma\nu})_{;\mu} = (\delta\Gamma^\sigma_{\mu\nu})_{;\sigma} - (\delta\Gamma^\sigma_{\sigma\nu})_{;\mu}. \quad (2.76)$$

To go from the partial derivative to covariant derivative, we used the fact that the result is a tensor, and hence it should be in the same in any frame. We can hence conclude that

$$\int_V g^{\mu\nu} \sqrt{-g} \delta R_{\mu\nu} d^4x = \int_V \sqrt{-g} \left[(g^{\mu\nu} \delta \Gamma_{\mu\nu}^\sigma)_{;\sigma} - (g^{\mu\nu} \delta \Gamma_{\sigma\nu}^\sigma)_{;\mu} \right] d^4x, \quad (2.77)$$

on any volume V . The integrand is therefore of the form $\sqrt{-g} I_{;\mu}^\mu$ which can be reexpressed, using the property (2.59), as $(\sqrt{-g} I^\mu)_{;\mu}$. This is therefore the integral of a total derivative, which can be reduced to an integral on the boundary of the volume V so that it does not contribute to the equations of motion. We therefore obtain

$$\delta \int R \sqrt{-g} d^4x = \int \sqrt{-g} G_{\mu\nu} \delta g^{\mu\nu} d^4x, \quad (2.78)$$

where the Einstein tensor $G_{\mu\nu}$ is defined in (2.70). The variation of the term Λ is trivial and gives

$$\delta \int 2\Lambda \sqrt{-g} d^4x = - \int \Lambda \sqrt{-g} g_{\mu\nu} \delta g^{\mu\nu} d^4x. \quad (2.79)$$

The variation of the matter action with respect to the metric is given by

$$\delta \int \mathcal{L}_{mat} \sqrt{-g} d^4x = \int \frac{\delta (\mathcal{L}_{mat} \sqrt{-g})}{\sqrt{-g} \delta g^{\mu\nu}} \delta g^{\mu\nu} \sqrt{-g} d^4x, \quad (2.80)$$

which we may write as

$$\delta \int \mathcal{L}_{mat} \sqrt{-g} d^4x = -\frac{1}{2} \int \sqrt{-g} T_{\mu\nu} \delta g^{\mu\nu} d^4x, \quad (2.81)$$

where the energy-momentum tensor $T_{\mu\nu}$, defined by

$$T_{\mu\nu} = -\frac{2}{\sqrt{-g}} \frac{\delta (\mathcal{L}_{mat} \sqrt{-g})}{\delta g^{\mu\nu}} = g_{\mu\nu} \mathcal{L}_{mat} - 2 \frac{\delta \mathcal{L}_{mat}}{\delta g^{\mu\nu}}, \quad (2.82)$$

is a rank 2 symmetric tensor. Using the above results, we obtain the general form of Einstein's equations

$$G_{\mu\nu} + \Lambda g_{\mu\nu} = \kappa T_{\mu\nu} \quad (2.83)$$

2.3.1 Conservation Equation

The Bianchi identities (2.66) impose $G_{;\nu}^{\mu\nu} = 0$ which implies, using Einstein's equations and the fact that $g_{\mu\nu;\alpha} = 0$, that

$$T_{;\nu}^{\mu\nu} = 0. \quad (2.84)$$

This equation is satisfied by the total energy-momentum tensor. The energy-momentum tensor is a symmetric tensor of rank 2 that describes material characteristics. T^{00} represents energy density, T^{i0} represents momentum density, T^{ii} represents pressure $T^{ii} > 0$, T^{ii} represents stress $T^{ii} < 0$, and T^{ij} represents shear forces $i \neq j$. For a Newtonian fluid we have the following energy-momentum tensor:

$$\begin{aligned} T^{00} &= \rho & T^{i0} &= \rho v^i \\ T^{ij} &= \rho v^i v^j + p \delta^{ij} \end{aligned} \quad (2.85)$$

where p is pressure, assumed isotropic here. We choose a locally Cartesian coordinate system in an inertial frame such that the covariant derivatives are reduced to partial derivatives. The divergence of the energy-momentum tensor, $T_{;\nu}^{\mu\nu}$ has 4 components, one for each value of μ . The zeroth component is

$$\begin{aligned} T_{;\nu}^{0\nu} &= T_{,\nu}^{0\nu} = T_{,0}^{00} + T_{,i}^{0i} \\ &= \frac{\partial \rho}{\partial t} + \frac{\partial (\rho v^i)}{\partial x^i} \end{aligned} \quad (2.86)$$

which by comparison to Newtonian hydrodynamics implies that $T_{;\nu}^{0\nu} = 0$ is the continuity equation. This equation represents the conservation of energy. The i th component of the divergence is

$$\begin{aligned} T_{;\nu}^{i\nu} &= T_{,0}^{i0} + T_{,j}^{ij} \\ &= \frac{\partial (\rho v^i)}{\partial t} + \frac{\partial (\rho v^i v^j + p \delta^{ij})}{\partial x^j} \\ &= \rho \frac{\partial v^i}{\partial t} + v^i \frac{\partial \rho}{\partial t} + v^i \frac{\partial \rho v^j}{\partial x^j} + \rho v^j \frac{\partial v^i}{\partial x^j} + \frac{\partial p}{\partial x^i} \end{aligned} \quad (2.87)$$

now, according to the continuity equation

$$\begin{aligned} \frac{\partial \rho}{\partial t} &= - \frac{\partial (\rho v^i)}{\partial x^i} \\ \Rightarrow T_{;\nu}^{i\nu} &= \rho \frac{\partial v^i}{\partial t} + v^i \frac{\partial \rho}{\partial t} - v^i \frac{\partial \rho}{\partial t} + \rho v^j \frac{\partial v^i}{\partial x^j} + \frac{\partial p}{\partial x^i} \\ &= \rho \frac{Dv^i}{Dt} + \frac{\partial p}{\partial x^i} \\ T_{;\nu}^{i\nu} &= 0 \Rightarrow \rho \frac{Dv^i}{Dt} = - \frac{\partial p}{\partial x^i} \end{aligned} \quad (2.88)$$

which is Euler's equation of motion. It represents the conservation of momentum. The equations $T_{;\nu}^{i\nu} = 0$ are general expressions for energy and momentum conservation. A perfect fluid is a fluid with no viscosity and is given by the energy-momentum tensor

$$T_{\mu\nu} = (\rho + p) u_\mu u_\nu + p g_{\mu\nu} \quad (2.89)$$

where ρ and p are the mass density and the stress, respectively, measured in the fluids rest frame, u_μ are the components of the 4-velocity of the fluids. In a comoving orthonormal basis the components of the 4-velocity are $u^{\hat{\mu}} = (c, 0, 0, 0)$. Then the energy-momentum tensor is given by

$$T^{\hat{\mu}\hat{\nu}} = \begin{pmatrix} \rho & 0 & 0 & 0 \\ 0 & p & 0 & 0 \\ 0 & 0 & p & 0 \\ 0 & 0 & 0 & p \end{pmatrix} \quad (2.90)$$

where $p > 0$ is pressure and $p < 0$ is tension. There are three different types of perfect fluids that are useful:

1. *Dust* or *non-relativistic gas* is given by $p = 0$ and the energy-momentum tensor $T_{\mu\nu} = \rho u_\mu u_\nu$.

2. *Radiation* or *ultra-relativistic gas* is given by a traceless energy-momentum tensor, i.e. $T^\mu_\mu = 0$. It follows that $p = \frac{1}{3}\rho$.
3. *Vacuum energy*: If we assume that no velocity can be measured relatively to vacuum, then all the components of the energy-momentum tensor must be Lorentz-invariant. It follows that $T_{\mu\nu} \propto g_{\mu\nu}$. If vacuum is defined as a perfect fluid we get $p = -\rho$ so that $T_{\mu\nu} = pg_{\mu\nu} = -\rho g_{\mu\nu}$.

In Newtonian limit the metric may be written

$$ds^2 = -(1 + 2\phi) dt^2 + (1 + h_{ii})(dx^2 + dy^2 + dz^2), \quad (2.91)$$

where the Newtonian potential $|\phi| \ll 1$, and h_{ii} is a perturbation of the metric satisfying $|h_{ii}| \ll 1$. We also have $T_{00} \gg T_{kk}$ and $T \approx -T_{00}$. Then the 00-component of the field equations becomes

$$R_{00} \approx \frac{\kappa}{2} T_{00}. \quad (2.92)$$

Furthermore we have

$$\begin{aligned} R_{00} = R_{0\mu 0}^\mu &= R_{0i0}^i \\ &= \Gamma_{00,i}^i - \Gamma_{0i,0}^i \\ &= \frac{\partial \Gamma_{00}^k}{\partial x^k} = \nabla^2 \phi. \end{aligned} \quad (2.93)$$

Since $T_{00} \approx \rho$ eq.(2.93) can be written $\nabla^2 \phi = \frac{1}{2}\kappa\rho$. Comparing this equation with the Newtonian law of gravitation on local form: $\nabla^2 \phi = 4\pi G\rho$, we see that $\kappa = 8\pi G$.

Chapter 3

Cosmology

The material of this chapter is mainly based on [1], [2], [3], [4], [5] and [6].

The first cosmological solution of Einstein's equation was given by Einstein himself in 1917. At the expense of introducing a cosmological constant, he was able to construct a closed and static space. The general solutions were discovered independently by Alexandre Friedmann and Georges Lemaître in 1922 and 1927. In this chapter we will give the derivation of these solutions from Einstein's equations. We will also study the kinematics and dynamics of these solutions.

3.1 Cosmological and Copernican Principles

The matter in the universe seems to be spread isotropically around us, just as the cosmic microwave background radiation. This indicates that the space-time describing the observable universe should have a spherical symmetry around us. There are two possible explanation: either our Galaxy lies in a special place in the universe so that it is not homogeneous and must have a center. Or the space-time is homogeneous; every point is then similar and the universe is isotropic around each point. To construct cosmological models, we distinguish two uniformity principles. The *cosmological principle* supposes that the Universe is spatially isotropic and homogeneous, and this implies that any observer sees an isotropic Universe around him. We distinguish this principle from the *Copernican principle* that states that we do not lie in a special place (the center) of the universe.

The cosmological principle makes definite predictions about all unobservable regions beyond the observable Universe. It completely determines the entire structure of the universe, even for regions that cannot be observed. From this point of view, this hypothesis, which cannot be tested, is very strong. The Copernican principle has more modest consequence and leads to the same conclusions but, only for the observable Universe where isotropy has been verified. It does not make any prediction on the structure of the universe for unobserved regions.

3.1.1 The Friedmann-Robertson-Walker Metric

The *homogeneity* of space means that at every moment, each point of space is similar to any other one. *Isotropy* means that at every point of the universe can be seen as isotropic. For a spatially homogeneous and isotropic spacetime it is possible to choose a set of coordinates, known as comoving coordinates, where the metric takes the simple form

$$ds^2 = -dt^2 + a^2(t) \left(\frac{dr^2}{1 - kr^2} + r^2 d\Omega^2 \right), \quad (3.1)$$

where

$$d\Omega^2 = d\theta^2 + \sin^2 \theta d\phi^2$$

This metric is called the Friedmann-Robertson-Walker metric. Here, $a(t)$ is the scale factor and gives us the relative size of space. The curvature of the space is described by parameter

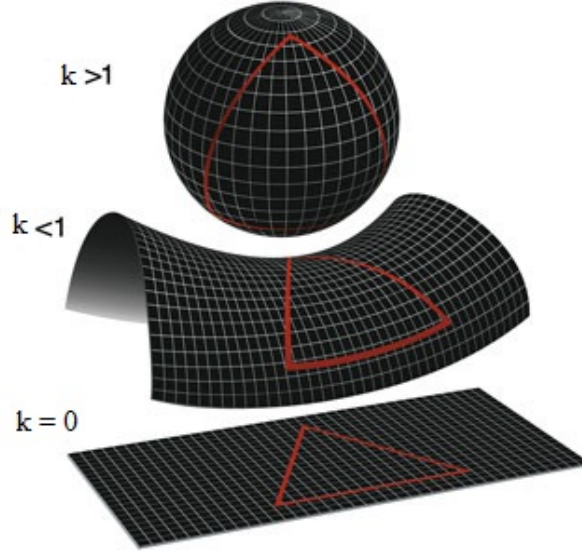


Figure 3.1: The curvature of space given by k . This image is taken from Nasa's WMAP universe cite http://map.gsfc.nasa.gov/universe/uni_shape.html

k . When $k > 0$ we have a closed space because the space is positively curved and the spatial geometry is spherical. If $k < 0$ we have a open space because the space have negative curvature and the spatial geometry is hyperbolic. The case where $k = 0$ the space is flat because it has no curvature, see figure 3.1.

3.1.2 The Cosmological Solution of Friedmann-Lemaître

From the metric (3.1) we can now calculate the Ricci tensor and Ricci scalar R , and then the Einstein tensor

$$G_{\mu\nu} = R_{\mu\nu} - \frac{1}{2}Rg_{\mu\nu}, \quad (3.2)$$

corresponding to the left hand side of Einsteins field equations. The actual calculations are found in appendix B. The non-vanishing components of the Einstein tensor $G_{\mu\nu}$ are

$$G_{tt} = \frac{3}{a^2} [(\partial_t a)^2 + k] \quad (3.3)$$

$$G_{rr} = (1 - kr^2)^{-1} [-2a\partial_t^2 a - (\partial_t a)^2 - k] \quad (3.4)$$

$$G_{\theta\theta} = r^2 [-2a\partial_t^2 a - (\partial_t a)^2 - k] \quad (3.5)$$

$$G_{\phi\phi} = r^2 \sin^2 \theta [-2a\partial_t^2 a - (\partial_t a)^2 - k] \quad (3.6)$$

3.1.3 Kinematic

Without knowing the evolution law for the scale factor, $a(t)$, a few general consequences can be obtained simply from the form of the Friedmann-Robertson-Walker metric. In the metric (3.1) the coordinates x^i are comoving. In a comoving reference frame, an observer has a four-velocity

$$u^\mu = \delta_0^\mu. \quad (3.7)$$

We can re-express this metric in the form

$$ds^2 = -(u_\mu dx^\mu)^2 + \hat{\gamma}_{\mu\nu}(t) dx^\mu dx^\nu, \quad (3.8)$$

where $\hat{\gamma}_{\mu\nu} = g_{\mu\nu} + u_\mu u_\nu$ is the projector tensor. We see that the expansion of the universe allows a comoving observer to naturally decompose any vector P^μ into a time-like and space-like component as

$$P^\mu = -(P^\nu u_\nu) u^\mu + \hat{\gamma}^\mu_\nu P^\nu \quad (3.9)$$

Let us now consider two comoving observers with trajectories given by $\mathbf{x} = \mathbf{x}_1$ and $\mathbf{x} = \mathbf{x}_2$. In the physical space, their separation is given by

$$\dot{\mathbf{r}}_{12} = a(t) (\mathbf{x}_1 - \mathbf{x}_2).$$

It follows that

$$\dot{\mathbf{r}}_{12} = H \mathbf{r}_{12}, \quad (3.10)$$

where $H = \dot{a}/a$ is the Hubble parameter, and a dot represents the derivative with respect to the cosmic time. The further the observers are from each other, the greater is their relative velocity. This is what is usually called the Hubble law. Since the physical distance \mathbf{r} is related to the comoving distance \mathbf{x} with the relation $\dot{\mathbf{r}} = a(t)\dot{\mathbf{x}}$, we deduce that

$$\dot{\mathbf{r}} = H \mathbf{r} + a(t)\dot{\mathbf{x}} \equiv \mathbf{v}_{rec} + \mathbf{v}_{proper}. \quad (3.11)$$

The recession velocity, \mathbf{v}_{rec} , is a time-dependent quantity and represents the component of the velocity related to the Hubble flow. As for \mathbf{v}_{proper} , it is the proper velocity of the object with respect to the cosmological reference frame privileged by the expansion.

The Cosmic Redshift

In special relativity light rays move along lines of constant proper time, $ds^2 = 0$. This implies

$$\frac{\sqrt{dx^2 + dy^2 + dz^2}}{dt} = \pm c \quad (3.12)$$

which describes motion at the speed of light. Since it is always possible locally, at a given time, to find a reference frame where the metric reduces to that of flat space, we can carry this over to general relativity. $ds^2 = 0$ is valid in all reference frames for a light ray, because ds^2 is a scalar and it is the same in any reference frame.

We consider light rays emitted from a point P and moving towards us at the origin O . The first peak of the wave is emitted at a cosmic time t_e , and the second at an infinitesimally later time $t_e + \delta t_e$. We receive them at times t_0 and $t_0 + \delta t_0$, respectively. The light wave travels along a line of constant θ and ϕ and follows a path defined by $ds^2 = 0$. Inserting this in the FRW line element gives

$$ds^2 = 0 = dt^2 - a^2(t) \frac{dr^2}{1 - kr^2}, \quad (3.13)$$

and since $dr < 0$ for $dt > 0$ we have

$$\frac{dt}{a(t)} = -\frac{dr}{\sqrt{1 - kr^2}}, \quad (3.14)$$

For the first peak we then have

$$\int_{t_e}^{t_o} \frac{dt}{a(t)} = - \int_r^0 \frac{dr}{\sqrt{1 - kr^2}} = \int_0^r \frac{dr}{\sqrt{1 - kr^2}},$$

and for the second peak we have

$$\int_{t_e + \delta t_e}^{t_o + \delta t_o} \frac{dt}{a(t)} = \int_0^r \frac{dr}{\sqrt{1 - Kr^2}}.$$

Thus

$$\int_{t_e}^{t_o} \frac{dt}{a(t)} = \int_{t_e + \delta t_e}^{t_o + \delta t_o} \frac{cdt}{a(t)}.$$

We can rewrite the integrals on each side as

$$\int_{t_e}^{t_e + \delta t_e} \frac{dt}{a(t)} + \int_{t_e + \delta t_e}^{t_o} \frac{dt}{a(t)} = \int_{t_e + \delta t_e}^{t_o} \frac{dt}{a(t)} + \int_{t_o}^{t_o + \delta t_o} \frac{dt}{a(t)},$$

and hence

$$\int_{t_e}^{t_e + \delta t_e} \frac{dt}{a(t)} = \int_{t_o}^{t_o + \delta t_o} \frac{dt}{a(t)}.$$

We can take the integrand to be constant, because both integrals are taken over an infinitesimally short time. We obtain

$$\frac{\delta t_e}{a(t_e)} = \frac{\delta t_o}{a(t_o)}.$$

This implies that

$$\delta t_e = \frac{a(t_e)}{a(t_o)} \delta t_o < \delta t_o.$$

This means that pulses received with a separation in time δt_o were emitted with a shorter separation in time δt_e by the object. Since $c\delta t_e = \lambda_e$ and $\delta t_o = \lambda_o$, we can rewrite the relation above as

$$\frac{\lambda_o}{\lambda_e} = \frac{a(t_o)}{a(t_e)}.$$

This means that since the universe is expanding, the wavelength of a light wave that we receive will be longer than at the time of emission by a factor equal to the ratio of the scale factors of the universe at the two times. The cosmic redshift is defined by

$$1 + z = \frac{\lambda_o}{\lambda_e} = \frac{a(t_o)}{a(t_e)}, \quad (3.15)$$

and measures how much the universe has expanded between the times of emission and reception of the light signal.

3.1.4 Friedmann and Continuity Equations

To investigate the dynamics of Friedmann-Lemaître space-times, we must obtain the equations of the motion deriving from the Einstein equation. From Chapter 2 we know that the energy-momentum tensor for a perfect fluid is given by

$$T_{\mu\nu} = (\rho + p) u_\mu u_\nu + p g_{\mu\nu} \quad (3.16)$$

where ρ and p are the energy density and the pressure, respectively. Using the expressions for the Einstein tensor and the energy-momentum tensor, we can easily deduce that the two Einstein equations reduce to two independent equations

$$H^2 = \frac{\kappa}{3}\rho - \frac{k}{a^2} + \frac{\Lambda}{3}, \quad (3.17)$$

$$\frac{\ddot{a}}{a} = -\frac{\kappa}{6}(\rho + 3p) + \frac{\Lambda}{3}, \quad (3.18)$$

recalling that $\kappa \equiv 8\pi G_N$. As for the matter conservation equation $(\nabla_\mu T^{\mu\nu})$, it reduces to a single equation

$$\dot{\rho} + 3H(\rho + p) = 0. \quad (3.19)$$

We can see that these three equations (3.17), (3.18) and (3.19) are not independent. Differentiating (3.17) with respect to time and expressing \ddot{a}/a using (3.18) and (3.17) to eliminate H^2 , we find (3.19). This is a consequence of the Bianchi identities.

Equations in Conformal Time

It will sometimes be convenient to work in terms of the conformal time. Remembering that $dt = a d\eta$, we find that the derivative of any quantity X with respect to η , X' , is related to that with respect to t by $X' = a\dot{X}$. It will be convenient to remember that

$$X' = a\dot{X}, \quad X'' - \mathcal{H}X' = a^2\ddot{X}.$$

The comoving Hubble parameter is given by $\mathcal{H} = a'/a$, which satisfies

$$\mathcal{H} = aH, \quad a\ddot{a} = \frac{a''}{a} - \mathcal{H}^2 \quad a^2\dot{H} = \mathcal{H}' - \mathcal{H}^2.$$

We deduce that the Friedmann and conservation equations take the form

$$\mathcal{H}^2 = \frac{\kappa}{3}\rho a^2 - k + \frac{\Lambda}{3}a^2, \quad (3.20)$$

$$\mathcal{H}' = -\frac{\kappa}{6}a^2(\rho + 3p) + \frac{\Lambda}{3}a^2, \quad (3.21)$$

$$\rho' + 3\mathcal{H}(\rho + p) = 0. \quad (3.22)$$

We also notice that if the scale factor is a power law in cosmic time, then

$$a(t) \propto t^n \quad \Leftrightarrow \quad a(\eta) \propto \eta^{\frac{n}{1-n}}, \quad (3.23)$$

as long as $n \neq 1$.

The Spatial Curvature Parameter and Equation of State

From the Friedmann equations we can see that there are four unknowns: the scale factor a , the spatial curvature parameter k , the energy density ρ , and the pressure p . Since only two of the Friedmann equations are independent, we have only two equations for four unknowns. We can determine the spatial curvature parameter in the following way: we rewrite equation (3.17) as

$$k = \frac{8\pi G}{3}\rho(t)a^2(t) - \dot{a}^2(t),$$

which is a the differential equation. In order to solve this equation we must have some boundary or initial conditions. We choose to impose these boundary conditions at the present time, which we will denote by t_0 . The present value of the Hubble parameter is given by $H_0 = H(t_0) = \dot{a}(t_0)/a(t_0)$, and if we furthermore define $\rho(t_0) \equiv \rho_0$, we can therefore write

$$\frac{k}{a_0^2} = \frac{8\pi G}{3}\rho_0 - H_0^2.$$

We thus see that if we specify initial conditions by choosing values for H_0 and ρ_0 , e.g. by using measurements of them, then the spatial curvature is determined for all times. However, there still remains three unknown functions $a(t)$, $\rho(t)$, and $p(t)$, and we have only two independent equations for them. We therefore need some additional information to solve Friedmann equations. For that, it is common to give an *equation of state*, that is, a relation between pressure p and energy density ρ as

$$p = w\rho \quad (3.24)$$

where w is a constant. For instance, dust will be described by $w = 0$ whereas for radiation we will have $w = 1/3$. For the cosmological constant, which corresponds to a constant energy density, (3.19) implies $p = -\rho$ and thus $w = -1$. Inserting (3.24) in equation (3.19), we can rewriting equation (3.19) as

$$\frac{d\rho}{(1+w)\rho} = -3\frac{da}{a} \quad (3.25)$$

Integration of equation (3.26) gives

$$\rho \propto a^{-3(1+w)}. \quad (3.26)$$

For the case of dust, $w = 0$, this gives

$$\rho \propto a^{-3}. \quad (3.27)$$

The energy density decreases inversely proportional to the volume. For radiation, $w = 1/3$, we obtain

$$\rho \propto a^{-4}. \quad (3.28)$$

Comparing the general result (3.26) with equations (3.17) and (3.18), we can see that the curvature term can be assimilated with a fluid with equation of state $w = -1/3$.

Reduced Form

It is useful to rewrite the Friedmann equations in a dimensionless form in terms of reduced quantities. For that, we introduce the energy density parameters

$$\Omega = \frac{\kappa\rho}{3H^2}, \quad \Omega_\Lambda = \frac{\Lambda}{3H^2}, \quad \Omega_k = \frac{k}{3H^2}, \quad (3.29)$$

respectively, for the matter, cosmological constant and the curvature. The matter term can be decomposed as a sum of components with different equations of state as $\Omega = \sum_X \Omega_X$ with

$$\Omega_X = \frac{\kappa\rho_X}{3H^2}, \quad (3.30)$$

and we will denote by Ω_{X0} its value today. The first Friedmann equation (3.17) then takes the form of a constant

$$\sum_X \Omega_X + \Omega_\Lambda + \Omega_k = 1. \quad (3.31)$$

Using the solutions of the conservation equation, it follows that

$$\Omega_X = \Omega_{X0} \left(\frac{a}{a_0} \right)^{-3(1+w_{X0})} \left(\frac{H_0}{H} \right)^2, \quad (3.32)$$

for a constant equation of state $w_X = w_{X0}$, so that $E(a) \equiv H/H_0$ can be expressed

$$E^2(a) \equiv (H/H_0^2) = \sum_X \Omega_{X0} \left(\frac{a}{a_0} \right)^{-3(1+w_X)} + \Omega_{k0} \left(\frac{a}{a_0} \right)^{-2} + \Omega_{\Lambda 0}. \quad (3.33)$$

Quantities with an index 0 are evaluated today. Thus, t_0 will be the dynamical age of the universe and $a_0 = a_0(t)$. Notice that E only depends on the redshift $x = (1+z) = a_0/a$. For the matter, the following different components can be distinguished

$$\Omega = \Omega_m + \Omega_r + \Omega_\Lambda, \quad \Omega_m = \Omega_b + \Omega_c \quad \Omega_r = \Omega_\gamma + \Omega_\nu$$

where the total matter component is decomposed into matter and radiation and then, respectively, into baryons (b), cold dark matter (c), photons (γ) and neutrinos (ν).

3.2 Dynamics of Friedmann-Lemaître Space-Time

3.2.1 Solutions

Using the Friedmann equation (3.17), the evolution law for the scale factor can be determined as a function of time for some simple cases.

$k = 0$ **and** $w \neq -1$

As seen earlier, if $w \neq -1$, the conservation implies that $\rho \propto a^{-3(1+w)}$, so that the Friedmann equation (3.17) implies $H^2 \propto a^{-3(1+w)}$. It follows that $\dot{a} \propto a^{-3(1+w)/2}$. By integrating this relation, we obtain,

$$a(t) \propto t^{\frac{2}{3(1+w)}}. \quad (3.34)$$

From this expression, the conformal time can be computed by integrating $d\eta = dt/a(t)$, given $\eta \propto t^{\frac{1+3w}{3(1+w)}}$ if $w \neq -1/3$. We deduce that

$$a(\eta) \propto \eta^{\frac{2}{1+3w}} \quad \text{if} \quad w \neq -\frac{1}{3}, \quad (3.35)$$

and $a(\eta) \propto e^\eta$ otherwise.

$k = 0$ **and** $w = -1$

If the matter density is dominated by a cosmological constant, we have $H^2 \propto \rho \propto a^0$, so that $\dot{a} \propto a$. By integrating this relation, we get,

$$a(t) \propto e^{Ht}. \quad (3.36)$$

This space has an accelerated expansion and is called de Sitter space. In terms of the conformal time, the scale factor is of the form

$$a(\eta) \propto -\frac{1}{H\eta} \quad \eta < 0. \quad (3.37)$$

This space can also be written in such a way that it has spherical spatial sections

$$ds^2 = -dt^2 + \frac{\cosh^2(Ht)}{H^2} (d\chi^2 + \sin^2 \chi d\Omega^2). \quad (3.38)$$

$k = \pm 1$ **and** $w \neq -1/3$

It is more convenient to work in conformal time to obtain $a(t)$ in the parametric form $\{a(\eta), t(\eta)\}$. Using $\rho = \rho_0(a/a_0)^{-3(1+w)}$ and (3.17), we get

$$\mathcal{H}^2 = \frac{\Omega_0}{|1 - \Omega_0|} (a/a_0)^{-3(1+w)} - k, \quad (3.39)$$

in units such that $|k| = 1$. This equation can be integrated to give

$$\left(\frac{a}{a_0}\right) = \left(\frac{\Omega_0}{|1 - \Omega_0|}\right)^{1/2\alpha} \begin{cases} (\sinh \alpha \eta)^{1/\alpha} & \text{if } k = -1, \\ (\sin \alpha \eta)^{1/\alpha} & \text{if } k = +1, \end{cases} \quad (3.40)$$

with $2\alpha = 1 + 3w$. This solution valid for all constant $w \neq -1/3$. The case $w = -1/3$ corresponds to a universe with no matter since matter can then be absorbed into the curvature term.

$k = 0$, $w = 0$ **and** $\Lambda \neq 0$

Let us mention the solution for a spatially Euclidean model dominated by a pressure less fluid and a cosmological constant

$$a(t) = \left(\frac{1}{\Omega_{\Lambda_0}} - 1\right)^{1/3} \sinh^{2/3} \left(\frac{3\alpha t}{2}\right), \quad (3.41)$$

where we $\alpha = H_0 \sqrt{\Omega_{\Lambda_0}}$. This solution is relevant for describing the late time evolution of a flat Λ CDM model.

Another interesting solution is the one obtained for an empty Universe with hyperbolic spatial section ($k = -1$). This space, called the Milne space, has following metric

$$ds^2 = -dt^2 + t^2 (d\chi^2 + \sin^2 \chi d\Omega^2). \quad (3.42)$$

It can be shown that this metric corresponds to a Minkowski metric by an approximate change of coordinates ($T = t \cosh \chi$, $R = t \sinh \chi$ leads to the Minkowski metric in spherical coordinates), but this space only covers a quarter of the Minkowski space-time.

3.2.2 Dynamical Evolution

In order to study the general dynamics of the solutions of the Friedmann equations, it is interesting to rewrite the system (3.17) and (3.18) in the form of a dynamical system for quantities Ω , Ω_Λ and Ω_k (see ref. [8]). Using $\dot{H} = \ddot{a}/a - H^2$ and expressing \ddot{a}/a with (3.18) and H^2 with (3.17) leads to

$$\frac{\dot{H}}{H^2} = -(1 + q), \quad (3.43)$$

q is the deceleration parameter defined by

$$2q \equiv (3\gamma - 2)(1 - \Omega_k) - 3\gamma\Omega_\Lambda, \quad (3.44)$$

with $\gamma \equiv w + 1$. The system of Friedmann equations can thus be rewritten using the new time variable $u \equiv \ln(a/a_0)$. The derivative, X' , with respect to u of any quantity X is then given by $X' = \dot{X}/H$. The evolution equation for the Hubble parameter (3.43) then becomes

$$H' = -(1 + q)H. \quad (3.45)$$

If we differentiate Ω, Ω_Λ and Ω_k with respect to u and use (3.45) to express H' , noticing that $a' = a$ and that (3.22) can be used to obtain $\rho' = -3\gamma\rho$, we then obtain the system

$$\Omega' = (2q + 2 - 3\gamma)\Omega, \quad (3.46)$$

$$\Omega'_\Lambda = 2(1 + q)\Omega_\Lambda, \quad (3.47)$$

$$\Omega'_k = 2q\Omega_k. \quad (3.48)$$

It is useless to keep all of these equations since (i) H does not enter in (3.46)-(3.48) and (ii) Ω can be deduced algebraically using (3.31). The dynamics of Friedmann-Lemaître space-time can thus be studied by considering the dynamical system

$$\begin{cases} \Omega'_\Lambda &= 2(1 + q)\Omega_\Lambda, \\ \Omega'_K &= 2q\Omega_K, \end{cases} \quad (3.49)$$

where q is a function of Ω_Λ and Ω_K given by (3.44).

3.2.3 Expansion and Contraction

When the total density vanishes, the expansion rate of the universe can change sign. For a universe with non-flat spatial sections and with matter, radiation and a cosmological constant, there are four possibilities

- The expansion lasts eternally starting from the Big Bang. This is the case if $k = 0$ or -1 for a universe without cosmological constant.
- The expansion is followed by a contracting phase leading to a big crunch. This is the case for a universe with $k = +1$ with no cosmological constant.
- The expansion lasts eternally but was preceded by a contracting phase; there must therefore have been a *bounce*. This situation can occur when the universe has spherical spatial sections ($k = +1$).
- The universe undergoes a series of contraction and expansion phases; this is an oscillating universe.

The separation between a universe with infinite expansion and a Universe with a big crunch is obtained when

$$\begin{aligned} \Omega_{m0} &\leq 1, & \Omega_{\Lambda 0} &= 0, \\ \text{or} \\ \Omega_{m0} &\geq 1, & \Omega_{\Lambda 0} &= 1 - \Omega_{m0} + \frac{2}{3} \cos [\arctan (\Xi_{m0}^{-1}) - \pi]. \end{aligned} \quad (3.50)$$

with $\Xi_{m0} = \sqrt{|2\Omega_{m0} - 1|}$. The separation between a universe with infinite expansion and a bouncing universe is obtained when

$$\begin{aligned} \Omega_{m0} &= 0, & \Omega_{\Lambda 0} &\leq 0, \\ \text{or} \\ 0 &\leq \Omega_{m0} \leq \frac{1}{2}, & \Omega_{\Lambda 0} &= 1 - \Omega_{m0} + \frac{3}{2(\Omega_{m0})^{1/3}} \left[(1 - \Omega_{m0} + \Xi_{m0})^{1/3} + (1 - \Omega_{m0} - \Xi_{m0})^{1/3} \right], \\ \text{or} \\ \Omega_{m0} &\geq \frac{1}{2}, & \Omega_{\Lambda 0} &= 1 - \Omega_{m0} + \frac{2}{3} \cos [\arctan (\Xi_{m0}^{-1}) + \pi]. \end{aligned} \quad (3.51)$$

3.3 Time and Distances

The characteristic distance and time scales of any Friedmann-Lemaître Universe is fixed by the value of the Hubble constant. We define the Hubble time and distance by

$$t_H = \frac{1}{H}, \quad D_H = \frac{c}{H}. \quad (3.52)$$

The order of magnitude of these quantities is obtained by expressing the current value of the Hubble parameter in following way

$$H_0 = 100 h \text{ km} \cdot \text{s}^{-1} \cdot \text{Mpc}^{-1}, \quad (3.53)$$

with h typically of the order of 0.7. We obtain that

$$t_{H_0} = 9.78 h^{-1} \times 10^9 \text{ years}, \quad D_{H_0} = 9.26 h^{-1} \times 10^{25} \text{ m}. \quad (3.54)$$

3.3.1 Age of the Universe

From the definition of the Hubble parameter, it follows that $dt = da/aH$. Thus, the expression (3.33) for the Hubble constant gives

$$dt = t_{H_0} \frac{da}{aE(a)}.$$

The age of the universe is thus obtained by integrating this equality between $a = 0$ and $a = a_0$, or equivalently between $z = 0$ and $z = \infty$,

$$t_0 = t_{H_0} \int_0^1 \frac{dx}{xE(x)} = t_{H_0} \int_0^\infty \frac{dz}{(1+z)E(z)}. \quad (3.55)$$

The analogous expression in conformal time is

$$\eta_0 = t_{H_0} \int_0^1 \frac{dx}{x^2 E(x)}. \quad (3.56)$$

In a similar way, the age of the Universe at the time when a photon with redshift z_* was emitted is defined by

$$t(z_*) = t_{H_0} \int_{z_*}^\infty \frac{dz}{(1+z)E(z)}. \quad (3.57)$$

3.3.2 Proper Distance

The proper distance is the length of the spatial geodesic (shortest path in space) between two points at a specified time t , so that the scale factor describing the expansion of the universe is held fixed at $a(t)$. It is denoted by $dp(t)$, and can be obtained as follows. We place one point at the origin $(0, 0, 0)$ and let the other point have coordinates (r, θ, ϕ) . Along the spatial geodesic between the two points, only the coordinate r varies. The time t is fixed so the FRW metric gives for an infinitesimal displacement along the geodesic

$$|ds| = a(t) \frac{dr}{\sqrt{1 - kr^2}}. \quad (3.58)$$

The proper distance is found by summing up all contributions along the geodesic, hence

$$d_p(t) = a(t) \int_0^r \frac{dr}{\sqrt{1 - kr^2}} = a(t) \delta^{-1}(r), \quad (3.59)$$

where $\delta^{-1}(r) = \sin^{-1} r$ for $k = +1$, $\delta^{-1}(r) = r$ for $k = 0$ and $\delta^{-1}(r) = \sinh^{-1} r$ for $k = -1$. We can see for the spatially flat case, $k = 0$, the proper distance is $d_p(t) = a(t)r$, which means that the proper distance is the comoving coordinate r of the point, which is a constant in time, times the scale factor which describes how much the universe has expanded since a given reference time.

3.3.3 Comoving Radial Distance

In order to find the radial comoving distance we consider a light ray propagating from a source towards an observer at the origin. The light ray travels at constant θ and ϕ along a null geodesic $ds^2 = 0$. Using this information, the FRW metric gives

$$\begin{aligned} 0 &= dt^2 - \frac{a^2(t)dr^2}{1 - kr^2} \\ \Rightarrow \frac{dr}{\sqrt{1 - Kr^2}} &= -\frac{dt}{a(t)} \end{aligned} \quad (3.60)$$

where the $-$ sign is chosen because r decreases ($dr < 0$) as time increases ($dt > 0$) along the path of the light ray. Integrating equation (3.60) we obtain

$$\delta_k^{-1} \equiv \int_0^r \frac{dr}{\sqrt{1 - kr^2}} = \int_t^{t_0} \frac{dt}{a(t)}, \quad (3.61)$$

where δ_K^{-1} is the inverse of the function δ_K , which is equal to $\sin r$ for $k = +1$, r for $k = 0$ and $\sinh r$ for $k = -1$. Therefore, the comoving radial distance take the form

$$r = \delta_k \left[\int_t^{t_0} \frac{dt}{a(t)} \right]. \quad (3.62)$$

3.4 Horizons

An horizon is a frontier that separates observable events from non-observable ones. In cosmology to different horizons have to be distinguished; event horizon and particle horizon. The event horizon answers the question: if distant source emits a light ray in our direction now, will

it reach us at some point in the future no matter how far away this source is? The particle horizon answers a different question: Is there a limit to how distant a source, which we have received, or are receiving, light from by now, can be? Thus, the event horizon is related to events observable in our future, whereas the particle horizon is related to events observable at present and in our past. Here we cite Rindler's definitions of the two horizons [9]:

- Event horizon: for a given fundamental observer A , this is a hypersurface in spacetime which divides all events into two non-empty classes: those that have been, are, or will be observable by A , and those that are forever outside A 's possible powers of observation.
- Particle horizon: for a given fundamental observer A and cosmic time t_0 , this is a surface in the instantaneous 3-space $t = t_0$ which divides all events into two non-empty classes: those that have already been observable by A at time t_0 and those that have not.

3.4.1 Event Horizon

Here, we want to find if a light ray emitted by a source at r_1 at time t_1 ever will reach an observer at origin. The condition for existence of an event horizon is that the integral

$$\int_{t_1}^{\infty} \frac{cdt}{a(t)}, \quad (3.63)$$

is convergent. If this integral converges to a finite value, there is a maximum value r_{EH} of r_1 such that for $r_1 > r_{EH}$ light emitted from r_1 at t_1 will never reach the origin. We see that this value of r is determined by

$$\delta^{-1}(r_{EH}) = \int_{t_1}^{\infty} \frac{cdt}{a(t)}, \quad (3.64)$$

so that the light ray emitted towards the origin at time t_1 reaches the origin in the infinite future. Light rays emitted at the same time from sources with $\delta^{-1}(r) > \delta^{-1}(r_{EH})$ will never reach the origin. The time t_1 is arbitrary, so we can replace it by t to make it clear that the event horizon is in general a time-dependent quantity. The proper distance to the event horizon is given by

$$d_p^{EH} = a(t) \int_{t_1}^{\infty} \frac{cdt}{a(t)}, \quad (3.65)$$

3.4.2 Particle Horizon

The event horizon concerns events observable in the future, whereas the particle horizon is related to events which have been, or are being, observed by a given time t . Again, we consider a source at comoving radial coordinate r_1 which emits a light signal at time t_1 . We want to know whether there is a limit to which light rays can have reached the origin by the time t . To maximize the chance of the light reaching the origin, we consider a light ray emitted at the earliest possible moment, which normally means taking $t_1 = 0$ (but in the case of the de Sitter model, where there is no Big Bang, we have to take $t_1 = -\infty$). Since $a(t) \rightarrow 0$ as $t \rightarrow 0$, there is a possibility that the integral on the right hand side diverges. However, in the case where the integral does converge to a finite value, there will be points r_1 so that

$$\delta^{-1}(r_1) > \int_0^t \frac{cdt}{a(t)}, \quad (3.66)$$

and a light ray emitted from r_1 at $t = 0$ will then not yet have reached the origin by time t . We then say that there exist a particle horizon with comoving radial coordinate at time t determined by

$$\delta^{-1}(r_{PH}) = \int_0^t \frac{cdt}{a(t)}, \quad (3.67)$$

and the proper distance of this point from the origin is

$$d_p^{PH} = a(t) \int_0^t \frac{cdt}{a(t)}. \quad (3.68)$$

Chapter 4

Statefinder Formalism

In this chapter, we will first give the definitions of the statefinder parameters. We will express this parameter both in terms of the Hubble parameter and its derivatives with respect to cosmic time, and in terms of the redshift, z . We will then go through some earlier applications of the statefinder diagnostics. At the end of this chapter, we will apply this formalism to a new coupled quintessence cosmological model.

With the statefinder method one introduces parameters depending on higher-order derivatives of the scale factor and generalizing the deceleration parameter. We can expand the scale factor around its value today as

$$a(t) = a_0 \left[1 + H_0(t - t_0) - \frac{1}{2}q_0 H_0^2(t - t_0)^2 + \frac{1}{6}r_0 H_0^3(t - t_0)^3 - \dots \right], \quad (4.1)$$

Based on Taylor expansion of the scale factor, eq. (4.1), the statefinder pair $\{r, s\}$, for flat universe models, are defined as

$$r \equiv \frac{\ddot{a}}{aH^3}, \quad (4.2)$$

$$s \equiv \frac{r - 1}{3(q - 1/2)}. \quad (4.3)$$

The deceleration parameter is defined as

$$q = -\frac{\ddot{a}}{aH^2} \quad (4.4)$$

Using the definition of Hubble parameter, $H = \frac{\dot{a}}{a}$, the second and third derivatives of scalar factor is given by

$$\dot{a} = aH, \quad \ddot{a} = \dot{a}H + a\dot{H}, \quad \dddot{a} = \ddot{a}H + 2\dot{a}\dot{H} + a\ddot{H} \quad (4.5)$$

We use these expressions to express the deceleration parameter and the statefinder parameters in terms of Hubble parameter and its derivatives with respect to cosmic time. We obtain

$$q = -1 - \frac{\dot{H}}{H^2}, \quad (4.6)$$

$$r = 1 + 3\frac{\dot{H}}{H^2} + \frac{\ddot{H}}{H^3}, \quad (4.7)$$

$$s = -\frac{2}{3H} \frac{3H\dot{H} + \ddot{H}}{3H^2 + 2\dot{H}}. \quad (4.8)$$

By changing coordinates from time to redshift, $x \equiv 1 + z = \frac{1}{a}$, we have

$$\dot{x} = \frac{dx}{dt} = \frac{da}{dt} \frac{dx}{da} = \dot{a} \left(-\frac{1}{a^2} \right) = -Hx, \quad (4.9)$$

Now taking the derivatives of the Hubble parameter with respect to x we get

$$\dot{H} = \frac{dH}{dt} = \frac{dx}{dt} \frac{dH}{dx} = -HH'x, \quad \ddot{H} = \frac{d}{dt}(-HH'x) = -\dot{x}(HH' + xH'^2 + xHH'') \quad (4.10)$$

With these expressions we can now express the deceleration parameter and the statefinder parameters in terms of x as

$$q = \frac{H'}{H}x - 1, \quad (4.11)$$

$$r = 1 - 2\frac{H'}{H}x + \left[\frac{H''}{H} + \left(\frac{H'}{H} \right)^2 \right] x^2, \quad (4.12)$$

$$s = \frac{-2\frac{H'}{H}x + \left[\frac{H''}{H} + \left(\frac{H'}{H} \right)^2 \right] x^2}{3 \left[\frac{H'}{H}x - \frac{3}{2} \right]}. \quad (4.13)$$

These expressions show that the statefinder parameters are only dependent on the space-time metric, regardless what cosmological model we consider.

4.1 Earlier Applications of the Statefinder Formalism

4.1.1 The Friedmann Universe

Friedmann's equation's for a universe model with curvature ($k \neq 0$) are given by

$$\left(\frac{\dot{a}}{a} \right)^2 + \frac{k}{a^2} = \frac{8\pi G}{3} \sum_i \rho_i, \quad (4.14)$$

$$\frac{\ddot{a}}{a} = -\frac{4\pi G}{3} \left(\sum_i \rho_i + 3 \sum_i p_i \right), \quad (4.15)$$

where $p_i = w_i \rho_i$. The continuity equation takes the form

$$\dot{\rho} = -3\frac{\dot{a}}{a} \left(\sum_i \rho_i + \sum_i p_i \right). \quad (4.16)$$

From chapter three we stated the definition of critical density, $\rho_{cr} \equiv \frac{3H^2}{8\pi G}$, and the definition of density parameter, $\Omega_i \equiv \frac{\rho_i}{\rho_{cr}}$. By using these definitions and the equations (eqs. 4.14-4.16) we get that

$$\begin{aligned} q = -\frac{\ddot{a}}{aH^2} &= \frac{4\pi G}{3H^2} \left(\sum_i \rho_i + 3 \sum_i p_i \right) \\ &= \frac{1}{2} \sum_i \frac{\rho_i}{\rho_{cr}} + \frac{3}{2} \sum_i w_i \frac{\rho_i}{\rho_{cr}} \\ &= \frac{1}{2} \left(\sum_i \Omega_i + 3 \sum_i w_i \Omega_i \right) \\ &= \frac{1}{2} \left(\Omega + 3 \sum_i w_i \Omega_i \right), \end{aligned} \quad (4.17)$$

where $\Omega \equiv \sum_i \Omega_i = 1 - \Omega_k$. Taking the derivative of Friedmann's second equation (4.15)

$$\begin{aligned} \frac{\ddot{a}a - \dot{a}\dot{a}}{a^2} &= -\frac{4\pi G}{3} \left(\sum_i \dot{\rho}_i + 3 \sum_i \dot{p}_i \right) \\ &= -\frac{4\pi G}{3} \left(\sum_i \dot{\rho}_i + 3 \sum_i (\dot{w}_i \rho_i + w_i \dot{\rho}_i) \right), \end{aligned} \quad (4.18)$$

and using the result above we can find the expression for the statefinder parameter r .

$$r = \frac{\ddot{a}}{aH^3} = \Omega + \frac{9}{2} \sum_i (w_i + w_i^2) \Omega_i - \frac{3}{2H} \sum_i \dot{w}_i \Omega_i. \quad (4.19)$$

The statefinder formalism was generalized to curved universe models by Evans et. Al [13]. In this generalization the statefinder parameter s is given by

$$s = \frac{r - \Omega}{3(q - \Omega/2)}. \quad (4.20)$$

We can see that this expression reduces to (4.3), for a flat universe model. This generalization gives us the following expression for s

$$s = 1 + \frac{\sum_i w_i^2 \Omega_i}{\sum_i w_i \Omega_i} - \frac{1}{3H} \frac{\sum_i \dot{w}_i \Omega_i}{\sum_i w_i \Omega_i}. \quad (4.21)$$

Going back to a flat universe model ($k = 0$) the deceleration parameter and statefinder parameters are given by

$$q = \frac{1}{2} \left(1 + 3 \sum_i w_i \Omega_i \right), \quad (4.22)$$

$$r = 1 + \frac{9}{2} \sum_i (w_i + w_i^2) \Omega_i - \frac{3}{2H} \sum_i \dot{w}_i \Omega_i, \quad (4.23)$$

$$s = 1 + \frac{\sum_i w_i^2 \Omega_i}{\sum_i w_i \Omega_i} - \frac{1}{3H} \frac{\sum_i \dot{w}_i \Omega_i}{\sum_i w_i \Omega_i}. \quad (4.24)$$

If we consider a flat universe model with cold matter (dust, ρ_m) and dark energy (ρ_X) obeying the equation of state

$$p_X = w\rho_X, \quad p_m = 0 \quad (4.25)$$

where p_X is the pressure of the dark energy and ρ_X its density, and w is a function of time, we can express the deceleration parameter using equation (4.17) as

$$q = \frac{1}{2} [\Omega_m + (1 + 3w)\Omega_x]. \quad (4.26)$$

From equation (4.19) we find that the statefinder parameter r is

$$r = \Omega_m + \left[1 + \frac{9}{2} (w + w^2) \right] \Omega_x - \frac{3}{2H} \dot{w} \Omega_x, \quad (4.27)$$

and from equation (4.21) we find that the statefinder parameter s is

$$s = 1 + w - \frac{1}{3H} \frac{\dot{w}}{w}. \quad (4.28)$$

Although r and s are not independent, r depends on Ω_X , w and \dot{w} , whereas s only depends on w and \dot{w} . By increasing the number of cosmological parameters evaluated today to three (H_0, q_0, r_0) , or equivalently (H_0, q_0, s_0) , we can hope to better constrain the recent history of the Universe.

We can now give an expression for the present value of the time derivative of the equation of state parameter w in terms of the statefinder parameter r_0 . First we make a Taylor expansion of w to first order in z ,

$$w(z) = w_0 - \frac{\dot{w}(t_0)}{H_0} z. \quad (4.29)$$

Using equation (4.26) we find

$$w_0 = \frac{2q_0\Omega_{m0} - \Omega_{x0}}{3\Omega_{x0}}, \quad (4.30)$$

and from equation (4.27) we obtain

$$\dot{w}(t_0) = \frac{2}{3} \frac{H_0}{\Omega_{x0}} \left[\Omega_{m0} + \left(1 + \frac{9}{2} w_0 (1 + w_0) \right) \Omega_{x0} - r_0 \right]. \quad (4.31)$$

Hence

$$w(z) \approx w_0 - \frac{2}{3} \left[1 + \frac{9}{2} w_0 (1 + w_0) + \frac{\Omega_{m0} - r_0}{\Omega_{x0}} \right] z. \quad (4.32)$$

By testing this expression against the observational data we may possibly determine the present value of statefinder parameter r_0 .

4.1.2 The Flat Λ CDM Model

The flat Λ CDM model, also known as the "standard model of cosmology", is a universe model dominated by dust, mostly in the form of so-called cold dark matter with the acronym CDM, and a positive cosmological constant. This model is in perfect agreement with astronomical observations. More specifically, the observations seem to prefer a flat model with $\Omega_{m0} \approx 0.3$ and $\Omega_{\Lambda 0} = 1 - \Omega_{m0} \approx 0.7$. The Λ CDM model has $w = -1$ and therefore $\dot{w} = 0$. Using this in equations (4.22)-(4.24), we find that the Λ CDM model corresponds to the fixed point $(r_0, s_0) = (1, 0)$.

4.1.3 The Chaplygin Gas

The Chaplygin gas model ([31]; [32]) is a model for dark energy fluid that does not have an equation of state of the form $p = w\rho$. We will now express deceleration parameter and statefinder parameters in terms of pressure p and density ρ , by using Friedmann's equations (4.14-4.16) and eqs. (4.17), (4.19), and (4.20) and we obtain

$$q = \frac{1}{2} \left(1 + 3 \frac{p}{\rho} \right) \Omega, \quad (4.33)$$

$$r = \left(1 - \frac{3}{2} \frac{\dot{p}}{H\rho} \right) \Omega, \quad (4.34)$$

$$s = -\frac{1}{3H} \frac{\dot{p}}{p}. \quad (4.35)$$

For a flat ($k = 0$) universe model these equations reduces to the following form

$$q = \frac{1}{2} \left(1 + 3 \frac{p}{\rho} \right), \quad (4.36)$$

$$r = 1 + \frac{9}{2} \frac{\rho + p}{\rho} \frac{\dot{p}}{\dot{\rho}}, \quad (4.37)$$

$$s = \frac{\rho + p}{p} \frac{\dot{p}}{\dot{\rho}}. \quad (4.38)$$

We assume that the universe contains only dark energy with an equation of state $p = p(\rho)$, then

$$\dot{p} = \dot{\rho} \frac{\partial p}{\partial \rho} = -3H(\rho + p) \frac{\partial p}{\partial \rho}. \quad (4.39)$$

Inserting this equation into (4.34) and (4.35), we obtain

$$r = \left[1 + \frac{9}{2} \left(1 + \frac{p}{\rho} \right) \frac{\partial p}{\partial \rho} \right] \Omega, \quad (4.40)$$

$$s = \left(1 + \frac{\rho}{p} \right) \frac{\partial p}{\partial \rho}. \quad (4.41)$$

If we instead assume that the universe contains cold matter and dark energy the expressions for the statefinder parameters are generalized to

$$r = \left[1 + \frac{9}{2} \frac{\rho_x + p_x}{\rho_m + \rho_x} \frac{\partial p_x}{\partial \rho_x} \right] \Omega, \quad (4.42)$$

$$s = \left(1 + \frac{\rho_x}{p_x} \right) \frac{\partial p_x}{\partial \rho_x}. \quad (4.43)$$

For the Chaplygin gas the equation of state is given by

$$p_C = -\frac{A}{\rho_C^\alpha}, \quad (4.44)$$

where A and α are positive constants. Energy conservation equation (4.16) is then given by

$$\dot{\rho} = -3 \frac{\dot{a}}{a} \left(\rho - \frac{A}{\rho_C^\alpha} \right). \quad (4.45)$$

Integrating this equation we obtain

$$\rho = \left(A + B a^{-3(1+\alpha)} \right)^{\frac{1}{1+\alpha}}, \quad (4.46)$$

where B is a constant of integration. We rewrite this equation as

$$\rho = \rho_0 \left(A_s + (1 - A_s) x^{3(1+\alpha)} \right)^{\frac{1}{1+\alpha}}. \quad (4.47)$$

where $\rho_0 = (A + B)^{1/(1+\alpha)}$, and $A_s = A/(A + B)$. We know from the previous chapter that the density of matter in terms of scale factor, or redshift is given by

$$\rho_m = \rho_{m0} \left(\frac{a_0}{a} \right)^3 = \rho_{m0} x^3, \quad (4.48)$$

where $x = 1 + z$ is the redshift.

If we consider a flat universe with matter and Chaplygin gas, the Friedmann' 1. equation gives the following expression for the Hubble parameter

$$\begin{aligned} \frac{\dot{a}^2}{a^2} &= \frac{\kappa}{3} (\rho_m + \rho_x) \\ &\rightarrow \frac{H^2(x)}{H_0^2} = \Omega_{m0}x^3 + (1 - \Omega_{m0}) \left[A_s + (1 - A_s)x^{3(1+\alpha)} \right]^{\frac{1}{1+\alpha}}. \end{aligned} \quad (4.49)$$

In order to find the expression for the deceleration parameter, we first differentiate equation (4.49) with respect to the redshift, and obtain

$$2HH'(x) = 3H_0^2 \left[\Omega_{m0}x^2 + (1 - \Omega_{m0})(1 - A_s) \left[A_s + (1 - A_s)x^{3(1+\alpha)} \right]^{\frac{1}{1+\alpha}-1} x^{3(1+\alpha)-1} \right].$$

Then, we insert H' and the expression for the Hubble parameter into the equation (4.11), and we get the following expression for $q(x)$:

$$q(x) = \frac{3}{2} \frac{\Omega_{m0}x^3 + (1 - \Omega_{m0})(1 - A_s)v^{\frac{3}{\beta}-1}x^\beta}{\Omega_{m0}x^3 + (1 - \Omega_{m0})v^{\frac{3}{\beta}}} - 1, \quad (4.50)$$

where we have defined $\beta \equiv 3(1 + \alpha)$ and

$$v = A_s + (1 - A_s)x^\beta. \quad (4.51)$$

Now we define $h(x) \equiv H(x)/H_0$, and

$$f(x) \equiv \Omega_{m0}x^2 + (1 - \Omega_{m0})(1 - A_s)v^{\frac{3}{\beta}-1}x^{\beta-1}, \quad (4.52)$$

and we use these definitions to give the expression for the statefinder parameter r by using equation (4.12), and we obtain

$$r(x) = 1 - 3 \frac{x}{h^2(x)} f(x) + \frac{3}{2} \frac{x^2}{h^2(x)} f'(x). \quad (4.53)$$

The expression for the statefinder parameter is

$$s(x) = \frac{-\frac{x}{h^2(x)} f(x) + \frac{1}{2} \frac{x^2}{h^2(x)} f'(x)}{\frac{3}{2} \left(\frac{x}{h^2(x)} f(x) - 1 \right)}. \quad (4.54)$$

To see the $r - s$ plane for the Chaplygin model we give the following expression

$$r = 1 - \frac{9}{2\alpha} s(1 + s). \quad (4.55)$$

Bertolami et al. (2004) [43], have compared the Chaplygin gas model with SNIa data and found evidence for $\alpha > 1$. But, most recently, R. C. Freitas et al. (2010) [40] have found, with a high dispersion, that a negative value for α is favoured by their analysis. They have found that $\alpha = -4.25^{+4.80}_{-15.50}$. In Fig. 4.1 we have drawn the s - r - plane for this model for different values of α . From these figures, we can see that when $s = 0$, $r = 1$.

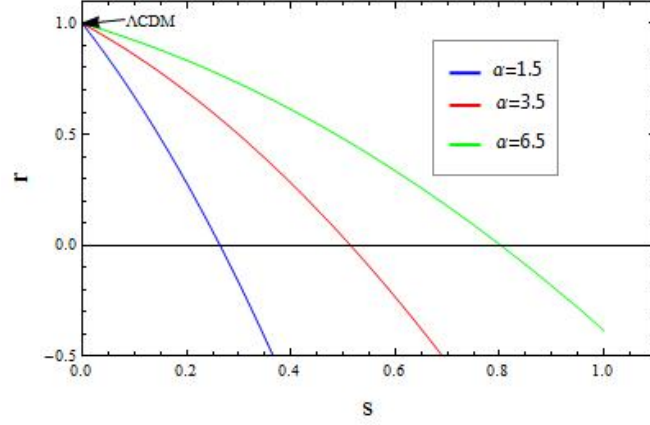
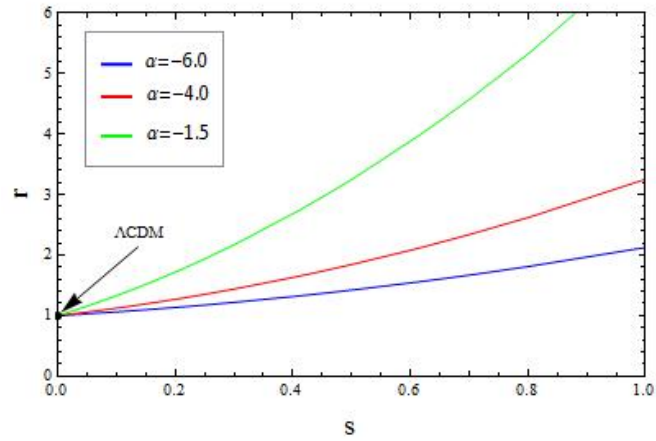
(a) $r(s)$ for $\alpha > 0$.(b) $r(s)$ for $\alpha < 0$.

Figure 4.1: The s - r plane for the Chaplygin gas model for different values of α . Fig.4.1(a) shows s - r plane for positive values of α . Fig.4.1(b) shows s - r plane for negative values of α . The point $\{0, 1\}$ corresponds to the values of statefinder parameters for the Λ CDM model.

4.1.4 Universe Models with a Scalar Field

There are many phenomena in nature which we describe by the concept of a field, e.g. the electric and magnetic fields. These are vector fields, because we are associating a vector with a given point in space at a given time. By analogy, a scalar field is a rule for associating a number with a point in space at a given time. There are many phenomena in nature which we describe by scalar fields, for example the temperature of the Earth's atmosphere can be considered as a scalar field. The Higgs field in theoretical particle physics which is introduced in the electroweak theory to provide the elementary particles with rest masses, is also a scalar field.

A scalar field has a kinetic and a potential energy associated with it, and hence an energy density and a pressure. We will in the following consider a homogeneous scalar field ϕ . Homogeneity means that ϕ is a function of time only, not of the spatial coordinates. Then, measuring ϕ in units of energy, the energy density of the field is given by

$$\rho_\phi = \frac{1}{2}\dot{\phi}^2 + V(\phi), \quad (4.56)$$

and the pressure is given by

$$p_\phi = \frac{1}{2}\dot{\phi}^2 - V(\phi), \quad (4.57)$$

If the source of the dark energy is a scalar field ϕ with the potential $V(\phi)$ and the equation of state $p_\phi = w\rho_\phi$, the equation of state factor w is then

$$w = \frac{p_\phi}{\rho_\phi} = \frac{\dot{\phi}^2 - 2V(\phi)}{\dot{\phi}^2 + 2V(\phi)}. \quad (4.58)$$

We see that whenever $\dot{\phi}^2 \ll V(\phi)$, which is the case when the field varies slowly in time, the equation of state is given by $w \approx -1$ and the scalar field will behave like a cosmological constant. This is the slowroll mechanism for providing a dark energy fluid.

If we differentiate this equation and multiply it with eq. (4.56) we obtain

$$\dot{w}\rho_\phi = \frac{2\dot{\phi}(2\ddot{\phi}V - \dot{\phi}\dot{V})}{\dot{\phi}^2 + 2V(\phi)}. \quad (4.59)$$

Summation of eqs. (4.56) and (4.57) gives

$$\rho_\phi + p_\phi = \dot{\phi}^2. \quad (4.60)$$

Differentiation of eq. (4.56) gives

$$\dot{\rho}_\phi = \dot{\phi}\ddot{\phi} + \dot{V}. \quad (4.61)$$

Inserting this two equations (eqs. (4.60) and (4.61)) into the continuity equation (4.16) we obtain the equation of motion of the scalar field

$$\ddot{\phi} = -3H\dot{\phi} - \frac{dV}{d\phi}. \quad (4.62)$$

We will assume that the scalar field dominates the energy density of the universe, and that the universe has curvature (which will be driven rapidly to zero anyway if inflation works the

way it is supposed to). We can now give the expressions for the deceleration parameter and statefinder parameters by using equations (4.17) (4.19) and (4.21). In this case

$$q = \frac{\Omega}{2} + \frac{\kappa}{2H^2} \left(\frac{1}{2}\dot{\phi}^2 - V(\phi) \right), \quad (4.63)$$

$$r = \Omega + \frac{3}{2}\kappa \frac{\dot{\phi}^2}{H^2} + \kappa \frac{\dot{V}}{H^3}, \quad (4.64)$$

$$s = 2 \frac{\dot{\phi}^2 + \frac{2}{3}\frac{\dot{V}}{H}}{\dot{\phi}^2 - 2V}. \quad (4.65)$$

The dark energy in a model where the energy is described by a slowrolling scalar-field is often called *quintessence*. We consider a model with matter, quintessence and curvature. The Friedmann equations governing the background evolution are

$$\frac{\dot{a}^2 + k}{a^2} = \frac{\kappa}{3} (\rho_m + \rho_k + \rho_\phi), \quad (4.66)$$

$$\frac{\ddot{a}}{a} = -\frac{\kappa}{6} (\rho_m + 2\rho_k + \rho_\phi + 3p_\phi). \quad (4.67)$$

Using the two above equations we obtain

$$\dot{H} = -3H^2 + \frac{1}{2M^2} \left(\frac{1}{2}\rho_m - V(\phi) + \frac{2}{3}\rho_k \right), \quad (4.68)$$

$$\frac{1}{2}\dot{\phi}^2 = 3H^2M^2 - \rho_m - V(\phi) - \rho_k \quad (4.69)$$

The energy conservation equation gives

$$\dot{\rho}_m = -3H\rho_m, \quad (4.70)$$

$$\dot{\rho}_k = -2H\rho_k. \quad (4.71)$$

The deceleration and statefinder parameters expressed in terms of density parameters are

$$q = \frac{1}{2}\Omega_m + 2\Omega_{kin} - \Omega_{pot}, \quad (4.72)$$

$$r = \Omega_m + 10\Omega_{kin} + \Omega_{pot} + 3\sqrt{6\Omega_{kin}} \frac{MV'}{\rho_{cr}} \quad (4.73)$$

$$s = \frac{6\Omega_{kin} + 2\sqrt{6\Omega_{kin}} \frac{MV'}{\rho_{cr}}}{3(\Omega_{kin} - \Omega_{pot})}. \quad (4.74)$$

where we have introduced the Planck mass $M^2 \equiv 1/8\pi G$ and we have defined $\Omega_{kin} \equiv \dot{\phi}^2/2\rho_{cr}$, and $\Omega_{pot} \equiv V(\phi)/\rho_{cr}$.

Statefinder parameters for an exponential potential

We will now consider two different potentials, and find statefinder parameters for both cases. For an exponential potential

$$V(\phi) = A \exp(-\lambda\phi/M), \quad (4.75)$$

the derivative with respect to ϕ is

$$V'(\phi) = -\frac{A\lambda}{M} \exp(-\lambda\phi/M). \quad (4.76)$$

Inserting equation (4.76) in equation (4.73) we obtain for the present epoch

$$q_0 = \frac{1}{2}\Omega_{m0} + 2\Omega_{kin0} - \Omega_{pot0}, \quad (4.77)$$

$$r_0 = \Omega_{m0} + 10\Omega_{kin0} + \Omega_{pot0} - 3\lambda\sqrt{6\Omega_{kin0}\Omega_{pot0}} \quad (4.78)$$

$$s_0 = \frac{6\Omega_{kin0} - 2\lambda\sqrt{6\Omega_{kin0}\Omega_{pot0}}}{3(\Omega_{kin0} - \Omega_{pot0})}. \quad (4.79)$$

We use $\Omega_{m0} + \Omega_{kin0} + \Omega_{pot0} + \Omega_{k0} = 1$ to eliminate Ω_{pot0} , and we obtain

$$q_0 = \frac{3}{2}\Omega_{m0} - (1 - \Omega_{k0}) + 3\Omega_{kin0}, \quad (4.80)$$

$$r_0 = (1 - \Omega_{k0}) + 9\Omega_{kin0} - 3\lambda\sqrt{6\Omega_{kin0}}(1 - \Omega_{k0} - \Omega_{m0} - \Omega_{kin0}) \quad (4.81)$$

$$s_0 = \frac{6\Omega_{kin0} - 2\lambda\sqrt{6\Omega_{kin0}}(1 - \Omega_{k0} - \Omega_{m0} - \Omega_{kin0})}{3(2\Omega_{kin0} + \Omega_{m0} + \Omega_{k0} - 1)}. \quad (4.82)$$

We choose $\Omega_{m0} = 0.27$ and $\Omega_{k0} = 0$. Now we plot the values of q_0 , r_0 and s_0 for varying Ω_{kin0} ; see figure 4.2(a). We can see from equations (4.80)-(4.82), that when $\Omega_{kin0} = 0$, q_0 , r_0 and s_0 are independent of λ . And $s_0 = 0$ and $r_0 = 1$ which is the same value as in the Λ CDM model. So, when taking away the kinetic term quintessence will reduce to Lorentz-invariant-vacuum-energy (*LIVE*). We can also see that, when $\Omega_{kin0} > 0$, we can make r_0 as large or as small as we like, by choosing $|\lambda|$ sufficiently large. We know that in order to get an accelerating universe today we must have $\lambda^2 < 2$. It seems that in order to get a universe close to what we observe, r and q for models with matter and quintessence with an exponential potential will essentially lie within the same area as models with matter and dark energy with a time-independent equation of state (also called quiescence). In figures 4.2(b) and 4.2(c) we have plotted the trajectories in the s_0 - r_0 -plane and the s_0 - q_0 -plane for the this model.

Statefinder parameters for a power-law potential

Now we look at a power-law potential

$$V(\phi) = A\phi^{-\alpha}, \quad (4.83)$$

that gives

$$V' = -\frac{\alpha}{\phi}V. \quad (4.84)$$

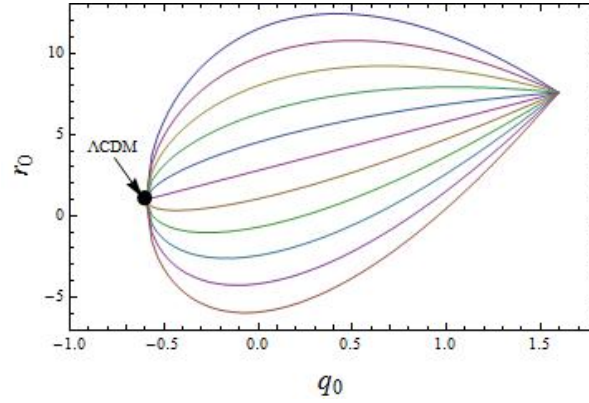
Inserting this equation (4.84) into equations (4.72-4.74) we obtain the following expressions for the deceleration and statefinder parameters

$$q = \frac{1}{2}\Omega_m + 2\Omega_{kin} - \Omega_{pot}, \quad (4.85)$$

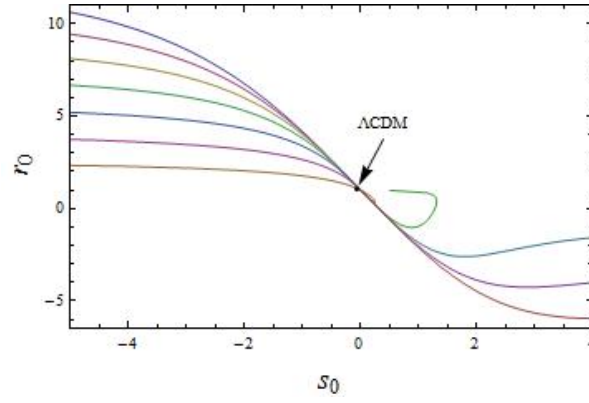
$$r = \Omega_m + 10\Omega_{kin} + \Omega_{pot} + 3\alpha\frac{M}{\phi}\sqrt{6\Omega_{kin}\Omega_{pot}} \quad (4.86)$$

$$s = \frac{6\Omega_{kin} - 2\frac{\alpha M}{\phi}\sqrt{6\Omega_{kin}\Omega_{pot}}}{3(\Omega_{kin} - \Omega_{pot})}. \quad (4.87)$$

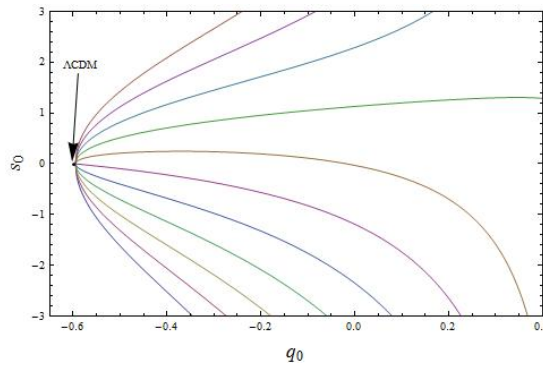
In figure 4.3(a) we have drawn the q_0 - r_0 -plane for the case $\alpha = 2$. And figure 4.3(b) shows the s_0 - r_0 -plane for the statefinder parameters with ($\phi_0 = M, \Omega_{kin0} = 0.05, \Omega_{m0} = 0.27, \Omega_{k0} = 0, h = 0.71$). From the figure 4.3(a) we see that for $\phi_0 = M$ we get the same curves in the q_0 - r_0 -plane when varying α as we got when varying λ in the exponential potential, see figure 4.2(a). We also see that varying ϕ_0 for a given value of α is essentially the same as varying α .



(a) The q_0 - r_0 plane for a universe model with matter and quintessence with an exponential potential. $\lambda = -5, -4, -3, -2, -1, 0, 1, 2, 3, 4, 5$ corresponds to curves from top to bottom, respectively. All curves starts at the point $(q_0, r_0) = (1.595, 7.57)$ which corresponds to $\Omega_{kin} = 0.73$. When we decrease Ω_{kin} , we move to the left and curves join at the point $(q_0, r_0) = (-0.595, 1)$ which corresponds to $\Omega_{kin} = 0$

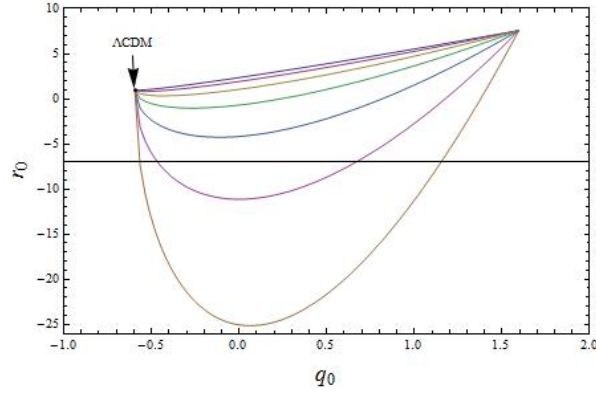


(b) The s_0 - r_0 plane for a universe model with matter and quintessence with an exponential potential.

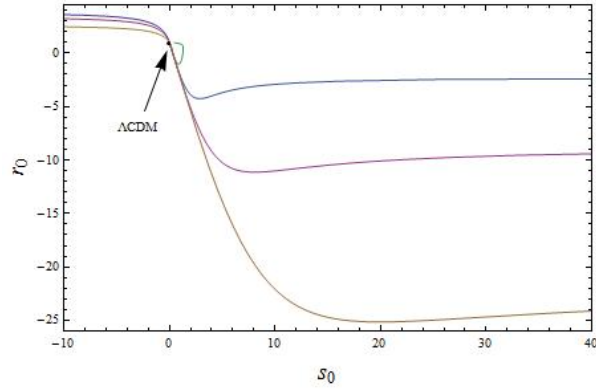


(c) The s_0 - q_0 plane for a universe model with matter and quintessence with an exponential potential.

Figure 4.2: $r_0(q_0)$, $r_0(s_0)$ and $s_0(q_0)$ for a universe model with matter and quintessence with an exponential potential.



(a) The q_0 - r_0 plane for a universe model with matter and quintessence with a power-law potential with $\alpha = 2$. $\phi = 8M, 4M, 2M, M, \frac{M}{2}, \frac{M}{4}, \frac{M}{8}$ corresponds to curves from top to bottom, respectively.



(b) The s_0 - r_0 plane for a universe model with matter and quintessence with a power-law potential with $\alpha = 2$. $\phi = 8M, 4M, 2M, M, \frac{M}{2}, \frac{M}{4}, \frac{M}{8}$ corresponds to curves from top to bottom, respectively.

Figure 4.3: $r_0(q_0)$ and $r_0(s_0)$ for a universe model with matter and quintessence with a power-law potential.

4.1.5 Universe Models with Two Interacting Fluids

We will in this subsection apply the statefinder formalism to universe models with two interacting fluids ([26], [27], [28]-[30]). These universe models are cosmological models whose evolution is dominated by interacting components. We will here study the case where dark matter interacts with dark energy. These models in which the energy components do evolve together and interact with each other are of special interest because they may solve the "coincidence problem". This problem states "Why the energy densities of the two main components happen to be of the same order today?" We will first focus on a universe filled with two components, namely, dark matter (subscript m) and dark energy (subscript x). As we have mentioned earlier the dark matter has a negligible pressure, $p_m \approx 0$, and dark energy has a equation of state $p_x = w\rho_x$. The interaction of the dark matter with the dark energy is given by

$$\dot{\rho}_m + 3H\rho_m = Q, \quad \dot{\rho}_x + 3H\rho_x(1+w) = -Q, \quad (4.88)$$

where $Q \geq 0$, and it is a measure of the strength of the interaction. It is more convenience to write $Q = -3PH$, where P has the dimension of pressure. Friedmann's equations are

$$H^2 = \frac{\kappa}{3}(\rho_m + \rho_x). \quad (4.89)$$

$$\frac{\ddot{a}}{a} = -\frac{\kappa}{6}[\rho_m + (1+3w)\rho_x]. \quad (4.90)$$

And hence

$$\dot{H} = -\frac{\kappa}{2}[\rho_m + (1+w)\rho_x]. \quad (4.91)$$

Using equation (4.6) we find the following expression for the deceleration parameter

$$q = \frac{1}{2}(1 + 3w\Omega_x). \quad (4.92)$$

From this expression we see that the deceleration parameter does not depend on the interaction of the two components.

We differentiate equation (4.91) and obtain

$$\ddot{H} = \frac{3}{2}\kappa H \left[\rho + p_x + w(1+w)\rho_x - wP - \frac{\dot{w}\rho_x}{3H} \right]. \quad (4.93)$$

We can rewrite this equation as

$$\frac{\ddot{H}}{H^3} = \frac{9}{2} \left(1 + \frac{p_x}{\rho} \right) + \frac{9}{2} \left[w(1+w)\frac{\rho_x}{\rho} - w\frac{P}{\rho} - \frac{\dot{w}}{3H}\frac{\rho_x}{\rho} \right], \quad (4.94)$$

where $\rho = \rho_m + \rho_x$ is the total energy density. Inserting this expression into equation (4.7) we obtain the following expression for the statefinder parameter r

$$r = 1 + \frac{9}{2} \left[w(1+w)\frac{\rho_x}{\rho} - w\frac{P}{\rho} - \frac{\dot{w}}{3H}\frac{\rho_x}{\rho} \right]. \quad (4.95)$$

Introducing the density ratio $\alpha \equiv \frac{\rho_m}{\rho_x}$, we obtain

$$r = 1 + \frac{9}{2} \frac{w}{1+\alpha} \left[1 + w - \frac{P}{\rho_x} - \frac{\dot{w}}{3wH} \right]. \quad (4.96)$$

Then, the statefinder parameter s is

$$s = 1 + w - \frac{P}{\rho_x} - \frac{\dot{w}}{3wH}. \quad (4.97)$$

From these expressions we see that when there is no interaction between the two components, i.e. when $P = 0$, these parameters reduce to the expressions in equations (4.27) and (4.28). We see also that statefinder parameters depend on the interaction between the components. Consequently, we can use the statefinder parameters to discriminate between models with different interactions or between interacting and non-interacting models.

Now, we want to study the density ratio α . Differentiation of α gives

$$\dot{\alpha} = \frac{\dot{\rho}_m \rho_x - \rho_m \dot{\rho}_x}{\rho_x^2}.$$

Using the equations in (4.88), we obtain

$$\dot{\alpha} = -3H \left[\left(\frac{\rho_m + \rho_x}{\rho_x \rho_m} \right) P - w \right] \alpha. \quad (4.98)$$

Solving this equation we can find the evolution of the interaction between the dark matter and dark energy. In order to solve the coincidence problem the density ratio should be a constant of the order of unity at late times.

It has been shown that solutions of the form (also called *scaling* solutions) $\rho_m/\rho_x \propto a^{-\beta}$, where $\beta \in [0, 3]$ is a constant, can be obtained when the dark energy component decays into the dark matter, (ref. [46]). Inserting the scaling solutions, $\alpha = \alpha_0 \left(\frac{a}{a_0} \right)^{-\beta}$, in equation (4.98) and assuming that w is a constant, we obtain

$$\frac{P}{\rho_x} = \left(w + \frac{\beta}{3} \right) \frac{\alpha_0 (1+z)^\beta}{1 + \alpha_0 (1+z)^\beta}, \quad (4.99)$$

where α_0 is the present energy density ratio, and z is the redshift. We insert this expression in equations (4.96) and (4.97) and get

$$r = 1 + \frac{9}{2} \frac{w}{1 + \alpha_0 (1+z)^\beta} \left[1 + w - \left(w + \frac{\beta}{3} \right) \frac{\alpha_0 (1+z)^\beta}{1 + \alpha_0 (1+z)^\beta} \right]. \quad (4.100)$$

$$s = 1 + w - \left(w + \frac{\beta}{3} \right) \frac{\alpha_0 (1+z)^\beta}{1 + \alpha_0 (1+z)^\beta}. \quad (4.101)$$

In figure (4.4) we have plotted the s - r -plane for different values of β . If $\beta = 3$ and $w = -1$ we get from the equations above that $P = 0$ and $\{s, r\} = \{0, 1\}$, which corresponds to the Λ CDM model. If $\beta = 0$ we get a stable and stationary solution $\alpha = \text{constant}$, and it solves the coincidence problem. If $z = 0$ we get the current values of the statefinder parameters

$$r_0 = 1 + \frac{9}{2} \frac{w}{1 + \alpha_0} s_0. \quad (4.102)$$

$$s_0 = 1 + w - \left(w + \frac{\beta}{3} \right) \frac{\alpha_0}{1 + \alpha_0}. \quad (4.103)$$

The current value of the deceleration parameter is

$$q_0 = \frac{1}{2} \frac{1 + \alpha_0 + 3w}{1 + \alpha_0}. \quad (4.104)$$

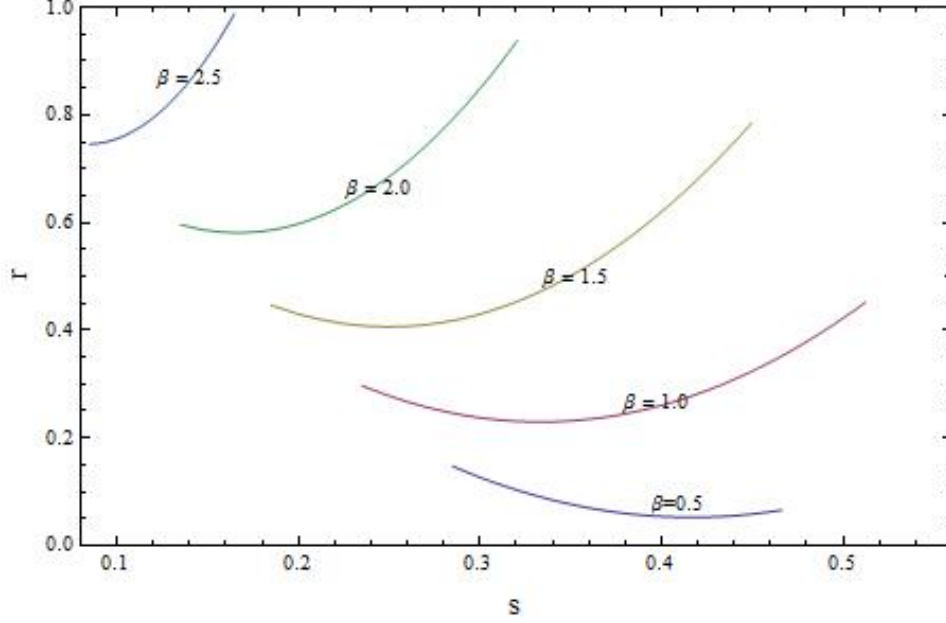


Figure 4.4: The s_0 - r_0 plane for a universe model with two interacting fluids, non-relativistic matter and dark energy. The curves are plotted in the redshift interval $[0, 6]$ with $\alpha_0 = 3/7$ and $w = -0.95$ for different values of β

If $w = -1$, we obtain

$$q_0(w = -1) = \frac{1}{2} \frac{1 + \alpha_0 - 3}{1 + \alpha_0}. \quad (4.105)$$

$$r_0(w = -1) = 1 + \frac{9}{2} \left(\frac{\beta}{3} - 1 \right) \frac{\alpha_0}{(1 + \alpha_0)^2}. \quad (4.106)$$

$$s_0(w = -1) = \left(1 - \frac{\beta}{3} \right) \frac{\alpha_0}{1 + \alpha_0}. \quad (4.107)$$

From these equations we see that $\beta = 3$ corresponds to the Λ CDM model with $\{s, r\} = \{0, 1\}$. We assume $\alpha_0 = 3/7$ and for stationary solution, $\beta = 0$, we get $\{s, r\} = \{0.30, 0.055\}$. Similar considerations hold for other values of w . Thus, the statefinder parameters are able to discriminate between different scaling models, characterized by the same deceleration parameter.

4.2 Statefinder Parameters for a New Coupled Quintessence Cosmological Model

J. F. Jesus, R. C. Santos, J. S. Alcaniz and J. A. S. Lima [48] have proposed a new cosmological model where radiation and baryons are conserved, while the dark energy component is decaying into cold dark matter (CDM). The dark energy component is decaying into CDM particles and therefore the CDM component will dilute more slowly compared to its standard (conserved)

evolution, $\rho_m = \rho_{m0}a^{-3}$. We assume the deviation from the standard evolution is characterized by a positive constant ϵ and given as

$$\rho_{\text{CDM}} = \rho_{\text{CDM0}}a^{-3+\epsilon}. \quad (4.108)$$

The dark energy satisfies the equation of state $p_x = w\rho_x$ ($w < 0$). For a spatially flat, homogeneous and isotropic universe model with matter (baryonic + dark) and radiation and a negative-pressure dark energy component, the Einstein field equations can be written as

$$H^2 = \frac{\kappa}{3}(\rho_\gamma + \rho_b + \rho_{\text{CDM}} + \rho_x), \quad (4.109)$$

$$\frac{\ddot{a}}{a} = -\frac{\kappa}{6}(\rho_\gamma + \rho_b + \rho_{\text{CDM}} + \rho_x + 3p_\gamma + 3p_x) \quad (4.110)$$

where ρ_γ , ρ_b , ρ_{CDM} and ρ_x are the energy densities of the radiation, baryons, cold dark matter and dark energy, respectively, while p_γ and p_x are the radiation and dark energy pressures.

We assume that the radiation and baryonic fluids are separately conserved. The energy conservation law for the two interacting components (dark energy and cold dark matter) is then given by

$$\dot{\rho}_{\text{CDM}} + 3\frac{\dot{a}}{a}\rho_{\text{CDM}} = -\dot{\rho}_x - 3\frac{\dot{a}}{a}(\rho_x + p_x). \quad (4.111)$$

Now, we insert equation (4.108) in equation (4.111), integrate and obtain the following expression for the energy density of the dark energy component

$$\rho_x = \tilde{\rho}_{x0}a^{-3(1+w)} + \frac{\epsilon\rho_{\text{CDM0}}}{3|w| - \epsilon}a^{-3+\epsilon}, \quad (4.112)$$

where $\tilde{\rho}_{x0}$ is the present-day fraction of dark energy density. We neglect the radiation contribution and write Friedmann's first equation (4.109) in terms of the density parameters as

$$\left(\frac{H}{H_0}\right)^2 = \Omega_{b0}a^{-3} + \frac{3|w|\Omega_{\text{CDM0}}}{3|w| - \epsilon}a^{-3+\epsilon} + \tilde{\Omega}_{x0}a^{-3(1+w)}, \quad (4.113)$$

where Ω_{b0} and Ω_{CDM0} are the present-day baryons and CDM density parameters. The density parameter $\tilde{\Omega}_{x0}$ is defined, in terms of the density parameter of the dark energy Ω_{x0} , as

$$\tilde{\Omega}_{x0} = \Omega_{x0} - \frac{\epsilon\Omega_{\text{CDM0}}}{3|w| - \epsilon}. \quad (4.114)$$

From the equations above we can see that when there is no interaction between the dark energy component and the CDM component, i.e., $\epsilon = 0$, the conventional non-interacting quintessence model is fully recovered.

J. F. Jesus, R. C. Santos, J. S. Alcaniz and J. A. S. Lima [48] have done statistical analyses based on cosmological observations such as distance measurements from SNe Ia [49], the current estimates of the baryon acoustic oscillations found in the SDSS data [50] and the shift parameter from WMAP observations [24]. At 68.3%, 95.4% and 99.7% confidence intervals, they have found respectively

$$\epsilon = 0.000_{-0.000}^{+0.027}, \quad \epsilon = 0.000_{-0.000}^{+0.057}, \quad \epsilon = 0.000_{-0.000}^{+0.088}, \quad (4.115)$$

$$w = -1.006_{-0.119}^{+0.117}, \quad w = -1.006_{0.205}^{+0.188} \quad \text{and} \quad w = -1.006_{-0.296}^{+0.258}. \quad (4.116)$$

Based on these results from the analyses we see that the standard Λ CDM is preferred. We make use of these results to find the exact expressions for deceleration parameter and statefinder parameters. Then, we will plot these parameters for different values of ϵ and w .

The deceleration parameter, defined as $q = -\frac{a\ddot{a}}{\dot{a}^2}$, for this model in terms of the redshift takes the following form

$$q(z) = \frac{1}{2} \frac{1 + \frac{3|w|-3|w|\epsilon}{3|w|-\epsilon} \frac{\Omega_{\text{CDM}0}}{\Omega_{b0}} (1+z)^{-\epsilon} + (1+3w) \frac{\tilde{\Omega}_{x0}}{\Omega_{b0}} (1+z)^{3w}}{1 + \frac{3|w|}{3|w|-\epsilon} \frac{\Omega_{\text{CDM}0}}{\Omega_{b0}} (1+z)^{-\epsilon} + \frac{\tilde{\Omega}_{x0}}{\Omega_{b0}} (1+z)^{3w}}. \quad (4.117)$$

Using the definitions in (4.7) and (4.8), we obtain the following expressions for the statefinder parameters

$$r(z) = \frac{8 + \frac{24|w|-\frac{27}{2}|w|\epsilon+\frac{3}{2}|w|\epsilon^2}{3|w|-\epsilon} \frac{\Omega_{\text{CDM}0}}{\Omega_{b0}} (1+z)^{-\epsilon} + (8 + \frac{27}{2}w + \frac{9}{2}w^2) \frac{\tilde{\Omega}_{x0}}{\Omega_{b0}} (1+z)^{3w}}{1 + \frac{3|w|}{3|w|-\epsilon} \frac{\Omega_{\text{CDM}0}}{\Omega_{b0}} (1+z)^{-\epsilon} + \frac{\tilde{\Omega}_{x0}}{\Omega_{b0}} (1+z)^{3w}}. \quad (4.118)$$

$$s(z) = \frac{2}{3} \frac{7 + \frac{24|w|-\frac{27}{2}|w|\epsilon+\frac{3}{2}|w|\epsilon^2}{3|w|-\epsilon} \frac{\Omega_{\text{CDM}0}}{\Omega_{b0}} (1+z)^{-\epsilon} + (8 + \frac{27}{2}w + \frac{9}{2}w^2) \frac{\tilde{\Omega}_{x0}}{\Omega_{b0}} (1+z)^{3w}}{\frac{3w\epsilon}{3|w|-\epsilon} \frac{\Omega_{\text{CDM}0}}{\Omega_{b0}} (1+z)^{-\epsilon} + 3w \frac{\tilde{\Omega}_{x0}}{\Omega_{b0}} (1+z)^{3w}}. \quad (4.119)$$

We have drawn the deceleration parameter and statefinder parameters and the s - r -plane for this model for different values of ϵ and w . From the figures (4.5), (4.6), (4.7) and (4.8), we see that the effect of ϵ is to decrease the value of $q(z)$, $r(z)$, $r(q)$ and $s(q)$, and for values of the dark energy equation of state parameter w close to the LIVE value ($w = -1$), the value of deceleration parameter and statefinder parameter r increases for increasing w . Figures (4.9) show the s - r -plane and the point $\{s, r\} = \{0, 1\}$ for the Λ CDM model. We see that for $w \leq -1$, the values of the statefinder parameters move toward the values of the Λ CDM model. But, for $w > -1$ the values of the statefinder parameters move toward, but do not reach the values of the Λ CDM model.

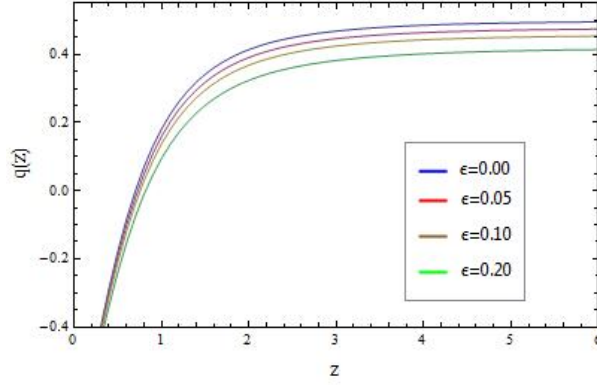
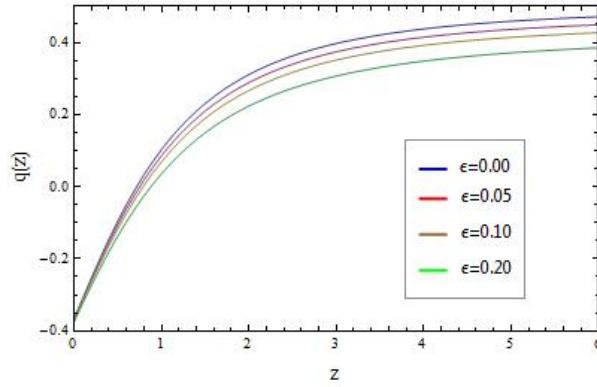
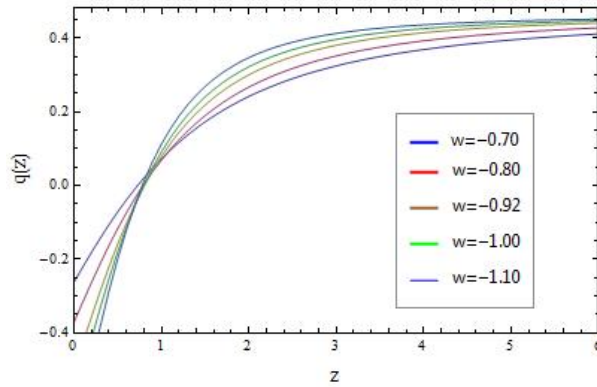
(a) $q(z)$ for $w = -1.2$.(b) $q(z)$ for $w = -0.8$.(c) $q(z)$ for $\epsilon = 0.1$.

Figure 4.5: $q(z)$ for the coupled quintessence model. Fig.4.5(a) shows deceleration parameter as a function of redshift z for $w = -1.2$ and different values of interaction parameter ϵ . Fig.4.5(b) also shows $q(z)$, for $w = -0.8$ and different values of ϵ . Fig.4.5(c) shows $q(z)$, for $\epsilon = 0.1$ and different values of w . We see from the figures that the effect of ϵ is to decrease the value of $q(z)$. We also see that the value of deceleration parameter increases for increasing equation of state parameter w

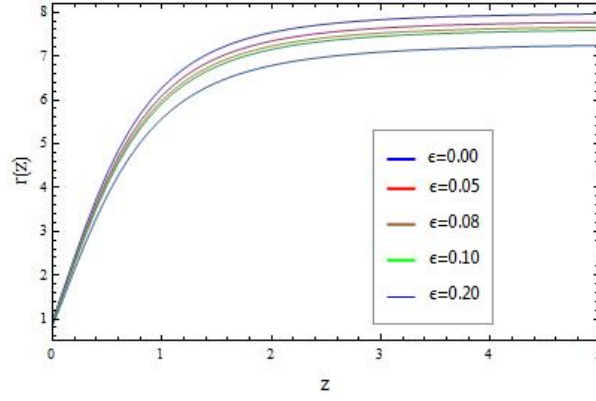
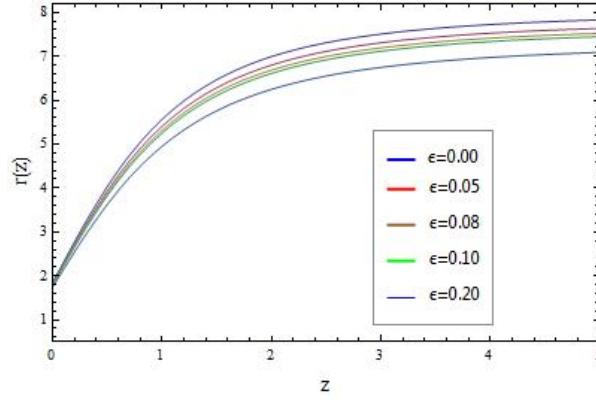
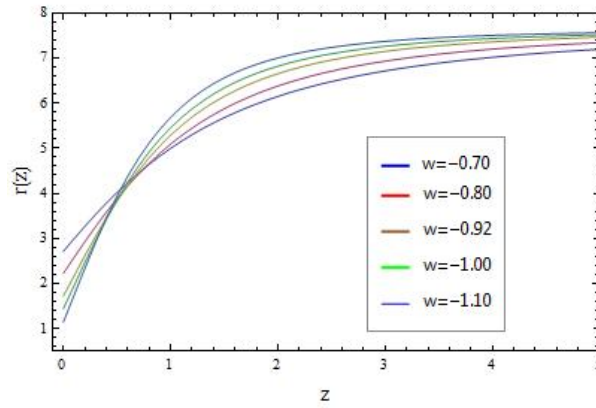
(a) $r(z)$ for $w = -1.2$.(b) $r(z)$ for $w = -0.9$.(c) $r(z)$ for $\epsilon = 0.1$.

Figure 4.6: $r(z)$ for the coupled quintessence model. Fig.4.6(a) shows statefinder parameter r as a function of redshift z for $w = -1.2$ and different values of interaction parameter ϵ . Fig.4.6(b) also shows $r(z)$, for $w = -0.8$ and different values of ϵ . Fig.4.6(c) shows $r(z)$, for $\epsilon = 0.1$ and different values of w . We see from the figures that the effect of ϵ is to decrease the value of $r(z)$.

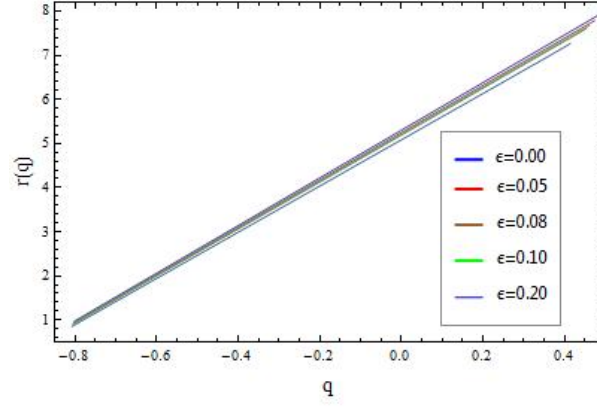
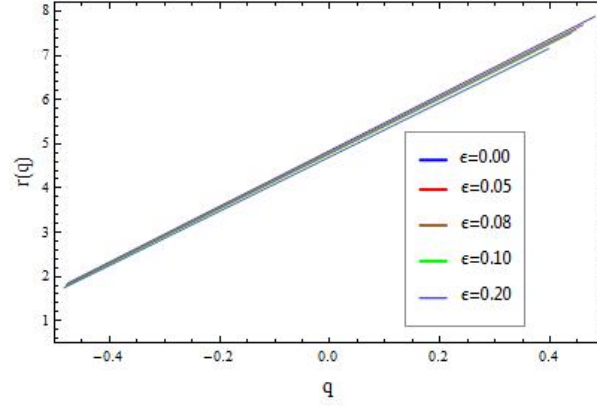
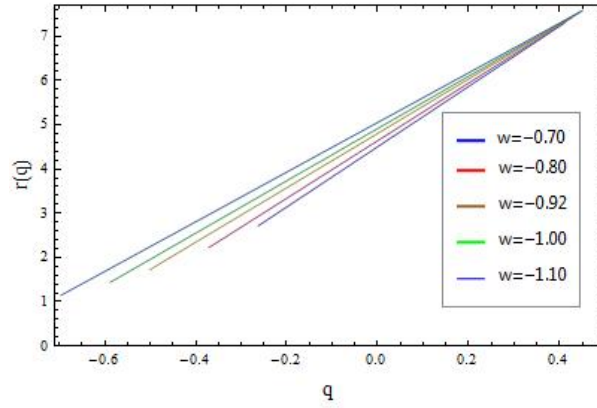
(a) $r(q)$ for $w = -1.2$.(b) $r(q)$ for $w = -0.9$.(c) $r(q)$ for $\epsilon = 0.1$.

Figure 4.7: The q - r -plane for the coupled quintessence model. Fig.4.7(a) shows the statefinder parameter r as a function of the deceleration parameter for $w = -1.2$ and different values of interaction parameter ϵ . Fig.4.7(b) also shows $r(q)$, for $w = -0.8$ and different values of ϵ . Fig.4.7(c) shows $r(q)$, for $\epsilon = 0.1$ and different values of w . We see from the figures that the effect of ϵ is to decrease the value of $r(q)$.

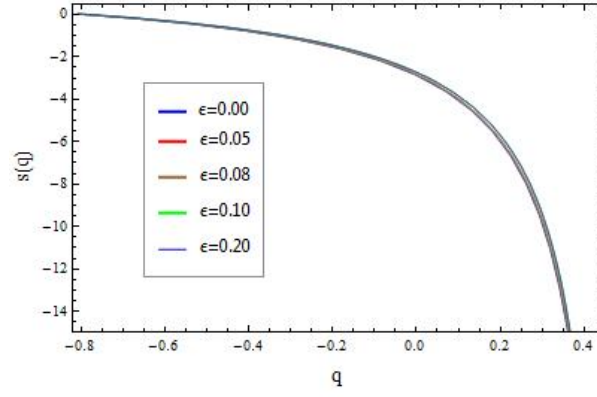
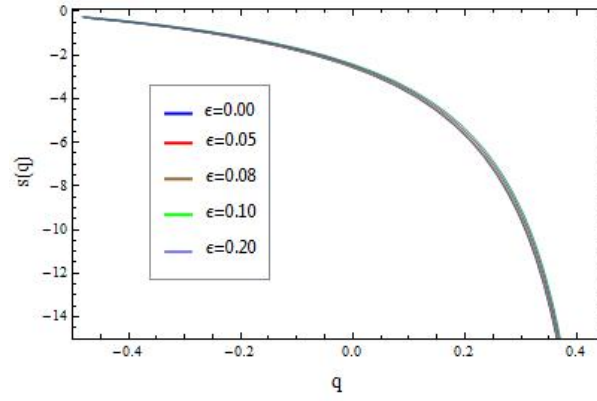
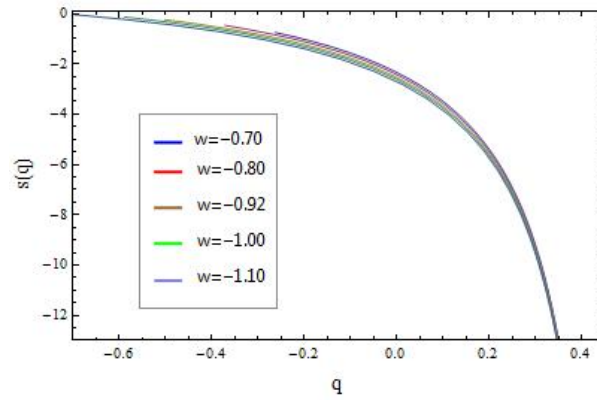
(a) $s(q)$ for $w = -1.2$.(b) $s(q)$ for $w = -0.9$.(c) $s(q)$ for $\epsilon = 0.1$.

Figure 4.8: The q - s -plane for the coupled quintessence model. Fig.4.8(a) shows statefinder parameter s as a function of deceleration parameter for $w = -1.2$ and different values of interaction parameter ϵ . Fig.4.8(b) also shows $s(q)$, for $w = -0.8$ and different values of ϵ . Fig.4.8(c) shows $s(q)$, for $\epsilon = 0.1$ and different values of w . We see from the figures that the effect of ϵ is to decrease the value of $s(q)$.

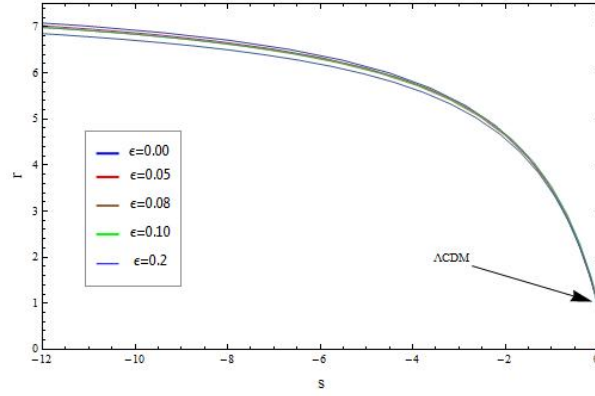
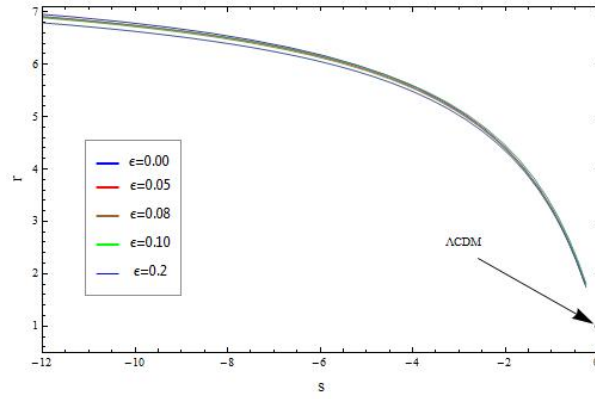
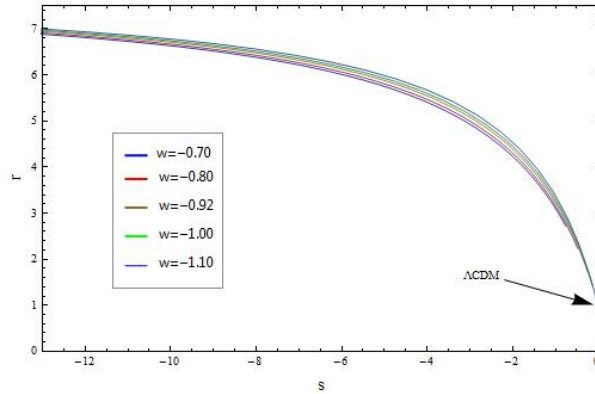
(a) $r(s)$ for $w = -1.2$.(b) $r(s)$ for $w = -0.8$.(c) $r(s)$ for $\epsilon = 0.1$.

Figure 4.9: The s - r -plane for the coupled quintessence model. Fig.4.9(a) shows deceleration parameter as a function of redshift z for $w = -1.2$ and different values of interaction parameter ϵ . Fig.4.9(b) also shows $r(s)$, for $w = -0.8$ and different values of ϵ . Fig.4.9(c) shows $r(s)$, for $\epsilon = 0.1$ and different values of w . The point $\{s, r\} = \{0, 1\}$ is the values for the standard Λ CDM model. We see that for $w \leq -1$, the values of the statefinder parameters move toward the values of the Λ CDM model. But, for $w > -1$ the values of the statefinder parameters move toward, but do not reach the values of the Λ CDM model.

Chapter 5

Viscous Universe Models

In hydrodynamics [58] [59], viscosity is defined as a measure of the resistance to flow of a fluid, and is related to velocity gradient. We will, in this thesis, consider to types of viscosity, namely, shear and bulk viscosity. The shear viscosity characterizes a change in shape of a fixed volume of the fluid, whereas the bulk viscosity characterizes a change in volume of the fluid of a fixed shape. In particular, the bulk viscosity being therefore relevant only for compressible liquids. The shear viscosity represents the ability of particles to transport momentum. It is usual to use shear viscosity in connection with spacetime anisotropy, and bulk viscosity with an isotropic cosmological model.

Many cosmological models deal with a perfect fluid behaviour. Because, it is easier to deal with this behaviour and these models seem to be in good agreement with cosmological observations [19] [24]. But, on a more physical and realistic basis we can replace the energy-momentum tensor for the simplest perfect fluid by the introduction of cosmic viscosity media contribution, which is another practical method to modify the equation of state.

We will, in this chapter, only consider flat and isotropic universe models. Therefore, we only use bulk viscosity.

5.1 Flat Friedmann-Robertson-Walker Universe Model with Viscous Dark Energy

We will, in this section, consider homogeneous and isotropic Friedmann-Robertson-Walker (FRW) universe models with bulk viscosity. In these models we can add a bulk viscosity term to the energy-momentum tensor as

$$T_{\mu\nu} = (\rho + p - \xi\theta)u_\mu u_\nu + (p - \xi\theta)g_{\mu\nu}, \quad (5.1)$$

where ξ is bulk viscosity, and θ is the expansion scalar, defined as $\theta \equiv 3H$. Writing out the Einstein equations

$$R_{\mu\nu} - \frac{1}{2}Rg_{\mu\nu} = 8\pi GT_{\mu\nu}, \quad (5.2)$$

for the Friedmann-Robertson-Walker metric of a flat universe and using equation (5.1), we obtain

$$\frac{\dot{a}^2}{a^2} = \frac{\kappa}{3}\rho, \quad (5.3)$$

$$\frac{\ddot{a}}{a} = -\frac{\kappa}{6}(\rho + 3p - 9\xi H) \quad (5.4)$$

The continuity equation takes the form

$$\dot{\rho} = -3H(\rho + p - 3\xi H), \quad (5.5)$$

Using the definitions of the deceleration parameter and statefinder parameters from chapter four

$$q = -1 - \frac{\dot{H}}{H^2}, \quad (5.6)$$

$$r = 1 + 3\frac{\dot{H}}{H^2} + \frac{\ddot{H}}{H^3}, \quad (5.7)$$

$$s = -\frac{2}{3H} \frac{3H\dot{H} + \ddot{H}}{3H^2 + 2\dot{H}}. \quad (5.8)$$

and combining with Eqs. (5.3)-(5.5), we obtain

$$q = \frac{3}{2} \frac{p}{\rho} - \frac{9}{2} \sqrt{\frac{\kappa}{3}} \frac{\xi}{\sqrt{\rho}} + \frac{1}{2}, \quad (5.9)$$

$$r = -\frac{3}{2} \left[\sqrt{\frac{3}{\kappa}} \frac{\dot{p}}{\rho^{\frac{3}{2}}} - 3 \frac{\dot{\xi}}{\rho} + \sqrt{3\kappa}(q+1) \frac{\xi}{\sqrt{\rho}} \right] + 1, \quad (5.10)$$

$$s = \frac{3\dot{\xi}\sqrt{\rho} - \sqrt{\frac{3}{\kappa}}\dot{p} - \sqrt{3\kappa}(q+1)\xi\rho}{3(\sqrt{\rho}p - \sqrt{3\kappa}\rho\xi)}. \quad (5.11)$$

From the above equations, we can see that the deceleration parameter and statefinder parameters are expressed by quantities ρ , p , \dot{p} , ξ and $\dot{\xi}$. But if we know the equation of state, ρ , p and \dot{p} reduces to one quantity. In what follows we will find the statefinder parameters for models with bulk viscosity.

5.2 Flat FRW Universe Models with Matter and Viscous Dark Energy

In this section we will consider a flat FRW universe model with matter and viscous dark energy, and then deduce the expressions for the statefinder parameters in terms of the Hubble parameter. We assume that the equation of state for the dark energy is

$$p_X = w\rho_X, \quad (5.12)$$

where w is a constant. Friedmann's equations for this model are then

$$H^2 = \frac{\kappa}{3} (\rho_m + \rho_X), \quad (5.13)$$

$$\frac{\ddot{a}}{a} = -\frac{\kappa}{6} (\rho_m + \rho_X + 3p_{\text{eff}}), \quad (5.14)$$

where ρ_m and ρ_X are the density of the matter and the dark energy, respectively, and

$$p_{\text{eff}} = p_X - 3\xi H = w\rho_X - 3\xi_0 H, \quad (5.15)$$

is the effective pressure of the dark energy, and ξ_0 is the usual viscosity coefficient which we assume to be a constant. Furthermore we assume that the matter and the dark energy does not interact with each other. The continuity equation is then for the dark matter and dark energy given as

$$\dot{\rho}_m = -3H\rho_m, \quad (5.16)$$

$$\dot{\rho}_X = -3H[(1+w)\rho_X - 3H\xi_0]. \quad (5.17)$$

Using equation (5.13) and inserting equation (5.15) in equation (5.14), we can rewrite Friedmann's 2. equation as

$$\frac{\ddot{a}}{a} = -\frac{H^2}{2} - \frac{\kappa}{2}w\rho_X + \frac{3}{2}H\kappa\xi_0. \quad (5.18)$$

The density parameters for the dark matter and dark energy are given as

$$\Omega_X \equiv \frac{\kappa}{3H^2}\rho_X, \quad (5.19)$$

$$\Omega_m \equiv \frac{\kappa}{3H^2}\rho_m = 1 - \Omega_X. \quad (5.20)$$

From the previous chapter we know that when we differentiate the Hubble parameter we obtain

$$\dot{H} = \frac{\ddot{a}}{a} - \left(\frac{\dot{a}}{a}\right)^2. \quad (5.21)$$

Inserting Friedmann's 2. equation (5.14) into the equation above we obtain the Raychaudhuri equation, which is the equation of motion of the cosmic expansion, and has the form

$$\dot{H} + \frac{3}{2}H^2 - \frac{3}{2}\kappa\xi_0H - \frac{1}{2}\kappa w\rho_X = 0. \quad (5.22)$$

Inserting the total energy density and pressure for this model, which is given as

$$\rho = \rho_m + \rho_X \quad p = p_X, \quad (5.23)$$

in equations (5.9)-(5.11), and using the expression for the density parameter for the dark energy in equation (5.19), the expressions for deceleration parameter and statefinder parameters take the following form

$$q = \frac{1}{2} \left(1 + 3w\Omega_X - 3\kappa \frac{\xi_0}{H} \right). \quad (5.24)$$

$$r = 1 + \frac{9}{2}w(1+w)\Omega_X - \frac{9}{4} \left(1 + 2w + w\Omega_X - \frac{\kappa\xi_0}{H} \right) \frac{\kappa\xi_0}{H}. \quad (5.25)$$

$$s = \frac{1}{2} \left(1 + 2w - \frac{\kappa\xi_0}{H} + \frac{1}{1 - \frac{\kappa\xi_0}{w\Omega_X H}} \right). \quad (5.26)$$

Now that we have given the general expressions for the deceleration parameter and the statefinder parameters for a flat FRW model, we will, in what follows, look at some specific cases. In the next section we will consider the Λ CDM model with viscosity.

5.3 Bulk Viscous Dark Energy and the Λ CDM Model

The Λ CDM Model consists of two components, the non-relative matter component, m , and the dark energy component, given as the cosmological constant, Λ . The equation of state of the dark energy is given by $p_\Lambda = -\rho_\Lambda$. Thus, the total pressure and density are given by

$$p = p_m + p_\Lambda = -\rho_\Lambda, \quad (5.27)$$

$$\rho = \rho_m + \rho_\Lambda. \quad (5.28)$$

For this model equation (5.5) can be rewritten as

$$\frac{d\rho_m}{\rho_m - \sqrt{3\kappa\xi_0}\sqrt{\rho_m + \rho_\Lambda}} = -3\frac{da}{a}. \quad (5.29)$$

Integrating both sides of this equation we obtain

$$(\rho - \sqrt{3\kappa\xi_0}\sqrt{\rho} - \rho_\Lambda) \left(\frac{\frac{2\sqrt{\rho}\xi}{\sqrt{3\kappa\xi_0}} - \xi - 1}{\frac{2\sqrt{\rho}\xi}{\sqrt{3\kappa\xi_0}} - \xi + 1} \right)^\xi = \frac{B}{a^3}, \quad (5.30)$$

where B is a integration constant and ξ is a constant defined as

$$\xi \equiv \frac{\sqrt{3\kappa\xi_0}}{\sqrt{4\rho_\Lambda + 3\kappa\xi_0^2}}. \quad (5.31)$$

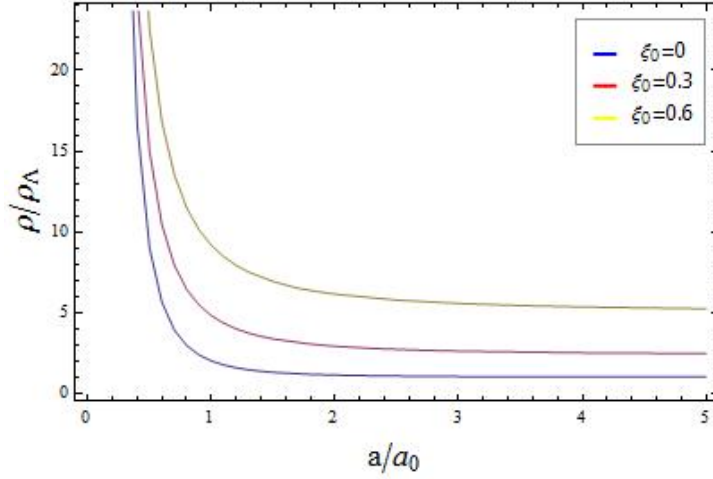


Figure 5.1: The relation between density ρ and the scale factor a for the three different values of ξ_0 . Here we set for simplicity $\rho_\Lambda = 1$ and $B = 1$.

From the equation (5.30) we can see that for a given value of the constant ξ_0 , there is a limit for the value of the density, ρ , which corresponds to $a \rightarrow \infty$, see Fig 5.1. And the expression for this value, which we denote as $\rho_\Lambda^{\text{eff}}$ and call it the effective vacuum energy density, is given by

$$\rho_\Lambda^{\text{eff}} = \frac{1}{4} \left(\sqrt{3\kappa\xi_0} + \sqrt{4\rho_\Lambda + 3\kappa\xi_0^2} \right)^2 = \frac{3}{4} \kappa \xi_0^2 \left(1 + \frac{1}{\xi} \right)^2. \quad (5.32)$$

In the limit of non-viscous case this expression reduces to

$$\lim_{\xi_0 \rightarrow 0} \rho_\Lambda^{\text{eff}} = \rho_\Lambda. \quad (5.33)$$

From this result we see that the effect of the bulk viscosity is to govern the value of the effective vacuum energy density. We will now define the relative changing rate, ς , of the density as

$$\varsigma = \left| \frac{\Delta\rho}{\rho(a)} \right| = \frac{|\rho(a + \Delta a) - \rho(a)|}{\rho(a)}, \quad (5.34)$$

where the Δa denotes a small change in the scale factor $a(t)$. From this definition we can see another effect of the bulk viscosity. The larger the bulk viscosity is, the bigger the value of the effective vacuum energy density will be and the smaller the relative changing rate. We can conclude that the bulk viscosity stabilizes the density evolution and blocks the rapid change of the universe. Now we will give the expressions for deceleration parameter and statefinder parameters for this model, by inserting the total pressure, Eq. (5.27), and density, Eq. (5.28), into Eqs.(5.9),(5.10) and (5.11). We obtain

$$q = \frac{1}{2} \left(1 - 3\Omega_\Lambda - 3\kappa \frac{\xi_0}{H} \right), \quad (5.35)$$

$$r = \frac{9}{4} \left[\frac{\kappa^2 \xi_0^2}{H^2} - (1 - \Omega_\Lambda) \frac{\kappa \xi_0}{H} \right] + 1, \quad (5.36)$$

$$s = -\frac{1}{2} \frac{\kappa \xi_0}{H} \left(1 - \frac{1}{\Omega_\Lambda + \frac{\kappa \xi_0}{H}} \right), \quad (5.37)$$

where the Ω_Λ is the vacuum density parameter defined by $\Omega_\Lambda \equiv \frac{\kappa \rho_\Lambda}{3H^2}$. Thus, the deceleration parameter and statefinder parameters are expressed by one variable parameter, H . In what follows, we will find the expression for the Hubble parameter.

For this model the differential equation for the Hubble parameter, eq. (5.22), reduces to

$$\dot{H} + \frac{3}{2}H^2 - \frac{3}{2}\kappa\xi_0H + \frac{\kappa}{2}\rho_\Lambda = 0. \quad (5.38)$$

Integrating equation (5.38), we obtain

$$H(t) = \frac{\kappa\xi_0}{2} + \alpha \frac{1 + Ce^{-3\alpha(t-t_0)}}{1 - Ce^{-3\alpha(t-t_0)}}, \quad (5.39)$$

where we have defined α and C as

$$\alpha = \sqrt{\left(\frac{\kappa\xi_0}{2} \right)^2 + \frac{\kappa\rho_\Lambda}{3}}, \quad (5.40)$$

$$C = \frac{H_0 - \frac{\kappa\xi_0}{2} - \alpha}{H_0 - \frac{\kappa\xi_0}{2} + \alpha}, \quad (5.41)$$

where H_0 and t_0 are the present Hubble parameter and the present time, respectively. Using the definition of the Hubble parameter, $H = \frac{\dot{a}}{a}$, we can rewrite equation (5.39) as

$$\frac{da}{a} = \left[\frac{\kappa\xi_0}{2} + \alpha \frac{1 + Ce^{-3\alpha(t-t_0)}}{1 - Ce^{-3\alpha(t-t_0)}} \right] dt. \quad (5.42)$$

Integrating both sides of equation (5.42) we obtain

$$a(t) = a_0 e^{\left(\frac{\kappa\xi_0}{2} + \alpha \right)(t-t_0)} \left[\frac{1 - Ce^{-3\alpha(t-t_0)}}{1 - C} \right]^{2/3}, \quad (5.43)$$

where $a(t_0) = a_0$, is the present scale factor.

The continuity equation for this model has the form

$$\dot{\rho}_m = -3H(\rho_m - 3\xi_0 H). \quad (5.44)$$

We have inserted equation (5.39) in equation (5.44), and have found some numerical solutions for the energy density, ρ_m , for different values of ξ_0 . The results are plotted in Fig.5.3. In Fig.5.2, we have plotted the scale factor, $a(t)$, and the Hubble parameter, $H(t)$, for different values of ξ_0 . From these figures we can see that when the bulk viscosity is zero, i.e. $\xi_0 = 0$, or when it has values very close to zero, the scale factor starts with zero and the Hubble parameter is infinitely large at a point of time, t . Depending on the value of ξ_0 this time could be at $t = 0$, $t > 0$ or $t < 0$, which shows that there is a point singularity at the initial epoch. We can also see that the energy density diverge at this point. It means that the universe starts with a big bang. As $t \rightarrow \infty$, the scale factor becomes infinite, whereas the Hubble parameter and the energy density become finite. If the bulk viscosity is zero, the energy density tends to zero as $t \rightarrow \infty$. Therefore, this model will give an empty universe for large times t . For the Λ CDM model with bulk viscosity, as $t \rightarrow \infty$ the energy density converges to a finite value. It means that for this model the energy density will stay constant for large times, t .

We can also see that when we increase the value of the bulk viscosity, the initial singularity will be removed, and the universe will begin at $t = -\infty$ with an infinitely large scale factor and a finite but negative Hubble parameter. As t increases, the scale factor will decay to a minimum. When it has reached this minimum it will start to increase, and as $t \rightarrow \infty$, the scale factor will increase exponentially. The Hubble parameter increases and becomes zero when the scale factor has reached its minimum value. After this point of time, the Hubble parameter increases, and as $t \rightarrow \infty$, it will reach its maximum value, and stay constant. From Fig.5.3(b) we can that the energy density starts with a finite but negative value at $t = -\infty$. It will decrease to a minimum at some point of time, and then, it will start to increase and becomes positive. As $t \rightarrow \infty$, the energy density will increase, and it will reach a maximum value. The bigger the value of the bulk viscosity is, the bigger the maximum value of the energy density will be.

We have plotted the time evolution of the deceleration parameter and the statefinder parameters in Fig.5.4. From this figure we can see that the deceleration parameter has its minimum value at $t = -\infty$ and $t = \infty$. As t increases, it will increase and reach a maximum value at a point where the Hubble parameter is infinitely large, i.e. at the singularity. As $t \rightarrow \infty$, the deceleration parameter will increase and it will reach its minimum value at $t = \infty$. When the bulk viscosity is zero, i.e. $\xi_0 = 0$, the statefinder parameters have the values $\{s, r\} = \{0, 1\}$, which is what we would expect for the Λ CDM model. Statefinder parameter r starts with a negative value at $t = -\infty$. As t increases, r will also increase. For a short period, r will decrease until it has reached zero. From that point on, it will increase, and as $t \rightarrow \infty$, r reaches a maximum. What we should notice from the time evolution of the statefinder parameter s , is that there exists a point of time where s diverges. The statefinder parameter s has a positive value at $t = -\infty$, and as $t \rightarrow \infty$, it reaches a negative value.

In Fig.5.5 we have also plotted the q - r -, q - s - and s - r -plane for this model for different values of the bulk viscosity ξ_0 . The point $\{0, 1\}$ corresponds to $\{s, r\}$ for the Λ CDM model with no viscosity. From these figures we can see that when the statefinder parameters have the values $s = 0$ and $r = 1$, the deceleration parameter has the value $q = -1$. By use of this diagnostic method we can differentiate the viscous Λ CDM models from non-viscous cases.

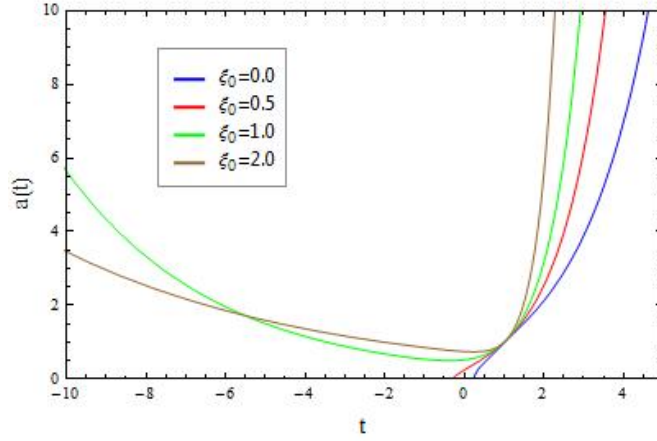
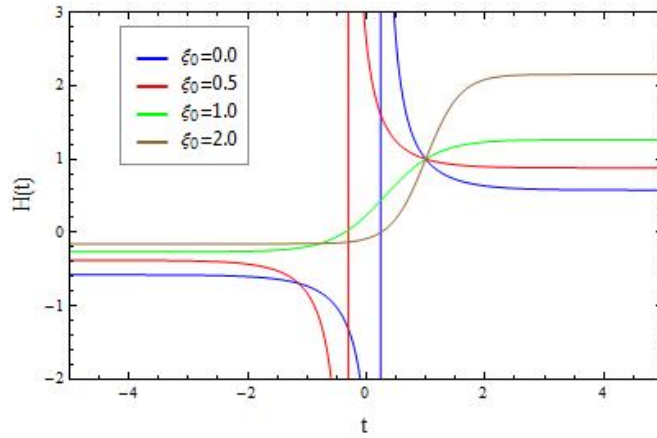
(a) $a(t)$.(b) $H(t)$.

Figure 5.2: The scale factor as a function of time for the Λ CDM model with and without viscosity is plotted in Fig.5.2(a). Fig.5.2(b) shows the Hubble parameter as a function of time for the Λ CDM model with and without viscosity. Here we have set $\rho_\Lambda = t_0 = H_0 = \kappa = 1$, for simplicity.

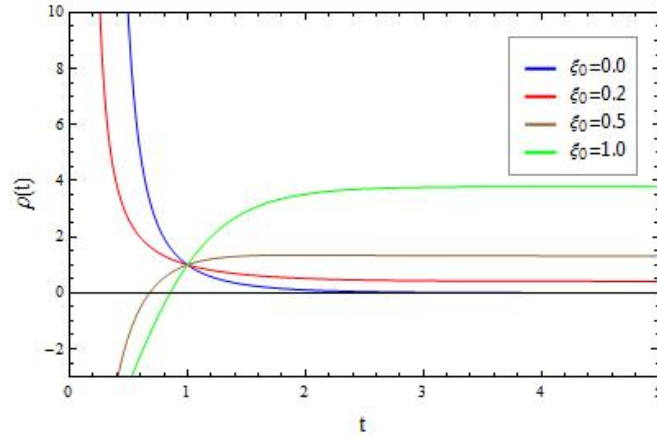
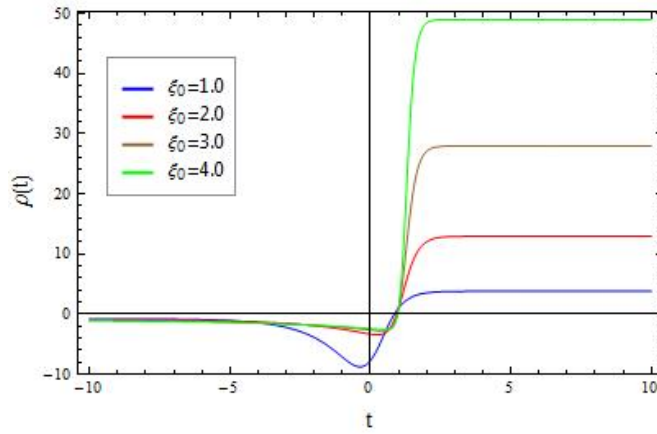
(a) $\rho(t)$.(b) $\rho(t)$.

Figure 5.3: The energy density for the non-relativistic matter as a function of time for the Λ CDM model with and without viscosity is displayed in Fig.5.3(a). Fig.5.3(b) shows the energy density for the non-relativistic matter as a function of time for the Λ CDM model with bigger values of the bulk viscosity. Here we have set $\rho_\Lambda = \rho_0 = t_0 = H_0 = \kappa = 1$, for simplicity.

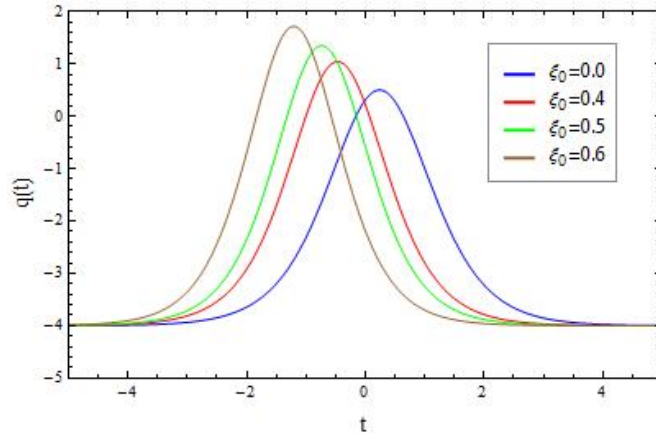
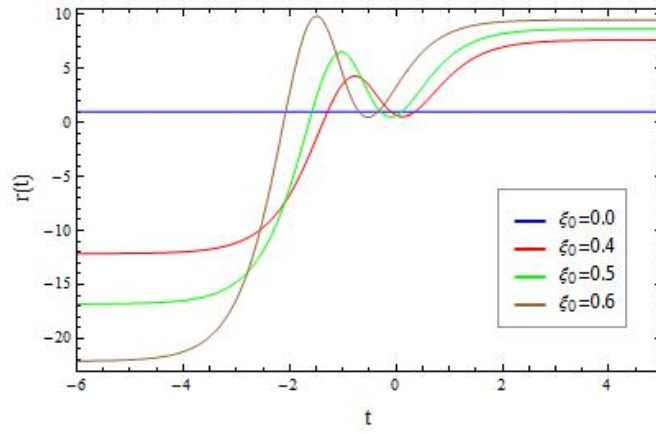
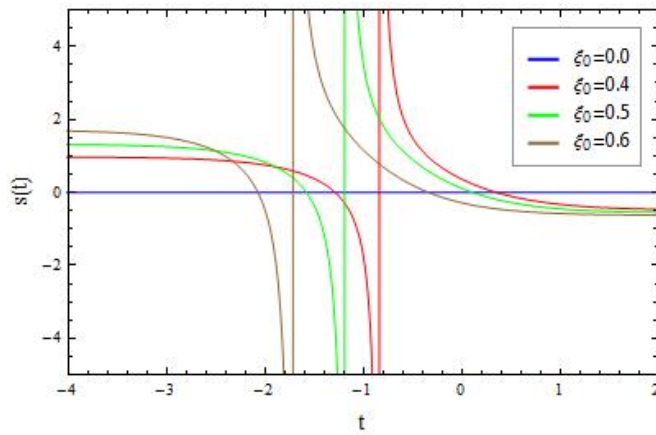
(a) $q(t)$.(b) $r(t)$.(c) $s(t)$.

Figure 5.4: The deceleration parameter as a function of time for the Λ CDM model with and without viscosity is displayed in Fig.5.4(a). Fig.5.4(b) shows the statefinder parameter r as a function of time for the Λ CDM model with and without viscosity. Fig.5.4(c) shows the statefinder parameter s as a function of time for the Λ CDM model with and without viscosity. Here we have set $\rho_\Lambda = t_0 = H_0 = \kappa = 1$, for simplicity.

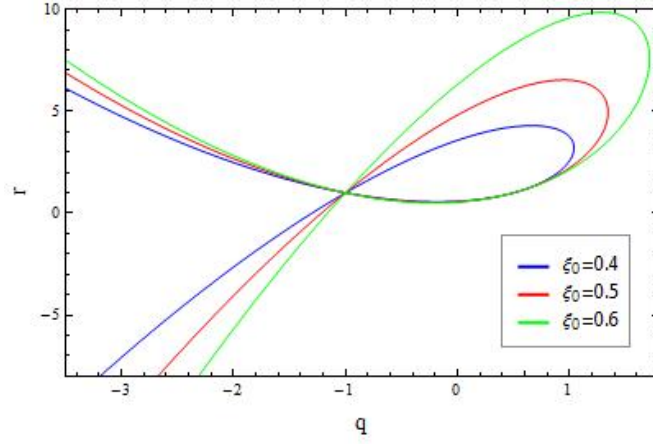
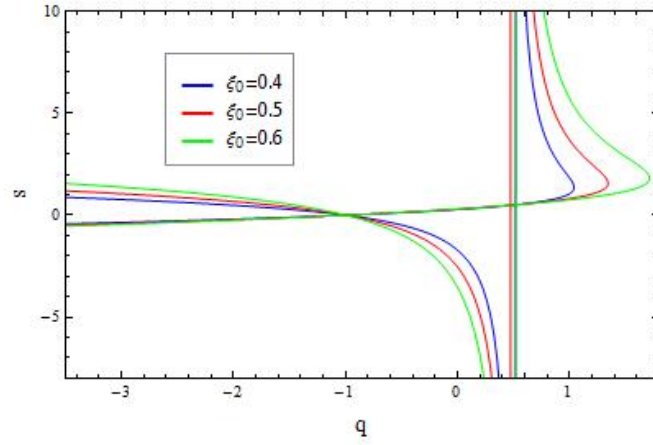
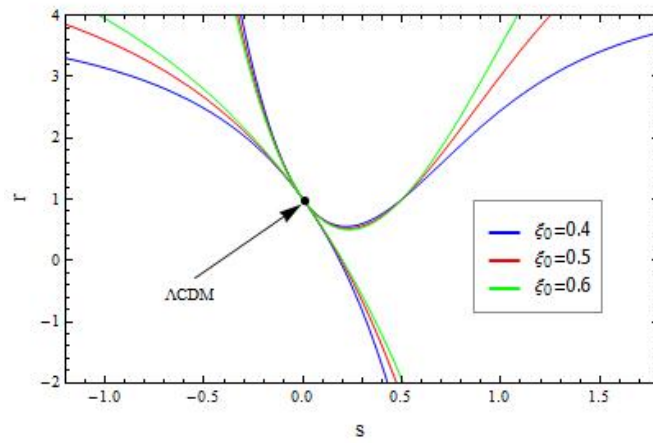
(a) q - r -plane.(b) q - s -plane.(c) s - r -plane

Figure 5.5: The q - r plane for the Λ CDM model with and without viscosity is plotted in Fig.5.5(a). Fig.5.5(b) shows the q - s plane for the Λ CDM model with and without viscosity. Fig.5.5(c) shows the s - r plane for the Λ CDM model with and without viscosity. The point $\{0,1\}$ corresponds to the values of the statefinder parameters for the Λ CDM model with no viscosity. Here we have set $\rho_\Lambda=t_0=H_0=\kappa=1$, for simplicity.

5.4 Universe Models Dominated by a Viscous Cosmic Fluid

We will in this section consider flat universe models dominated by a viscous cosmic fluid with $w > -1$. For this model Friedmann's equations in (5.13) and (5.14) reduces to

$$H^2 = (\kappa/3)\rho, \quad (5.45)$$

$$\frac{\ddot{a}}{a} = -\frac{\kappa}{6}(\rho + 3p_{\text{eff}}), \quad (5.46)$$

where ρ is the density of the viscous fluid, and p_{eff} is the effective pressure of the fluid given by equation (5.15).

The Raychaudhuri equation for this model is then given by

$$\dot{H} + \frac{3}{2}(1+w)H^2 - \frac{3}{2}\kappa\xi_0 H = 0. \quad (5.47)$$

The solution of equation (5.47) is

$$a(t) = a_0 \left[1 + \frac{3}{2}H_0(1+w)t_\xi \left(e^{(t-t_0)/t_\xi} - 1 \right) \right]^{\frac{2}{3(1+w)}}, \quad (5.48)$$

where a_0 and t_0 are constants of integration, and t_ξ is defined as

$$t_\xi = \left(\frac{3}{2}\kappa\xi_0 \right)^{-1}. \quad (5.49)$$

If we assume that $a(0) = 0$, the equation (5.48) will give the following condition

$$H_0 t_\xi = \frac{2}{3(1+w)(1 - e^{-t_0/t_\xi})}. \quad (5.50)$$

When we use the normalization $a(t_0) = a_0 = 1$, the equation (5.48) for the scale factor, reduces to

$$a(t) = \left(\frac{e^{t/t_\xi} - 1}{e^{t_0/t_\xi} - 1} \right)^{\frac{2}{3(1+w)}}. \quad (5.51)$$

The Hubble parameter is then

$$H(t) = H_0 \frac{1 - e^{t_0/t_\xi}}{1 - e^{t/t_\xi}}. \quad (5.52)$$

For this model the equation (5.24) for the deceleration parameter and equation (5.25) for the statefinder parameter r reduces to

$$q = \frac{1}{2}(1 + 3w\Omega_X - 3\kappa\xi_0/H). \quad (5.53)$$

$$r = 1 + \frac{9}{2}w(1+w) - \frac{9}{4}\left(1 + 3w - \frac{\kappa\xi_0}{H}\right)\frac{\kappa\xi_0}{H}. \quad (5.54)$$

The statefinder parameter s for this universe model is then

$$s = \frac{1}{2} \left(1 + 2w - \frac{\kappa\xi_0}{H} + \frac{1}{1 - \frac{\kappa\xi_0}{wH}} \right). \quad (5.55)$$

When we factorize the expression (5.54), we obtain

$$r = 1 + \frac{9}{4} \left(1 + w - \frac{\kappa \xi_0}{H} \right) \left(2w - \frac{\kappa \xi_0}{H} \right). \quad (5.56)$$

Then, the statefinder parameter s is given by

$$s = \frac{1}{2} \frac{\left(1 + w - \frac{\kappa \xi_0}{H} \right) \left(2w - \frac{\kappa \xi_0}{H} \right)}{w - \frac{\kappa \xi_0}{H}}. \quad (5.57)$$

Now that we have the expression for the Hubble parameter (5.52) we can insert this equation into equations (5.56) and (5.57), and by using equation (5.49) and (5.50), we will get the following expressions for the statefinder parameters

$$r = 1 - \frac{9}{4} (1 + w^2) e^{-t/t_\xi} + \frac{9}{4} (1 + w)^2 e^{-2t/t_\xi}. \quad (5.58)$$

$$s = \frac{1}{2} (1 + w) \frac{1 - w - (1 + w) e^{-t/t_\xi}}{e^{t/t_\xi} - 1 - w}. \quad (5.59)$$

In Fig.5.6 we have drawn the s - r plane for this model. The trajectories with bigger values of w are more parabola-like.

The effective pressure of this viscous fluid was given by

$$p_{\text{eff}} = p - 3\xi_0 H. \quad (5.60)$$

Using Friedmann's 1. equation, the expression for the effective pressure becomes

$$p_{\text{eff}} = w\rho - \xi_0 \sqrt{3\kappa\rho}. \quad (5.61)$$

The equation of continuity for this model is given by

$$\dot{\rho} + \sqrt{3\kappa}(1 + w)\rho^{3/2} - 3\kappa\xi_0\rho = 0, \quad (5.62)$$

If we consider a flat FRW universe model dominated by a dark energy with a non-linear equation of state (see Refs. [38] [16]) given by

$$p = w\rho + A\sqrt{\rho}, \quad (5.63)$$

where w and A are constants, we obtain the same equation of continuity as in (5.62). We can interpret the expression for the effective pressure as a nonlinear equation of state for a fluid. This means that the expansion behaviour of a model dominated by a viscous fluid, is the same as for a model dominated by a fluid with a nonlinear equation of state. Furthermore the expressions for the statefinder parameters will be the same, and this means that we can not distinguish these two models just with statefinder parameters.

From the expression for the Hubble parameter we see that the initial value of the Hubble parameter is $H(0) = \infty$, and when $t \rightarrow \infty$ we get the following value for the Hubble parameter

$$\begin{aligned} \lim_{t \rightarrow \infty} H(t) &= \lim_{t \rightarrow \infty} H_0 \frac{1 - e^{t_0/t_\xi}}{1 - e^{t/t_\xi}} \\ &= H_0 \left(1 - e^{-t_0/t_\xi} \right) \\ &= \frac{2}{3(1 + w)t_\xi} = \frac{\kappa \xi}{1 + w} \equiv H_\infty. \end{aligned} \quad (5.64)$$

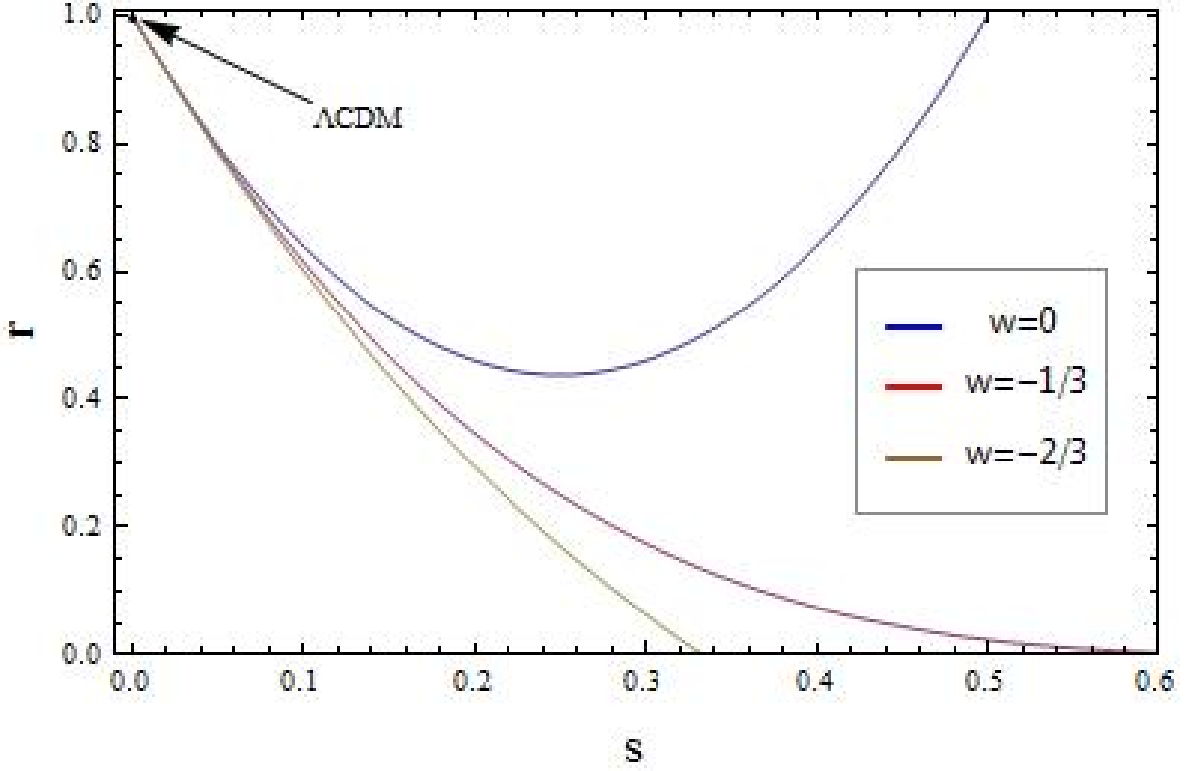


Figure 5.6: The s - r plane for a model dominated by a viscous cosmic fluid. The trajectories are plotted for $t \in [0, \infty]$. We can see from this figure that the bigger the value of w is, the more parabola-like the trajectory is.

I. Brevik [37] has given an estimation for the value of ξ . From the definition of the time t_ξ in equation (5.49), we know that it depends on the value of the ξ , and for small values of viscosity we will get larger values for t_ξ . Brevik has found that at $t = 1000s$ after the Big Bang $t_\xi \approx 10^{21}y$. Hence, for $t > 1000s$ we have that $e^{t/t_\xi} \approx 1$. Equation (5.50) then gives to lowest order in t/t_ξ ,

$$w \approx \frac{2}{3H_0 t_0} - 1 \approx -\frac{1}{3}. \quad (5.65)$$

The values of the statefinder parameters for the Λ CDM which are favoured by observations are $\{r, s\} = \{1, 0\}$. For the universe models in this section we obtain these values for the statefinder parameters at two points of time

$$H(t_1) = \frac{\kappa\xi}{1+w}, \quad H(t_2) = \frac{\kappa\xi}{2w}. \quad (5.66)$$

For $w < 0$ only t_1 corresponds to an expanding universe. Comparing with equation (5.64) we see that $H(t_1) = H_\infty$. Hence, the statefinder parameters of these universe models approach the favoured value in the infinite future.

5.5 Quiescence Model with Constant Bulk Viscosity

The quiescence model is one of the simplest models of dark energy with an equation of state in the form

$$p_x = w_x \rho_x, \quad (5.67)$$

where $w_x < -1/3$, is a constant. We will assume that there is no interaction between the dark energy component x and the matter component m . For this model the equations (5.3) and (5.5) are satisfied for both components. For the dark energy component, x , equation (5.5) can be rewritten as

$$\frac{d\rho_x}{(1 + w_x)\rho_x - \sqrt{3\kappa\xi_0}\sqrt{\rho_x}} = -3\frac{da}{a}. \quad (5.68)$$

Integrating this equation we obtain

$$\rho_x = \left(\frac{\kappa\xi_0}{1 + w_x} + B(1 + z)^{\frac{3(1+w_x)}{2}} \right)^2, \quad (5.69)$$

where z is the redshift and B is an integration constant given as

$$B = \rho_{x0}^{1/2} - \frac{\kappa\xi_0}{1 + w_x}, \quad (5.70)$$

where ρ_{x0} is the present dark energy density. For the non-relativistic matter component the equations (5.3) and (5.5) give the following solution

$$\rho_m = \rho_{m0}(1 + z)^3, \quad (5.71)$$

where ρ_{m0} is the present matter density. The total energy density, which is given by the equation 5.28, is then

$$\rho = \left(\frac{\kappa\xi_0}{1 + w_x} + B(1 + z)^{\frac{3(1+w_x)}{2}} \right)^2 + \rho_{m0}(1 + z)^3. \quad (5.72)$$

In Fig.5.7, we have drawn the relation between energy density, ρ , and redshift, z . We have divided the trajectories into two classes, trajectories with $w_x > -1$ and trajectories with $w_x < -1$, while $w_x = -1$ corresponds to a singularity that is shown in equation (5.69).

We will now investigate the effects of the bulk viscosity for this model by using the relative changing rate parameter ς . For a small change of the redshift, Δz , we have the following expression for the ς

$$\varsigma = \frac{|\rho(z + \Delta z) - \rho(z)|}{\rho(z)}. \quad (5.73)$$

After using the same analysis as in the previous subsection, we can conclude that the bulk viscosity stabilizes the evolution of the density in this model.

Inserting equation (5.72) in equation (5.3) we obtain the following expression for the Hubble parameter

$$H(z) = H_0 \left[\frac{\kappa}{3H_0^2} \left(\frac{3\xi_0}{1 + w_x} + B(1 + z)^{\frac{3(1+w_x)}{2}} \right)^2 + \Omega_{m0}(1 + z)^3 \right]^{\frac{1}{2}}. \quad (5.74)$$

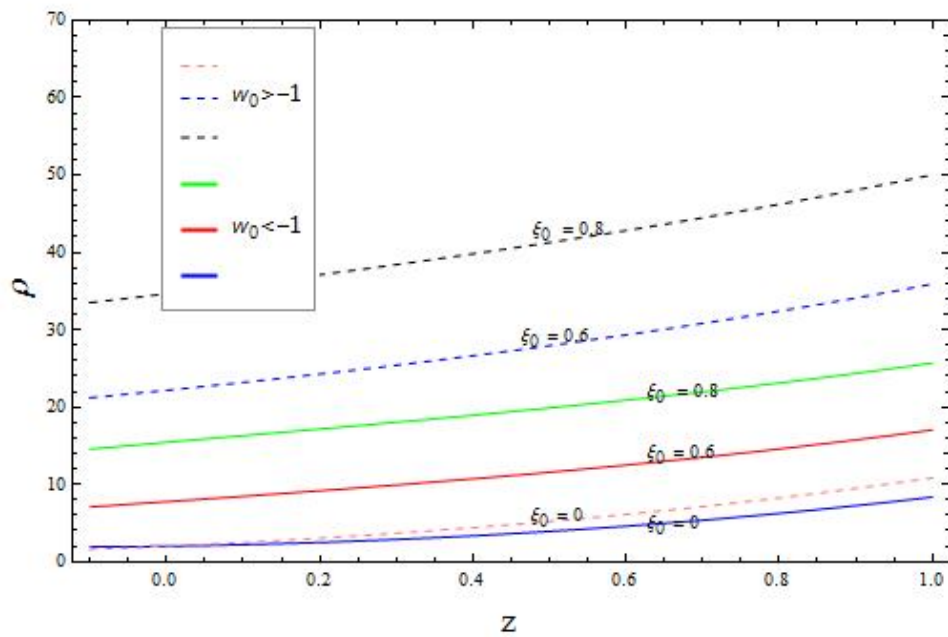


Figure 5.7: The relation between density ρ and the redshift z for the three different values of ξ_0 and two different values of w_0 . Here we set for simplicity $B = C = 1$ and $w_0 = -0.5$ ($w_0 > -1$) and $w_0 = -1.5$ ($w_0 < -1$).

The deceleration parameter and the statefinder pair of the quiescence model can be obtained, if we insert the total density $\rho = \rho_m + \rho_x$ and pressure $p = w_x \rho_x$ into Eqs.(5.9),(5.10) and (5.11). The results are

$$q = \frac{1}{2} \left(3w_x \Omega_x - 3 \frac{\kappa \xi_0}{H} + 1 \right), \quad (5.75)$$

$$r = \frac{9}{2} (1 + w_x) w_x \Omega_x - \frac{9}{4} \frac{\kappa \xi_0}{H} \left[w_x \Omega_x - \frac{\kappa \xi_0}{H} + 1 \right] + 1, \quad (5.76)$$

$$s = \frac{(1 + 2w_x) w_x \Omega_x}{2 \left(w_x \Omega_x - \frac{\kappa \xi_0}{H} \right)} - \frac{1}{2} \frac{\kappa \xi_0}{H} + \frac{1}{2}, \quad (5.77)$$

where the Ω_x is the dark energy density parameter defined by $\Omega_x \equiv \frac{\kappa \rho_x}{3H^2}$. Thus, the deceleration parameter and statefinder parameters are expressed by the redshift z after considering equations (5.3) and (5.74).

In Fig.5.8 we have drawn the s - r plane for this model. From this figure we see that $w_x = -1$ in Fig.5.8(c) is the border-case and divides trajectories into curves with $w_x < -1$ in Fig.5.8(a) and curves with $w_x > -1$ in Fig.5.8(b). This border case is also called 'phantom divide' (see Ref. [36]). The point $\{0, 1\}$, which is the statefinder parameter value for Λ CDM model, represents the situation $w_x = -1$ and divides the trajectories. From the evolution directions we see that the universe is approaching a state with $w_x = -1$ and will keep itself stable there, which is consistent with results from lots of data analysis and cosmic simulations as favored to the Λ CDM model for describing later stage universe evolutions.

5.6 Quiescence Model with Variable Bulk Viscosity

In order to discuss the dark energy properties, some authors (see Refs. [39] [41]) have proposed a possible form of bulk viscosity as

$$\xi = \xi_1 H, \quad (5.78)$$

where ξ_1 is a constant. But, this is just a particular situation of the general form

$$\xi = \xi_0 + \xi_1 \frac{\dot{a}}{a} + \xi_2 \frac{\ddot{a}}{a}, \quad (5.79)$$

which is proposed in [42]. In this section we will consider a quiescence model with variable bulk viscosity given by (5.78). For this model Friedmann's 1. equation has the usual form

$$H^2 = \frac{\kappa}{3} (\rho_m + \rho_x), \quad (5.80)$$

Inserting (5.78) in continuity equation (5.5), we obtain the following expression for the dark energy component

$$\dot{\rho}_x = -3H [(1 + w - \kappa \xi_1) \rho_x]. \quad (5.81)$$

We can rewrite this expression as

$$\frac{d\rho_x}{(1 + w - \kappa \xi_1) \rho_x} = -3 \frac{da}{a}. \quad (5.82)$$

Integration of (5.82) gives

$$\rho_x(a) = \rho_{x0} \left(\frac{a_0}{a} \right)^{3(1+w-\kappa \xi_1)} \quad (5.83)$$

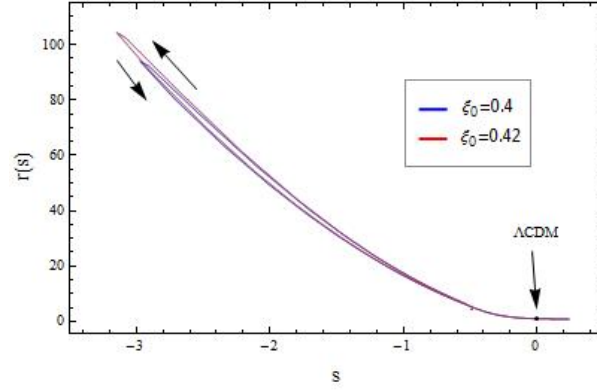
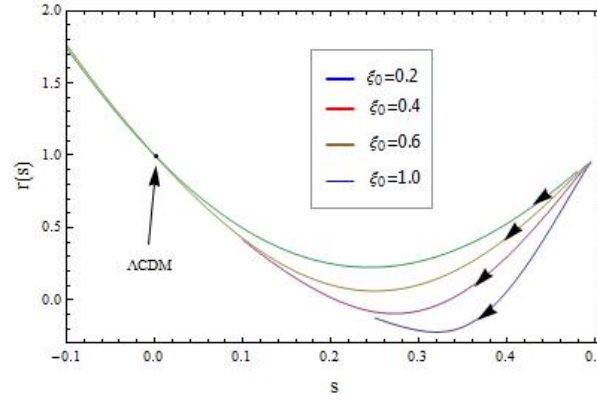
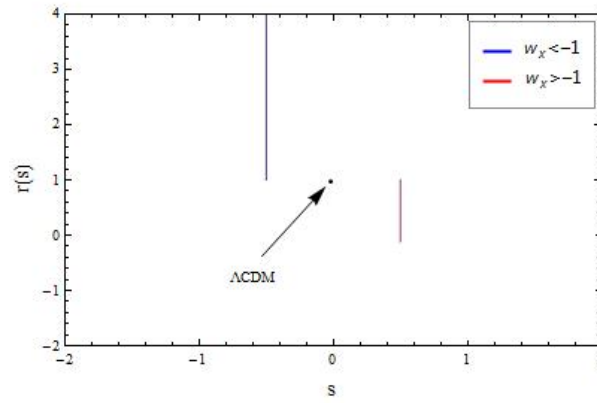
(a) $r(s)$ for $w_x = -1.5$.(b) $r(s)$ for $w_x = -0.5$.(c) $r(s)$ for $\xi_0 = 0.0$.

Figure 5.8: The s - r -plane for the quiescence model. Fig.5.8(a) shows r - s plane for $w_x = -1.5$ and different values of viscosity constant ξ_0 . Fig.5.8(b) also shows $r(s)$, for $w = -0.5$ and different values of ξ_0 . Fig.5.8(c) shows $r(s)$, for $\xi_0 = 0.0$ and for $w_x > -1.0$ and $w_x < -1.0$. The point $\{s, r\} = \{0, 1\}$ is the values for the standard Λ CDM model. Arrows show the direction of the evolution of statefinder parameters with time.

Using the definition of the redshift, $1 + z = \frac{a_0}{a}$, equation (5.83) takes the form

$$\rho_x(z) = \rho_{x0} (1 + z)^{3(1+w-\kappa\xi_1)}. \quad (5.84)$$

Using equation (5.84) and (5.71), we find the following expression for the Hubble parameter

$$H(z) = \left[\frac{\kappa\rho_{x0}}{3} (1 + z)^{3(1+w-\kappa\xi_1)} + \frac{\kappa\rho_{m0}}{3} (1 + z)^3 \right]^{1/2}. \quad (5.85)$$

Replacing ξ_0 in (5.75)-(5.77) with the variable bulk viscosity ξ in (5.78), we find the following expressions for the deceleration parameter and statefinder parameters

$$q = \frac{1}{2} (3w_x\Omega_x - 3\kappa\xi_1 + 1), \quad (5.86)$$

$$r = \frac{9}{2} (1 + w_x)w_x\Omega_x - \frac{9}{4}\kappa\xi_1 (w_x\Omega_x - \kappa\xi_1 + 1) + 1, \quad (5.87)$$

$$s = \frac{(1 + 2w_x)w_x\Omega_x}{2(w_x\Omega_x - \kappa\xi_1)} - \frac{1}{2}\kappa\xi_1 + \frac{1}{2}. \quad (5.88)$$

In Fig.5.9 and Fig.5.10 we have plotted the Hubble parameter and the energy density, respectively. From these figures we can see that for the different values of w_x and ξ_1 that we use here, the Hubble parameter and the energy density have infinitely large values at the initial epoch of the cosmic evolution. As $z \rightarrow 0$, the Hubble parameter and the energy density will decay to

$$H(0) \equiv H_0 = \sqrt{\frac{\kappa}{3}(\rho_{x0} + \rho_{m0})}, \quad \text{and} \quad \rho(0) \equiv \rho_0 = \frac{\kappa}{3}(\rho_{x0} + \rho_{m0}), \quad (5.89)$$

respectively. From $z = 0$ and as z decreases, for smaller values of w_x and for bigger values of ξ_1 , the Hubble parameter and the energy density will increase rapidly, and they will eventually be infinitely large. The bigger the value of ξ_1 is, the faster they will diverge. For bigger values of w_x and for smaller values of ξ_1 , the Hubble parameter and the energy density will tend to zero as $z \rightarrow -\infty$.

In Fig.(5.11) we have drawn r - s plane by using the Hubble parameter in (5.85). From Fig.5.11(c) we can see that when there is no viscosity, i.e. $\xi_1 = 0$, we obtain the same plot as in Fig.5.8(c), which is what we will expect. From Fig.5.11(a), which shows the r - s plane for $w_x = -1.5$ and different values of ξ_1 , we can see that for small values of ξ_1 the curves will go through the point $\{0, 1\}$, which is the statefinder parameter value for Λ CDM model and represents the situation with no viscosity and $w_x = -1$. In Fig.5.11(b) we have plotted the r - s plane for $w_x = -0.7$ and different values of ξ_1 . We can see from this figure that only the curve with $\xi_1 = 0.3$ that goes through the point for Λ CDM model.

5.7 Models with variable bulk viscosity and equation of state

In this section we will discuss the viscous dark energy model with variable equation of state parameter w , and a variable bulk viscosity given by (5.78). We will consider a universe model with one component that follows the equation of state

$$p = (\gamma - 1)\rho + p_1, \quad (5.90)$$

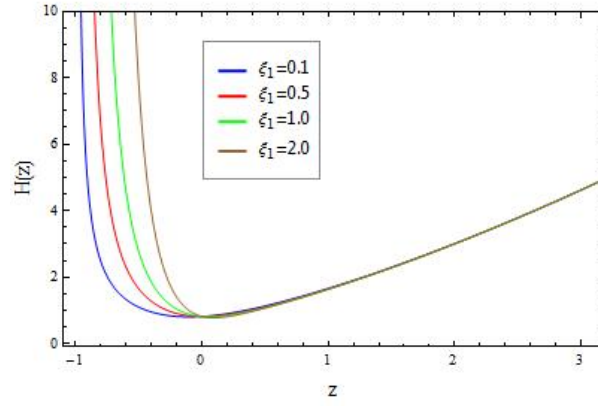
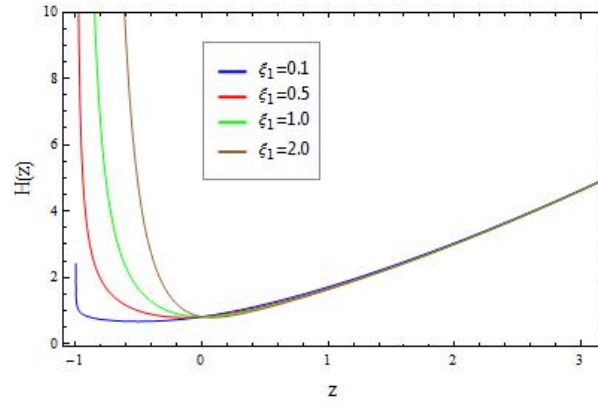
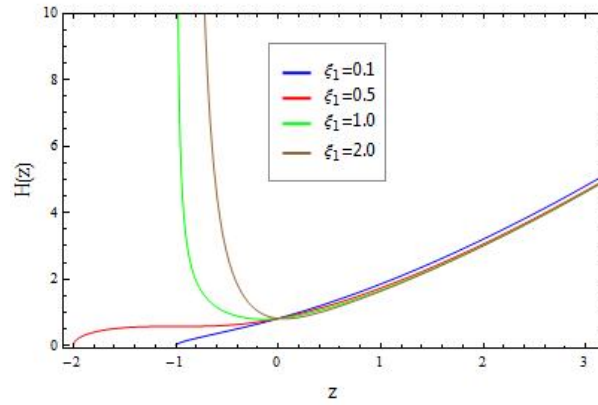
(a) $H(z)$ for $w_x = -1.5$.(b) $H(z)$ for $w_x = -1.0$.(c) $H(z)$ for $w_x = -0.5$.

Figure 5.9: The Hubble parameter as a function of the redshift for the quiescence model for different values of w_x and ξ_1 . Here we set $\rho_{x0} = \rho_{m0} = \kappa = 1$, for simplicity.

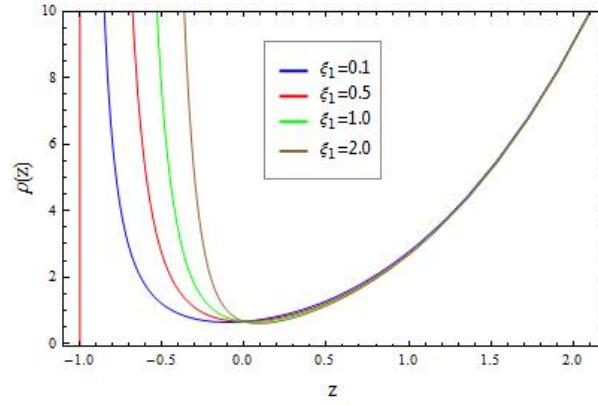
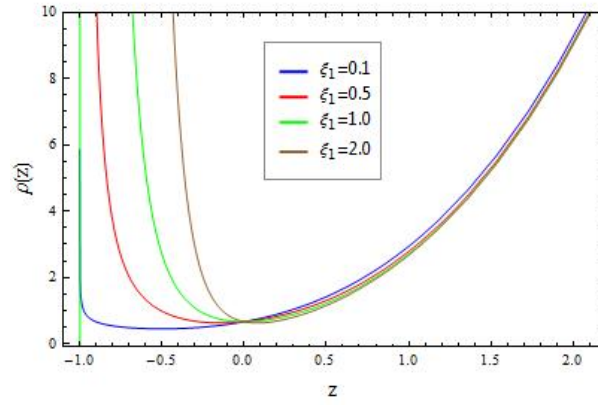
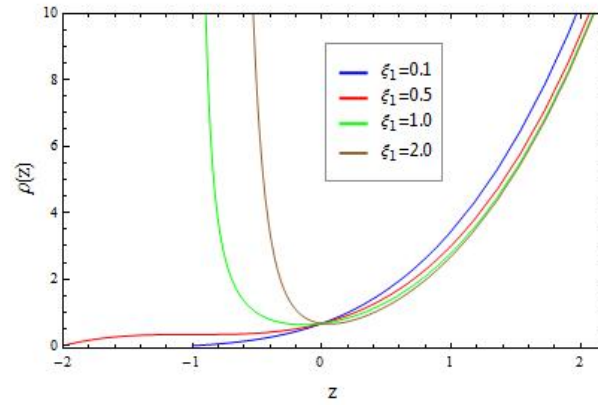
(a) $\rho(z)$ for $w_x = -1.5$.(b) $\rho(z)$ for $w_x = -1.0$.(c) $\rho(z)$ for $w_x = -0.5$.

Figure 5.10: The total energy density as a function of the redshift for the quiescence model for different values of w_x and ξ_1 . Here we set $\rho_{x0} = \rho_{m0} = \kappa = 1$, for simplicity.

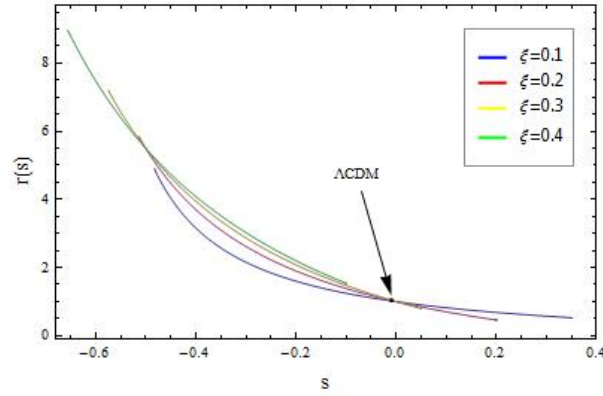
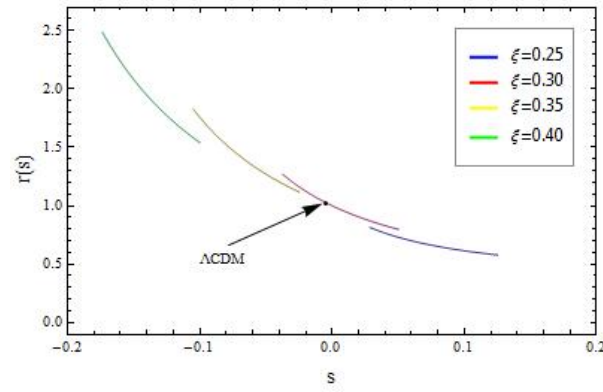
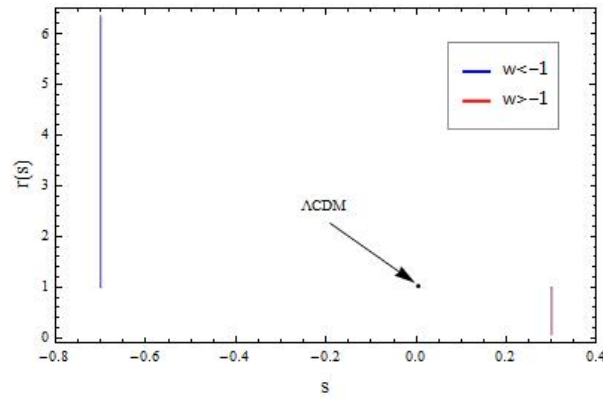
(a) $r(s)$ for $w_x = -1.5$.(b) $r(s)$ for $w_x = -0.7$.(c) $r(s)$ for $\xi_1 = 0.0$.

Figure 5.11: The s - r -plane for the quiescence model. Fig.5.11(a) shows r - s plane for $w_x = -1.5$ and different values of viscosity constant ξ_1 . Fig.5.11(b) also shows $r(s)$, for $w = -0.7$ and different values of ξ_1 . Fig.5.11(c) shows $r(s)$, for $\xi_1 = 0.0$ and for $w_x > -1.0$ and $w_x < -1.0$. The point $\{s, r\} = \{0, 1\}$ is the values for the standard Λ CDM model.

where p_1 is a constant, and $\gamma - 1$ is equivalent to the state parameter w . In this section, we set $\frac{\kappa}{3} = 1$, for simplicity. We put equations (5.78) and (5.90) into the continuity equation (5.5), and by using equation (5.3) we obtain

$$\begin{aligned}\dot{\rho} &= -3H [\rho + (\gamma - 1)\rho + p_1 - 3\xi_1 H^2] \\ &= -3H [p_1 + (\gamma - 3\xi_1)\rho].\end{aligned}\quad (5.91)$$

We can rewrite this equation as

$$\frac{d\rho}{p_1 + (\gamma - 3\xi_1)\rho} = -3\frac{da}{a}.\quad (5.92)$$

By integrating both sides of this equation we obtain

$$\rho(a) = \rho_0 \left[\left(1 + \frac{p_1}{\rho_0 \tilde{\gamma}} \right) \left(\frac{a}{a_0} \right)^{-3\tilde{\gamma}} - \frac{p_1}{\rho_0 \tilde{\gamma}} \right],\quad (5.93)$$

or

$$\rho(z) = \rho_0 \left[\left(1 + \frac{p_1}{\rho_0 \tilde{\gamma}} \right) (1+z)^{3\tilde{\gamma}} - \frac{p_1}{\rho_0 \tilde{\gamma}} \right],\quad (5.94)$$

where $\tilde{\gamma} \equiv \gamma - 3\xi_1$. Now that we have the expression for the density, we can solve Friedmann's first equation (5.3). Inserting equation (5.93) in equation (5.3) we obtain

$$\left(\frac{\dot{a}}{a} \right)^2 = \rho_0 \left[\left(1 + \frac{p_1}{\rho_0 \tilde{\gamma}} \right) \left(\frac{a}{a_0} \right)^{-3\tilde{\gamma}} - \frac{p_1}{\rho_0 \tilde{\gamma}} \right].\quad (5.95)$$

We rewrite this equation as

$$\sqrt{\frac{\tilde{\gamma}}{p_1}} \frac{da}{a \sqrt{\left(1 + \frac{\rho_0 \tilde{\gamma}}{p_1} \right) \left(\frac{a}{a_0} \right)^{-3\tilde{\gamma}} - 1}} = dt\quad (5.96)$$

Now we can integrate both sides of this equation by substitution. If $\tilde{\gamma} > 0$ we obtain

$$a(t) = a_0 \left[\cos \left(\frac{t - t_0}{2T_2} \right) + \theta_0 \tilde{\gamma} T_2 \sin \left(\frac{t - t_0}{2T_2} \right) \right]^{\frac{2}{3\tilde{\gamma}}},\quad (5.97)$$

and if $\tilde{\gamma} < 0$ we obtain

$$a(t) = a_0 \left[\cosh \left(\frac{t - t_0}{2T_1} \right) + \theta_0 \tilde{\gamma} T_1 \sinh \left(\frac{t - t_0}{2T_1} \right) \right]^{\frac{2}{3\tilde{\gamma}}},\quad (5.98)$$

where $T_1 \equiv \frac{1}{3\sqrt{-\tilde{\gamma}p_1}}$ and $T_2 \equiv \frac{1}{3\sqrt{\tilde{\gamma}p_1}}$ and ρ_0 , θ_0 and t_0 are the present energy density, expansion scalar and cosmic time, respectively.

For $\tilde{\gamma} = 0$, equation (5.92) reduces to

$$\frac{d\rho}{p_1} = -3\frac{da}{a}.\quad (5.99)$$

Integrating (5.99), we obtain

$$\rho = \rho_0 + 3p_1 \ln \left(\frac{a_0}{a} \right),\quad (5.100)$$

or

$$\rho = \rho_0 + 3p_1 \ln(1+z). \quad (5.101)$$

Inserting equation (5.100) in equation (5.3) we obtain

$$\left(\frac{\dot{a}}{a}\right)^2 = \rho_0 + 3p_1 \ln\left(\frac{a_0}{a}\right). \quad (5.102)$$

We rewrite this equation as

$$\frac{da}{a\sqrt{\rho_0 + 3p_1 \ln\left(\frac{a_0}{a}\right)}} = dt. \quad (5.103)$$

Integrating equation (5.103) we obtain

$$a(t) = a_0 e^{\sqrt{\rho_0}(t-t_0) - \frac{3p_1}{4}(t-t_0)^2}. \quad (5.104)$$

In Fig.5.12 we have drawn the scalar factor as a function of time for these three cases in equations (5.97), (5.98) and (5.104). For the case when $\tilde{\gamma} = 0$, we can see from Fig.5.12(b), that at $t = -\infty$ the scale factor is zero, but, the Hubble parameter and the energy density diverge. This means that there is singularity at $t = -\infty$, and the universe starts with a big bang. As t increases, the scale factor will also increase, whereas the Hubble parameter and the energy density decrease. At a point of time, $t > 0$, the scale factor reaches its maximum value, but, at this point the energy density and the Hubble parameter are zero. From this point on, and as $t \rightarrow \infty$, the scale factor decays to zero, whereas the Hubble parameter and the energy density diverge. We can see that for this model the universe both starts and ends up with a bang.

From Fig.5.12(a) we can compare the two cases $\tilde{\gamma} > 0$ and $\tilde{\gamma} < 0$, and we can find which of them are in accordance with cosmic acceleration expansion. We can see that for the case $\tilde{\gamma} < 0$, $a(t)$ can explain the cosmic acceleration expansion in the late evolution universe. But in the case of $\tilde{\gamma} > 0$ it is impossible to do so, because there are periods where the scale factor, $a(t)$, disappears. Therefore we only consider the case $\tilde{\gamma} < 0$ in equation (5.98).

From the equation (5.98), we calculate \dot{a}

$$\dot{a}(t) = \frac{a}{3\tilde{\gamma}T_1} x^{\frac{3\tilde{\gamma}}{2}} \left[\sinh\left(\frac{t-t_0}{2T_1}\right) + W \cosh\left(\frac{t-t_0}{2T_1}\right) \right], \quad (5.105)$$

where $x = 1+z = a_0/a$ is the redshift, and W is defined as $W \equiv \theta_0 \tilde{\gamma} T_1$. We know that in the late universe evolution $\dot{a} > 0$ and $a > 0$, and for $\tilde{\gamma} < 0$ we get $T_1 > 0$. Then, by using equation (5.105) we find that

$$W < \frac{1 - \exp\left(\frac{t-t_0}{T_1}\right)}{1 + \exp\left(\frac{t-t_0}{T_1}\right)}. \quad (5.106)$$

For $t \rightarrow \infty$, the right hand side of the above equation becomes

$$-1 < \frac{1 - \exp\left(\frac{t-t_0}{T_1}\right)}{1 + \exp\left(\frac{t-t_0}{T_1}\right)},$$

which gives the following constraint on W

$$W \leq -1.$$

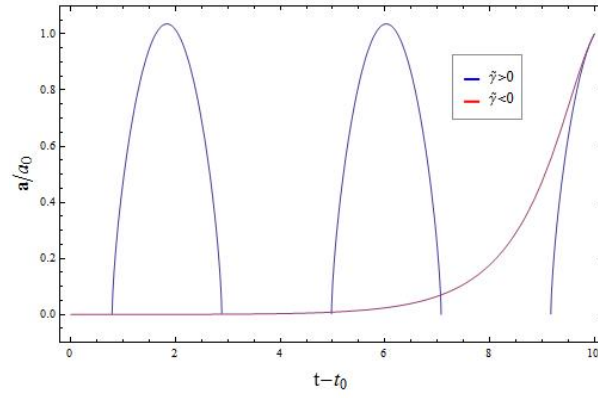
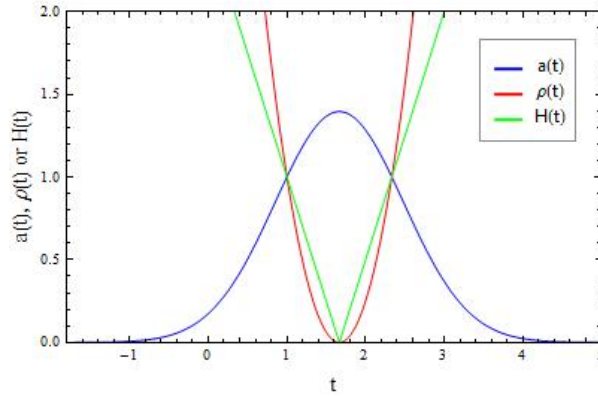
(a) $a(t)$.(b) $a(t)$, $\rho(t)$ and $H(t)$ for $\tilde{\gamma} = 0$.

Figure 5.12: Fig.5.12(a) shows the scale factor $a(t)$ for the two cases $\tilde{\gamma} > 0$ and $\tilde{\gamma} < 0$. Fig.5.12(b) shows the scale factor, $a(t)$, the energy density, $\rho(t)$ and the Hubble parameter $H(t)$ for the case when $\tilde{\gamma} = 0$. Here we have set $\rho_0 = H_0 = a_0 = t_0 = p_1 = 1$, for simplicity.

Hu and Meng [21] have done statistical analyses based on cosmological observations data presented by Riess et al. [19], and they have found that the best value of W which is consistent with $\tilde{\gamma} < 0$ is $W = -1$. This gives for the parameter $\tilde{\gamma}$

$$\tilde{\gamma} = \gamma - 3\xi_1 = -\frac{9p_1}{\theta_0^2} = -\frac{p_1}{\rho_0}.$$

using this result the equation (5.93) reduces to

$$\rho = \rho_0,$$

which is a constant, and consequently the pressure p also is a constant. In this case equation (5.98) reduces to

$$a(t) = a_0 e^{\sqrt{\rho_0}(t-t_0)}, \quad (5.107)$$

Which is the scale factor for the de Sitter model. This means that when we use the observational data to determine W , we find that the energy density is a constant and scale factor is given by (5.107), therefore, we obtain a de Sitter universe model.

Now we will give the expressions for deceleration parameter and statefinder parameters for this model. Using the definitions for this parameters, equations (5.9)-(5.11), we obtain

$$q = \frac{3}{2}V - 1, \quad (5.108)$$

$$r = \frac{9}{2}V(\tilde{\gamma} - 1) + 1, \quad (5.109)$$

$$s = \frac{V(\tilde{\gamma} - 1)}{V - 1}, \quad (5.110)$$

where V is defined as $V \equiv \left(\frac{p_1}{\rho} + \tilde{\gamma}\right)$.

For the de Sitter model that we found above, when the parameter W takes the value $W = -1$, we obtain $V = 0$ and $\{r, s\} = \{1, 0\}$, which are the same values for statefinder parameters as in the Λ CDM model. We have plotted the s - r plane for the universe model with $\tilde{\gamma} < 0$ in Fig.5.13. From this figure we can see that the trajectories have a hyperbola-like form, and the statefinder parameters are moving toward the point for the Λ CDM model in the late cosmic evolution.

In Fig.5.14, we have plotted the deceleration parameter, the statefinder parameters and the s - r plane for this model when $\tilde{\gamma} = 0$. From Fig.5.14(a) we can see the time evolution of the deceleration parameter and the statefinder parameters. At $t = -\infty$ the deceleration parameter is $q = -1$, and the statefinder parameters r and s , are very close to 1 and 0, respectively. As t increases they will differ from these values. And, at a point of time they will diverge. As $t \rightarrow \infty$ the deceleration parameter will approach the value $q = -1$, and the statefinder parameters will come close to the values $s = 0$ and $r = 1$. From Fig.5.14(b) we can see that from $t = -\infty$, as t increases, the statefinder parameters go away from the point $\{0, 1\}$ for the Λ CDM model. From a point of time, $t > 0$, as $t \rightarrow \infty$ the statefinder parameters will start to move toward the point $\{0, 1\}$ for the Λ CDM model.

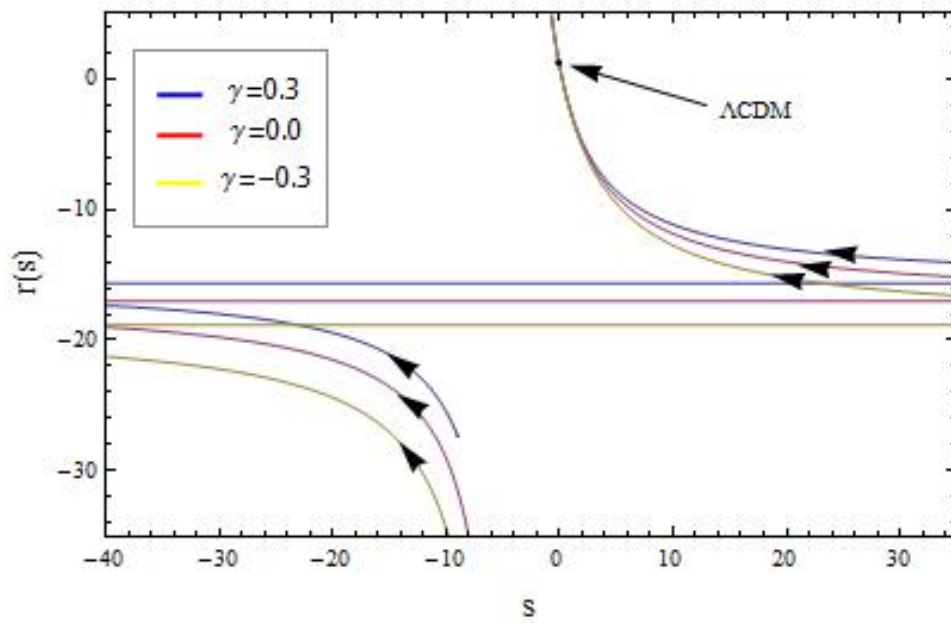


Figure 5.13: The s - r plane for a model with variable bulk viscosity and equation of state. The trajectories have a hyperbola-like form. The arrows shows how the statefinder parameters are changing with time, and that they move toward the point for the ΛCDM model in the late cosmic evolution.

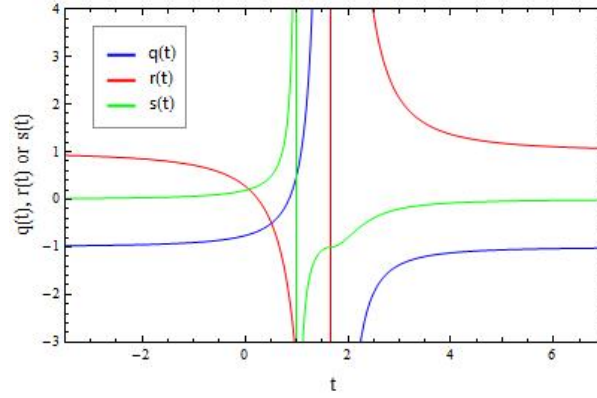
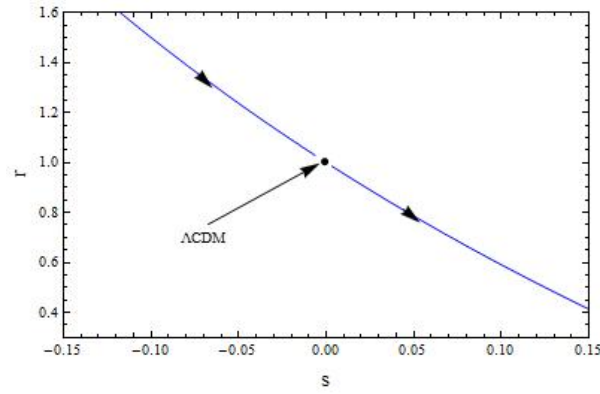
(a) $q(t)$, $r(t)$ and $s(t)$ for the case $\tilde{\gamma} = 0$.(b) s - r -plane for the case $\tilde{\gamma} = 0$.

Figure 5.14: Fig.5.14(a) shows the deceleration parameter $q(t)$, statefinder parameters $r(t)$ and $s(t)$ for the case $\tilde{\gamma} = 0$. Fig.5.14(b) shows the s - r plane for the case when $\tilde{\gamma} = 0$. Here we have set $\rho_0 = H_0 = a_0 = t_0 = p_1 = 1$, for simplicity.

Chapter 6

Bianchi Type-I Universe Models

Spatially homogeneous and isotropic universes can be well described by Friedmann-Robertson-Walker (FRW) model. However, the FRW model has the disadvantage of being unstable near the singularity and it fails to describe the early universe. Therefore spatially homogeneous and anisotropic Bianchi type-I models are undertaken to understand the universe at its early stage of evolution. In this chapter we will consider Bianchi type-I universe models, after the Italian mathematician Luigi Bianchi (1856-1928).

Bianchi type-I universe model is the simplest model of anisotropic universe that describes a homogeneous and spatially flat space-time and if filled with perfect fluid with the equation of state $p = w\rho$, $w < 1$, eventually evolves into a FRW universe [47]. The isotropy of present-day universe makes BI model a prime candidate for studying the possible effects of an anisotropy in the early universe on modern-day data observations.

Bianchi type-I universe model with viscous fluid have been studied by some cosmologists. The influence of viscosity on Bianchi type-I model have been investigated by Belinski and Khalatnikov [64], and they have concluded that asymptotically for large times, Bianchi type-I model will approach an isotropic steady-state universe model with a de Sitter space which expands exponentially. And, for asymptotically small times, there exist a Kasner era in which the effects of matter, radiation and viscosity are negligible. Other authors ([65] [66] [67]) have also concluded that anisotropical models have in general a vacuum stage near an unavoidable initial singularity in which the energy-momentum tensor has no influence on the cosmic evolution. But, Grøn [12] have found that in a Bianchi type-I universe model filled with viscous Zel'dovich fluid, the bulk viscosity may remove the initial singularity. And, he also concluded that the viscosity has an important role in isotropization of the universe. In the last section of this chapter, we find results which are in agreement with Grøn's conclusion.

Bijan Saha [51] have studied Bianchi type-I universe model with viscous fluid. And, he have found that when the shear viscosity is proportional to the Hubble parameter, the universe has an oscillatory mode of expansion, accompanied by an exponential mode. He also concluded that the oscillation is due to viscosity. We will, in this chapter, show that this conclusion has to be modified.

In this chapter, we will study the evolution and the influence of viscosity on a homogeneous and anisotropic Bianchi type-I cosmological model, filled with viscous fluid, both with and without a cosmological constant, Λ . Then, we will apply the statefinder diagnostics to these models, to find which models are in agreement with the observational data.

6.1 Viscous Fluid Cosmology of Bianchi Type-I

The gravitational field in the spatially homogeneous and anisotropic case is given by a Bianchi type I metric, and it has the form

$$ds^2 = dt^2 - R_i^2(t)(dx^i)^2, \quad (6.1)$$

where $R_1 = a(t)$, $R_2 = b(t)$, $R_3 = c(t)$, and $dx^1 = dx$, $dx^2 = dy$ and $dx^3 = dz$. The energy momentum tensor gives the influence of the viscous fluid in the evolution of the Universe, and it acts as the source of the corresponding gravitational field. The energy momentum tensor of a viscous field has the form

$$T_\nu^\mu = \left(\rho + p'\right) u^\mu u_\nu - \delta_\nu^\mu p_{\text{eff}} + \eta g^{\mu\beta} [u_{\nu;\beta} + u_{\beta;\nu} - u_\nu u^\alpha u_{\beta;\alpha} - u_\beta u^\alpha u_{\nu;\alpha}], \quad (6.2)$$

where

$$p_{\text{eff}} = p - \left(\xi - \frac{2}{3}\eta\right) u^\nu_{;\nu}. \quad (6.3)$$

is the effective pressure. Here ξ and η are the coefficients of bulk and shear viscosity, respectively. The bulk and shear viscosities, ξ and η , are both positively definite, i.e., $\xi > 0$, $\eta > 0$. They may be either constant or function of time or energy. The pressure p is connected to the energy density by means of an equation of state describing a perfect fluid, given by

$$p = w\rho. \quad (6.4)$$

In a comoving system of reference such that $u^\mu = (1, 0, 0, 0)$, we have

$$T_0^0 = \rho, \quad (6.5)$$

$$T_1^1 = -p_{\text{eff}} + 2\eta \frac{\dot{a}}{a}, \quad (6.6)$$

$$T_2^2 = -p_{\text{eff}} + 2\eta \frac{\dot{b}}{b}, \quad (6.7)$$

$$T_3^3 = -p_{\text{eff}} + 2\eta \frac{\dot{c}}{c}, \quad (6.8)$$

We will now give the definitions of some physical parameters. We first introduce the volume expansion as

$$\theta \equiv u^\mu_{;\mu} = 3H, \quad (6.9)$$

where we have introduced a generalized Hubble parameter H , in analogy with Hubble parameter in a FRW universe, as

$$3H \equiv \frac{\dot{\tau}}{\tau} \quad (6.10)$$

$$= \left(\frac{\dot{a}}{a} + \frac{\dot{b}}{b} + \frac{\dot{c}}{c} \right) \quad (6.11)$$

$$= H_1 + H_2 + H_3, \quad (6.12)$$

where τ is the volume scale of the BI space-time, and is defined as

$$\tau \equiv abc. \quad (6.13)$$

The definition of the anisotropy parameter, A , is given by

$$A = \frac{1}{3} \sum_{i=1}^3 \left(\frac{\Delta H_i}{H} \right)^2 = \frac{1}{9} \sum_{i < j} \left(\frac{H_i - H_j}{H} \right)^2, \quad \Delta H_i = H_i - H. \quad (6.14)$$

This parameter tells how anisotropic the space is, and $A = 0$ represents an isotropic space. The shear scalar σ is defined by

$$\sigma^2 \equiv \frac{1}{2} \sigma^{\mu\nu} \sigma_{\mu\nu}, \quad (6.15)$$

where

$$\sigma_{\mu\nu} = \frac{1}{2} [u_{\mu;\alpha} (\delta_\nu^\alpha - u^\alpha u_\nu) + u_{\nu;\alpha} (\delta_\mu^\alpha - u^\alpha u_\mu)] - \frac{1}{3} \theta (g_{\mu\nu} - u_\mu u_\nu). \quad (6.16)$$

This gives

$$2\sigma^2 = \sum_{i=1}^3 H_i^2 - 3H^2 \quad (6.17)$$

$$= \frac{1}{3} A \theta^2 \quad (6.18)$$

$$= \frac{\dot{a}^2}{a^2} + \frac{\dot{b}^2}{b^2} + \frac{\dot{c}^2}{c^2} - \frac{1}{3} \theta^2. \quad (6.19)$$

6.1.1 Field equations and their solutions

The Einstein's field equation with the Λ -term is given by

$$G_\nu^\mu = R_\nu^\mu - \frac{1}{2} \delta_\nu^\mu R = \kappa T_\nu^\mu - \delta_\nu^\mu \Lambda. \quad (6.20)$$

Einstein's field equations, (6.20), can be written as

$$\frac{\dot{a}\dot{b}}{ab} + \frac{\dot{b}\dot{c}}{bc} + \frac{\dot{c}\dot{a}}{ca} = \kappa\rho - \Lambda \quad (6.21)$$

$$\frac{\ddot{b}}{b} + \frac{\ddot{c}}{c} + \frac{\dot{b}\dot{c}}{bc} = \kappa \left(-p_{\text{eff}} + 2\eta \frac{\dot{a}}{a} \right) - \Lambda \quad (6.22)$$

$$\frac{\ddot{c}}{c} + \frac{\ddot{a}}{a} + \frac{\dot{c}\dot{a}}{ca} = \kappa \left(-p_{\text{eff}} + 2\eta \frac{\dot{b}}{b} \right) - \Lambda \quad (6.23)$$

$$\frac{\ddot{a}}{a} + \frac{\ddot{b}}{b} + \frac{\dot{a}\dot{b}}{ab} = \kappa \left(-p_{\text{eff}} + 2\eta \frac{\dot{c}}{c} \right) - \Lambda. \quad (6.24)$$

The calculations for finding the Ricci tensor and Ricci scalar R are found in appendix B. Let us now solve the Einstein equations and find the expressions for the metric functions. Subtracting (6.22) from (6.23), (6.22) from (6.24) and (6.23) from (6.24), one finds

$$\frac{\ddot{a}}{a} - \frac{\ddot{b}}{b} + \frac{\dot{c}}{c} \left[\frac{\dot{a}}{a} - \frac{\dot{b}}{b} \right] = -2\kappa\eta \left[\frac{\dot{a}}{a} - \frac{\dot{b}}{b} \right] \quad (6.25)$$

$$\frac{\ddot{a}}{a} - \frac{\ddot{c}}{c} + \frac{\dot{b}}{b} \left[\frac{\dot{a}}{a} - \frac{\dot{c}}{c} \right] = -2\kappa\eta \left[\frac{\dot{a}}{a} - \frac{\dot{c}}{c} \right] \quad (6.26)$$

$$\frac{\ddot{b}}{b} - \frac{\ddot{c}}{c} + \frac{\dot{a}}{a} \left[\frac{\dot{b}}{b} - \frac{\dot{c}}{c} \right] = -2\kappa\eta \left[\frac{\dot{b}}{b} - \frac{\dot{c}}{c} \right] \quad (6.27)$$

Now, dividing (6.25) by $\left[\frac{\dot{a}}{a} - \frac{\dot{b}}{b} \right]$, (6.26) by $\left[\frac{\dot{a}}{a} - \frac{\dot{c}}{c} \right]$ and (6.27) by $\left[\frac{\dot{b}}{b} - \frac{\dot{c}}{c} \right]$, we obtain

$$\frac{\ddot{a}b - \ddot{b}a}{a\dot{b} - \dot{a}b} - \frac{\dot{c}}{c} = -2\kappa\eta \quad (6.28)$$

$$\frac{\ddot{a}c - \ddot{c}a}{a\dot{c} - \dot{a}c} - \frac{\dot{b}}{b} = -2\kappa\eta \quad (6.29)$$

$$\frac{\ddot{b}c - \ddot{c}b}{b\dot{c} - \dot{b}c} - \frac{\dot{a}}{a} = -2\kappa\eta \quad (6.30)$$

Integrating equations (6.28)-(6.30), we get the following relation between a and b , a and b , and a and b

$$\frac{a}{b} = D_1 \exp \left(X_1 \int \frac{e^{-2\kappa \int \eta dt}}{\tau} dt \right) \quad (6.31)$$

$$\frac{b}{c} = D_2 \exp \left(X_2 \int \frac{e^{-2\kappa \int \eta dt}}{\tau} dt \right) \quad (6.32)$$

$$\frac{c}{a} = D_3 \exp \left(X_3 \int \frac{e^{-2\kappa \int \eta dt}}{\tau} dt \right). \quad (6.33)$$

Here $D_1, D_2, D_3, X_1, X_2, X_3$ are integration constants. From the equations (6.31)-(6.37) we can write the metric functions as

$$a(t) = A_1 \tau^{1/3} \exp \left(\frac{B_1}{3} \int \frac{e^{-2\kappa \int \eta dt}}{\tau} dt \right) \quad (6.34)$$

$$b(t) = A_2 \tau^{1/3} \exp \left(\frac{B_2}{3} \int \frac{e^{-2\kappa \int \eta dt}}{\tau} dt \right) \quad (6.35)$$

$$c(t) = A_3 \tau^{1/3} \exp \left(\frac{B_3}{3} \int \frac{e^{-2\kappa \int \eta dt}}{\tau} dt \right). \quad (6.36)$$

where

$$A_1 = \sqrt[3]{(D_1/D_3)}, \quad A_2 = \sqrt[3]{(D_2/D_1)}, \quad A_3 = \sqrt[3]{(D_3/D_2)},$$

$$B_1 = X_1 - X_3, \quad B_2 = X_2 - X_1, \quad B_3 = -X_2 + X_3.$$

And

$$A_1 A_2 A_3 = 1, \quad B_1 + B_2 + B_3 = 0. \quad (6.37)$$

Thus, the metric functions are found explicitly in terms of τ and viscosity. As seen from (6.34)-(6.36) for $\tau = t^n$ with $n > 1$ the exponent tends to unity at large t , and the anisotropic model becomes isotropic.

6.1.2 Equations for determining τ , H and ρ

Summation of Einstein equations (6.22)-(6.24) and 3 times (6.21) gives the following differential equation for τ

$$\ddot{\tau} - \frac{3}{2} \kappa \xi \dot{\tau} = \frac{3}{2} \kappa (\rho - p) \tau - 3\Lambda \tau. \quad (6.38)$$

From Einstein's field equations and the second Bianchi identity follows that the energy-momentum is conserved, i.e.,

$$T_{\nu;\mu}^{\mu} = T_{\nu,\mu}^{\mu} + \Gamma_{\rho\mu}^{\mu} T_{\nu}^{\rho} - \Gamma_{\nu\mu}^{\rho} T_{\rho}^{\mu} = 0, \quad (6.39)$$

which in our case has the form

$$\frac{1}{\tau} (\tau T_0^0) - \frac{\dot{a}}{a} T_1^1 - \frac{\dot{b}}{b} T_2^2 - \frac{\dot{c}}{c} T_3^3 = 0. \quad (6.40)$$

After a little manipulation we obtain

$$\dot{\rho} - \frac{\dot{\tau}}{\tau} (\rho + p) - \left(\xi + \frac{4}{3} \eta \right) \frac{\dot{\tau}^2}{\tau^2} + 4\eta (\kappa \rho - \Lambda) = 0. \quad (6.41)$$

Now, we write the equations (6.38) and (6.41), using the generalized Hubble parameter H in (6.10), as

$$\dot{H} = \frac{\kappa}{2} (3\xi H - (1+w)\rho) - (3H^2 - \kappa\rho + \Lambda), \quad (6.42)$$

$$\dot{\rho} = 3H (3\xi H - (1+w)\rho) + 4\eta (3H^2 - \kappa\rho + \Lambda). \quad (6.43)$$

Using equations (6.34)-(6.36) we can rewrite the shear scale as

$$2\sigma^2 = \frac{6(X_1^2 + X_1X_3 + X_3^2)}{9\tau^2} e^{-4\kappa \int \eta dt}. \quad (6.44)$$

From the 00-component of the field equations, equation (6.21), we obtain

$$\frac{1}{3}\theta^2 - \sigma^2 = \kappa\rho - \Lambda. \quad (6.45)$$

Writing equations (6.42) and (6.43) in terms of θ and σ we obtain

$$\dot{\theta} = \frac{3\kappa}{2} (\xi\theta - (1+w)\rho) - 3\sigma^2, \quad (6.46)$$

$$\dot{\rho} = \theta (\xi\theta - (1+w)\rho) + 4\eta\sigma^2. \quad (6.47)$$

The system of equations that we have to solve is

$$\dot{\tau} = 3H\tau, \quad (6.48)$$

$$\dot{H} = \frac{\kappa}{2} (3\xi H - (1+w)\rho) - (3H^2 - \kappa\rho + \Lambda), \quad (6.49)$$

$$\dot{\rho} = 3H (3\xi H - (1+w)\rho) + 4\eta (3H^2 - \kappa\rho + \Lambda). \quad (6.50)$$

6.1.3 The Special Solutions with Constant Deceleration Parameter

Some authors, (see refs. [63] [62] [61]) have proposed that the Hubble's parameter is related to the scale factor by the relation

$$H = DR^{-n}, \quad (6.51)$$

where $D \geq 0$, $n > 0$ and $R = (abc)^{1/3}$ is the average scale factor. We will here, assume that the generalized mean Hubble parameter is related to the volume expansion by

$$H = D\tau^{-n}. \quad (6.52)$$

Using equation (6.52), we can rewrite equation (6.10) as

$$\tau^{n-1} d\tau = 3D dt. \quad (6.53)$$

Integrating equation (6.53), we obtain

$$\tau(t) = (\tau_0^n + 3nD(t-t_0))^{\frac{1}{n}}, \quad \text{if } n \neq 0 \quad (6.54)$$

$$\tau(t) = C_0 e^{3D(t-t_0)}, \quad \text{if } n = 0 \quad (6.55)$$

where $C_0 = \tau_0 e^{-3Dt_0}$. Using the definition of the deceleration parameter from Chapter 4, we find that the 'average' deceleration parameter is a constant given by

$$q = n - 1 = \text{constant}. \quad (6.56)$$

This is an 'average' over all directions. From recent observational data, (see refs. [20] [19]), we know that

$$-1 \leq q < 0 \quad (6.57)$$

which means that the present day universe is undergoing an accelerating expansion. This gives the following constraint on the value of n

$$0 \leq n < 1 \quad (6.58)$$

If we assume that $\tau(0) = 0$, we obtain

$$\tau = (3nDt)^{\frac{1}{n}}, \quad (6.59)$$

and, the statefinder parameters, representing again an average over all direction, take the following form

$$r = (n-1)(2n-1), \quad (6.60)$$

$$s = \frac{2}{3}n. \quad (6.61)$$

And hence

$$r = 3 \left(n - \frac{2}{3} \right) s + 1, \quad (6.62)$$

We see from this expression that the statefinder parameters are linearly dependent, and we have illustrated this in Fig.6.1.

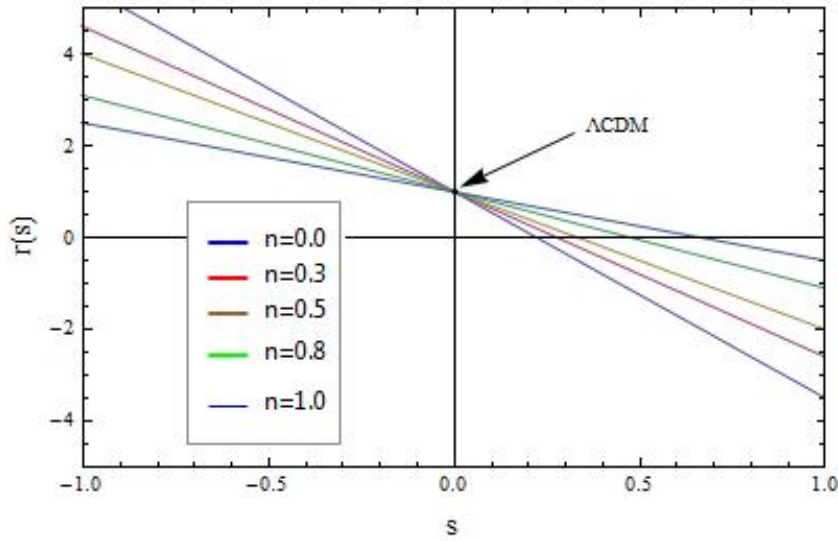


Figure 6.1: The s - r plane for a model with constant deceleration parameter.

In what follows we give the exact solutions of Bianchi type-I model for $n \neq 0$ and $n = 0$. We assume that the shear viscosity, η , is proportional to the expansion scalar

$$\eta = \eta_0 \theta = 3\eta_0 H, \quad (6.63)$$

where η_0 is proportionality constant.

Solutions for $n \neq 0$

Inserting equation (6.54) and equation (6.63) in equations (6.34)-(6.36), we find the following expressions for scale factors

$$a(t) = A_1(3nDt)^{\frac{1}{3n}} \exp \left[\frac{B_1}{9D(n-2\kappa\eta_0-1)} (3nDt)^{\frac{n-2\kappa\eta_0-1}{n}} \right] \quad (6.64)$$

$$b(t) = A_2(3nDt)^{\frac{1}{3n}} \exp \left[\frac{B_2}{9D(n-2\kappa\eta_0-1)} (3nDt)^{\frac{n-2\kappa\eta_0-1}{n}} \right] \quad (6.65)$$

$$c(t) = A_3(3nDt)^{\frac{1}{3n}} \exp \left[\frac{B_3}{9D(n-2\kappa\eta_0-1)} (3nDt)^{\frac{n-2\kappa\eta_0-1}{n}} \right]. \quad (6.66)$$

From this solutions we find the following expressions for the directional Hubble parameters

$$H_i = (3nt)^{-1} + \frac{B_i}{3} (3nDt)^{\frac{-2\kappa\eta_0-1}{n}}. \quad (6.67)$$

The generalized Hubble parameter and expansion scalar are then

$$H = (3nt)^{-1} \quad (6.68)$$

$$\theta = (nt)^{-1} \quad (6.69)$$

Using equations (6.14) and (6.17), we find that the anisotropy parameter and shear scalar are given by

$$A = \frac{\beta}{27D^2} (3nDt)^{\frac{2n-4\kappa\eta_0-2}{n}}. \quad (6.70)$$

$$\sigma^2 = \frac{\beta}{18} (3nDt)^{\frac{-4\kappa\eta_0-2}{n}}. \quad (6.71)$$

where $\beta \equiv (B_1^2 + B_2^2 + B_3^2)$. Using equation (6.21), we find the following expression for the energy density

$$\rho = \frac{3}{\kappa} (3nt)^{-2} - \frac{\beta}{18\kappa} (3nDt)^{\frac{-4\kappa\eta_0-2}{n}} + \frac{\Lambda}{\kappa}. \quad (6.72)$$

In the view of (6.3), (6.4) and (6.63), we find that the expression for pressure and shear viscosity are given by

$$p = \frac{3w}{\kappa} (3nt)^{-2} - \frac{w\beta}{18\kappa} (3nDt)^{\frac{-4\kappa\eta_0-2}{n}} + \frac{w\Lambda}{\kappa} \quad (6.73)$$

$$\eta = 3\eta_0 (3nt)^{-1} \quad (6.74)$$

From equations (6.64)-(6.74) and Figs.(6.2)-(6.5), we can see that the spatial volume is zero at $t = 0$ and expansion scalar is infinite. This means that the universe starts to evolve with zero volume at $t = 0$ with a big bang. We can also see that this model has a singularity point at $t = 0$, because the scale factors vanish at this point. The physical parameters that diverge at this point are: the pressure, energy density, shear viscosity, directional Hubble parameters, anisotropy parameter and shear scalar. After the big bang, the universe will experience a power-law expansion, and as t increases, the scale factors and spatial volume increase, but the expansion scalar, Hubble parameters, shear viscosity, anisotropy parameter and shear scalar decrease and will tend to zero. The anisotropy parameter, A , goes faster to zero because of shear viscosity. Therefore, the shear viscosity has an important role in isotropizing the universe.

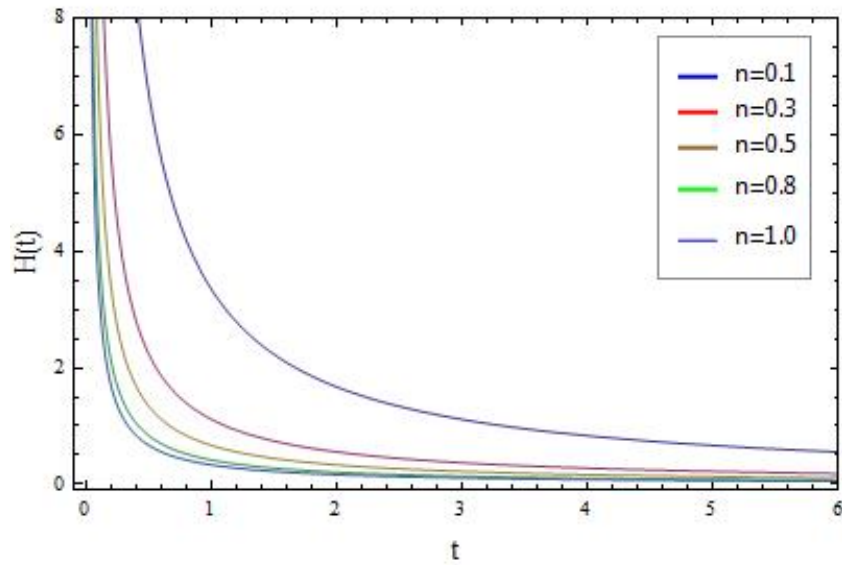


Figure 6.2: The generalized Hubble parameter as a function of time for $0 < n \leq 1$.

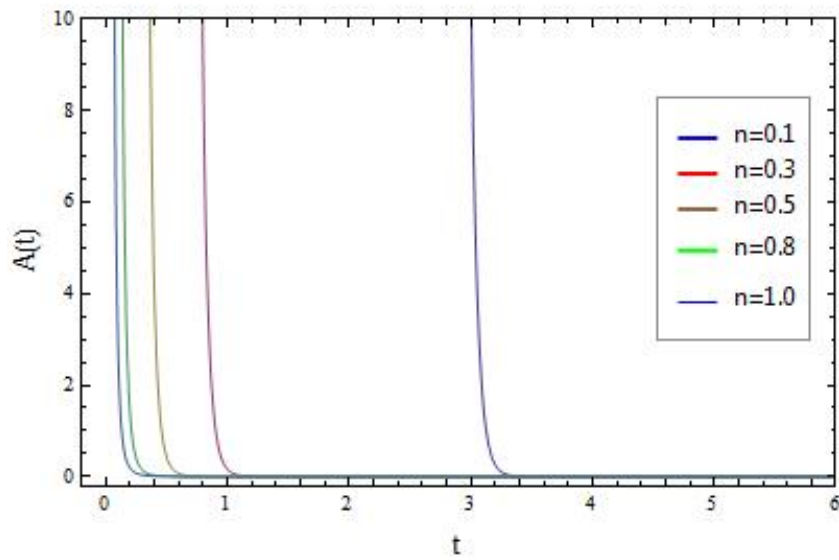


Figure 6.3: The anisotropy parameter as a function of time for $0 < n \leq 1$. Here we set $D = \eta_0 = \kappa = 1$ and $\beta = \frac{2}{3}$ for simplicity.

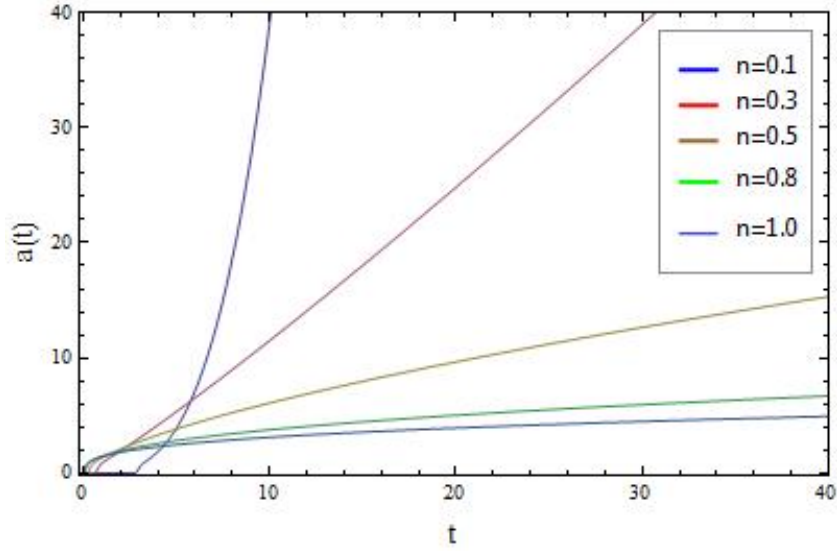
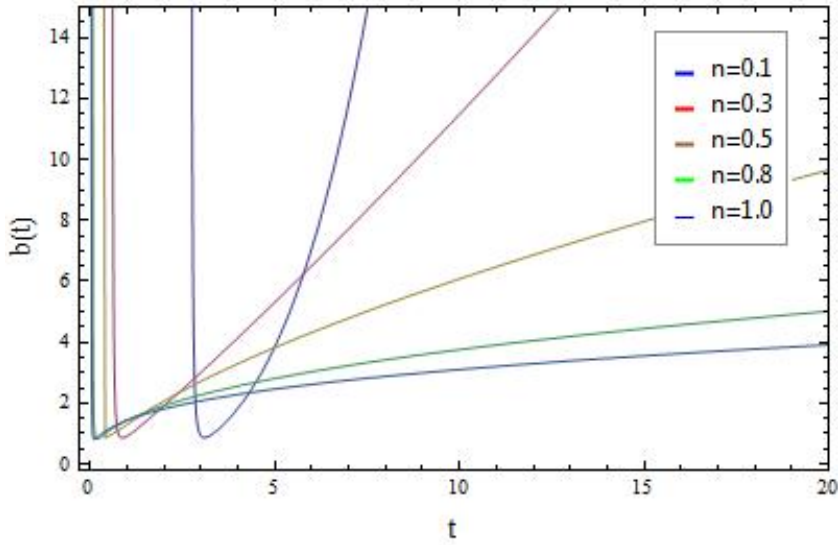
(a) $a(t)$ for $0 < n \leq 1$.(b) $b(t)$ for $0 < n \leq 1$.

Figure 6.4: The metric functions of cosmic time for $0 < n \leq 1$. Fig.6.4(a) shows $a(t)$ for $B_1 = \frac{2}{3}$ and different values of n . Fig.6.4(b) shows $b(t)$ for $B_2 = -\frac{1}{3}$ and different values of n .

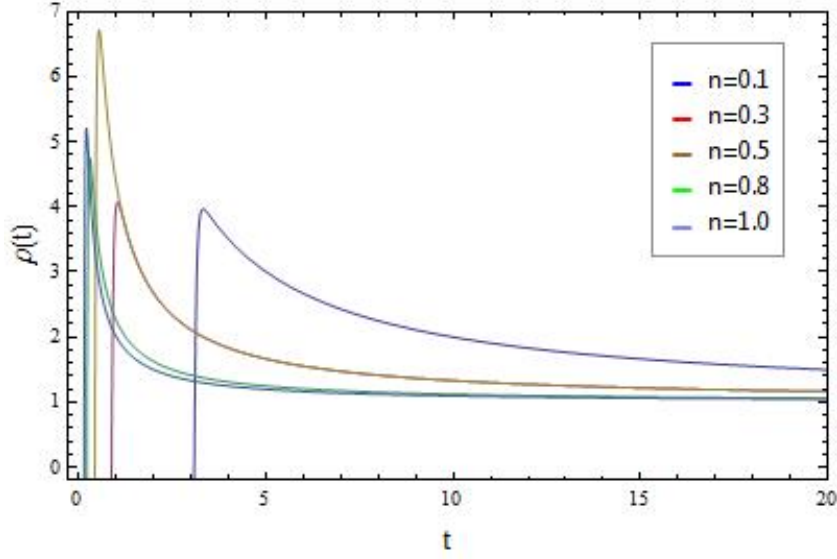


Figure 6.5: Energy density, $\rho(t)$, as a function of time for different values of n . Here we set $\eta_0 = \kappa = \Lambda = D = 1$ for simplicity.

The energy density approaches $\frac{\Lambda}{\kappa}$, as $t \rightarrow \infty$. Therefore, in this model the universe would only contain the cosmological constant for large times, t . But, in the case with no cosmological constant, i.e. $\Lambda = 0$, the energy density goes to zero for large values of t , and we would get an empty universe. The ratio of shear and expansion scalars is given by

$$\frac{\sigma^2}{\theta^2} = \frac{\beta}{162D^2}(3nDt)^{\frac{2n-4\kappa\eta_0-2}{n}}. \quad (6.75)$$

Equation (6.75) shows that the universe in this model becomes isotropic because this ratio goes to zero as $t \rightarrow \infty$. In Fig.6.6, we have plotted the ratio of energy density and expansion scalar, which have the form

$$\frac{\rho}{\theta^2} = \frac{1}{3\kappa} + \frac{\Lambda}{\kappa}(nt)^2 - \frac{\beta}{162\kappa D^2}(3nDt)^{\frac{2n-4\kappa\eta_0-2}{n}}, \quad (6.76)$$

for different values of n and with $\Lambda = 1$. From this figure we can see that $\frac{\rho}{\theta^2} \rightarrow \infty$ as $t \rightarrow \infty$. But, in the absence of the cosmological constant, this ratio has its maximum value, $\frac{1}{3\kappa}$, at $t = \infty$.

Solutions with $n = 0$

Inserting equation (6.55) and equation (6.63) in equations (6.34)-(6.36), we find, in the case when $n = 0$, the following expressions for the scale factors

$$a(t) = A_1 C_0^{\frac{1}{3}} \exp \left[Dt - \frac{B_1}{9C_0 D(1+2\kappa\eta_0)} e^{-3D(1+2\kappa\eta_0)t} \right] \quad (6.77)$$

$$b(t) = A_2 C_0^{\frac{1}{3}} \exp \left[Dt - \frac{B_2}{9C_0 D(1+2\kappa\eta_0)} e^{-3D(1+2\kappa\eta_0)t} \right] \quad (6.78)$$

$$c(t) = A_3 C_0^{\frac{1}{3}} \exp \left[Dt - \frac{B_3}{9C_0 D(1+2\kappa\eta_0)} e^{-3D(1+2\kappa\eta_0)t} \right]. \quad (6.79)$$

In this case, the expressions for directional Hubble parameters, generalized Hubble parameter, energy density, expansion scalar, anisotropy parameter, shear scalar and shear viscosity are then given by

$$H = D \quad (6.80)$$

$$\theta = 3D \quad (6.81)$$

$$H_i = D + \frac{B_i}{3C_0} e^{-3D(1+2\kappa\eta_0)t} \quad (6.82)$$

$$A = \frac{\beta}{27C_0^2 D^2} e^{-6D(1+2\kappa\eta_0)t} \quad (6.83)$$

$$\sigma^2 = \frac{\beta}{18C_0^2} e^{-6D(1+2\kappa\eta_0)t} \quad (6.84)$$

$$\rho = \frac{3D^2}{\kappa} - \frac{\beta}{18\kappa C_0^2} e^{-6D(1+2\kappa\eta_0)t} + \frac{\Lambda}{\kappa} \quad (6.85)$$

$$\eta = 3\eta_0 D. \quad (6.86)$$

From equations (6.77)-(6.86) and figures 6.7-6.10, we can see that this model has no initial singularity, because the scale factors, energy density, shear viscosity and directional Hubble parameters have a finite value at $t = 0$. The scale factors and spatial volume increase exponentially with time. Because of the shear viscosity the anisotropy parameter decreases faster. Therefore, the shear viscosity has an important role in isotropizing the universe in this model. We also see that for this model the expansion scalar is always a constant and, therefore, the universe will expand exponentially. When $t \rightarrow \infty$, the anisotropy parameter and shear scalar go to zero, whereas, the scale factors and volume of the universe become infinitely large. But, energy density becomes a constant. The ratio of shear and expansion scalars

$$\frac{\sigma^2}{\theta^2} = \frac{\beta}{162C_0^2 D^2} e^{-6D(1+2\kappa\eta_0)t}. \quad (6.87)$$

decays exponentially and goes to zero as $t \rightarrow \infty$. And, this shows that the universe in this model becomes isotropic at late times. The ratio of energy density and expansion scalar

$$\frac{\rho}{\theta^2} = \frac{1}{3\kappa} + \frac{\Lambda}{9\kappa D^2} - \frac{\beta}{162\kappa C_0^2 D^2} e^{-6D(1+2\kappa\eta_0)t}, \quad (6.88)$$

shows that when $t \rightarrow \infty$, this ratio approaches its maximum value, which is given by

$$\left(\frac{\rho}{\theta^2} \right)_{\max} = \frac{1}{3\kappa} + \frac{\Lambda}{9\kappa D^2}. \quad (6.89)$$

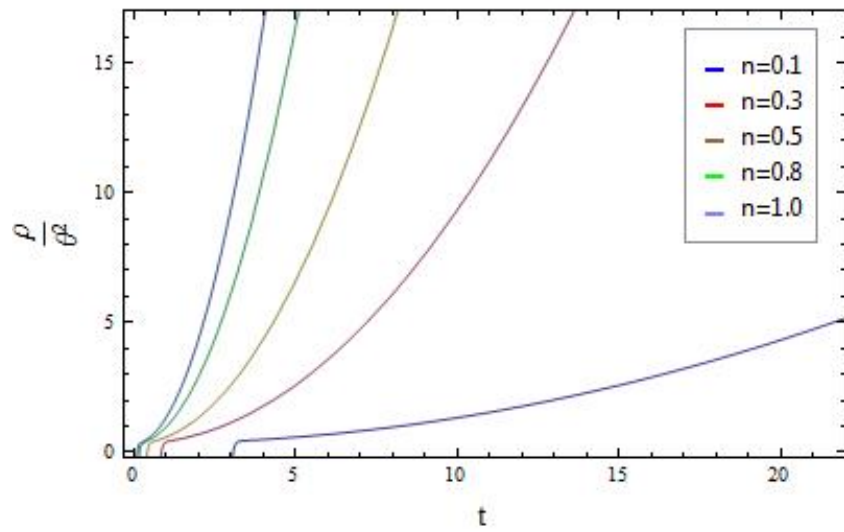


Figure 6.6: The ratio of energy density and expansion scalar. Here we set $\Lambda = 1$.

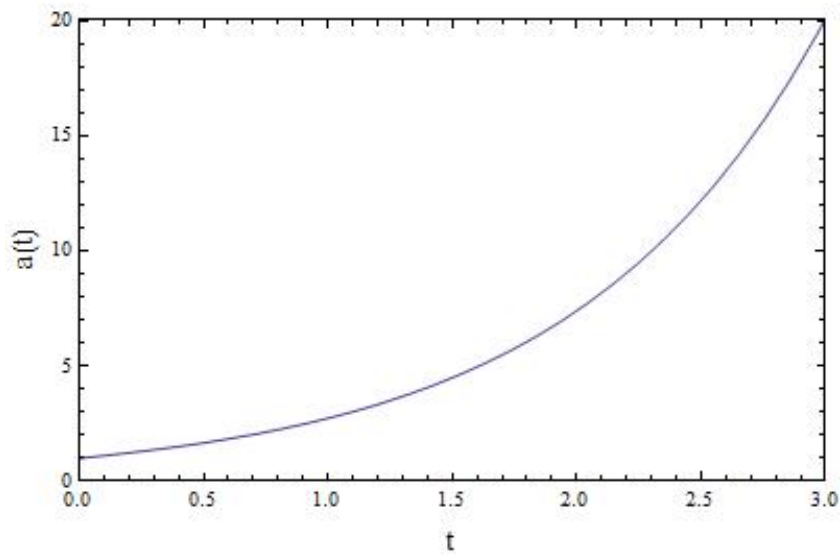


Figure 6.7: The scale factor as a function of time, $a(t)$, for the solution with $n = 0$. Here we set $D = \kappa = \eta_0 = C_0 = 1$, for simplicity.

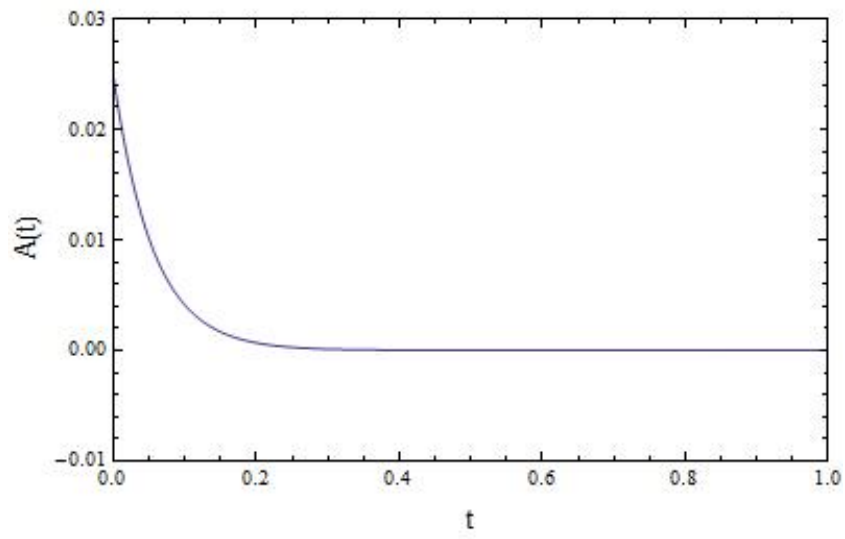


Figure 6.8: Anisotropy parameter as a function of cosmic time for $n = 0$. Here we set $\Lambda = 1$ for simplicity.

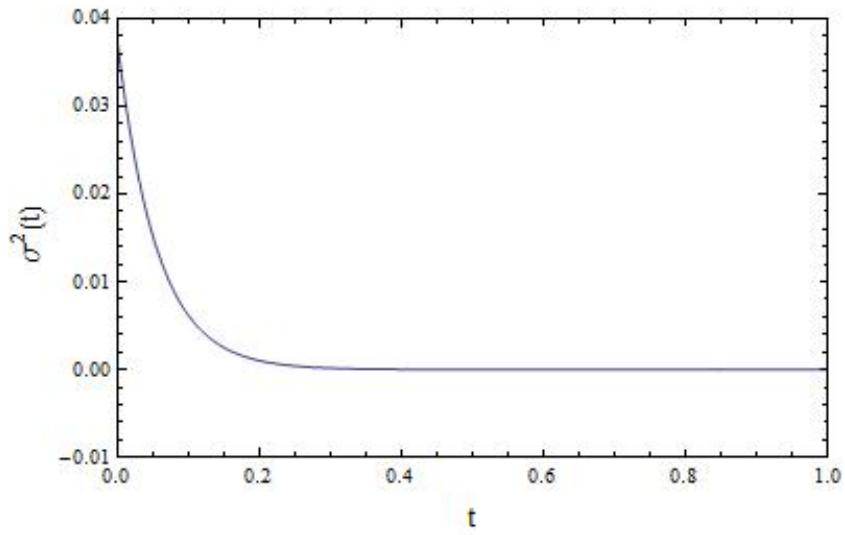


Figure 6.9: Shear scalar as a function of cosmic time for $n = 0$. Here we set $\Lambda = 1$ for simplicity.

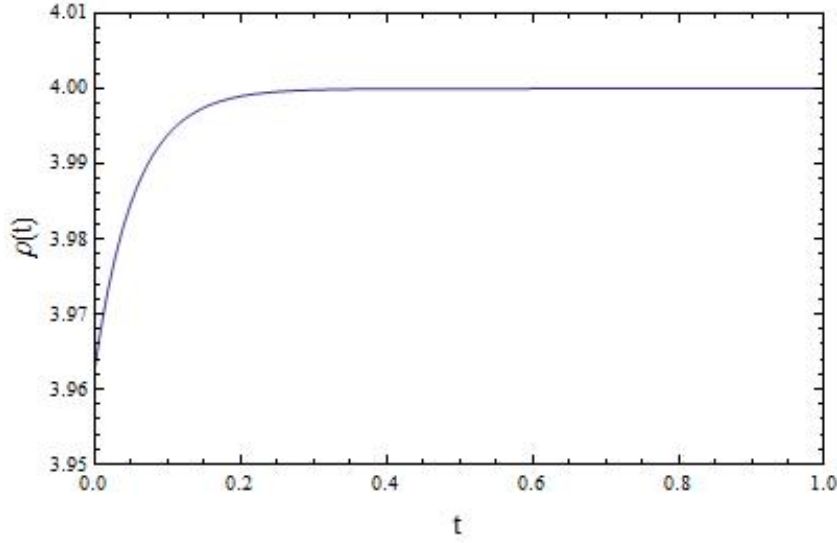


Figure 6.10: Energy density as a function of cosmic time for $n = 0$. Here we set $\Lambda = 1$ for simplicity.

6.1.4 Special Solutions in the Case with Variable Shear Viscosity and Constant Bulk Viscosity

In this section, we will study Bianchi type-I universe model with variable shear viscosity and constant bulk viscosity. We consider the case with shear viscosity being proportional to the expansion, given by

$$\eta = -\frac{1}{2\kappa}\theta = -\frac{3}{2\kappa}H. \quad (6.90)$$

Inserting equation (6.90) in equation (6.50), we find

$$\dot{\rho} = \left[\frac{\kappa}{2} (3\xi H - (1+w)\rho) - (3H^2 - \kappa\rho + \Lambda) \right] \frac{6}{\kappa} H. \quad (6.91)$$

Using equation (6.49), equation (6.91) reduces to

$$\kappa\dot{\rho} = 6H\dot{H}. \quad (6.92)$$

We rewrite this equation as

$$\kappa d\rho = 6H dH. \quad (6.93)$$

Integrating both sides of equation (6.93), we obtain

$$3H^2 = \kappa\rho + C, \quad (6.94)$$

where $C = 3H_0^2 - \kappa\rho_0$, is a constant, and H_0 and ρ_0 are the present Hubble parameter and energy density, respectively. From equation (6.94) we can see that at the initial stage of expansion of the universe, when energy density is large, the Hubble parameter is also large. We can also see

that the Hubble parameter and energy density will decrease with the expansion of the universe. Now, inserting equation (6.94) in equation (6.49), we find

$$\dot{H} = AH^2 + BH + D, \quad (6.95)$$

where we have introduced

$$A = -\frac{3}{2}(1+w), \quad B = \frac{3}{2}\kappa\xi \quad \text{and} \quad D = \frac{1}{2}(w-1)C - \Lambda.$$

We rewrite equation (6.95) as

$$\frac{dH}{AH^2 + BH + D} = dt. \quad (6.96)$$

Integrating (6.96), we obtain

$$H(t) = -\frac{B}{2A} - \frac{\alpha}{A} \frac{De^{2\alpha(t-t_0)} + 1}{De^{2\alpha(t-t_0)} - 1}, \quad \text{when} \quad \frac{1}{4}B^2 - AD > 0 \quad (6.97)$$

or

$$H(t) = \frac{\beta}{A} \tan \beta(t-t_0) + \phi - \frac{B}{2A}, \quad \text{when} \quad \frac{1}{4}B^2 - AD < 0 \quad (6.98)$$

or

$$H(t) = -\frac{1}{A} \left(\frac{1}{T-t} - \frac{B}{2} \right), \quad \text{when} \quad \frac{1}{4}B^2 - AD = 0 \quad (6.99)$$

where we have defined

$$\alpha = \sqrt{\frac{1}{4}B^2 - AD}, \quad \beta = \sqrt{AD - \frac{1}{4}B^2} \quad \text{and} \quad T = t_0 + \frac{1}{AH_0 + B/2},$$

where $H_0 = H(t_0)$ in equation (6.99), is the present Hubble parameter. Using equation (6.48), we find the following expressions for the volume expansion, τ , corresponding to the Hubble parameters in (6.97), (6.98) and (6.99), respectively,

$$\tau(t) = \tau_0 e^{\left[\frac{3\alpha}{A} - \frac{3B}{2A}\right](t-t_0)} \left(\frac{Ee^{2\alpha(t-t_0)} - 1}{E - 1} \right)^{-\frac{3}{A}}, \quad (6.100)$$

$$\tau(t) = \tau_0 e^{-\frac{3B}{2A}(t-t_0)} \left(\frac{\cos \phi}{\cos \beta(t-t_0) + \phi} \right)^{\frac{3}{A}}, \quad (6.101)$$

$$\tau(t) = \tau_0 e^{-\frac{3B}{2A}(t-t_0)} \left(\frac{T-t}{T-t_0} \right)^{-\frac{3}{A}}, \quad (6.102)$$

where we have introduced

$$\phi = \arctan \frac{AH + \frac{1}{2}B}{\beta} \quad \text{and} \quad E = \frac{AH_0 + \frac{B}{2} - \alpha}{AH_0 + \frac{B}{2} + \alpha}.$$

In Fig.6.11-Fig.6.13 we have plotted these volume expansions for three different values of w ; $w = 0$ for dust, $w = 1/3$ for radiation and $w = 1$ for stiff matter, also called Zel'dovich fluid, and for some appropriate values of Λ given in table 6.1. For the solution in (6.100), we can see from Fig.6.11 that when $w = 0$ and $w = 1/3$ the cosmological constant must be less than zero. In the case when $w = 0$ the universe starts with large volume at $t = -\infty$, and, as $t \rightarrow 0$, the volume will decrease, but, there is no singularity at time $t = 0$. As $t \rightarrow \infty$, the volume will

	$\frac{1}{4}B^2 - AD > 0$	$\frac{1}{4}B^2 - AD = 0$	$\frac{1}{4}B^2 - AD < 0$
$w = 0$	$\Lambda < \frac{3}{8}\kappa^2\xi^2 - \frac{1}{2}C$	$\Lambda = \frac{3}{8}\kappa^2\xi^2 - \frac{1}{2}C$	$\Lambda > \frac{3}{8}\kappa^2\xi^2 - \frac{1}{2}C$
$w = 1/3$	$\Lambda < \frac{9}{16}\kappa^2\xi^2 - \frac{2}{3}C$	$\Lambda = \frac{9}{16}\kappa^2\xi^2 - \frac{2}{3}C$	$\Lambda > \frac{9}{16}\kappa^2\xi^2 - \frac{2}{3}C$
$w = 1$	$\Lambda < \frac{3}{16}\kappa^2\xi^2$	$\Lambda = \frac{3}{16}\kappa^2\xi^2$	$\Lambda > \frac{3}{16}\kappa^2\xi^2$

Table 6.1: Possible values of Λ , for the three solutions in eqs.(6.100)-(6.102) and three different values of w .

start to increase exponentially. And, the smaller the value of Λ is, the faster the volume will decrease for $t < 0$, and the faster it will increase for $t > 0$. When $w = 1/3$, for small values of Λ , the universe will behave in the same way as in the case of $w = 0$. But, for bigger values of Λ , the universe starts with zero volume at some point of time, $t < 0$, and as $t \rightarrow \infty$, the universe will expand exponentially. For $w = 1$, we find that the universe starts with negative volume at $t = -\infty$, and, at some point of time, $t > 0$, the volume becomes zero, and after this point the universe will expand exponentially.

Fig.6.12 shows the volume expansion in equation (6.102), for three cases, namely, $w = 0$, $w = 1/3$ and $w = 1$. For these solutions $\Lambda = 0$. For $w = 0$, the universe starts with zero volume at some point of time $t < 0$, and then the volume expands exponentially. For $w = 1/3$, the universe starts with zero volume at $t = 0$, and as $t \rightarrow \infty$, it will expand exponentially. For a Bianchi type-I universe model filled with Zel'dovich fluid, i.e. $w = 1$, the universe starts with zero volume at $t = -\infty$. As $t \rightarrow 0$ the volume becomes negative. And, at some point of time $t > 0$, the volume becomes positive, and then the universe expands exponentially.

The solution in equation (6.101) have been plotted in Fig. 6.13. When $w = 1$, the cosmological constant must be positive, i.e. $\Lambda > 0$. In this case the universe starts with zero volume at $t = -\infty$. For small values of Λ , as $t \rightarrow \infty$, the universe expands exponentially. But, for bigger values of Λ , the volume of the universe will first have a periodic behavior, it becomes negative and positive several times, and when t becomes larger, the universe starts to expand exponentially. For $w = 0$, the universe starts with zero volume at $t = -\infty$. As t increases, the volume will also increase, but, the expansion will stop at some point of time, and then, the volume will decay to zero. When the volume reaches zero, and as $t \rightarrow \infty$ the universe will start to expand exponentially. For $w = 1/3$, the universe will behave in a very strange way. It will start with zero volume at $t = -\infty$, and it will disappear several times before it starts to expand. After a period of expansion, the universe will stop expanding and it begins to contract, and when the volume approaches zero it will again disappear. After a period, the universe begins with zero volume, and as $t \rightarrow \infty$, it will start to expand exponentially.

Now, we will use the definitions

$$q = -1 - \frac{\dot{H}}{H^2}, \quad (6.103)$$

$$r = 1 + 3\frac{\dot{H}}{H^2} + \frac{\ddot{H}}{H^3}, \quad (6.104)$$

$$s = \frac{r - 1}{3(q - \frac{1}{2})}, \quad (6.105)$$

to find the expressions for the deceleration parameter and statefinder parameters, for these solutions. Because of the complexity of the form of the deceleration parameter and statefinder parameters for the solution when $\frac{1}{4}B^2 - AD > 0$, we will not give this expressions here. But,

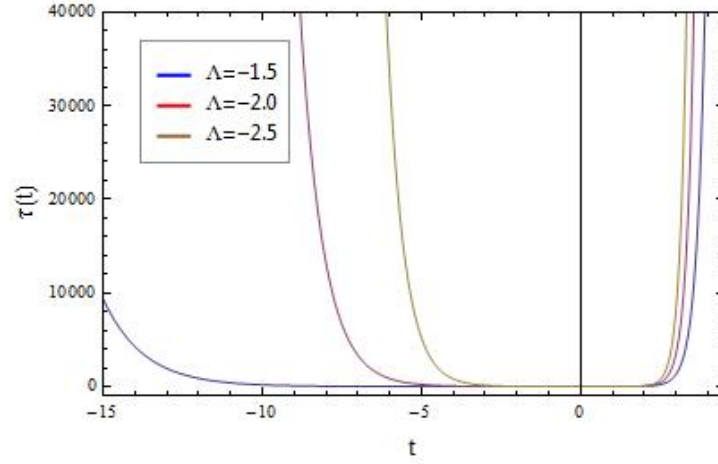
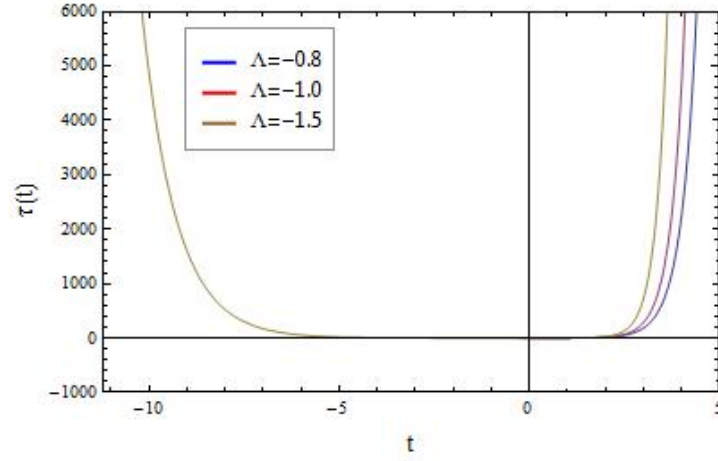
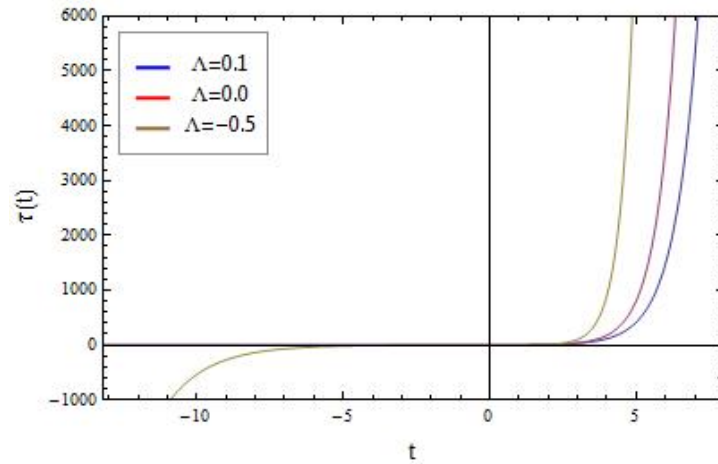
(a) $\tau(t)$ for $w = 0$.(b) $\tau(t)$ for $w = 1/3$.(c) $\tau(t)$ for $w = 1$.

Figure 6.11: The volume expansion as a function of cosmic time for the solution when $\frac{1}{4}B^2 - AD > 0$, for three different values of w , and different values of Λ . Here we set $\kappa=\xi=\rho_0=H_0=\tau_0=t_0=1$, for simplicity.

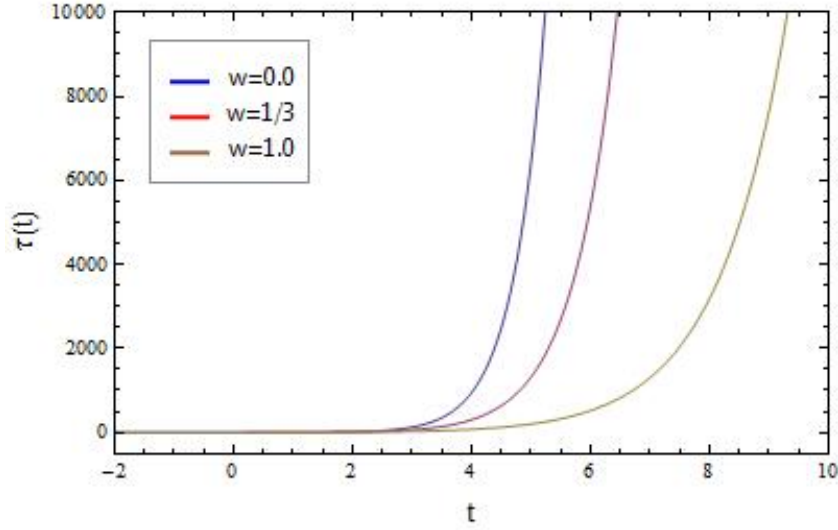


Figure 6.12: The volume expansion τ , for the solution when $\frac{1}{4}B^2 - AD = 0$, for three different values of w . These solutions does not depend on Λ . Here we set $\kappa=\xi=\rho_0=H_0=\tau_0=t_0=1$, for simplicity.

we have plotted these parameters in Fig.6.18-Fig.6.21. For the solution when $\frac{1}{4}B^2 - AD = 0$ we find the following expressions

$$q = -1 - \frac{A}{\left[\frac{B}{2}(t-T) + 1\right]^2}, \quad (6.106)$$

$$r = 1 + \frac{3A}{\left[\frac{B}{2}(t-T) + 1\right]^2} + \frac{2A^2}{\left[\frac{B}{2}(t-T) + 1\right]^3}, \quad (6.107)$$

$$s = -\frac{2}{9} \frac{2A^2 + 3A \left[\frac{B}{2}(t-T) + 1\right]}{\left[\frac{B}{2}(t-T) + 1\right]^3 + 2A \left[\frac{B}{2}(t-T) + 1\right]}, \quad (6.108)$$

In Fig.6.14 we have plotted the q - r -, q - s - and s - r -plane. The curves in the q - r - and q - s -plane are parabola-like. But, in the s - r -plane, the curves are not parabola-like. For $w = 1/3$ and $w = 1$ the curves go through the point $\{0, 1\}$, which corresponds to the values of the statefinder parameters for the Λ CDM model. The curve corresponding to $w = 0$, does not go through the point $\{0, 1\}$, but, it will approach this point for large times, t .

For the solution when $\frac{1}{4}B^2 - AD < 0$, we find the following expressions for deceleration parameter and statefinder parameters

$$q = -1 - \frac{A\beta^2}{g(t)^2}, \quad (6.109)$$

$$r = 1 + \frac{3A\beta^2}{g(t)^2} + \frac{2A^2\beta^3 \sin[\beta(t-t_0) + \phi]}{g(t)^3}, \quad (6.110)$$

$$s = -\frac{1}{3} \frac{2A^2\beta^3 \sin[\beta(t-t_0) + \phi] + 3A\beta^2 g(t)}{\frac{3}{2}g(t)^3 + A\beta^2 g(t)}, \quad (6.111)$$

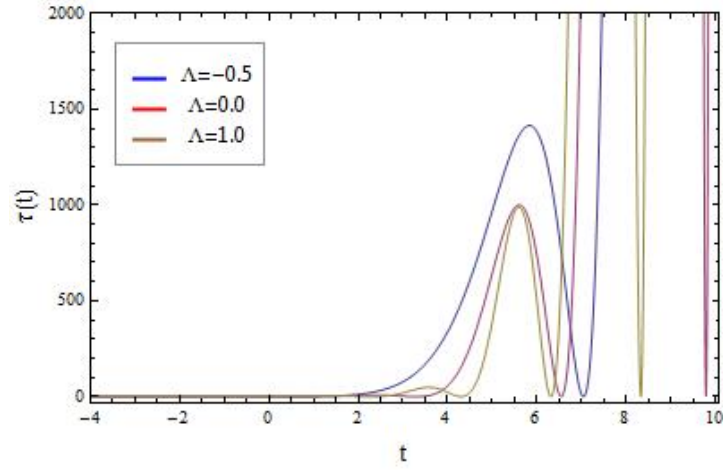
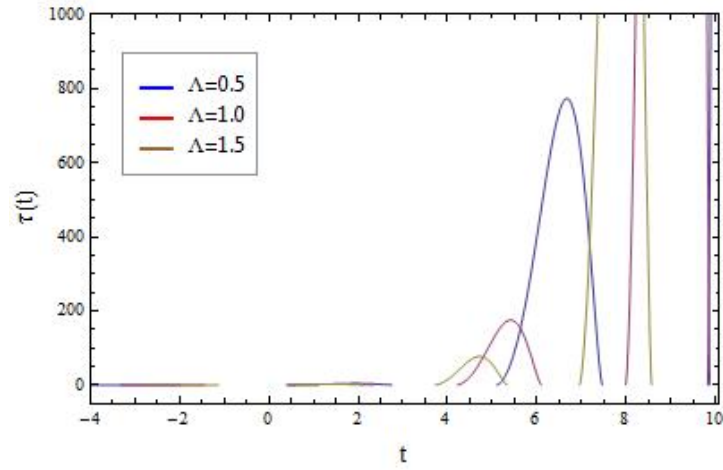
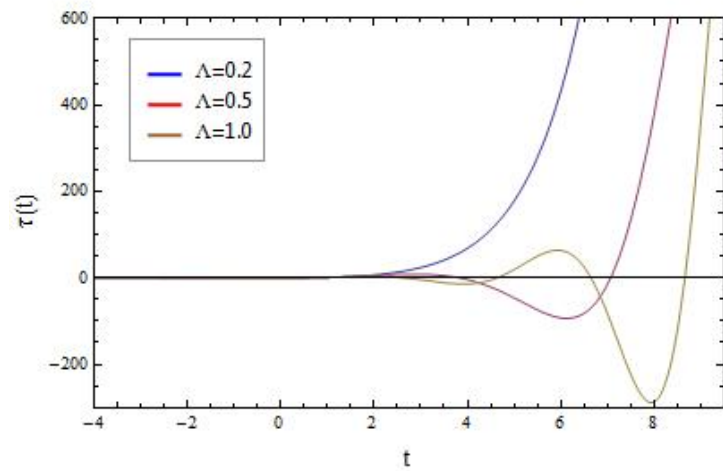
(a) $\tau(t)$ for $w = 0$.(b) $\tau(t)$ for $w = 1/3$.(c) $\tau(t)$ for $w = 1$.

Figure 6.13: The volume expansion as a function of cosmic time for the solution when $\frac{1}{4}B^2 - AD < 0$, for three different values of w , and different values of Λ . Here we set $\kappa=\xi=\rho_0=H_0=\tau_0=t_0=1$, for simplicity.

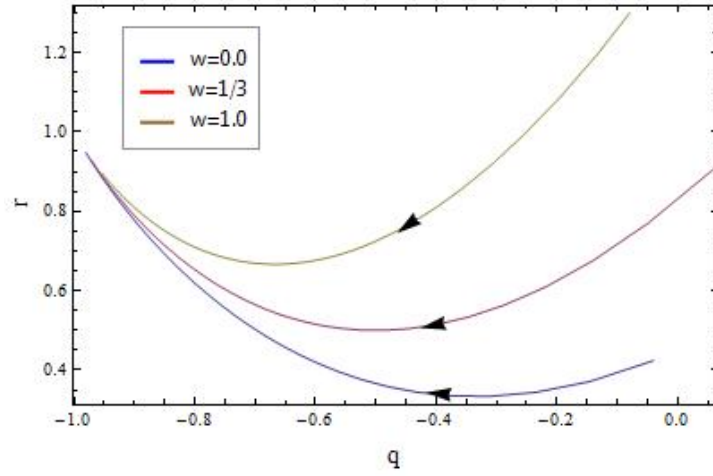
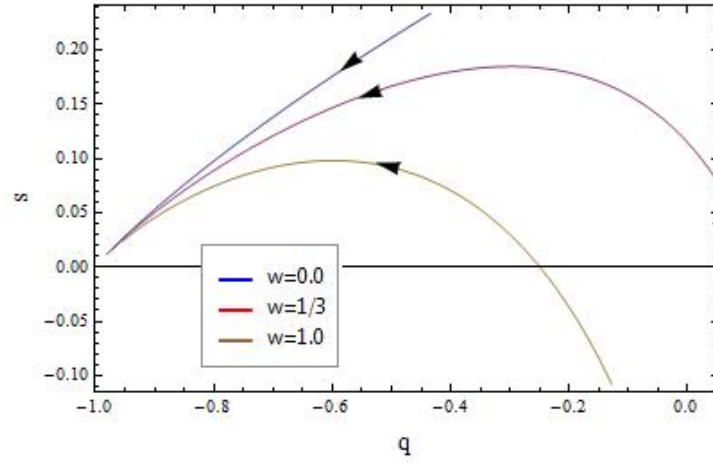
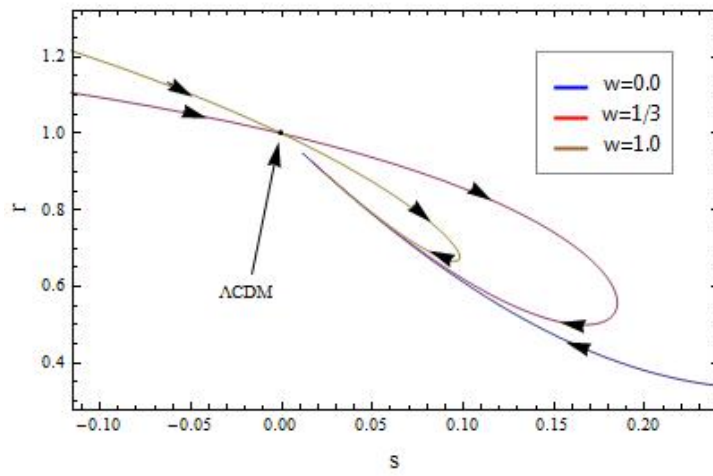
(a) $r(q)$.(b) $s(q)$.(c) $r(s)$.

Figure 6.14: Fig.6.14(a) shows q - r plane for the solution when $\frac{1}{4}B^2 - AD = 0$, for three different values of w . Fig.6.14(b) shows q - s plane, and Fig.6.14(c) shows s - r plane. The arrows indicate the direction of the time evolution.

where we have defined

$$g(t) = \beta \sin [\beta(t - t_0) + \phi] - \frac{B}{2} \cos [\beta(t - t_0) + \phi].$$

Using these expressions, we have plotted the q - r -, q - s - and s - r -plane in Fig.6.15-Fig.6.17. From these figures, we can see that for $w = 1/3$ and $w = 1$, the curves in s - r -plane will go through the point $\{0, 1\}$ at a point of time. But, for $w = 0$, the curves will not go through the point $\{0, 1\}$.

For the solution in equation (6.97) we have plotted the q - r -, q - s - and s - r -plane in Fig.6.18-Fig.6.21. From these figures we can see that for $w = 0$ and $w = 1/3$, the curves in s - r -plane will go through the point $\{0, 1\}$ at a point of time. For $w = 1$, when $\Lambda = 0$ the curve will approach the point $\{0, 1\}$ for large times, t . But, For $\Lambda > 0$ or $\Lambda < 0$, the curves will go through this point.

6.2 Bianchi Type-I Universe Models with Nonlinear Viscosity

In this section, we will first give the energy-momentum tensor for a nonlinear viscous fluid, and then we will write down Einstein's field equations with the cosmological constant. We will also give the equation of energy conservation for this fluid. We use then the field equations to give some special solutions for these models. At the end, we will apply the statefinder formalism to these models.

6.2.1 Energy-Momentum Tensor for a Fluid with Nonlinear Viscosity

The energy-momentum tensor for a fluid with linear viscosity was given in (6.2). In a comoving reference frame with diagonal metric tensor, the nonvanishing components was given in (6.5)-(6.8). In the same reference frame the nonvanishing components of the energy-momentum tensor of a nonlinear viscous fluid is given by (see refs [10])

$$T_{N0}^0 = \rho_N, \quad T_{Ni}^i = -p_N + \alpha\theta^2 + \beta\theta H_i + \lambda(H_i)^2, \quad (6.112)$$

where H_i are the directional Hubble parameters, and α , β and λ are constants, and they satisfy the following constraints relation

$$(3\alpha + \beta)9H^2 + \lambda \sum_{i=1}^3 H_i^2 = 0. \quad (6.113)$$

The subscript N denotes nonlinear viscous fluid. We will here consider an energy-momentum tensor that is given by

$$T = T_L + T_N, \quad (6.114)$$

where T_L is the energy-momentum tensor of a fluid with linear viscosity, given in (6.2). In this case, in a comoving reference frame with diagonal metric tensor the nonvanishing components of (6.114), are

$$T^0_0 = \rho, \quad T^i_i = -p + 2\eta H_i + (3\xi - 2\eta)H + 9\alpha H^2 + 3\beta H H_i + \lambda(H_i)^2, \quad (6.115)$$

where

$$\begin{aligned} \rho &= \rho_L + \rho_N, \\ p &= p_L + p_N. \end{aligned}$$

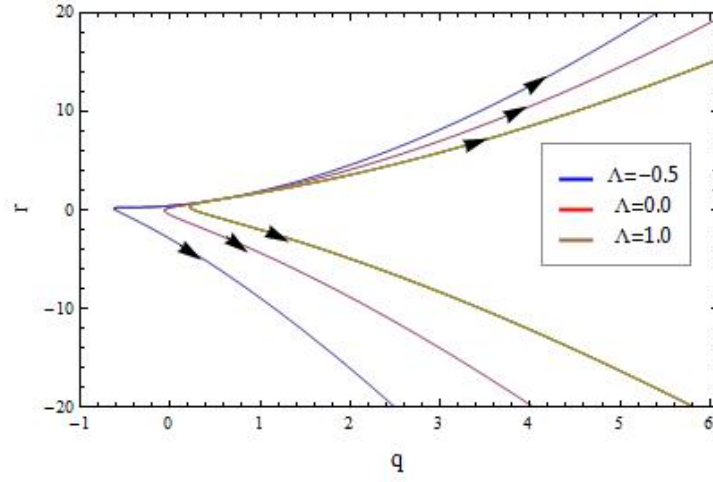
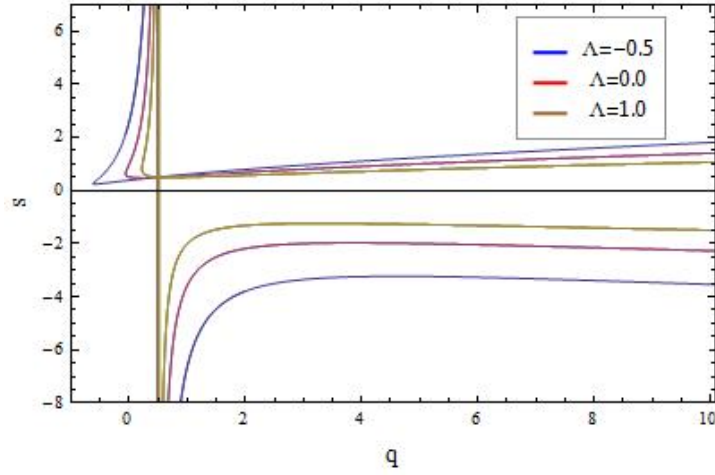
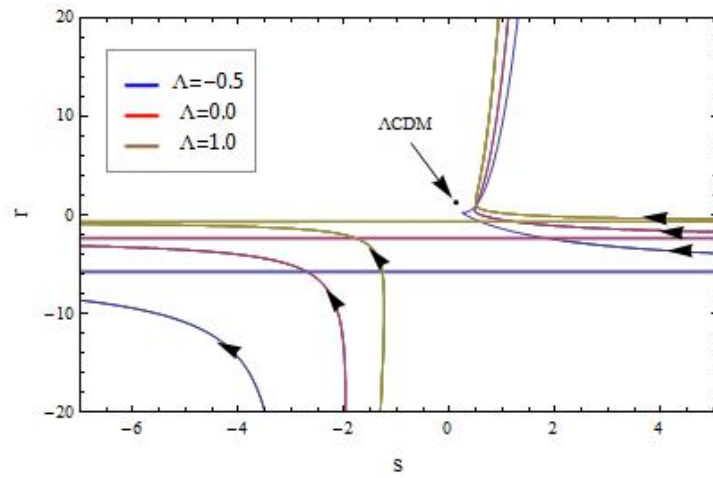
(a) $r(q)$ for $w = 0$.(b) $s(q)$ for $w = 0$.(c) $r(s)$ for $w = 0$.

Figure 6.15: Fig.6.15(a) shows q - r plane for the solution when $\frac{1}{4}B^2 - AD < 0$, for $w = 0$, and three different values of Λ . Fig.6.15(b) shows q - s plane. Fig.6.15(c) shows s - r plane.

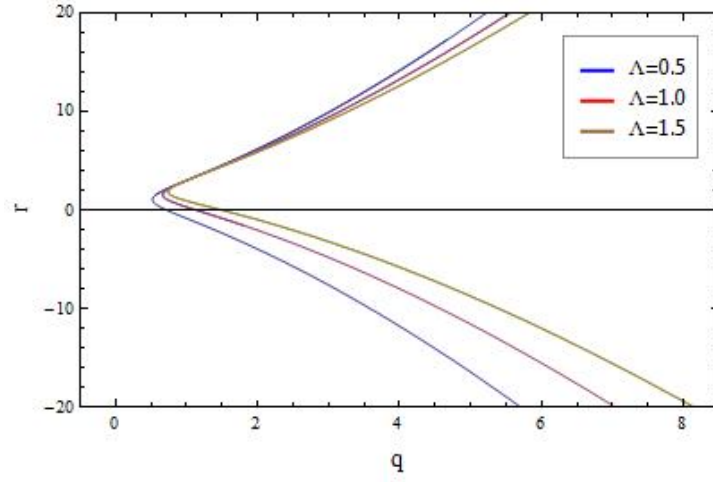
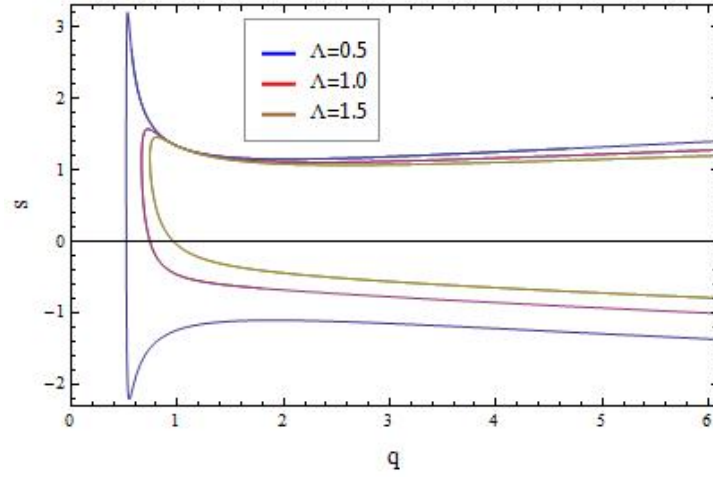
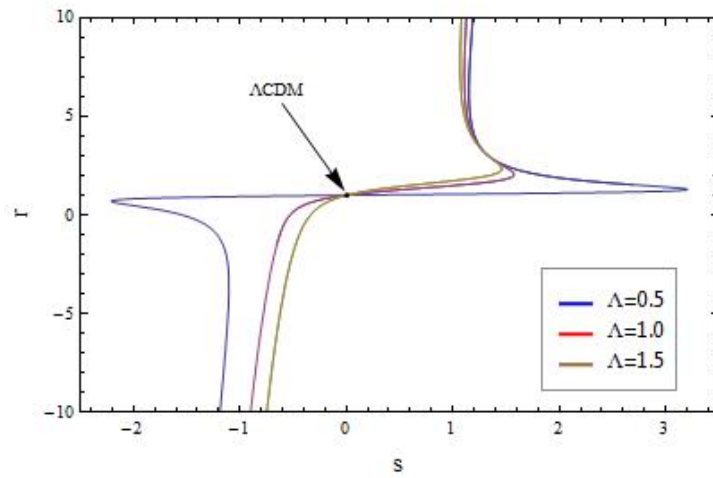
(a) $r(q)$ for $w = 1/3$.(b) $s(q)$ for $w = 1/3$.(c) $r(s)$ for $w = 1/3$.

Figure 6.16: Fig.6.16(a) shows q - r plane for the solution when $\frac{1}{4}B^2 - AD < 0$, for $w = 1/3$, and three different values of Λ . Fig.6.16(b) shows q - s plane. Fig.6.16(c) shows s - r plane.

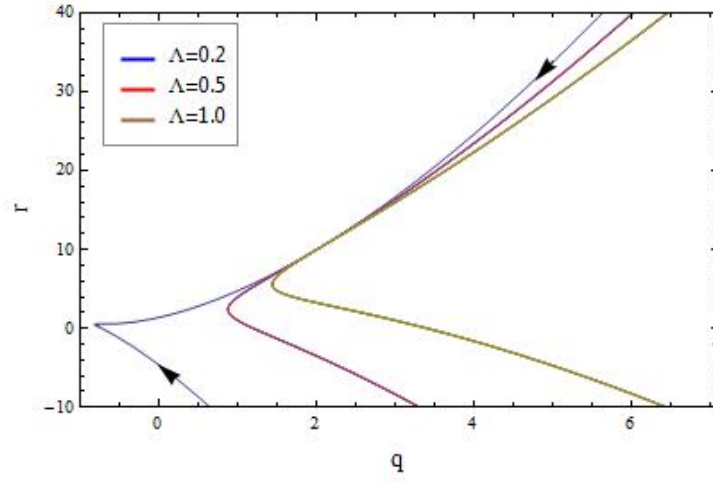
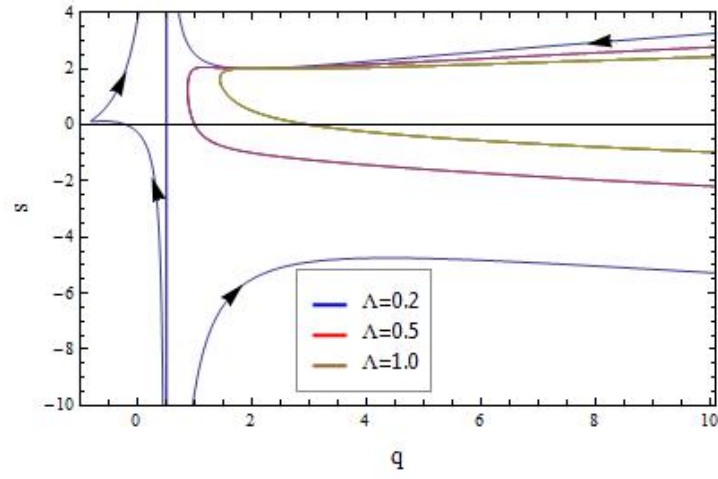
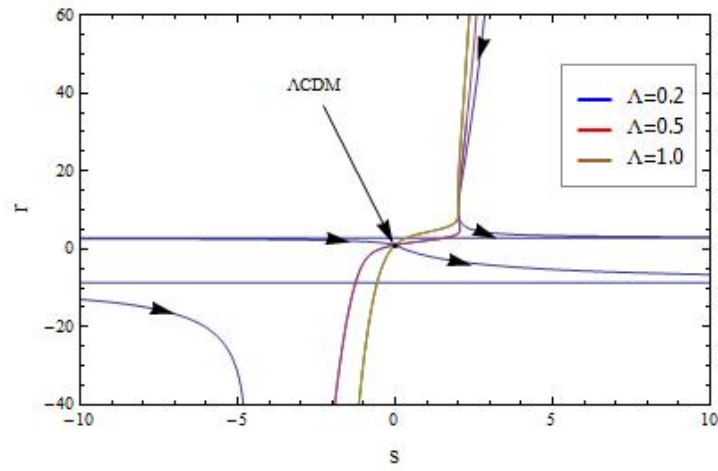
(a) $r(q)$ for $w = 1$.(b) $s(q)$ for $w = 1$.(c) $r(s)$ for $w = 1$.

Figure 6.17: Fig.6.17(a) shows q - r plane for the solution when $\frac{1}{4}B^2 - AD < 0$, for $w = 1$, and three different values of Λ . Fig.6.17(b) shows q - s plane. Fig.6.17(c) shows s - r plane.

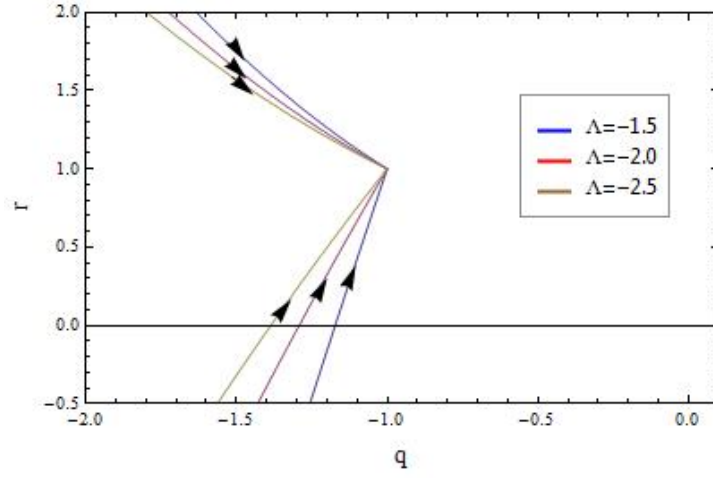
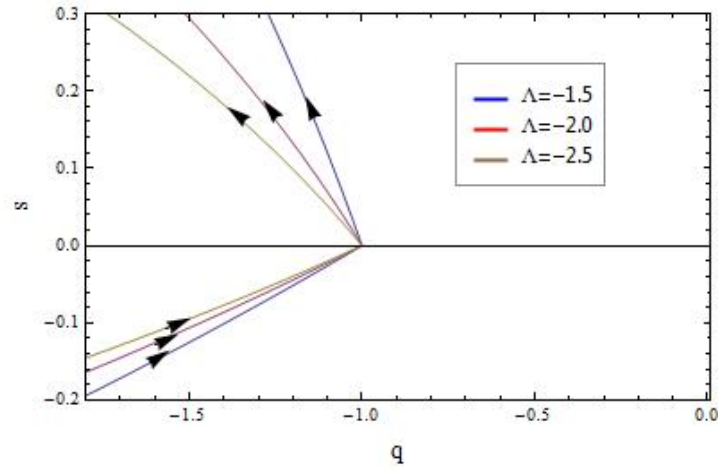
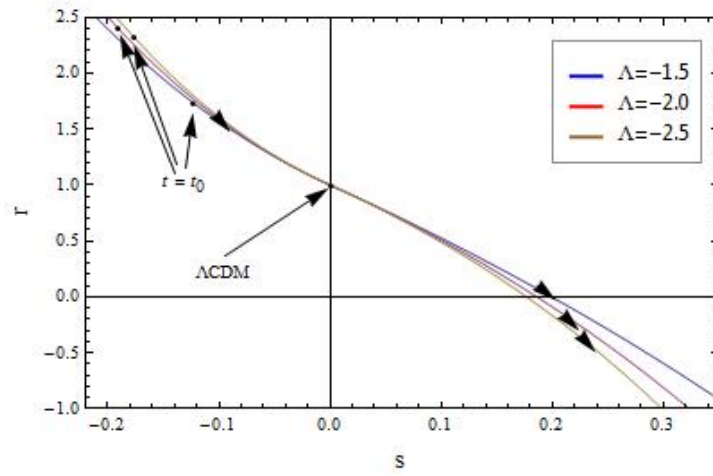
(a) $r(q)$ for $w = 0$.(b) $s(q)$ for $w = 0$.(c) $r(s)$ for $w = 0$.

Figure 6.18: Fig.6.18(a) shows q - r plane for the solution when $\frac{1}{4}B^2 - AD > 0$, for $w = 0$, and three different values of Λ . Fig.6.18(b) shows q - s plane. Fig.6.18(c) shows s - r plane.

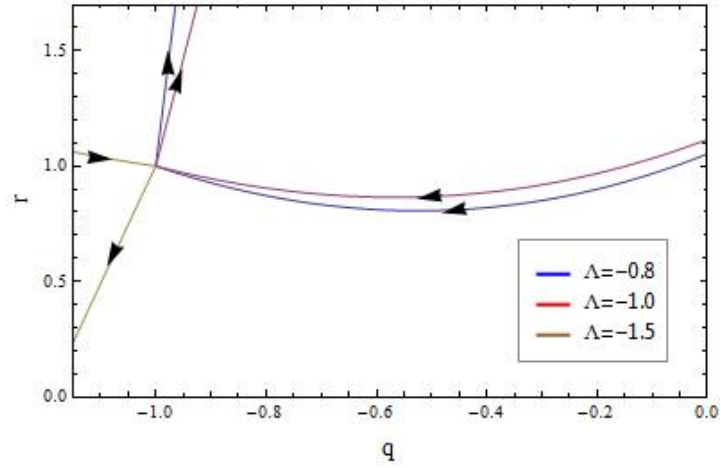
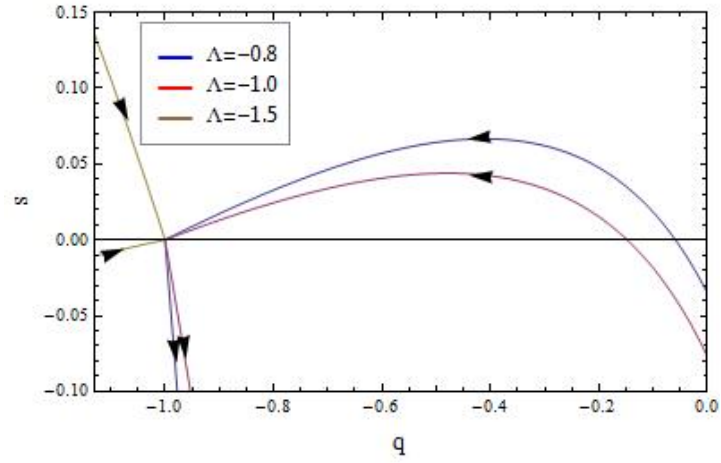
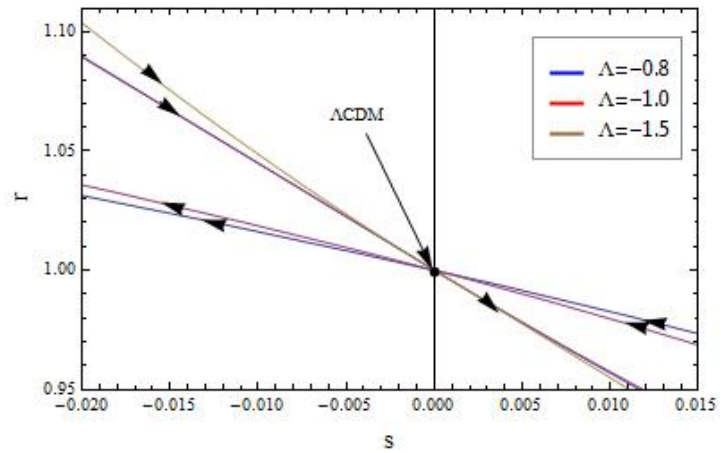
(a) $r(q)$ for $w = 1/3$.(b) $s(q)$ for $w = 1/3$.(c) $r(s)$ for $w = 1/3$.

Figure 6.19: Fig.6.19(a) shows q - r plane for the solution when $\frac{1}{4}B^2 - AD > 0$, for $w = 1/3$, and three different values of Λ . Fig.6.19(b) shows q - s plane. Fig.6.19(c) shows s - r plane.

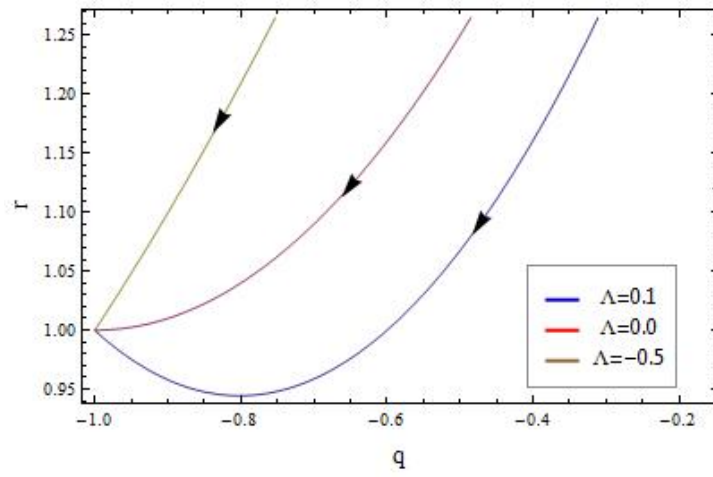
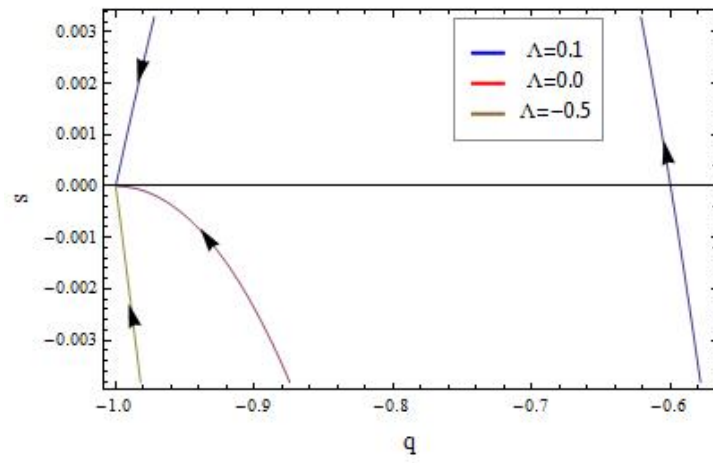

 (a) $r(q)$ for $w = 1$.

 (b) $s(q)$ for $w = 1$.

 Figure 6.20: Fig.6.20(a) shows q - r plane for the solution when $\frac{1}{4}B^2 - AD > 0$, for $w = 1$, and three different values of Λ . Fig.6.20(b) shows q - s plane.

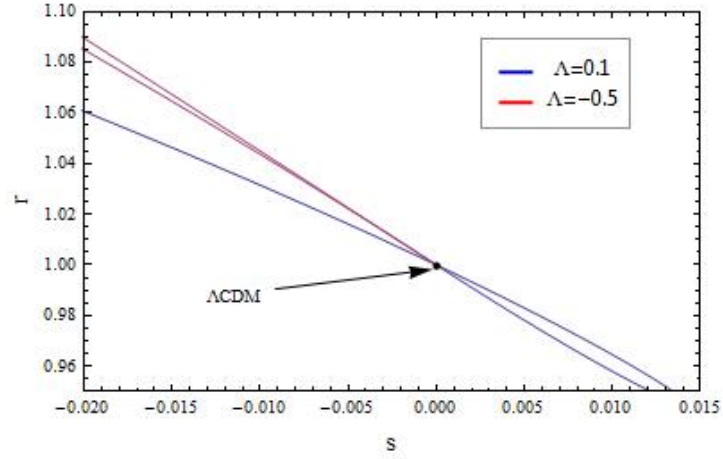
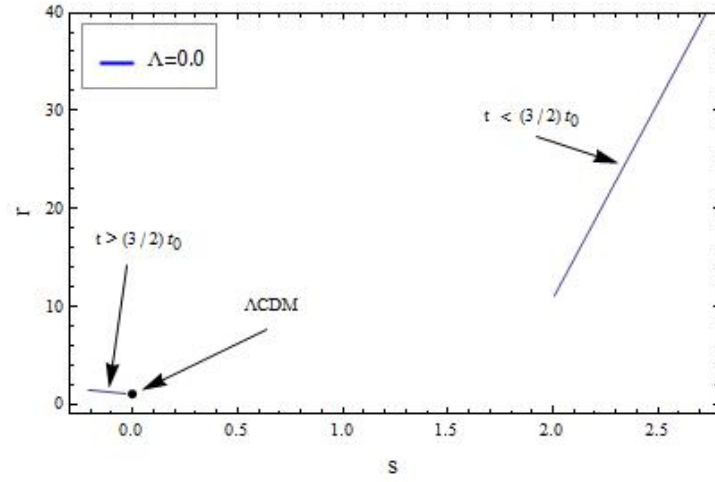
(a) $r(s)$ for $w = 1$.(b) $r(s)$ for $w = 1$.

Figure 6.21: Fig.6.21(a) shows s - r plane for the solution when $\frac{1}{4}B^2 - AD > 0$, for $w = 1$, and for two different values of Λ . Fig.6.21(b) shows s - r plane for the same solution, and for $w = 1$, but for $\Lambda = 0$.

6.2.2 Einstein's field equations

The line-element for the Bianchi type-I universe model is given by (6.1). The expansion volume, the average Hubble parameter and the directional Hubble parameters are defined as usual, as

$$\begin{aligned}\tau &= abc, \\ H_i &= \dot{R}_i/R_i, \\ 3H &= H_1 + H_2 + H_3 \\ &= \frac{\dot{\tau}}{\tau}\end{aligned}\tag{6.116}$$

Einstein's field equations with the cosmological are given by

$$R^\mu_\nu - \frac{1}{2}\delta^\mu_\nu R = T^\mu_\nu - \delta^\mu_\nu \Lambda,\tag{6.117}$$

where we have set $\kappa = 8\pi G = 1$. The field equations take the form

$$\begin{aligned}\frac{\ddot{b}}{b} + \frac{\ddot{c}}{c} + \frac{\dot{b}\dot{c}}{bc} &= -p + 2\eta H_1 + (3\xi - 2\eta)H + 9\alpha H^2 + 3\beta H H_1 + \lambda H_1^2 \\ &\quad - \Lambda,\end{aligned}\tag{6.118}$$

$$\begin{aligned}\frac{\ddot{a}}{a} + \frac{\ddot{c}}{c} + \frac{\dot{a}\dot{c}}{ac} &= -p + 2\eta H_2 + (3\xi - 2\eta)H + 9\alpha H^2 + 3\beta H H_2 + \lambda H_2^2 \\ &\quad - \Lambda,\end{aligned}\tag{6.119}$$

$$\begin{aligned}\frac{\ddot{a}}{a} + \frac{\ddot{b}}{b} + \frac{\dot{a}\dot{b}}{ab} &= -p + 2\eta H_3 + (3\xi - 2\eta)H + 9\alpha H^2 + 3\beta H H_3 + \lambda H_3^2 \\ &\quad - \Lambda,\end{aligned}\tag{6.120}$$

$$\frac{\dot{a}\dot{b}}{ab} + \frac{\dot{b}\dot{c}}{bc} + \frac{\dot{c}\dot{a}}{ca} = \rho - \Lambda.\tag{6.121}$$

Using the definition of the anisotropy parameter, A , in equation (6.14), we can write equation (6.121) as

$$\rho = \left(1 - \frac{A}{2}\right) 3H^2 + \Lambda.\tag{6.122}$$

Expressing this equation by the volume expansion, i.e. $\theta = 3H$, and the shear scalar σ , equation (6.15), we obtain

$$\rho = \frac{1}{3}\theta^2 - \sigma^2 + \Lambda.\tag{6.123}$$

We will now solve these equations, equations (6.118)-(6.120), and find the expressions for the metric functions. We will go through the same steps as in the case of linear viscosity in section 6.1.1. Subtracting (6.118) from (6.119), (6.118) from (6.120) and (6.119) from (6.120), one finds

$$\frac{\ddot{a}}{a} - \frac{\ddot{b}}{b} + \frac{\dot{c}}{c} \left[\frac{\dot{a}}{a} - \frac{\dot{b}}{b} \right] = [-2\eta - 3\beta H] \left[\frac{\dot{a}}{a} - \frac{\dot{b}}{b} \right] - \lambda \left[\left(\frac{\dot{a}}{a} \right)^2 - \left(\frac{\dot{b}}{b} \right)^2 \right]\tag{6.124}$$

$$\frac{\ddot{a}}{a} - \frac{\ddot{c}}{c} + \frac{\dot{b}}{b} \left[\frac{\dot{a}}{a} - \frac{\dot{c}}{c} \right] = [-2\eta - 3\beta H] \left[\frac{\dot{a}}{a} - \frac{\dot{c}}{c} \right] - \lambda \left[\left(\frac{\dot{a}}{a} \right)^2 - \left(\frac{\dot{c}}{c} \right)^2 \right]\tag{6.125}$$

$$\frac{\ddot{b}}{b} - \frac{\ddot{c}}{c} + \frac{\dot{a}}{a} \left[\frac{\dot{b}}{b} - \frac{\dot{c}}{c} \right] = [-2\eta - 3\beta H] \left[\frac{\dot{b}}{b} - \frac{\dot{c}}{c} \right] - \lambda \left[\left(\frac{\dot{c}}{c} \right)^2 - \left(\frac{\dot{b}}{b} \right)^2 \right]\tag{6.126}$$

We divide (6.124) by $\left[\frac{\dot{a}}{a} - \frac{\dot{b}}{b}\right]$, (6.125) by $\left[\frac{\dot{a}}{a} - \frac{\dot{c}}{c}\right]$ and (6.126) by $\left[\frac{\dot{b}}{b} - \frac{\dot{c}}{c}\right]$, and we obtain

$$\frac{\ddot{a}b - \ddot{b}a}{\dot{a}\dot{b} - \dot{a}b} = -2\eta - 3\beta H - \frac{\dot{c}}{c} - \lambda \left(\frac{\dot{a}}{a} + \frac{\dot{b}}{b} \right) \quad (6.127)$$

$$\frac{\ddot{a}c - \ddot{c}a}{\dot{a}\dot{c} - \dot{a}c} = -2\eta - 3\beta H - \frac{\dot{b}}{b} - \lambda \left(\frac{\dot{a}}{a} + \frac{\dot{b}}{b} \right) \quad (6.128)$$

$$\frac{\ddot{b}c - \ddot{c}b}{\dot{b}\dot{c} - \dot{b}c} = -2\eta - 3\beta H - \frac{\dot{a}}{a} - \lambda \left(\frac{\dot{a}}{a} + \frac{\dot{b}}{b} \right) \quad (6.129)$$

Integrating equations (6.127)-(6.129), we get the following relation between H_1 and H_2 , H_2 and H_3 , and H_1 and H_3

$$\frac{\dot{a}}{a} - \frac{\dot{b}}{b} = X_1 \tau^{-1-\beta} (ab)^{-\lambda} \exp \left(-2 \int \eta dt \right), \quad (6.130)$$

$$\frac{\dot{b}}{b} - \frac{\dot{c}}{c} = X_2 \tau^{-1-\beta} (bc)^{-\lambda} \exp \left(-2 \int \eta dt \right), \quad (6.131)$$

$$\frac{\dot{a}}{a} - \frac{\dot{c}}{c} = X_3 \tau^{-1-\beta} (ac)^{-\lambda} \exp \left(-2 \int \eta dt \right). \quad (6.132)$$

Here X_1, X_2, X_3 are integration constants. We have here, used

$$(\ln \tau)' = 3H, \quad \Rightarrow \tau = e^{3 \int H dt}. \quad (6.133)$$

Integrating equations (6.130)-(6.132), we find

$$\frac{a}{b} = D_1 \exp \left[X_1 \tau^{-1-\beta} (ab)^{-\lambda} e^{-2 \int \eta dt} dt \right], \quad (6.134)$$

$$\frac{b}{c} = D_2 \exp \left[X_2 \tau^{-1-\beta} (bc)^{-\lambda} e^{-2 \int \eta dt} dt \right], \quad (6.135)$$

$$\frac{a}{c} = D_3 \exp \left[X_3 \tau^{-1-\beta} (ac)^{-\lambda} e^{-2 \int \eta dt} dt \right], \quad (6.136)$$

where D_1, D_2, D_3 are integration constants. From the equations (6.134)-(6.136) we can write the metric functions as

$$a(t) = A_1 \tau^{1/3} \exp \left[\tau^{-1-\beta-\lambda} e^{-2 \int \eta dt} \left(\frac{X_1}{3} c^\lambda + \frac{X_3}{3} b^\lambda \right) dt \right] \quad (6.137)$$

$$b(t) = A_2 \tau^{1/3} \exp \left[\int \tau^{-1-\beta-\lambda} e^{-2 \int \eta dt} \left(\frac{X_2}{3} a^\lambda - \frac{X_1}{3} c^\lambda \right) dt \right] \quad (6.138)$$

$$c(t) = A_3 \tau^{1/3} \exp \left[- \int \tau^{-1-\beta-\lambda} e^{-2 \int \eta dt} \left(\frac{X_3}{3} b^\lambda + \frac{X_2}{3} a^\lambda \right) dt \right], \quad (6.139)$$

where

$$A_1 = \sqrt[3]{(D_1 D_3)}, \quad A_2 = \sqrt[3]{(D_2 / D_1)}, \quad A_3 = \sqrt[3]{1 / (D_2 D_3)},$$

We will now give the Raychaudhuri equation for this model by using equation (6.113) and summation of Einstein equations (6.118), (6.119) and (6.120), and we obtain

$$\dot{H} = -3H^2 + \frac{1}{2}(\rho - p) + \frac{3}{2}\xi H - \Lambda. \quad (6.140)$$

Using the equation of state

$$p = w\rho, \quad (6.141)$$

we can rewrite equation (6.140) as

$$\dot{H} = -3H^2 + \frac{1}{2}(1-w)\rho + \frac{3}{2}\xi H - \Lambda. \quad (6.142)$$

6.2.3 Energy Conservation Equation

The equation of energy conservation is given by equation (6.39). Using the energy-momentum tensor in (6.115), we obtain

$$\dot{\rho} + 3H(\rho + p) = 3(3\xi - 2\eta)H^2 + 2\eta \sum_{i=1}^3 H_i^2 + 27\alpha H^3 + 3\beta \sum_{i=1}^3 3H_i^2 + \lambda \sum_{i=1}^3 3H_i^3. \quad (6.143)$$

Using the definition of the anisotropy parameter, we can rewrite this equation as

$$\dot{\rho} + 3H(\rho + p) = 3(3\xi + 2\eta A)H^2 + [3\alpha + \beta(1 + A)]9H^3 + \lambda \sum_{i=1}^3 3H_i^3. \quad (6.144)$$

From this equation we can see that at the early stage of the cosmic expansion, when the Hubble parameter has a large value, viscosity has an important role in energy production. We can also see that as the universe expands the energy density will increase.

6.2.4 Statefinder Formalism for Bianchi Type-I Universe Models with Non-linear Viscous Fluid

We will, in this subsection, give the general expressions for the deceleration parameter and statefinder parameters for Bianchi type-I universe models with nonlinear viscous fluid by using the definitions in equations (6.103)-(6.105). We first differentiate equation (6.140), and obtain

$$\ddot{H} = -6H\dot{H} + \frac{1}{2}(\dot{\rho} - \dot{p}) + \frac{3}{2}(\dot{\xi}H + \xi\dot{H}). \quad (6.145)$$

Inserting equation (6.140) and equation (6.145) in equations (6.103)-(6.105), gives the following expressions for the deceleration parameter and statefinder parameter

$$q = 2 - \frac{3}{2}\frac{\xi}{H} - \frac{1}{2}\frac{(\rho + p)}{H} + \frac{\Lambda}{H^2}, \quad (6.146)$$

$$r = 10 - 9\frac{\xi}{H} + \frac{1}{2}(\dot{\rho} - \dot{p})\frac{1}{H^3} + \frac{3}{2}(\rho - p)\left(\frac{1}{2}\xi - H\right)\frac{1}{H^3} + \frac{3}{2}\frac{\dot{\xi} - \frac{3}{2}\xi^2}{H^2} + \frac{\Lambda}{H^2}\left(1 - \frac{3}{2}\frac{\xi}{H}\right), \quad (6.147)$$

$$s = \frac{9 - 9\frac{\xi}{H} + \frac{1}{2}(\dot{\rho} - \dot{p})\frac{1}{H^3} + \frac{3}{2}(\rho - p)\left(\frac{1}{2}\xi - H\right)\frac{1}{H^3} + \frac{3}{2}\frac{\dot{\xi} - \frac{3}{2}\xi^2}{H^2} + \frac{\Lambda}{H^2}\left(1 - \frac{3}{2}\frac{\xi}{H}\right)}{\frac{9}{2} - \frac{9}{2}\frac{\xi}{H} - 3\frac{\Lambda}{H^2} - \frac{3}{2}\frac{(\rho - p)}{H^2}}. \quad (6.148)$$

From these expressions, we can see that if we know the equation of state, the deceleration parameter and statefinder parameter are related to the quantities H , ρ , ξ , $\dot{\xi}$ and Λ .

6.2.5 Bianchi Type-I Universe Filled with Zel'dovich Fluid

In this section, we consider a Bianchi type-I universe model with cosmological constant and filled with Zel'dovich fluid [12] [14] [15]. We assume the equation of state for the Zel'dovich fluid is given by

$$p_z = \rho_z, \quad (6.149)$$

i.e. $w = 1$. We also assume that the coefficient of bulk viscosity is a positive constant. In this case equation (6.140) reduces to

$$\dot{H} = -3H^2 + \frac{3}{2}\xi H - \Lambda. \quad (6.150)$$

We rewrite this equation as

$$\dot{H} = -3 \left[\left(H - \frac{\xi}{4} \right)^2 - \hat{H}^2 \right], \quad (6.151)$$

where

$$\hat{H}^2 = \left(\frac{\xi}{4} \right)^2 - \frac{\Lambda}{3}. \quad (6.152)$$

Now we rewrite equation (6.151) as

$$\frac{1}{\hat{H}} \frac{dH}{\left(\frac{H - \frac{\xi}{4}}{\hat{H}} \right)^2 - 1} = -3\hat{H}dt. \quad (6.153)$$

We integrate both sides of this equation, and obtain

$$H(t) = \frac{\xi}{4} + \hat{H} \frac{e^{6\hat{H}(t-t_0)} - \hat{C}}{e^{6\hat{H}(t-t_0)} + \hat{C}}, \quad (6.154)$$

where

$$\hat{C} = e^{-2\phi}, \quad (6.155)$$

and

$$\phi = \text{artanh} \left[\frac{1}{\hat{H}} \left(H_0 - \frac{\xi}{4} \right) \right], \quad (6.156)$$

and H_0 is the present Hubble parameter. Using equation (6.133), we find the following expression for the volume expansion

$$\tau(t) = \tau_0 \hat{D} e^{\frac{3\xi}{4}(t-t_0)} \left[e^{3\hat{H}(t-t_0)} + \hat{C} e^{-3\hat{H}(t-t_0)} \right], \quad (6.157)$$

where $\hat{D} = \frac{1}{1+\hat{C}}$. In Fig.6.22, we have plotted the Hubble parameter, which is given by equation (6.154), for different values of Λ and ξ . And, in Fig.6.23 we have plotted the volume expansion, which is given by equation (6.157), corresponding to the Hubble parameters in Fig.6.22. From these figures we can see that, for different values of Λ , when the value of the bulk viscosity is small, there exists a singularity at $t = 0$. But, when we decrease the value of the bulk viscosity, for the same values of Λ , the singularities vanish. For big values of ξ , and for $\Lambda > 0$, the universe starts with zero volume at $t = -\infty$. Up to $t = t_0$ there will be no accelerated expansion. From t_0 , as $t \rightarrow \infty$, the universe will have an accelerated expansion. And, the bigger the value of the bulk viscosity is, the bigger the expansion rate will be. For small values of ξ , if we decrease the

value of Λ , there exist singularities at $t = 0$. But, as $t \rightarrow \infty$, the universe will experience an accelerated expansion. If we decrease the value of Λ , but increase the value of ξ , the universe will begin with infinitely large volume, and, as $t \rightarrow t_0$, this volume will decrease, and then, as $t \rightarrow \infty$, the universe will start to expand at an accelerated rate.

Numerical Solutions to the Energy Density

Using the definition of the redshift, $1 + z = \frac{a_0}{a}$, and the transformation

$$\frac{d}{dt} \rightarrow -H(1+z) \frac{d}{dz}, \quad (6.158)$$

we can rewrite equation (6.150) as

$$H'(z) = -\frac{1}{1+z} \left(-3H + \frac{3}{2}\xi - \frac{\Lambda}{H} \right), \quad (6.159)$$

where $'$ denotes differentiation with respect to the redshift, z . We assume $\lambda = 0$ and the shear viscosity is a constant, therefore, in terms of the redshift, equation (6.144) takes the form

$$\rho'(z) = -\frac{1}{1+z} \left[-3(1+w)\rho(z) + 3(3\xi + 2\eta A)H(z) + [3\alpha + \beta(1+A)]9H^2(z) \right]. \quad (6.160)$$

We will, now, give a numerical solution to the energy density by using equation (6.159) and equation (6.160). Inserting $\lambda = 0$ in equation (6.113) we find the following constraint on the constants α and β

$$3\alpha + \beta = 0. \quad (6.161)$$

Hence, the equation (6.160) reduces to

$$\rho'(z) = -\frac{1}{1+z} \left[-3(1+w)\rho(z) + 3(3\xi + 2\eta A)H(z) + 9\beta AH^2(z) \right]. \quad (6.162)$$

We have plotted the numerical solutions of the energy density for different values of Λ , the bulk and the shear viscosity in Fig.6.24-Fig.6.26. Fig.6.24(a) shows the evolution of the energy density with no cosmological constant and no viscosity, i.e. $\Lambda = 0$, $\xi = 0$ and $\eta = 0$. From this figure we can see that in this case the energy density is infinitely large at the beginning of the cosmic evolution, and it will decay to ρ_0 at $z = 0$. From Fig.6.24(c), Fig.6.25(b) and Fig.6.26(b) we can see that regardless of what values the cosmological constant and the bulk viscosity have, the shear viscosity will not change the evolution of the energy density. In Fig.6.24(b), Fig.6.25(a) and Fig.6.26(a) we have plotted the evolution of the energy density in the case where the shear viscosity has the value $\eta = 1$, for $\Lambda = 1$, $\Lambda = 0$ and $\Lambda = -1$, respectively. From these figures we can see that for small values of the bulk viscosity, the value of the energy density is infinitely large at the beginning of the cosmic evolution, and, it will decay to ρ_0 at $z = 0$. And, the bigger the value of the bulk viscosity is, the faster the energy density decays to ρ_0 . When we increase the value of the bulk viscosity further, the universe starts with a finite value of energy density. Then, as the universe evolves, the energy density will decay to ρ_0 at $z = 0$.

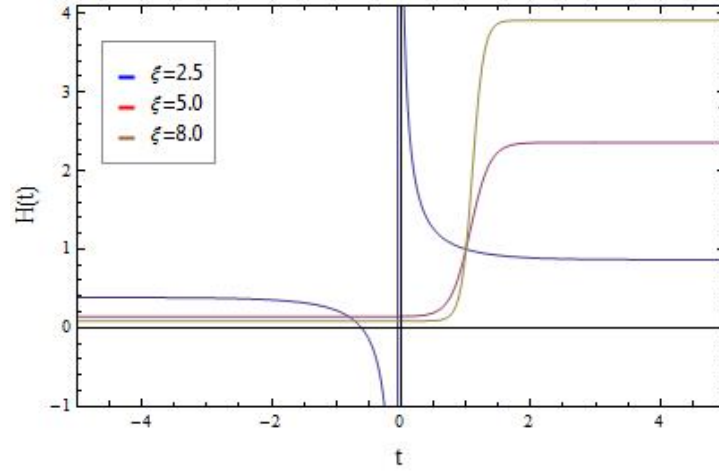
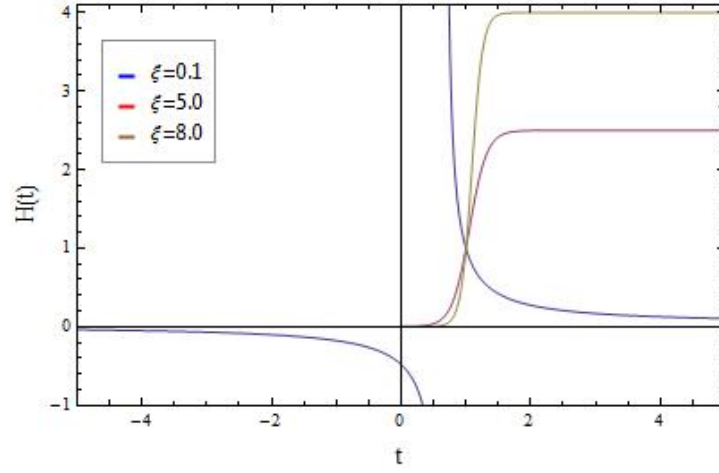
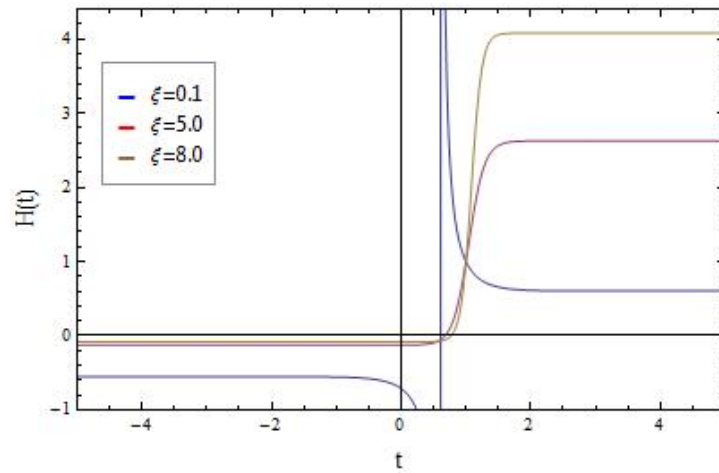
(a) $H(t)$ for $\Lambda = 1.0$.(b) $H(t)$ for $\Lambda = 0.0$.(c) $H(t)$ for $\Lambda = -1.0$.

Figure 6.22: The Hubble parameter as a function of cosmic time, for the BI universe model with cosmological constant and Zel'dovich fluid, for three different values of ξ , and different values of Λ . Here we set $\kappa=H_0=\tau_0=t_0=1$, for simplicity.

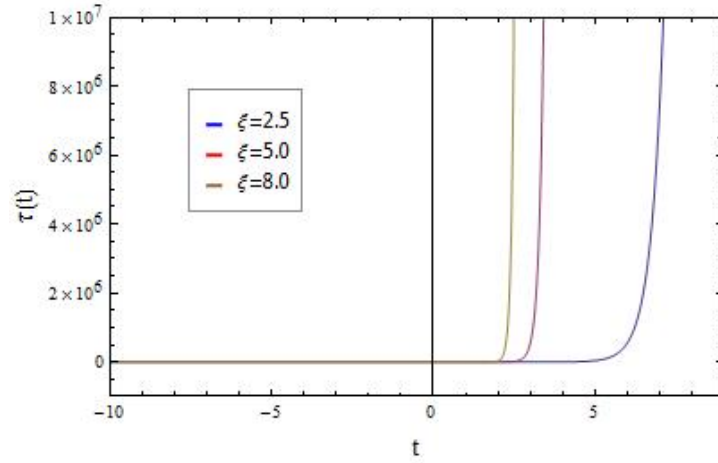
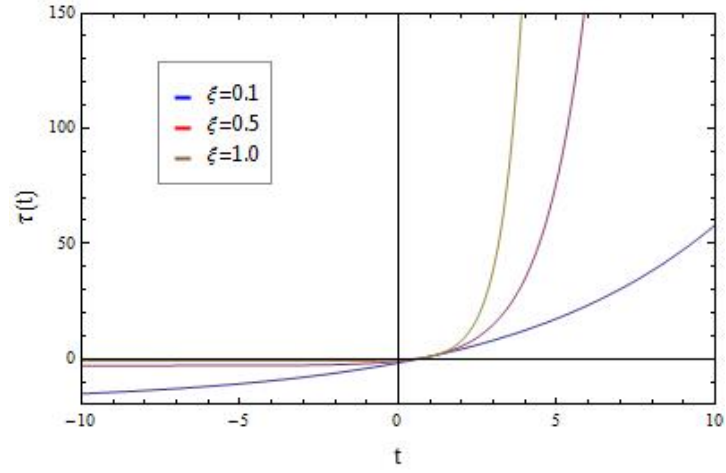
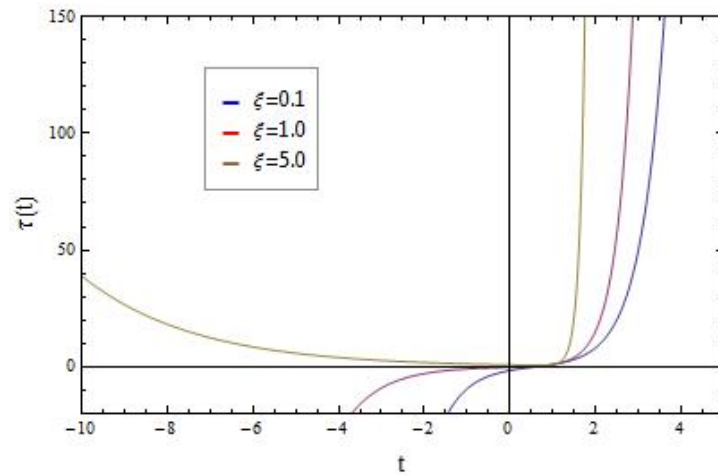
(a) $\tau(t)$ for $\Lambda = 1.0$.(b) $\tau(t)$ for $\Lambda = 0.0$.(c) $\tau(t)$ for $\Lambda = -1.0$.

Figure 6.23: The volume expansion as a function of cosmic time, for the BI universe model with cosmological constant and Zel'dovich fluid, for three different values of ξ , and different values of Λ . Here we set $\kappa=H_0=\tau_0=t_0=1$, for simplicity.

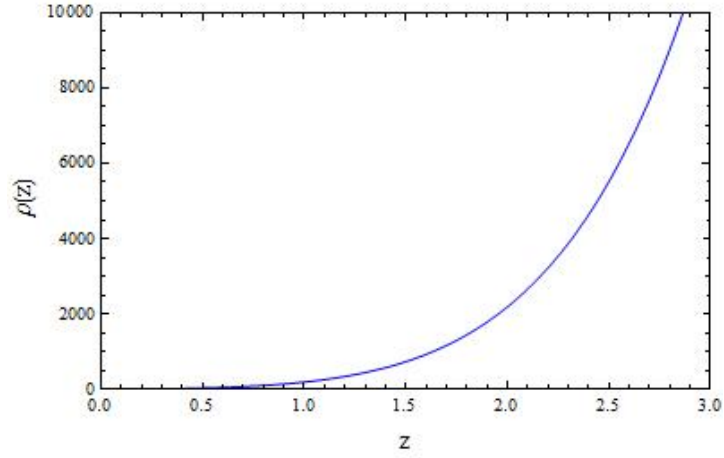
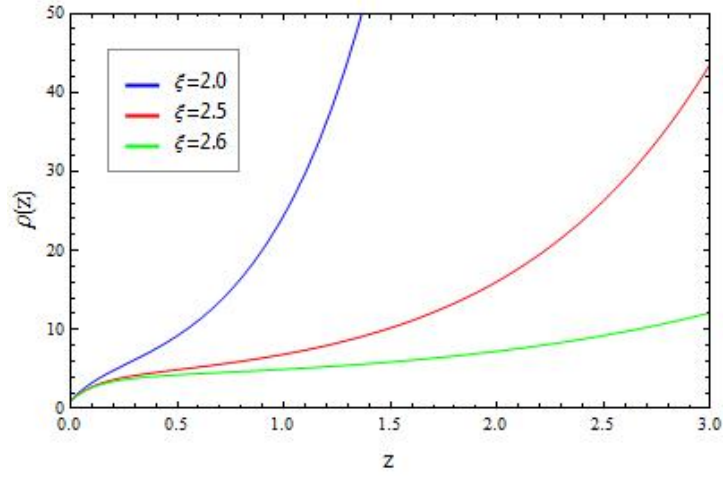
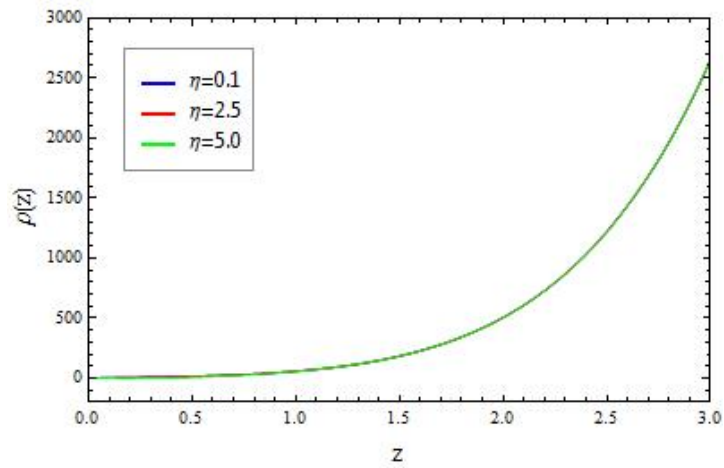
(a) $\rho(z)$ for $\eta = 0.0$, $\xi = 0.0$ and $\Lambda = 0.0$.(b) $\rho(z)$ for $\eta = 1.0$ and $\Lambda = 1$.(c) $\rho(z)$ for $\xi = 1.5$ and $\Lambda = 1$.

Figure 6.24: The energy density as a function of the redshift, for the BI universe model with cosmological constant and Zel'dovich fluid, for three different values of ξ and η . Here we set $H_0 = 1$, $\alpha = 1$, $\beta = -3$ and $\rho_0 = 1$.

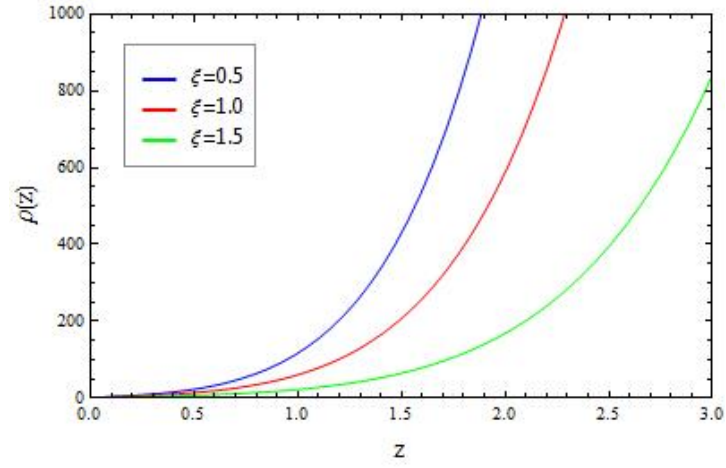
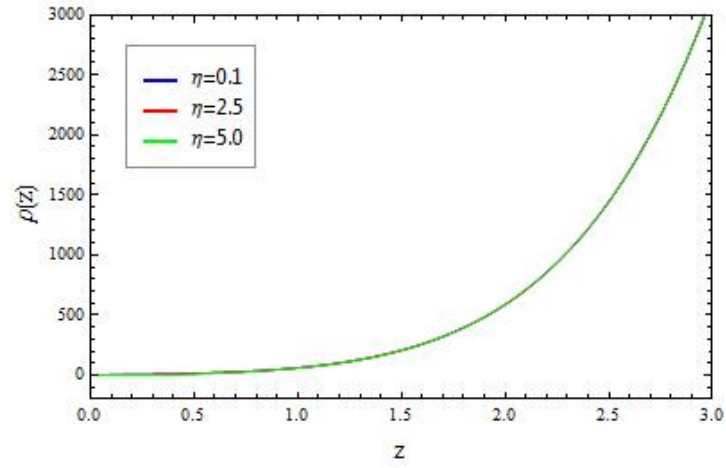
(a) $\rho(z)$ for $\eta = 1.0$ and $\Lambda = 0$.(b) $\rho(z)$ for $\xi = 1.0$ and $\Lambda = 0$.

Figure 6.25: The energy density as a function of the redshift, for the BI universe model with Zel'dovich fluid, for three different values of ξ , and different values of η . Here we set $H_0 = 1$, $\alpha = 1$, $\beta = -3$ and $\rho_0 = 1$.

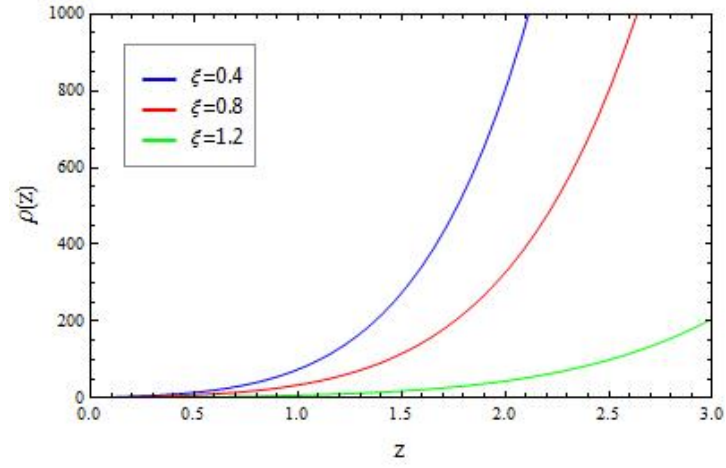
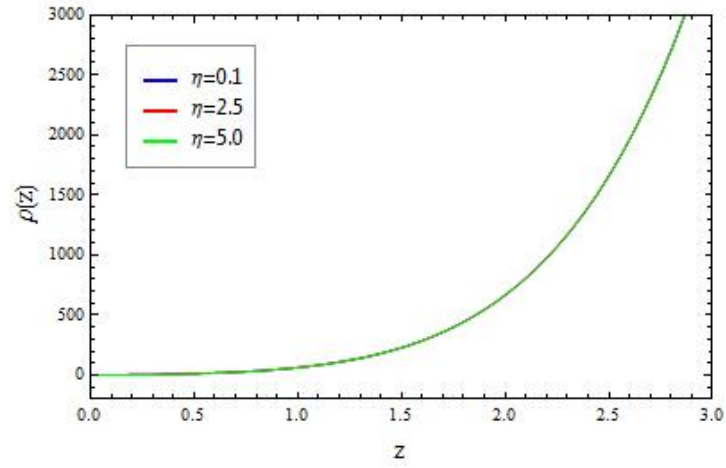
(a) $\rho(z)$ for $\eta = 1.0$ and $\Lambda = -1$.(b) $\rho(z)$ for $\eta = 0.5$ and $\Lambda = -1$.

Figure 6.26: The energy density as a function of the redshift, for the BI universe model with cosmological constant and Zel'dovich fluid, for different values of ξ , and η . Here we set $H_0 = 1$, $\alpha = 1$, $\beta = -3$ and $\rho_0 = 1$.

Deceleration Parameter and Statefinder Parameters

We will, in this subsection, give the deceleration parameter and statefinder parameters for this model. We shall first rewrite equation (6.154), as

$$H(t) = \frac{\xi}{4} + \hat{H} \tanh \left[3\hat{H}(t - t_0) + \phi \right], \quad (6.163)$$

The first and second derivatives of (6.163) are then given by

$$\dot{H} = \frac{3\hat{H}^2}{\cosh^2 \left[3\hat{H}(t - t_0) + \phi \right]}, \quad (6.164)$$

$$\ddot{H} = -18\hat{H}^3 \frac{\sinh \left[3\hat{H}(t - t_0) + \phi \right]}{\cosh^3 \left[3\hat{H}(t - t_0) + \phi \right]}, \quad (6.165)$$

Now, using the definitions in (6.103)-(6.105), we find the following expressions for deceleration parameter and statefinder parameters

$$q = -1 - \frac{3\hat{H}^2}{[f(t)]^2}, \quad (6.166)$$

$$r = 1 + \frac{9\hat{H}^2}{[f(t)]^2} - \frac{18\hat{H}^3 \sinh \left[3\hat{H}(t - t_0) + \phi \right]}{[f(t)]^3}, \quad (6.167)$$

$$s = -\frac{2}{9} \frac{9\hat{H}^2 f(t) - 18\hat{H}^3 \sinh \left[3\hat{H}(t - t_0) + \phi \right]}{[f(t)]^3 + 2\hat{H} f(t)}, \quad (6.168)$$

where

$$f(t) = \frac{\xi}{4} \cosh \left[3\hat{H}(t - t_0) + \phi \right] + \hat{H} \sinh \left[3\hat{H}(t - t_0) + \phi \right].$$

We have plotted the time evolution of the deceleration parameter, the statefinder parameter s and r , in Fig.6.29, Fig.6.28 and Fig.6.27, respectively. From these figures we can see that when $\Lambda = 0$, as t increases

$$q \rightarrow -1, \quad s \rightarrow 0 \quad \text{and} \quad r \rightarrow 1. \quad (6.169)$$

When $\Lambda < 0$ or $\Lambda > 0$, the universe starts with

$$q = -1, \quad s = 0, \quad r = 1, \quad (6.170)$$

and as $t \rightarrow 0$, the deceleration parameter and the statefinder parameters go away from the values in (6.170). From $t = 0$, as t increases, the deceleration parameter and the statefinder parameters will eventually approach the values in (6.170).

In Fig.6.30, Fig.6.31 and Fig.6.32 we have plotted the q - r -, q - s - and s - r -planes, respectively. From Fig.6.30 and Fig.6.31, we should notice that for different values of Λ , only for small values of the bulk viscosity that the deceleration parameter have the values

$$-1 < q < 0,$$

which are the preferred values of q by observational data (see refs. [20] [19]). For bigger values of ξ , the deceleration parameter has values smaller than -1 . We should also notice that when

$r = 1$ and $s = 0$, the deceleration parameter is equal -1 , i.e. $q = -1$. From Fig.6.32 we can see that for $\Lambda = 1$ and $\Lambda = -1$, and for all appropriate values of ξ , the curves have values very close to $\{0, 1\}$, which corresponds to the values of statefinder parameters in Λ CDM model. For $\Lambda = 0$, the curves will eventually approach the point $\{0, 1\}$.

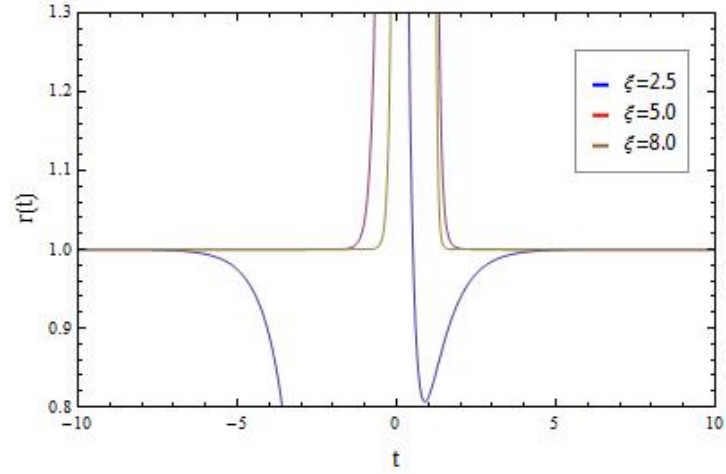
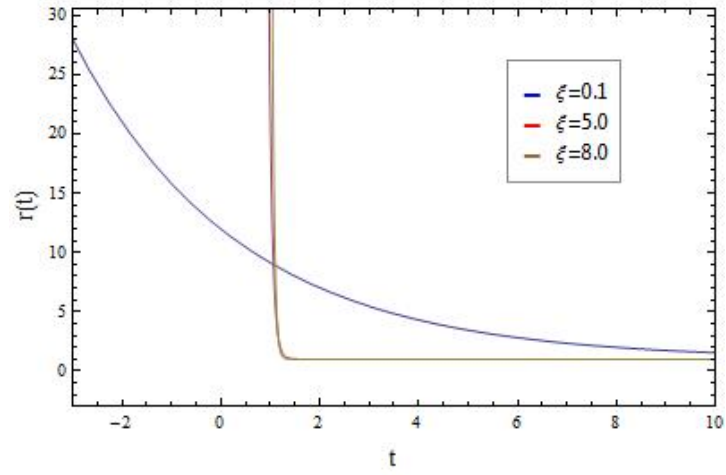
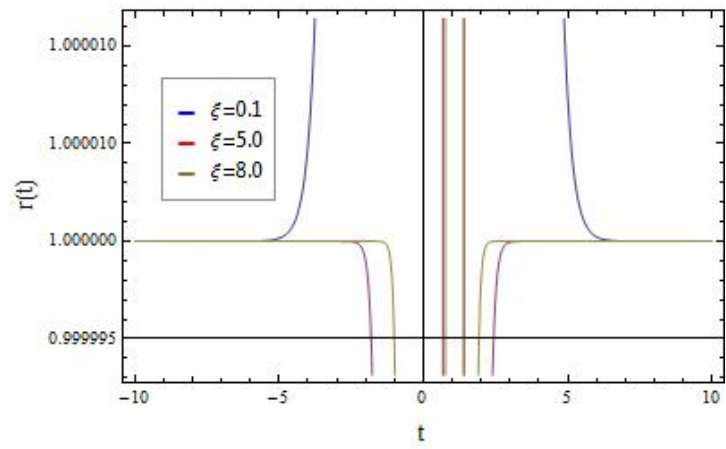
(a) $r(t)$ for $\Lambda = 1.0$.(b) $r(t)$ for $\Lambda = 0.0$.(c) $r(t)$ for $\Lambda = -1.0$.

Figure 6.27: Statefinder parameter r as a function of time, for the BI universe model with cosmological constant and Zel'dovich fluid, for three different values of ξ , and different values of Λ . Here we set $\kappa=H_0=\tau_0=t_0=1$, for simplicity.

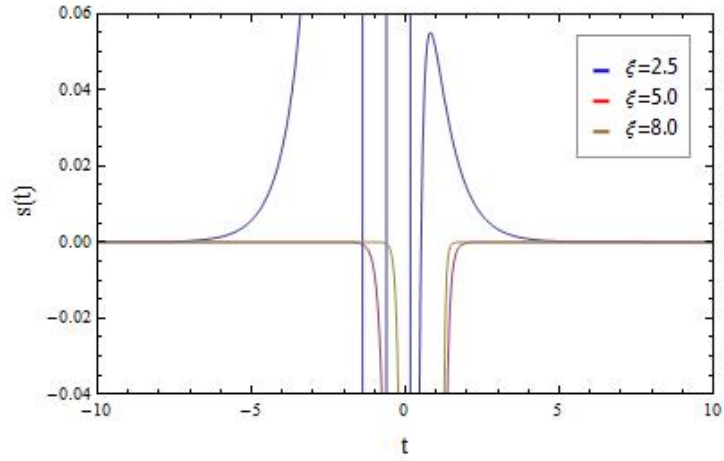
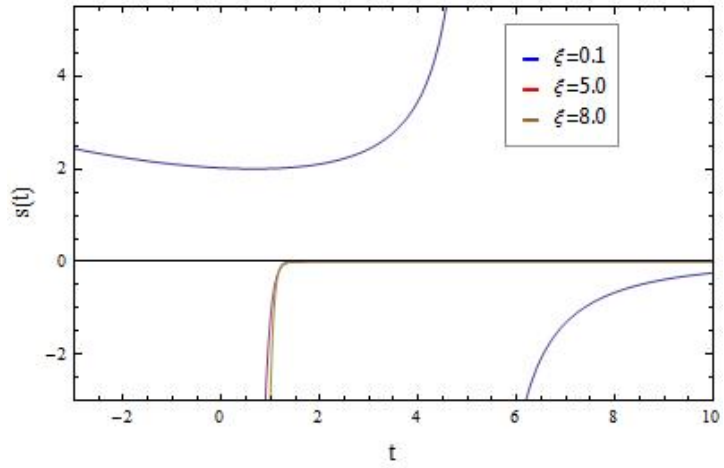
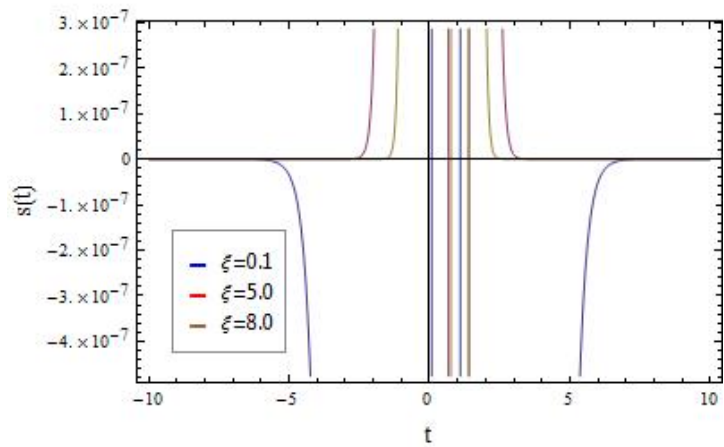
(a) $s(t)$ for $\Lambda = 1.0$.(b) $s(t)$ for $\Lambda = 0.0$.(c) $s(t)$ for $\Lambda = -1.0$.

Figure 6.28: Statefinder parameter s as a function of time, for the BI universe model with cosmological constant and Zel'dovich fluid, for three different values of ξ , and different values of Λ . Here we set $\kappa=H_0=\tau_0=t_0=1$, for simplicity.

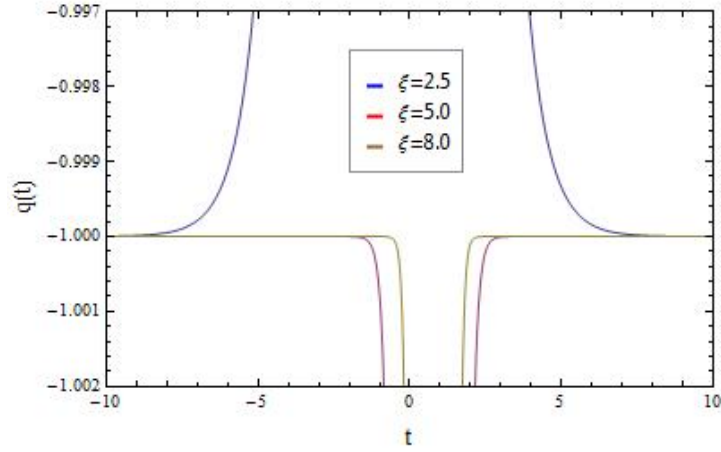
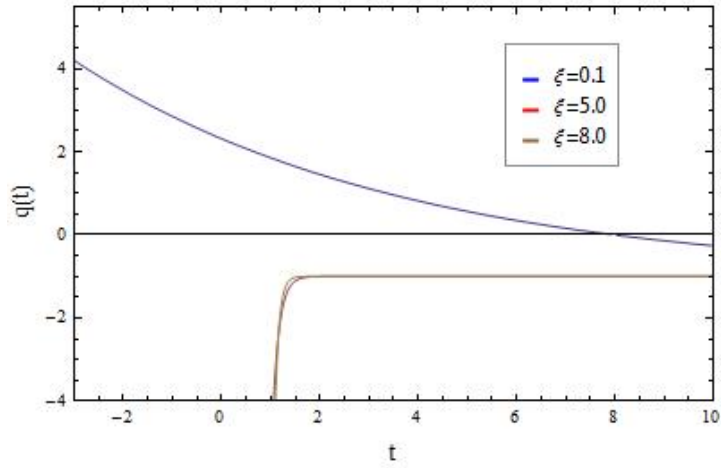
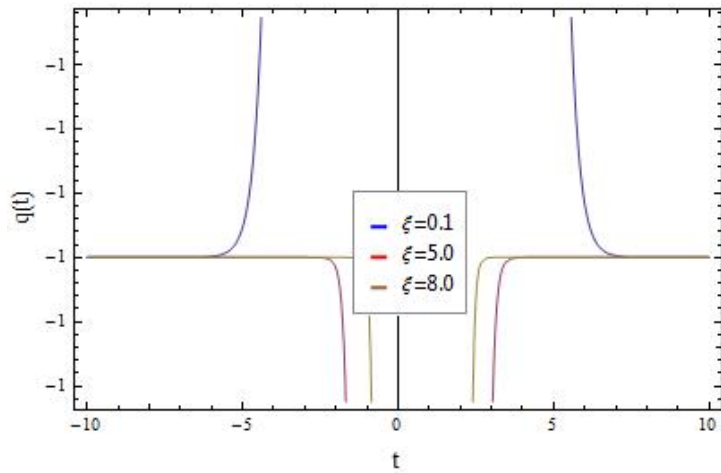
(a) $q(t)$ for $\Lambda = 1.0$.(b) $q(t)$ for $\Lambda = 0.0$.(c) $q(t)$ for $\Lambda = -1.0$.

Figure 6.29: Deceleration parameter q as a function of time, for the BI universe model with cosmological constant and Zel'dovich fluid, for three different values of ξ , and different values of Λ . Here we set $\kappa=H_0=\tau_0=t_0=1$, for simplicity.

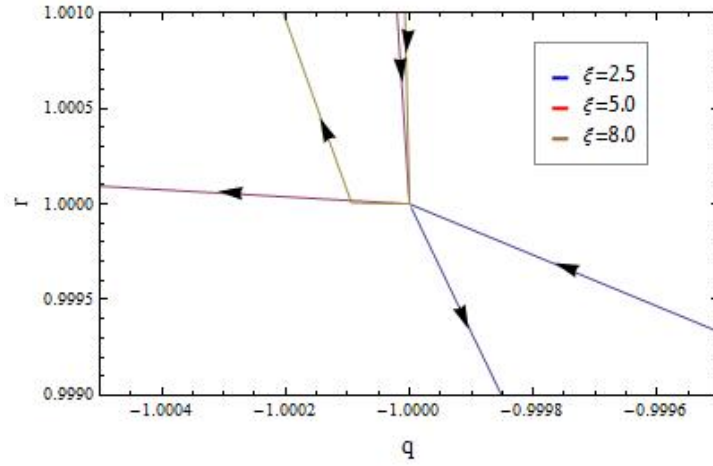
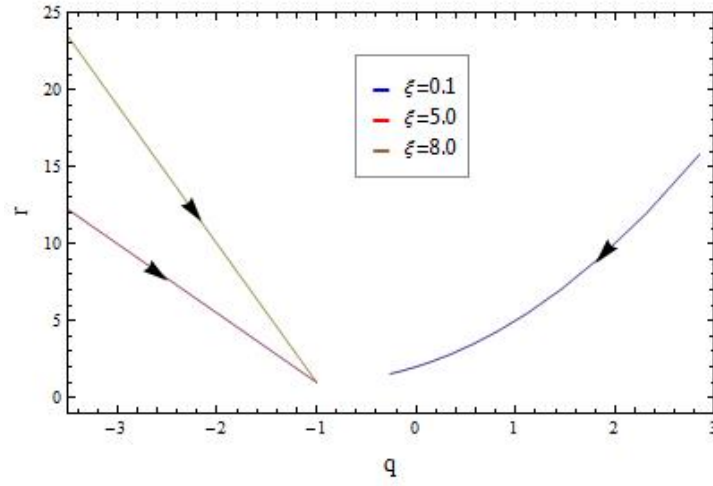
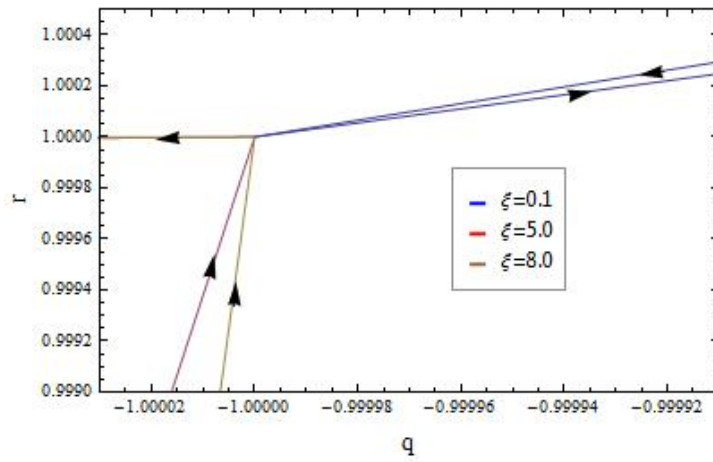
(a) $r(q)$ for $\Lambda = 1.0$.(b) $r(q)$ for $\Lambda = 0.0$.(c) $r(q)$ for $\Lambda = -1.0$.

Figure 6.30: The q - r plane for the BI universe model with cosmological constant and Zel'dovich fluid, for three different values of ξ , and different values of Λ . The arrows indicate the direction of the time evolution. Here we set $\kappa=H_0=\tau_0=t_0=1$, for simplicity.

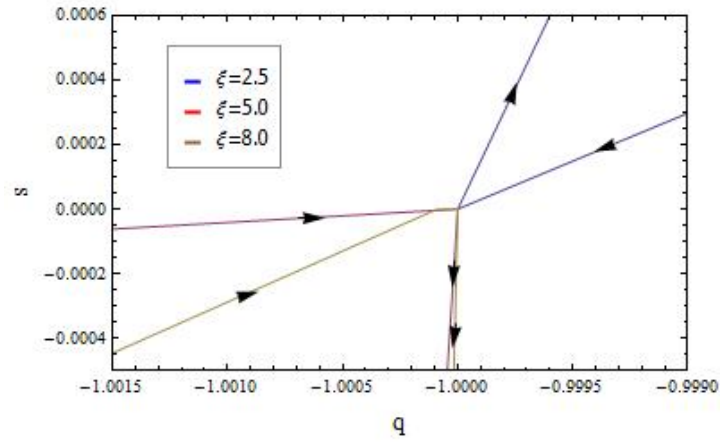
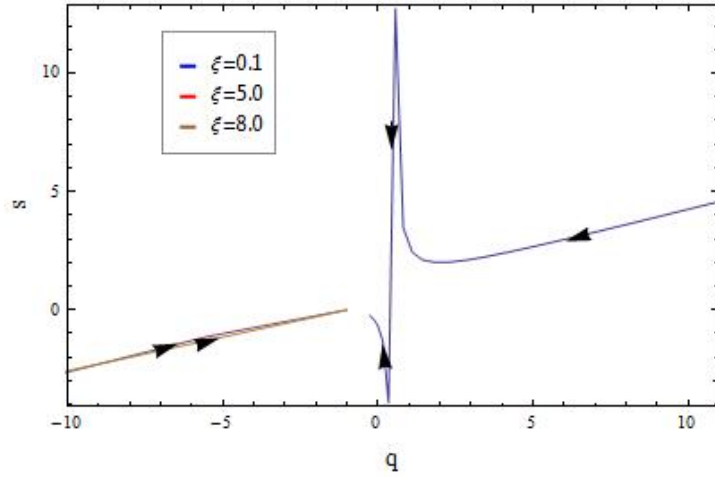
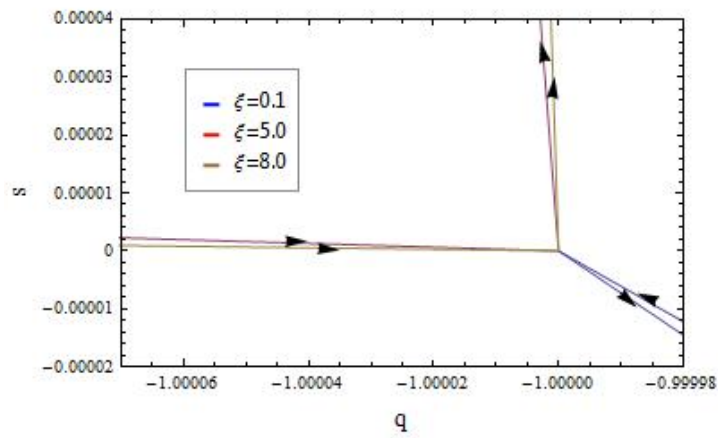
(a) $s(q)$ for $\Lambda = 1.0$.(b) $s(q)$ for $\Lambda = 0.0$.(c) $s(q)$ for $\Lambda = -1.0$.

Figure 6.31: The q - s plane for the BI universe model with cosmological constant and Zel'dovich fluid, for three different values of ξ , and different values of Λ . The arrows indicate the direction of the time evolution. Here we set $\kappa=H_0=\tau_0=t_0=1$, for simplicity.

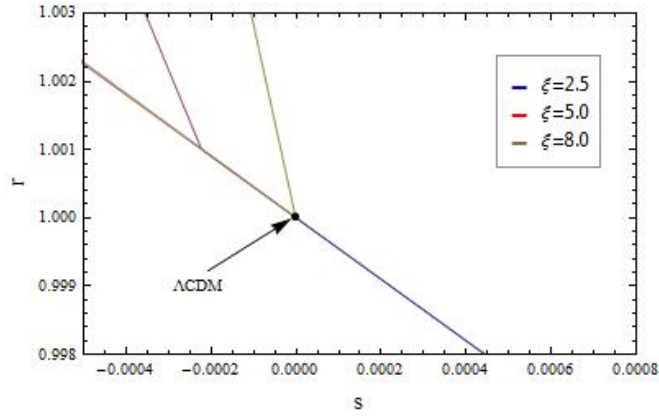
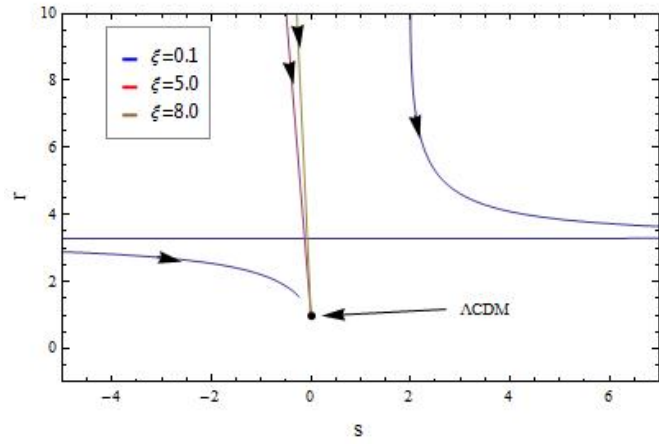
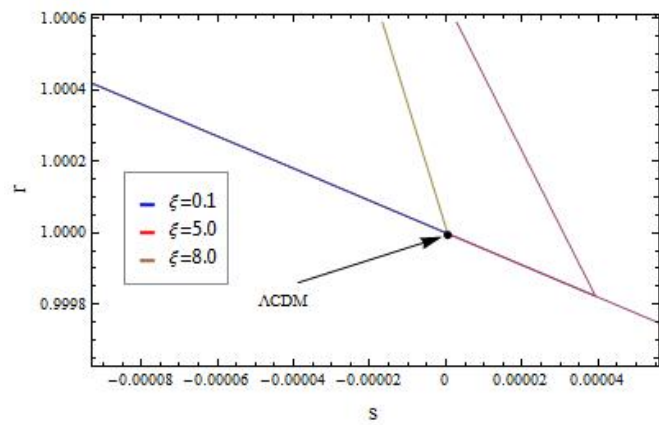
(a) $r(s)$ for $\Lambda = 1.0$.(b) $r(s)$ for $\Lambda = 0.0$.(c) $r(s)$ for $\Lambda = -1.0$.

Figure 6.32: The s - r plane for the BI universe model with cosmological constant and Zel'dovich fluid, for three different values of ξ and Λ . The arrows indicate the direction of the time evolution. The point $\{0, 1\}$ corresponds to the values of statefinder parameters for the Λ CDM model. Here we set $\kappa=H_0=\tau_0=t_0=1$, for simplicity.

Chapter 7

Conclusion and Outlook

7.1 Results and Conclusions

In this thesis we have reviewed the statefinder formalism and several universe models. We have considered the universe models listed in the introduction and applied the statefinder formalism to these models, and it is time to review our results.

- The new coupled quintessence cosmological model, presented by J. F. Jesus, R. C. Santos, J. S. Alcaniz and J. A. S. Lima [48]:

In this model the dark energy component is decaying into the cold dark matter (CDM) and therefore the CDM component will dilute more slowly compared to its standard evolution. The deviation from the standard evolution is characterized by a positive constant, ϵ . We have calculated the deceleration parameter and the statefinder parameters for this model and we have plotted the deceleration parameter, statefinder parameters and the s - r -plane for different values of ϵ and w . We have found that the effect of ϵ is to decrease the value of $q(z)$, $r(z)$, $r(q)$ and $s(q)$. When the equation of state parameter w has values close to the LIVE value, i.e. $w = -1$, the value of deceleration parameter and statefinder parameter r increases for increasing w . For this model when $w \leq -1$, the values of the statefinder parameters move toward the values of the Λ CDM model. For $w > -1$ the values of the statefinder parameters move toward, but do not reach the values of the Λ CDM model.

- The Λ CDM model with viscosity.

For this model we have found the expressions for the Hubble parameter, the scale factor, the deceleration parameter and the statefinder parameters. We have also given some numerical solutions to the energy density for the non-relativistic matter. When the viscosity is set to zero the standard Λ CDM model is recovered.

When the bulk viscosity has values very close to zero, we found a point singularity at the initial epoch of the cosmic evolution. For these models the universe starts with a big bang. For the Λ CDM model with bulk viscosity, as $t \rightarrow \infty$ the energy density converges to a finite value. This means that for this model the energy density of matter will stay constant for large times, t .

For bigger values of the bulk viscosity we have found that the initial singularity will be removed, and the universe will begin at $t = -\infty$ with an infinitely large volume. As t increases, the volume will decay to a minimum. When it has reached this minimum, it will start to increase, and as $t \rightarrow \infty$, it will increase exponentially. We have also found that for large times, t , the energy density and the Hubble parameter have finite values and they will stay constant. The bigger the value of the bulk viscosity is, the bigger the value of the energy density and the Hubble parameter will be.

All the curves on the s - r -plane for this model will go through the point $\{0,1\}$, which is the point for the Λ CDM model with no viscosity. By use of the statefinder formalism it is possible to differentiate the viscous Λ CDM models from non-viscous cases.

- Quiescence model with variable bulk viscosity.

For this model we have found the expressions for the Hubble parameter and the energy density. From the plots that we have made we found that the Hubble parameter and the energy density have infinitely large values at the initial epoch of the cosmic evolution. As $z \rightarrow 0$, the Hubble parameter and the energy density will decay to H_0 and ρ_0 , respectively. From $z = 0$ and as z decreases, for smaller values of w_x and for bigger values of ξ_1 , the Hubble parameter and the energy density will increase rapidly, and they will eventually be infinitely large. The bigger the value of ξ_1 is, the faster they will diverge. For bigger values of w_x and for smaller values of ξ_1 , the Hubble parameter and the energy density will tend to zero as $z \rightarrow -\infty$. This gives an empty universe that expands with a constant velocity.

On the r - s plane for this model we found that when $w_x = -1.5$, for small values of ξ_1 the curves will go through the point $\{0,1\}$, which is the statefinder parameter value for Λ CDM model. On the r - s plane for $w_x = -0.7$, we found that only the curve with $\xi_1 = 0.3$ will go through the point $\{0,1\}$.

- Bianchi type-I universe model with cosmological constant and with variable shear viscosity and constant bulk viscosity.

For this model we considered the case where the shear viscosity is proportional to the expansion. When we solved the Raychaudhuri equation we found three different solutions for the Hubble parameter for three different cases, and hence, we found three different expressions for the volume expansion. Because of the complexity of the form of one of the solutions, we only gave the expressions for the deceleration parameter and statefinder parameters, for two of the solutions. But, we have, for all solutions, plotted the q - r -, q - s - and s - r -plane. We have also plotted the volume expansions for three different values of w ; $w = 0$ for dust, $w = 1/3$ for radiation and $w = 1$ for Zel'dovich fluid and for some appropriate values of Λ .

For one of the solutions we found that $\Lambda = 0$. From the plots that we made we found that for $w = 0$, the universe starts with zero volume at some point of time $t < 0$, and then the volume expands exponentially. For $w = 1/3$, the universe starts with zero volume at $t = 0$, and as $t \rightarrow \infty$, it will also expand exponentially. For the Bianchi type-I universe model filled with Zel'dovich fluid, i.e. $w = 1$, we found that the universe starts with zero volume at $t = -\infty$. As $t \rightarrow 0$ the volume becomes negative. And, at some point of time $t > 0$, the volume becomes positive, and then the universe expands exponentially. From the s - r -plane for this model we found that at a point of time the curves will go through the point for the Λ CDM model.

For the other solutions we found some physically reasonable behaviour of the volume expansion, but we also found, for one of the solutions, that when $w = 1/3$ the universe will behave in a very strange and perhaps 'unphysical' way. From the s - r -plane for these solutions we found that for most cases the curves will, at a point of time, go through the point for the Λ CDM model.

- Nonlinear viscous fluid Bianchi type-I universe model filled with Zel'dovich fluid and with the cosmological constant.

For this model we first found the solutions for the Einstein's field equations. When we considered the case with constant bulk and shear viscosity we managed to find the expressions for the Hubble parameter and the volume expansion, and, based on these expressions we found a numerical solution for the energy density. We plotted the Hubble parameter, the volume expansion and the energy density for different values of Λ , ξ and η . We found that for different values of Λ , when the value of the bulk viscosity is small, there exists a singularity at $t = 0$. But, when we decrease the value of the bulk viscosity, for the same values of Λ , the singularities vanish. For these models as $t \rightarrow \infty$, the universe will experience an accelerated expansion. The bigger the value of the bulk viscosity is, the bigger the expansion rate will be.

For big values of ξ , and for $\Lambda > 0$, the universe starts with zero volume at $t = -\infty$. For $\Lambda < 0$, if we increase the value of ξ , the universe will begin with infinitely large volume at $t = -\infty$, and, as $t \rightarrow t_0$, this volume will decrease, and then, as $t \rightarrow \infty$, the universe will start to expand exponentially.

From the numerical solutions of the energy density we found that regardless of what values the cosmological constant and the bulk viscosity have, the shear viscosity will not change the evolution of the energy density. For different values of the bulk viscosity, the value of the energy density is infinitely large at the beginning of the cosmic evolution, and, it will decay to ρ_0 at $z = 0$. The bigger the value of the bulk viscosity is, the faster the energy density decays to ρ_0 . Based on the solutions for the Hubble parameter, the volume expansion and the energy density we found that these universe models will eventually evolve to a de Sitter universe.

For this model we found the expressions for the deceleration parameter and statefinder parameters, and we plotted the time evolution for these parameters. We found that for $\Lambda = 1$ and $\Lambda = -1$, and for all appropriate values of ξ , the curves have values very close to $\{0, 1\}$, and for $\Lambda = 0$, the curves will eventually approach the point $\{0, 1\}$ for the Λ CDM model.

7.2 General Overview and Outlook

In this thesis we have explored and analyzed different universe models by means of the statefinder parameter formalism. We have found the expressions for the Hubble parameter, the scale factor/the volume expansion and the energy density for these models.

In the case of the Bianchi type-I universe models, we have only considered some special cases, those provides exact solutions. For a better knowledge about the cosmic evolution, it is important to perform a detailed analysis and find some numerical solutions of this model.

We have also found the expressions for the deceleration parameter and the statefinder parameters for these models. It is the hope that someday we will be able to measure r and s to a good accuracy and by comparing these observations with different dark energy models we can find which model is the 'best' model of dark energy. One such way of measuring the statefinder parameters is via the data that is coming from SuperNova Acceleration Probe (SNAP) type experiments. This shows that the statefinder parameters can turn into a powerful diagnostic of dark energy in the future.

Appendix A

Numerical values

A.1 Physical constants

Speed of light	c	$2.99792458 \times 10^8 \text{m} \cdot \text{s}^{-1}$
Newton constant	G_N	$6.67428(67) \times 10^{-11} \text{m}^3 \cdot \text{kg}^{-1} \cdot \text{s}^{-2}$
Planck constant	h	$6.62606896(33) \times 10^{-34} \text{J} \cdot \text{s}$
Reduced Planck constant	$\hbar = \frac{h}{2\pi}$	$1.054571628(53) \times 10^{-34} \text{J} \cdot \text{s}$
Boltzmann constant	k_B	$1.3806504(24) \times 10^{-23} \text{J} \cdot \text{K}^{-1}$

A.2 Units

A.2.1 Natural units

When using the international system of units (SI), the laws of physics involve many constants, such as the Planck constant \hbar , the speed of light in vacuum c or the gravitational Newton constant G_N [60].

It turns out that one can choose a more adequate system of units that greatly simplifies calculations. This is achieved by imposing that the numerical value of some constant is unity. Cosmologists use the system of units in which ' $\hbar = c = 1$ '. In this system time and distance are expressed in the same units, and masses and energies are also expressed in same units, and both are inverse to space and time units

$$\hbar = c = 1 \quad \Leftrightarrow \quad [L] = [T] = [M^{-1}] = [E^{-1}]. \quad (\text{A.1})$$

In order to fix the system of units, one must use a third constant. For instance, one can impose that the numerical value of the Newton constant G_N be set to unity. In this case, one deals with the so-called Planck units. In this system, time, mass, energy and distance are all dimensionless, meaning that numbers found are in units of the Planck length, time and mass, namely

$$\ell_P = \sqrt{\frac{\hbar G_N}{c^3}}, \quad t_P = \sqrt{\frac{\hbar G_N}{c^5}}, \quad M_P = \sqrt{\frac{\hbar c}{G_N}}. \quad (\text{A.2})$$

A.2.2 Conversion factors

Planck mass	$M_P = \sqrt{\frac{\hbar c}{G_N}}$	$2.17644(11) \times 10^{-8} \text{kg}$
Planck time	$t_P = \sqrt{\frac{\hbar G_N}{c^3}}$	$5.391242(76) \times 10^{-44} \text{s}$
Planck length	$\ell_P = \sqrt{\frac{\hbar G_N}{c^3}}$	$1.616252(81) \times 10^{-35} \text{m}$
Planck temperature	$T_P = \sqrt{\frac{\hbar c^5}{G_N k_B^2}}$	$1.416785(71) \times 10^{32} \text{K}$

A.2.3 Cosmological quantities

Astronomical unit	AU	$1.49597870660(20) \times 10^{11} \text{m}$
parsec	pc	$3.0856775807(4) \times 10^{16} \text{m}$
sidereal year	yr	$3.155815 \times 10^7 \text{s}$
Hubble constant	H_0	$100 h \text{km} \cdot \text{s}^{-1} \text{Mpc}^{-1}$
	h	0.72 ± 0.05
Hubble time	$t_{H_0} = H_0^{-1}$	$9.7776 h^{-1} \times 10^9 \text{yr}$
Hubble distance	$D_{H_0} = c H_0^{-1}$	$29997.9 h^{-1} \text{Mpc}$
Critical density today	$\rho_{cr} = \frac{3H_0^2}{8\pi G_N}$	$1.87837(28) \times 10^{-29} h^2 \text{g} \cdot \text{cm}^{-3}$
CMB temperature	$T_{\gamma 0}$	$2.725 \Theta_{2.7} \text{K}$
Radiation energy density	ρ_{r0}	$7.8042 \times 10^{-34} \Theta_{2.7}^4 \text{g} \cdot \text{cm}^{-3}$

Appendix B

Einstein's Field Equations

In this appendix we will give Einstein's field equations for two cases. First, for the Friedmann-Lemaître universe model, which has spatially homogeneous and isotropic spacetime and it is used to find the Friedmann equations. And then, for Bianchi type-I universe model, which has a spatially homogeneous but anisotropic spacetime.

In both cases, we will first find Einstein tensor $G_{\mu\nu}$, which is given as

$$G_{\mu\nu} = R_{\mu\nu} - \frac{1}{2}Rg_{\mu\nu}, \quad (\text{B.1})$$

where $R_{\mu\nu}$ and R are the Ricci tensor and the Ricci scalar, respectively. And they are given as

$$R = g^{\mu\nu}R_{\mu\nu} = R^\mu_\mu, \quad (\text{B.2})$$

$$R_{\mu\nu} = \delta^\beta_\alpha R^\alpha_{\mu\beta\nu} = R^\alpha_{\mu\alpha\nu}, \quad (\text{B.3})$$

where $R^\alpha_{\mu\beta\nu}$ is the Riemann tensor. In coordinate basis the connection can be written in terms of the metric $g_{\mu\nu}$ as

$$\Gamma^\alpha_{\mu\nu} = \frac{1}{2}g^{\alpha\lambda}(\partial_\nu g_{\mu\lambda} + \partial_\mu g_{\lambda\nu} - \partial_\lambda g_{\mu\nu}) \quad (\text{B.4})$$

This expression can be used to find the components of the Riemann tensor $R^\alpha_{\mu\beta\nu}$

$$R^\alpha_{\mu\beta\nu} = \partial_\beta \Gamma^\alpha_{\mu\nu} - \partial_\nu \Gamma^\alpha_{\mu\beta} + \Gamma^\alpha_{\beta\lambda} \Gamma^\lambda_{\mu\nu} - \Gamma^\alpha_{\nu\lambda} \Gamma^\lambda_{\mu\beta}. \quad (\text{B.5})$$

B.1 Einstein's Field Equations for Friedmann-Lemaître Metric

The lineelement for a spatially homogeneous and isotropic spacetime in spherical coordinates (r, θ, ϕ) takes the form

$$ds^2 = -dt^2 + a^2(t) \left[\frac{1}{1 - kr^2} dr^2 + r^2 d\theta^2 + r^2 \sin^2 \theta d\phi^2 \right] \quad (\text{B.6})$$

B.1.1 Christoffel symbols $\Gamma^\alpha_{\mu\nu}$

In order to calculate Christoffel symbols for this lineelement, we use the fact that for a diagonal metric the inverse is given by $g^{\mu\nu} = \frac{1}{g_{\mu\nu}}$. Because of the symmetry in the lower indices we know that $\Gamma^\alpha_{\mu\nu} = \Gamma^\alpha_{\nu\mu}$. The non-vanishing Christoffel symbols are then

$$\Gamma^t_{rr} = \frac{1}{2}\partial_t g_{rr} = (1 - kr^2)^{-1} a \partial_t a \quad (\text{B.7})$$

$$\Gamma^t_{\theta\theta} = \frac{1}{2}\partial_t g_{\theta\theta} = r^2 a \partial_t a \quad (\text{B.8})$$

$$\Gamma^t_{\phi\phi} = \frac{1}{2}\partial_t g_{\phi\phi} = r^2 \sin^2 \theta a \partial_t a \quad (\text{B.9})$$

$$\Gamma_{tr}^r = \frac{1}{2}(1 - kr^2)a^{-2}\partial_t g_{rr} = \frac{\partial_t a}{a} \quad (\text{B.10})$$

$$\Gamma_{rr}^r = \frac{1}{2}(1 - kr^2)a^{-2}\partial_r g_{rr} = (1 - kr^2)^{-1}kr \quad (\text{B.11})$$

$$\Gamma_{\theta\theta}^r = -\frac{1}{2}(1 - kr^2)a^{-2}\partial_r g_{\theta\theta} = -(1 - kr^2)r \quad (\text{B.12})$$

$$\Gamma_{\phi\phi}^r = -\frac{1}{2}(1 - kr^2)a^{-2}\partial_r g_{\phi\phi} = -(1 - kr^2)r \sin^2 \theta \quad (\text{B.13})$$

$$\Gamma_{t\theta}^\theta = \frac{1}{2}r^{-2}a^{-2}\partial_t g_{\theta\theta} = \frac{\partial_t a}{a} \quad (\text{B.14})$$

$$\Gamma_{r\theta}^\theta = \frac{1}{2}r^{-2}a^{-2}\partial_r g_{\theta\theta} = \frac{1}{r} \quad (\text{B.15})$$

$$\Gamma_{\phi\phi}^\theta = \frac{1}{2}r^{-2}a^{-2}\partial_\theta g_{\phi\phi} = -\cos \theta \sin \theta \quad (\text{B.16})$$

$$\Gamma_{t\phi}^\phi = \frac{1}{2}r^{-2}\sin^{-2}\theta a^{-2}\partial_t g_{\phi\phi} = \frac{\partial_t a}{a} \quad (\text{B.17})$$

$$\Gamma_{r\phi}^\phi = \frac{1}{2}r^{-2}\sin^{-2}\theta a^{-2}\partial_r g_{\phi\phi} = \frac{1}{r} \quad (\text{B.18})$$

$$\Gamma_{\theta\phi}^\phi = \frac{1}{2}r^{-2}\sin^{-2}\theta a^{-2}\partial_\theta g_{\phi\phi} = \frac{\cos \theta}{\sin \theta} \quad (\text{B.19})$$

B.1.2 Riemann Tensor $R_{\mu\beta\nu}^\alpha$

In the view of (B.5) and the Christoffel symbols we can calculate the components of the Riemann tensor. The non-vanishing relevant components of the Riemann tensor for $R_{\mu\nu}$ are

$$R_{rtr}^t = \partial_t \Gamma_{rr}^t - \Gamma_{rr}^t \Gamma_{tr}^r = (1 - kr^2)^{-1}a\partial_t^2 a \quad (\text{B.20})$$

$$R_{\theta t\theta}^t = \partial_t \Gamma_{\theta\theta}^t - \Gamma_{\theta\theta}^t \Gamma_{t\theta}^\theta = r^2 a \partial_t^2 a \quad (\text{B.21})$$

$$R_{\phi t\phi}^t = \partial_t \Gamma_{\phi\phi}^t - \Gamma_{\phi\phi}^t \Gamma_{t\phi}^\phi = r^2 \sin^2 \theta a \partial_t^2 a \quad (\text{B.22})$$

$$R_{trt}^r = -\partial_t \Gamma_{tr}^r - \Gamma_{tr}^r \Gamma_{tr}^r = -\frac{\partial_t^2 a}{a} \quad (\text{B.23})$$

$$R_{\theta r\theta}^r = \partial_r \Gamma_{\theta\theta}^r + \Gamma_{tr}^r \Gamma_{\theta\theta}^t + \Gamma_{rr}^r \Gamma_{\theta\theta}^r - \Gamma_{\theta\theta}^r \Gamma_{r\theta}^\theta = r^2 \left[(\partial_t a)^2 + k \right] \quad (\text{B.24})$$

$$\begin{aligned} R_{\phi r\phi}^r &= \partial_r \Gamma_{\phi\phi}^r + \Gamma_{tr}^r \Gamma_{\phi\phi}^t + \Gamma_{rr}^r \Gamma_{\phi\phi}^r - \partial_\phi \Gamma_{\phi r}^r - \Gamma_{\phi\phi}^r \Gamma_{r\phi}^\phi \\ &= r^2 \sin^2 \theta \left[(\partial_t a)^2 + k \right] \end{aligned} \quad (\text{B.25})$$

$$R_{t\theta t}^{\theta} = -\partial_t \Gamma_{t\theta}^{\theta} - \left(\Gamma_{t\theta}^{\theta}\right)^2 = -\frac{\partial_t^2 a}{a} \quad (\text{B.26})$$

$$\begin{aligned} R_{r\theta r}^{\theta} &= -\partial_r \Gamma_{r\theta}^{\theta} - \left(\Gamma_{r\theta}^{\theta}\right)^2 + \Gamma_{t\theta}^{\theta} \Gamma_{rr}^t + \Gamma_{r\theta}^{\theta} \Gamma_{rr}^r \\ &= (1 - kr^2)^{-1} \left[(\partial_t a)^2 + k \right] \end{aligned} \quad (\text{B.27})$$

$$\begin{aligned} R_{\phi\theta\phi}^{\theta} &= \partial_{\theta} \Gamma_{\phi\phi}^{\theta} + \Gamma_{t\theta}^{\theta} \Gamma_{\phi\phi}^t + \Gamma_{r\theta}^{\theta} \Gamma_{\phi\phi}^r - \Gamma^{\phi} \theta \phi \Gamma_{\phi\phi}^{\theta} \\ &= r^2 \sin^2 \theta \left[(\partial_t a)^2 + k \right] \end{aligned} \quad (\text{B.28})$$

$$R_{t\phi t}^{\phi} = -\partial_t \Gamma_{t\phi}^{\phi} - \left(\Gamma_{t\phi}^{\phi}\right)^2 = -\frac{\partial_t^2 a}{a} \quad (\text{B.29})$$

$$\begin{aligned} R_{r\phi r}^{\phi} &= -\partial_r \Gamma_{r\phi}^{\phi} - \left(\Gamma_{r\phi}^{\phi}\right)^2 + \Gamma_{t\phi}^{\phi} \Gamma_{rr}^t + \Gamma_{r\phi}^{\phi} \Gamma_{rr}^r \\ &= (1 - kr^2)^{-1} \left[(\partial_t a)^2 + k \right] \end{aligned} \quad (\text{B.30})$$

$$R_{\theta\phi\theta}^{\phi} = -\partial_{\theta} \Gamma_{\theta\phi}^{\phi} - \left(\Gamma_{\theta\phi}^{\phi}\right)^2 + \Gamma_{t\phi}^{\phi} \Gamma_{\theta\theta}^t + \Gamma_{r\phi}^{\phi} \Gamma_{\theta\theta}^r = r^2 \left[(\partial_t a)^2 + k \right] \quad (\text{B.31})$$

B.1.3 Ricci Tensor $R_{\mu\nu}$ and Ricci Scalar R

Ricci Tensor $R_{\mu\nu}$

$$R^{tt} = R_{trt}^r + R_{t\theta t}^{\theta} + R_{t\phi t}^{\phi} = -3 \frac{\partial_t^2 a}{a} \quad (\text{B.32})$$

$$R_{rr} = R_{trt}^r + R_{r\theta r}^{\theta} + R_{r\phi r}^{\phi} = (1 - kr^2)^{-1} \left[a \partial_t^2 a + 2 (\partial_t a)^2 + 2k \right] \quad (\text{B.33})$$

$$R_{\theta\theta} = R_{t\theta t}^t + R_{\theta r \theta}^r + R_{\theta\phi\theta}^{\phi} = r^2 \left[a \partial_t^2 a + 2 (\partial_t a)^2 + 2k \right] \quad (\text{B.34})$$

$$R_{\phi\phi} = R_{t\phi t}^t + R_{\phi r \phi}^r + R_{\phi\theta\phi}^{\theta} = r^2 \sin^2 \theta \left[a \partial_t^2 a + 2 (\partial_t a)^2 + 2k \right] \quad (\text{B.35})$$

Ricci Scalar R

$$R = g^{tt} R_{tt} + g^{rr} R_{rr} + g^{\theta\theta} R_{\theta\theta} + g^{\phi\phi} R_{\phi\phi} = 6 \left[\frac{a \partial_t^2 a + (\partial_t a)^2 + k}{a^2} \right] \quad (\text{B.36})$$

B.1.4 Einstein Tensor $G_{\mu\nu}$

In the view of (B.1), (B.6), (B.32)-(B.35) and (B.36), the components of Einstein tensor are

$$G_{tt} = R_{tt} - \frac{1}{2} g_{tt} R = \frac{3}{a^2} \left[(\partial_t a)^2 + k \right] \quad (\text{B.37})$$

$$G_{rr} = R_{rr} - \frac{1}{2} g_{rr} R = (1 - kr^2)^{-1} \left[-2a \partial_t^2 a - (\partial_t a)^2 - k \right] \quad (\text{B.38})$$

$$G_{\theta\theta} = R_{\theta\theta} - \frac{1}{2} g_{\theta\theta} R = r^2 \left[-2a \partial_t^2 a - (\partial_t a)^2 - k \right] \quad (\text{B.39})$$

$$G_{\phi\phi} = R_{\phi\phi} - \frac{1}{2} g_{\phi\phi} R = r^2 \sin^2 \theta \left[-2a \partial_t^2 a - (\partial_t a)^2 - k \right] \quad (\text{B.40})$$

B.1.5 Energy-Momentum Tensor for a Perfect Fluid

Energy-momentum tensor for a perfect fluid is given as

$$T_{\mu\nu} = (\rho + p) u_\mu u_\nu + p g_{\mu\nu} \quad (\text{B.41})$$

In a comoving orthogonal basis the components of the fluids four-velocity is $u_\mu = (1, 0, 0, 0)$. Then, the non-zero components of the energy-momentum tensor are given as

$$T_{tt} = \rho, \quad T_{ii} = p g_{ii} \quad (\text{B.42})$$

Conservation of the energy-momentum is given by

$$\dot{\rho} = -3 \frac{\dot{a}}{a} (\rho + p). \quad (\text{B.43})$$

B.1.6 Einstein's Field Equations

Einstein's field equation is given by

$$G_{\mu\nu} = 8\pi G T_{\mu\nu} \quad (\text{B.44})$$

Using (B.37)-(B.40) and (B.42), we find that

- tt-component

$$\frac{\dot{a}^2 + k}{a^2} = 8\pi G \rho \quad (\text{B.45})$$

- ii-component

$$-2a\ddot{a} - \dot{a}^2 - k = 8\pi G p a^2. \quad (\text{B.46})$$

Summation of ii-components (B.46) and inserting (B.45), gives Friedmann's second equation

$$\frac{\ddot{a}}{a} = -\frac{4\pi G}{3} (\rho + 3p). \quad (\text{B.47})$$

B.2 Einstein's Field Equations for Bianchi Type-I Metric

The lineelement for the Bianchi type-I model, which is a spatially homogeneous and anisotropic spacetime, takes the form

$$ds^2 = dt^2 - a(t)^2 dx^2 - b(t)^2 dy^2 - c(t)^2 dz^2, \quad (\text{B.48})$$

The non-trivial Christoffel symbols for this metric are

$$\begin{aligned} \Gamma_{xt}^x &= \frac{\dot{a}}{a}, & \Gamma_{yt}^y &= \frac{\dot{b}}{b}, & \Gamma_{zt}^z &= \frac{\dot{c}}{c} \\ \Gamma_{xx}^t &= a\dot{a}, & \Gamma_{yy}^t &= b\dot{b}, & \Gamma_{zz}^t &= c\dot{c}. \end{aligned} \quad (\text{B.49})$$

The non-trivial components of Riemann tensors in this case are

$$\begin{aligned} R_{tx}^{tx} &= -\frac{\ddot{a}}{a}, & R_{ty}^{ty} &= -\frac{\ddot{b}}{b}, & R_{tz}^{tz} &= -\frac{\ddot{c}}{c} \\ R_{xy}^{xy} &= -\frac{\dot{a}\dot{b}}{a b}, & R_{yz}^{yz} &= -\frac{\dot{b}\dot{c}}{b c}, & R_{zx}^{zx} &= -\frac{\dot{a}\dot{c}}{a c}. \end{aligned} \quad (\text{B.50})$$

The non-trivial components of Ricci tensors are then

$$R_t^t = - \left(\frac{\ddot{a}}{a} + \frac{\ddot{b}}{b} + \frac{\ddot{c}}{c} \right), \quad (\text{B.51})$$

$$R_x^x = - \left[\frac{\ddot{a}}{a} + \frac{\dot{a}}{a} \left(\frac{\dot{b}}{b} + \frac{\dot{c}}{c} \right) \right], \quad (\text{B.52})$$

$$R_y^y = - \left[\frac{\ddot{b}}{b} + \frac{\dot{b}}{b} \left(\frac{\dot{c}}{c} + \frac{\dot{a}}{a} \right) \right], \quad (\text{B.53})$$

$$R_z^z = - \left[\frac{\ddot{c}}{c} + \frac{\dot{c}}{c} \left(\frac{\dot{a}}{a} + \frac{\dot{b}}{b} \right) \right]. \quad (\text{B.54})$$

The Ricci scalar for BI universe is

$$R = -2 \left(\frac{\ddot{a}}{a} + \frac{\ddot{b}}{b} + \frac{\ddot{c}}{c} + \frac{\dot{a}\dot{b}}{ab} + \frac{\dot{b}\dot{c}}{bc} + \frac{\dot{c}\dot{a}}{ca} \right). \quad (\text{B.55})$$

B.2.1 Energy-Momentum Tensor for a Viscous Fluid

Energy-momentum tensor for a viscous fluid has the form

$$T_{\mu\nu} = (\rho + p') u_\mu u_\nu - p' \delta_{\mu\nu} + \eta g_\nu^\beta [u_{\mu;\beta} + u_{\beta;\mu} - u_\mu u^\alpha u_{\beta;\alpha} - u_\beta u^\alpha u_{\mu;\alpha}], \quad (\text{B.56})$$

where

$$p' = p - \left(\xi - \frac{2}{3}\eta \right) u^\mu_{;\mu}. \quad (\text{B.57})$$

In a comoving system of reference such that $u^\mu = (1, 0, 0, 0)$ we have

$$T_{tt} = \rho, \quad (\text{B.58})$$

$$T_{xx} = -p' + 2\eta \frac{\dot{a}}{a}, \quad (\text{B.59})$$

$$T_{yy} = -p' + 2\eta \frac{\dot{b}}{b}, \quad (\text{B.60})$$

$$T_{zz} = -p' + 2\eta \frac{\dot{c}}{c}. \quad (\text{B.61})$$

B.2.2 Einstein Field Equations

In account of the Λ -term Einstein's field equations are given by

$$G_{\mu\nu} = R_{\mu\nu} - \frac{1}{2} g_{\mu\nu} R = \kappa T_{\mu\nu} - g_{\mu\nu} \Lambda. \quad (\text{B.62})$$

Using (B.51)-(B.54) and (B.55) for the BI for the space-time (B.48), we can rewrite equation (B.62) as

$$\frac{\ddot{b}}{b} + \frac{\ddot{c}}{c} + \frac{\dot{b}\dot{c}}{bc} = \kappa T_{xx} - \Lambda, \quad (\text{B.63})$$

$$\frac{\ddot{c}}{c} + \frac{\ddot{a}}{a} + \frac{\dot{c}\dot{a}}{ca} = \kappa T_{yy} - \Lambda, \quad (\text{B.64})$$

$$\frac{\ddot{a}}{a} + \frac{\ddot{b}}{b} + \frac{\dot{a}\dot{b}}{ab} = \kappa T_{zz} - \Lambda, \quad (\text{B.65})$$

$$\frac{\dot{a}\dot{b}}{ab} + \frac{\dot{b}\dot{c}}{bc} + \frac{\dot{c}\dot{a}}{ca} = \kappa T_{tt} - \Lambda, \quad (\text{B.66})$$

We define the volume scale of BI space-time as

$$\tau \equiv abc. \quad (\text{B.67})$$

In analogy with Hubble parameter in a FRW universe model we introduce a generalized Hubble parameter H

$$\frac{\dot{\tau}}{\tau} = \frac{\dot{a}}{a} + \frac{\dot{b}}{b} + \frac{\dot{c}}{c} = 3H. \quad (\text{B.68})$$

Summation of Einstein equations (B.63)-(B.65) and 3 times (B.66) gives

$$\ddot{\tau} - \frac{3}{2}\kappa\xi\dot{\tau} = \frac{3}{2}\kappa(\rho - p)\tau - 3\Lambda\tau. \quad (\text{B.69})$$

Conservation of the energy-momentum is given by

$$T_{\mu;\nu}^{\nu} = T_{\mu,\nu}^{\nu} + \Gamma_{\alpha\nu}^{\nu}T_{\mu}^{\alpha} - \Gamma_{\mu\nu}^{\alpha}T_{\alpha}^{\nu} = 0. \quad (\text{B.70})$$

Equation (B.70) gives

$$\frac{1}{\dot{\tau}}(\tau T_t^t)^{\cdot} - \frac{\dot{a}}{a}T_x^x - \frac{\dot{b}}{b}T_y^y - \frac{\dot{c}}{c}T_z^z = 0. \quad (\text{B.71})$$

Using (B.58)-(B.61), equation (B.71) becomes

$$\dot{\rho} + \frac{\dot{\tau}}{\tau}(\rho + p) - \left(\xi + \frac{4}{3}\eta\right)\frac{\dot{\tau}^2}{\tau^2} + 4\eta(\kappa\rho - \Lambda) = 0. \quad (\text{B.72})$$

References

- [1] Øyvind Grøn and S. Hervik, *Einstein's General Theory of Relativity With Modern Applications in Cosmology* (Springer, 2007).
- [2] S. Carroll, *Spacetime and Geometry: An Introduction to General Relativity* (Addison Wesley, 2004).
- [3] Øystein Elgarøy, *Lecture notes: AST4220 Cosmology I*
- [4] S. Weinberg, *Cosmology*, Oxford University Press, 2008.
- [5] S. Weinberg, *Gravitation and Cosmology*, Wiley, New York, 1972.
- [6] Patrick Peter and Jean-Philippe Uzan *Primordial Cosmology* Oxford university press 2009.
- [7] H. Goldstein, C. Pool, and J. Safko, *Classical Mechanics* (Addison Wesley, 2002).
- [8] J. Ehlers and W. Rindler, *A phase space representation of Friedmann-Lemaître Universe containing both dust and radiation and the inevitability of a Big Bang*, Month. Not. R. Astron. Soc. **238**, 503, 1989.
- [9] W. Rindler, *Visual horizons in world-models*, Month. Not. R. Astron. Soc. **116**, 622, 1953.
- [10] Novello, M. and d'Olival, J. B. S., *Nonlinear Viscous Cosmology* 1980, Acta Phys. Pol. B11, 3.
- [11] Sahni, V., Saini, T.D., Starobinsky, A. and Alam, U., *Statefinder - a new geometrical diagnostic of dark energy*, 2002, astro-ph/0201498.
- [12] Ø. Grøn, *Viscous inflationary universe models*. Astrophys. Space. Sci. 173 (1990) 191.
- [13] A. K. D. Evans, I. K. Wehus, Ø. Grøn and Ø. Elgarøy, *Geometric Constraints on Dark Energy*. Astron.Astrophys. 430 (2005) 399.
- [14] Liang, E. P. T. 1975, Monthly Notices Roy. Astron. Soc. 171, 551.
- [15] Liang, E. P. T. 1977, *Entropy generation in the very early universe* Phys. Rev. D16, 3369.
- [16] Øyvind Grøn *Statefinder analysis of universe models with a viscous cosmic fluid and a fluid with a non-linear equation of state* Astrophysics (astro-ph) arXiv:0812.2549
- [17] U. Alam, V. Sahni and T. D. Starobinsky, *Exploring the Expanding Universe and Dark Energy using Statefinder Diagnostic*. Mon. Not. Roy. Astron. Soc. 344 (2003) 1057.
- [18] S. G. Rabinovich, *Measurement Errors: Theory and Practice*, American Institute of Physics, NY, 1995.
- [19] A. G. Riess, *et al.* [Supernova Search Team Collaboration], Astron. J. 116 (1998) 1009 [arXiv:astro-ph/9805201].

- [20] S. Perlmutter, *et al.* [Supernova Cosmology Project Collaboration], *Astrophys. J.* 517 (1999) 565 [arXiv:astro-ph/9812133].
- [21] M. G. Hu and X. H. Meng, *Bulk viscous cosmology: statefinder and entropy*. *Phys. Lett. B* 635 (2006) 186.
- [22] M. Tegmark *et al.* [SDSS Collaboration], *Phys. Rev. D* 69 (2004) 103501 [arXiv:astro-ph/0310723].
- [23] K. Abazajian *et al.* [SDSS Collaboration], *Astron. J.* 128 (2004) 502 [arXiv:astro-ph/0403325].
- [24] D. N. Spergel *et al.* [WMAP Collaboration], *Astrophys. J. Suppl.* 148 (2003) 175 [arXiv:astro-ph/0302209];
D. N. Spergel *et al.*, *Astrophys. J. Suppl.* 170, 377 (2007);
J. Dunkley *et al.*, arXiv:0803.0586.
- [25] C. L. Bennett *et al.* [WMAP Collaboration], *Astrophys. J. Suppl.* 148 (2003) 1 [arXiv:astro-ph/0302207].
- [26] W. Zimdahl and D. Pavon, *Statefinder parameters for interacting dark energy*. *Gen. Rel. Grav.* 36 (2004), 1483.
- [27] J. Zhang, X. Zhang and H. Liu, *Statefinder diagnosis for the interacting model of holographic dark energy*. *Phys. Lett. B* 659 (2008) 26.
- [28] X. Zhang, *Statefinder diagnostic for coupled quintessence*. *Phys. Lett. B* 611 (2005) 1.
- [29] X. Zhang, F. Q. Wu and J. Zhang, *New generalized Chaplygin gas as a scheme for unification of dark energy and dark matter*. *JCAP*, 0601 (2006) 003.
- [30] X. Zhang, *Statefinder diagnostic for holographic dark energy model*. *Int. J. Mod. Phys. D* 14 (2005) 1597.
- [31] Kamenshchick, A., Moschella, U., Pasquier, V. 2001, *Phys. Lett. B*, 511, 265
- [32] Bilic, N., Tupper, G. G., Viollier, R. 2002, *Phys. Lett. B*, 535, 17
- [33] U. Alam, V. Sahni, T. D. Saini and A. A. Starobinsky, *Statefinder - A new geometrical diagnostic of dark energy* *Mon. Not. Roy. ast. Soc.* 344, 1057 (2003) [astro-ph/0303009].
- [34] V. Gorini, A. Kamenshchik and U. Moschella, *Can the Chaplygin gas be a plausible model for dark energy?* *Phys. Rev. D* 67 063509 (2003) [astro-ph/0209395].
- [35] S. Capozziello, V. F. Cardone, E. Elizalde, S. Nojiri, S. D. Odintsov, *Title: Observational constraints on dark energy with generalized equations of state* astro-ph/0508350.
- [36] W. Hu, *Crossing the Phantom Divide: Dark Energy Internal Degrees of Freedom* astro-ph/0410680;
B. Feng, M. Li, X. Wang, X. Zhang, *Dark Energy Constraints from the Cosmic Age and Supernova* astro-ph/0404224;
X. Meng, M. Hu, J. Ren, *Cosmology with extended Chaplygin gas media and $w = -1$ crossing* astro-ph/0510357.

- [37] I. Brevik, *Viscous Cosmology, Entropy, and the Cardy-Verlinde Formula*. Quantum Cosmology Research Trends. Horizon in World Physics, Volume 246. Edited by Albert Reimer. QB991.Q36Q36 2005; Nova Science Publishers, Inc., 2005, p.165. (arXiv: gr-qc/0404095)
- [38] I. Brevik, O. Gorbunova and A. V. Timoshkin, *Dark energy fluid with time-dependent, inhomogeneous equation of state*. Eur. Phys. J. 51C (2007) 179.
- [39] I. Brevik, O. Gorbunova, *Dark Energy and Viscous Cosmology* gr-qc/0504001;
I. Brevik, O. Gorbunova, Y. A. Shaibo, *Viscous FRW Cosmology in Modified Gravity* gr-qc/0508038;
D. J. Scheartz, *Accelerated expansion without dark energy* Cern-th/2002-246
- [40] R. C. Feritas, S. V. B. Goncalves and H. E. S. Velten, *Constraints on the Generalized Chaplygin Gas Model from Gamma-Ray Bursts*. arXiv:1004.5585v1 [astro-ph.CO] 30 Apr 2010.
- [41] X. Meng, J. Ren, M. Hu, *Friedmann cosmology with a generalized equation of state and bulk viscosity* astro-ph/0509250.
J. Ren, X. Meng, Phys. Lett. B 633 (2006) 1;
J. Ren, X. H. Meng, *Modified equation of state, scalar field, and bulk viscosity in Friedmann universe* astro-ph/0602462.
- [42] W. Hu, *Crossing the Phantom Divide: Dark Energy Internal Degrees of Freedom* astro-ph/0410680;
B. Feng, M. Li, X. Wang, X. Zhang, *Dark Energy Constraints from the Cosmic Age and Supernova* astro-ph/0404224;
X. Meng, M. Hu, J. Ren, *Cosmology with extended Chaplygin gas media and $w = -1$ crossing* astro-ph/0510357.
- [43] Bertolami, O., Sen, A. A., Sen, S., Silva, P., T., 2004, MNRAS, *Latest Supernova data in the framework of Generalized Chaplygin Gas model* astro-ph/0402387
- [44] Chiba, T. Nakamura, T. 1998, Prog. Theor. Phys., 100, 1077
- [45] Visser, M. 2004, Class. Quant. Grav., 21, 2603
- [46] W. Zimdahl and D. Pavòn, Gen. Relativ. Grav. 35, 413 (2003).
- [47] K. C. Jacobs, Astrophys. J. 153, 661 (1968).
- [48] J. F. Jesus, R. C. Santos, J. S. Alcaniz, and J. A. S. Lima
Statfinder parameters for a new quintessence cosmology arXiv:0806.1366v2 [astro-ph] 25 Nov 2008
- [49] T. M. Davis et al., Astrophys. J. 666, 716 (2007).
- [50] D. J. Eisenstein et al., Astrophys. J. 633, 560 (2005).
- [51] Bijan Saha *Bianchi type I universe with viscous fluid* arXiv:gr-qc/0409104v2 13 Oct 2004
- [52] V. Sahni and A. A. Starobinsky, *The Case for a Positive Cosmological Lambda-term* Int. J. Mod. Phys. D 9 (2000) 373 [arXiv:astro-ph/9904398]

- [53] P. J. E. Peebles and B. Ratra, *The Cosmological Constant and Dark Energy* Rev. Mod. Phys. 75 (2003) 559 [arXiv:astro-ph/0207347]
- [54] V. Sahni, *Dark Matter and Dark Energy* Lect. Notes Phys. 653, 141 (2004) [arXiv:astro-ph/0403324]
- [55] E. J. Copeland, M. Sami and S. Tsujikawa, *Dynamics of dark energy* Int. J. Mod. Phys. D 15 (2006) 1753 [arXiv:hep-th/0603057]
- [56] J. Frieman, M. Turner and D. Huterer, *Dark Energy and the Accelerating Universe* Ann. Rev. Astron. Astrophys. 46, 385 (2008) [arXiv:0803.0982 [astro-ph]].
- [57] Guth, A. H. *Inflationary universe: A possible solution to the horizon and flatness problems* 1981, Phys. Rev. D, 23, 347
- [58] Frank M. White *Viscous Fluid Flow* McGraw-Hill Education (ISE Editions); 3rd edition (April 1, 2005)
- [59] Pijush K. Kundu, Ira M. Cohen *Fluid Mechanics* Academic Press; 4 edition (February 5, 2010)
- [60] Recommended values of fundamental constants (CODATA) [<http://physics.nist.gov/cuu/Constants/>].
- [61] C. P. Singh, Suresh Kumar *Viscous Fluid Cosmology in Bianchi Type-I Space-Time* Springer Science+Business Media, LLC 2008.
- [62] M. S. Berman (1983). *Nuovo Cim.*, 74B, 182.
- [63] M. S. Berman and F. de Mello Gomide. *Cosmological Models with Constant Deceleration Parameter* Plenum Publishing Corporation 1987
- [64] Belinskij, V. A. and Khalitnikov I. M. *Influence of viscosity on the character of cosmological evolution* Zh. Eksp. Teor. Fiz. 69, 401-413, (August 1975)
- [65] Heller, M. Acta Cosmologica 7, 7 (1978)
- [66] Woszczyna, A. Acta Phys. Pol. B11, 15. (1980)
- [67] Woszczyna, A. and Betkowski, W. AstroPhys. Space Sci. 82, 489. (1982)